



FACULTY OF SCIENCE AND TECHNOLOGY

MASTER THESIS

Study programme / specialisation:

Engineering Structures and Materials –
Offshore structures

The spring semester, 2022

Open Access

Authors:

Ahmed Adel Mohamed Radwan,
Nikolas Bentzen


(Signature author)

Course coordinator:

Sudath Chaminda Siriwardane

Supervisor(s):

Sudath Chaminda Siriwardane,
Ivar Holta,
Gunnar Gjerde

Thesis title:

Wind Fatigue Analysis – Evaluation of Different Methods and Software Alternatives

Credits (ECTS):

30

Keywords:

Wind induced fatigue
Slender structures
Power spectral density approach
Time history non-linear dynamic approach
Rain flow counting

Pages: 154

Stavanger, 15/06/2022
date/year

Abstract

Wind induced fatigue damage affects most slender structures such as flare booms and bridges in offshore environment. Due to the irregular and dynamic nature of wind, wind loading might cause structures to vibrate near the structure's natural frequency. Even though a structure never experience wind loading over the ultimate limit, vibrations can cause micro plastic deformities such as micro cracks, that over time can lead to fatigue-induced failure. The process of fatigue is complex in nature and hard to estimate accurately. A widely used approach in the offshore industry for calculating fatigue induced damage on complex structures is the use of FEM models and annual probability of wind speed and directional data. Two design methods for estimating fatigue damage are used: the spectral density approach and time history non-linear dynamic analysis. Both methods are based on the hot spot stress assessment approach.

FRAMEWORK and WINDPACK are software which uses the spectral density approach, and USFOS can be used to perform a non-linear dynamic analysis. The time history approach is slightly more computationally demanding to set up; however, it is arguably more accurate. Time history analysis offers more control, since each load case can be analyzed and verified separately, whereas the spectral transforms all load history into spectral diagrams. The spectral equations however are well documented and based on site collected wind turbulence data. There is research demand for further development of both methods, mainly for confirmation with real structural behavior. However, since spectral approaches are generally less demanding, comparing the two methods is also of interest for the practicing industry.

The main objective of this thesis is to compare the results and parametric sensitivity of the three different software using the two methods of fatigue calculation, due to wind buffeting. The effect of vortex induced vibrations on individual members are not included in this thesis.

Multiple fatigue analyses of a typical flare tower in the North Sea (Flare 1) are done with the same FEM model, with as similar input as possible, for all three software. Parametric studies have been executed for the following parameters: weight factor, drag coefficient (C_d), wind block combination and relative velocity. Time increment effect has also been studied in USFOS but is not considered as a parameter as it is a case dependent. The results from different parameter cases have been stored for the 5 most critical joints, and graphs are plotted to study trends.

Before the main comparisons are made, the thesis goes through the reasoning behind certain parameter choices. Then all software results are presented separately to illustrate how different parameter affect fatigue life, then comparisons between the software and the spectral density method against time history method is presented.

The main findings of this thesis are that USFOS predicts on average 66% the fatigue life that FRAMEWORK finds. For weight factor 1.0 cases, the difference becomes 49%. FRAMEWORK predicts on average 41% of the fatigue life that WINDPACK predicts. FRAMEWORK seems to be rather sensitive to weight factor change in the range of 1.0 to 1.1, which does not correlate with the change in the same range in the other two software.

Acknowledgements

This thesis is submitted as a requirement to complete a master's degree in Engineering Structures and Materials – Offshore Structures at the University of Stavanger. The work presented has been done in cooperation with Aker Solutions in Stavanger.

We would like to express our gratitude to professor Sudath for all his valuable assistance and motivation during the thesis work and throughout the study program. We would also like to extend our gratitude and respect to Ivar Holta and Gunnar Gjerde for their continuous assistance, humble sharing of knowledge and guidance throughout the thesis work. With their support, this thesis has exceeded all our expectations.

Also, we would like to thank Aker Solutions and Ådne Hausberg for giving us the chance to work on this thesis as a group and providing us with all the required tools to maintain a high level of quality. We also show our appreciation to Tore Holmås and Anders Holstad for their support on using USFOS. Finally, thanks for Rakesh Bhongade for his assistance on setting WINDPACK to run the required analysis and his overseas guidance.

Stavanger, June 2022

Ahmed, Nikolas

Table of Contents

Abstract	I
Acknowledgements	II
Table of Contents	III
List of figures	VI
List of tables	XIII
1 Introduction	1
1.1 Background	1
1.2 Problem Statement	1
1.3 Objectives	2
1.4 Limitations	2
1.5 Thesis Outline	2
2 Literature Review on Wind-induced Fatigue	4
2.1 Wind-induced Fatigue on Slender Structures	4
2.2 Wind Turbulence and Gust	5
2.2.1 Wind Turbulence	5
2.2.2 Wind Gust	5
2.3 Fatigue Assessment Methods	6
2.3.1 Nominal Stress Approach	7
2.3.2 Notch Stress Approach	7
2.3.3 Hot-Spot Stress Approach	8
2.4 Power Spectral Density Method for Fatigue Analysis	9
2.5 Time Domain Fatigue Analysis Method and Rain Flow Counting	10
2.5.1 Rain Flow Counting Method	11
2.6 Stress Concentration	12
2.6.1 Hot-spot Stress Method in Welded Pipes	13
2.7 Fatigue Analysis Using S-N Curves	16
2.7.1 S-N Curves for Tubular Joints	16
2.8 Miner's Rule	17
2.9 Research Gap	18
3 Model and Methodology of FRAMEWORK, WINDPACK and USFOS	20
3.1 Flare Boom and Model	20
3.1.1 Critical Fatigue Points	21
3.1.2 Structural Weight	24
3.1.3 Material Properties	25
3.1.4 Coordinate System	25
3.1.5 Boundary Conditions	26
3.1.6 Wind Data	26
3.1.7 Drag Coefficient	29
3.1.8 S-N Curves	30

3.2	Parametric Study	31
3.2.1	Software Limitations	31
3.2.2	Number of Wind Blocks.....	31
3.2.3	Drag Coefficient	34
3.2.4	Weight and Eigen Frequency	34
3.2.5	Time Increment	34
3.2.6	Relative Velocity	35
3.2.7	Stress Concentration Factors	36
3.3	DNV SESAM FRAMEWORK Methodology	37
3.3.1	Assumptions	38
3.3.2	Wind Data.....	39
3.3.3	Wind Spectra	39
3.3.4	Spectral Forcing Function	40
3.3.5	Spectral Relationships	41
3.3.6	Mode Shape and Eigen Frequency of a Brace	41
3.3.7	Calculation of Member End Damage	43
3.3.8	Stress Concentration Factors	43
3.3.9	Hot Spot Stress Power Spectra.....	44
3.3.10	Fatigue Life Calculation	44
3.4	WINDPACK Methodology	46
3.4.1	Analysis Procedure.....	46
3.4.2	Units	47
3.4.3	Wind Speed and Direction Probabilities	47
3.4.4	Wind Turbulence Spectra.....	48
3.4.5	Stress Concentration Factors (SCFs).....	49
3.5	USFOS/FATAL Methodology	51
3.5.1	Structural Model.....	52
3.5.2	Wind Fields	53
3.5.3	Dynamic Analysis (USFOS)	55
3.5.4	SCF Calculation	57
3.5.5	Cycle Counting (FATAL)	57
4	Wind-induced Fatigue Analysis Using FRAMEWORK.....	58
4.1	Results Tables.....	58
4.2	Result Graphs	59
4.2.1	Fatigue life against weight factor for different drag coefficient values	60
4.2.2	Fatigue life against drag coefficient for different weight factor values	62
4.2.3	Fatigue life against weight factor for different wind blocks	64
4.2.4	Fatigue life against drag factor for different wind blocks	66
4.3	Summary and Discussion	69
5	Wind-induced Fatigue Analysis Using WINDPACK.....	70
5.1	Results Tables.....	70

5.2	Result Graphs	71
5.2.1	Fatigue life against weight factor for different drag coefficient values:	72
5.2.2	Fatigue life against drag coefficient for different weight factor values:	74
5.2.3	Fatigue life against weight factor for different wind block cases:	76
5.2.4	Fatigue life against drag coefficient for different wind blocks:	78
5.3	Summary and Discussion	80
6	Wind-induced Fatigue Analysis Using USFOS	82
6.1	USFOS Analysis with Time Increment (dt) of 0.10 seconds	82
6.1.1	Results Tables.....	82
6.1.2	Results Graphs.....	84
6.1.3	Summary and Discussion	94
6.2	USFOS Analysis with Time Increment (dt) of 0.05 seconds	95
6.2.1	Results Tables.....	95
6.2.2	Results Graphs.....	97
6.2.3	Summary and Discussion	107
6.3	Parameters	111
6.3.1	Decision on Time Increment	111
6.3.2	Relative Velocity.....	112
7	Comparisons and Discussions	114
7.1	Comparison Table	114
7.2	FRAMEWORK and WINDPACK.....	116
7.2.1	Results Tables.....	116
7.2.2	Results Graphs.....	117
7.2.3	Summary and Discussion	122
7.3	FRAMEWORK and USFOS.....	123
7.3.1	Results Tables.....	123
7.3.2	Results Graphs.....	125
7.3.3	Summary and Discussion	147
8	Conclusions	149
8.1	Concluding Remarks	149
8.2	Further Work	152
9	References	153

List of figures

Figure 2-1: Wind loading of structures (Holmes, 2018).....	6
Figure 2-2: Typical wind speed over time (Holmes, 2018).....	6
Figure 2-3: Nominal stress concept (Dikshant Singh Saini, 2016).....	7
Figure 2-4: Notch stress concept for welded joints (C.M. Sonsino, 2012).....	8
Figure 2-5: Hot-spot stress concept for welded joints (Hobbacher, 2008).....	9
Figure 2-6: Typical spectral density diagram of wind energy (Hoven, 1957).....	10
Figure 2-7: Element stress history due to wind loading.....	11
Figure 2-8: Stress history diagram (Yung-Li Lee, 2012).....	11
Figure 2-9: Rain flow counting method (Yung-Li Lee, 2012).....	12
Figure 2-10: Stress concentration around a hole (Arthur P. Boresi, 2003).....	13
Figure 2-11: Brace and chord configuration (DNV RP-C203, 2019).....	14
Figure 2-12: Hot-spot locations in pipes (DNV RP-C203, 2019).....	14
Figure 2-13: SCF naming for tubular joints (Karlsson, 2018).....	15
Figure 2-14: S-N curve example (DNV RP-C203, 2019).....	17
Figure 3-1: Flare boom model in GeniE.....	20
Figure 3-2: Flare boom model showing elevation above LAT (lowest astronomical tide).....	21
Figure 3-3: Isometric view of the model showing critical points.....	22
Figure 3-4: Elevation view of the model showing critical points.....	23
Figure 3-5: Side view of the model showing critical points.....	24
Figure 3-6: Flare boom model showing point added masses.....	25
Figure 3-7: Platform orientation relative to global coordinates.....	26
Figure 3-8: Flare boom model showing support points.....	26
Figure 3-9: All-year wind rose.....	27
Figure 3-10: Wind profiles at different wind speeds.....	28
Figure 3-11: S-N curve for tubular joints (DNV RP-C203, 2019).....	30
Figure 3-12: Generation of Hot Spot Stress Spectrum (DNV - Framework User Manual, 2020).....	37
Figure 3-13: Typical Hot Spot Stress Spectrum (DNV - Framework User Manual, 2020).....	38
Figure 3-14: Scatter Diagram.....	39
Figure 3-15: Flowchart of WINDPACK modules run sequence.....	46
Figure 3-16: Location of saddle and crown as defined in WINDPACK.....	50
Figure 3-17: USFOS fatigue methodology, flow chart example.....	52
Figure 3-18: USFOS Model showing the rotation of the flare boom.....	53

Figure 3-19: Wind profile for simulating wind fields (AAS_JAKOBSEN - WindSim User manual, 2020).....	54
Figure 3-20: Frøya Spectrum for simulating fluctuating wind (AAS_JAKOBSEN - WindSim User manual, 2020).....	54
Figure 3-21: Wind grid	55
Figure 3-22: Axial stress history of element 243 end 1 example.....	57
Figure 4-1: Fatigue life against weight factor with 8 wind blocks for different Cd values (FRAMEWORK).....	60
Figure 4-2: Fatigue life against weight factor with 10 wind blocks for different Cd values (FRAMEWORK).....	61
Figure 4-3: Fatigue life against weight factor with 12 wind blocks for different Cd values (FRAMEWORK).....	61
Figure 4-4: Fatigue life against Drag coefficient with 8 wind blocks for different weight factor values (FRAMEWORK).....	62
Figure 4-5: Fatigue life against Drag coefficient with 10 wind blocks for different weight factor values (FRAMEWORK)	63
Figure 4-6 Fatigue life against Drag coefficient with 12 wind blocks for different weight factor values (FRAMEWORK)	63
Figure 4-7: Fatigue life against weight factor with Cd=0.65 for different wind block cases (FRAMEWORK).....	64
Figure 4-8: Fatigue life against weight factor with Cd=1.0 for different wind block cases (FRAMEWORK).....	65
Figure 4-9: Fatigue life against weight factor with Cd=1.2 for different wind block cases (FRAMEWORK).....	65
Figure 4-10: Fatigue life against weight factor with Reynold's dependent Cd for different wind block cases (FRAMEWORK).....	66
Figure 4-11: Fatigue life against Cd with weight factor 0.5 for different wind block cases (FRAMEWORK).....	67
Figure 4-12: Fatigue life against Cd with weight factor 1.0 for different wind block cases (FRAMEWORK).....	67
Figure 4-13: Fatigue life against Cd with weight factor 1.1 for different wind block cases (FRAMEWORK).....	68
Figure 4-14: Fatigue life against Cd with weight factor 1.5 for different wind block cases (FRAMEWORK).....	68
Figure 5-1: Fatigue life against weight factor with 8 wind blocks for different Cd values (WINDPACK)	72

Figure 5-2: Fatigue life against weight factor with 10 wind blocks for different Cd values (WINDPACK)	73
Figure 5-3: Fatigue life against weight factor with 12 wind blocks for different Cd values (WINDPACK)	73
Figure 5-4: Fatigue life against Drag coefficient with 8 wind blocks for different weight factor values (WINDPACK)	74
Figure 5-5: Fatigue life against Drag coefficient with 10 wind blocks for different weight factor values (WINDPACK)	75
Figure 5-6: Fatigue life against Drag coefficient with 12 wind blocks for different weight factor values (WINDPACK)	75
Figure 5-7: Fatigue life against weight factor with Cd=0.65 for different wind block cases (WINDPACK)	76
Figure 5-8: Fatigue life against weight factor with Cd=1.0 for different wind block cases (WINDPACK)	77
Figure 5-9: Fatigue life against weight factor with Cd=1.2 for different wind block cases (WINDPACK)	77
Figure 5-10: Fatigue life against Cd with weight factor 0.5 for different wind block cases (WINDPACK)	78
Figure 5-11: Fatigue life against Cd with weight factor 1.0 for different wind block cases (WINDPACK)	79
Figure 5-12: Fatigue life against Cd with weight factor 1.1 for different wind block cases (WINDPACK)	79
Figure 5-13: Fatigue life against Cd with weight factor 1.5 for different wind block cases (WINDPACK)	80
Figure 6-1: Fatigue life against weight factor with dt=0.10 and 8 wind blocks for different Cd values	85
Figure 6-2: Fatigue life against weight factor with dt=0.10 and 10 wind blocks for different Cd values.....	85
Figure 6-3: Fatigue life against weight factor with dt=0.10 and 12 wind blocks for different Cd values.....	86
Figure 6-4: Fatigue life against weight factor with dt=0.10 and 16 wind blocks for different Cd values.....	86
Figure 6-5: Fatigue life against Cd with dt=0.10 and 8 wind blocks for different weight factors.....	87
Figure 6-6: Fatigue life against Cd with dt=0.10 and 10 wind blocks for different weight factors.....	88
Figure 6-7: Fatigue life against Cd with dt=0.10 and 12 wind blocks for different weight factors.....	88

Figure 6-8: Fatigue life against Cd with dt=0.10 and 16 wind blocks for different weight factors.....	89
Figure 6-9: Fatigue life against weight factor with dt=0.10 and Cd=0.65 for different wind block cases	90
Figure 6-10: Fatigue life against weight factor with dt=0.10 and Cd=0.10 for different wind block cases	90
Figure 6-11: Fatigue life against weight factor with dt=0.10 and Cd=1.2 for different wind block cases	91
Figure 6-12: Fatigue life against weight factor with dt=0.10 and Reynold's dependent Cd for different wind block cases.....	91
Figure 6-13: Fatigue life against Cd with dt=0.10 and weight factor 0.5 for different wind block cases	92
Figure 6-14: Fatigue life against Cd with dt=0.10 and weight factor 1.0 for different wind block cases	93
Figure 6-15: Fatigue life against Cd with dt=0.10 and weight factor 1.1 for different wind block cases	93
Figure 6-16: Fatigue life against Cd with dt=0.10 and weight factor 1.5 for different wind block cases	94
Figure 6-17: Fatigue life against weight factor with dt=0.05 and 8 wind blocks for different Cd values.....	98
Figure 6-18: Fatigue life against weight factor with dt=0.05 and 10 wind blocks for different Cd values.....	98
Figure 6-19: Fatigue life against weight factor with dt=0.05 and 12 wind blocks for different Cd values.....	99
Figure 6-20: Fatigue life against weight factor with dt=0.05 and 16 wind blocks for different Cd values.....	99
Figure 6-21: Fatigue life against Cd with dt=0.05 and 8 wind blocks for different weight factors.....	100
Figure 6-22: Fatigue life against Cd with dt=0.05 and 10 wind blocks for different weight factors.....	101
Figure 6-23: Fatigue life against Cd with dt=0.05 and 12 wind blocks for different weight factors.....	101
Figure 6-24: Fatigue life against Cd with dt=0.05 and 16 wind blocks for different weight factors.....	102
Figure 6-25: Fatigue life against weight factor with dt=0.05 and Cd=0.65 for different wind block cases	103

Figure 6-26: Fatigue life against weight factor with $dt=0.05$ and $Cd=1.0$ for different wind block cases	103
Figure 6-27: Fatigue life against weight factor with $dt=0.05$ and $Cd=1.2$ for different wind block cases	104
Figure 6-28: Fatigue life against weight factor with $dt=0.05$ and Reynold's dependent Cd for different wind block cases.....	104
Figure 6-29: Fatigue life against Cd with $dt=0.05$ and weight factor 0.5 for different wind block cases	105
Figure 6-30: Fatigue life against Cd with $dt=0.05$ and weight factor 1.0 for different wind block cases	106
Figure 6-31: Fatigue life against Cd with $dt=0.05$ and weight factor 1.1 for different wind block cases	106
Figure 6-32: Fatigue life against Cd with $dt=0.05$ and weight factor 1.5 for different wind block cases	107
Figure 6-33: Axial stress time history in element 243 from load case 192, with weight factor 0.5.....	108
Figure 6-34: Axial stress time history in element 243 from load case 192, with no weight factor	109
Figure 6-35: Axial stress time history in element 243 from 16 wind blocks' load case 192, with $Cd=0.65$	110
Figure 6-36: Axial stress time history in element 243 from 16 wind blocks' load case 192, with $Cd=1.0$	110
Figure 6-37: Fatigue life against weight factor for all cases of Cd of both $dt=0.05$ and $dt=0.10$	112
Figure 7-1: Fatigue life against weight factor with $Cd=0.65$ for different wind block cases in FRAMEWORK and WINDPACK	118
Figure 7-2: Fatigue life against weight factor with $Cd=1.0$ for different wind block cases in FRAMEWORK and WINDPACK	118
Figure 7-3: Fatigue life against weight factor with $Cd=1.2$ for different wind block cases in FRAMEWORK and WINDPACK	119
Figure 7-4: Fatigue life against Cd with weight factor 0.5 for all wind block cases in FRAMEWORK and WINDPACK	120
Figure 7-5: Fatigue life against Cd with weight factor 1.0 for all wind block cases in FRAMEWORK and WINDPACK	120
Figure 7-6: Fatigue life against Cd with weight factor 1.1 for all wind block cases in FRAMEWORK and WINDPACK	121
Figure 7-7: Fatigue life against Cd with weight factor 1.5 for all wind block cases in FRAMEWORK and WINDPACK	121

Figure 7-8: Fatigue life against weight factor with Cd=0.65 and 8 wind blocks for USFOS and FRAMEWORK.....	126
Figure 7-9: Fatigue life against weight factor with Cd=0.65 and 10 wind blocks for USFOS and FRAMEWORK.....	126
Figure 7-10: Fatigue life against weight factor with Cd=0.65 and 12 wind blocks for USFOS and FRAMEWORK.....	127
Figure 7-11: Fatigue life against weight factor with Cd=0.65 for all wind block cases in USFOS and FRAMEWORK	127
Figure 7-12: Fatigue life against weight factor with Cd=1.0 and 8 wind blocks for USFOS and FRAMEWORK.....	128
Figure 7-13: Fatigue life against weight factor with Cd=1.0 and 10 wind blocks for USFOS and FRAMEWORK.....	129
Figure 7-14: Fatigue life against weight factor with Cd=1.0 and 12 wind blocks for USFOS and FRAMEWORK.....	129
Figure 7-15: Fatigue life against weight factor with Cd=1.0 for all wind block cases in USFOS and FRAMEWORK	130
Figure 7-16: Fatigue life against weight factor with Cd=1.2 and 8 wind blocks for USFOS and FRAMEWORK.....	131
Figure 7-17: Fatigue life against weight factor with Cd=1.2 and 10 wind blocks for USFOS and FRAMEWORK.....	131
Figure 7-18: Fatigue life against weight factor with Cd=1.2 and 12 wind blocks for USFOS and FRAMEWORK.....	132
Figure 7-19: Fatigue life against weight factor with Cd=1.2 for all wind block cases in USFOS and FRAMEWORK	132
Figure 7-20: Fatigue life against weight factor with Reynold’s number dependent Cd and 8 wind blocks for USFOS and FRAMEWORK	133
Figure 7-21: Fatigue life against weight factor with Reynold’s number dependent Cd and 10 wind blocks for USFOS and FRAMEWORK	134
Figure 7-22: Fatigue life against weight factor with Reynold’s number dependent Cd and 12 wind blocks for USFOS and FRAMEWORK	134
Figure 7-23: Fatigue life against weight factor with Reynold’s number dependent Cd for all wind block cases in USFOS and FRAMEWORK.....	135
Figure 7-24: Fatigue life against Cd with weight factor 0.5 and 8 wind blocks for USFOS and FRAMEWORK.....	136
Figure 7-25: Fatigue life against Cd with weight factor 0.5 and 10 wind blocks for USFOS and FRAMEWORK.....	136

Figure 7-26: Fatigue life against Cd with weight factor 0.5 and 12 wind blocks for USFOS and FRAMEWORK.....	137
Figure 7-27: Fatigue life against Cd with weight factor 0.5 for all wind block cases in USFOS and FRAMEWORK.....	137
Figure 7-28: Fatigue life against Cd with weight factor 1.0 and 8 wind blocks for USFOS and FRAMEWORK.....	138
Figure 7-29: Fatigue life against Cd with weight factor 1.0 and 10 wind blocks for USFOS and FRAMEWORK.....	139
Figure 7-30: Fatigue life against Cd with weight factor 1.0 and 12 wind blocks for USFOS and FRAMEWORK.....	139
Figure 7-31: Fatigue life against Cd with weight factor 1.0 for all wind block cases in USFOS and FRAMEWORK.....	140
Figure 7-32: Fatigue life against Cd with weight factor 1.1 and 8 wind blocks for USFOS and FRAMEWORK.....	141
Figure 7-33: Fatigue life against Cd with weight factor 1.1 and 10 wind blocks for USFOS and FRAMEWORK.....	142
Figure 7-34: Fatigue life against Cd with weight factor 1.1 and 12 wind blocks for USFOS and FRAMEWORK.....	142
Figure 7-35: Fatigue life against Cd with weight factor 1.1 for all wind block cases in USFOS and FRAMEWORK.....	143
Figure 7-36: Fatigue life against Cd with weight factor 1.5 and 8 wind blocks for USFOS and FRAMEWORK.....	144
Figure 7-37: Fatigue life against Cd with weight factor 1.5 and 10 wind blocks for USFOS and FRAMEWORK.....	145
Figure 7-38: Fatigue life against Cd with weight factor 1.5 and 12 wind blocks for USFOS and FRAMEWORK.....	145
Figure 7-39: Fatigue life against Cd with weight factor 1.5 for all wind block cases in USFOS and FRAMEWORK.....	146

List of tables

Table 2-1: DNV S-N curve for tubular joints (DNV RP-C203, 2019).....	17
Table 3-1: Material properties of tubular members	25
Table 3-2: Scatter diagram provided by Metocean data	29
Table 3-3: S-N curve for tubular joints (DNV RP-C203, 2019).....	30
Table 3-4: Scatter diagram of 16 wind blocks	32
Table 3-5: Scatter diagram of 8 wind blocks	32
Table 3-6: Scatter diagram of 12 wind blocks	33
Table 3-7: Scatter diagram of 10 wind blocks	33
Table 3-8: Critical fatigue life for different time increments for cases with 8 wind-blocks and Cd = 1.0.....	35
Table 3-9: SCFs for WINDPACK and FRAMEWORK	36
Table 3-10: Eigen values and eigen frequency with no weight factor.....	43
Table 3-11: 8 wind blocks scatter diagram	43
Table 3-12: Scatter diagram of 8 wind blocks showing the input in WINDPACK.....	48
Table 4-1: All results with 8 wind blocks in FRAMEWORK.....	58
Table 4-2: All results with 10 wind blocks in FRAMEWORK.....	59
Table 4-3: All results with 12 wind blocks in FRAMEWORK.....	59
Table 5-1: All results with 8 wind blocks in WINDPACK	70
Table 5-2: All results with 10 wind blocks in WINDPACK	71
Table 5-3: All results with 12 wind blocks in WINDPACK	71
Table 6-1: All results with 8 wind blocks in USFOS with dt=0.10.....	82
Table 6-2: All results with 10 wind blocks in USFOS with dt=0.10.....	83
Table 6-3 All results with 12 wind blocks in USFOS with dt=0.10.....	83
Table 6-4: All results with 16 wind blocks in USFOS with dt=0.10.....	84
Table 6-5: All results with 8 wind blocks in USFOS with dt=0.05	95
Table 6-6: All results with 10 wind blocks in USFOS with dt=0.05	96
Table 6-7: All results with 12 wind blocks in USFOS with dt=0.05	96
Table 6-8: All results with 16 wind blocks in USFOS with dt=0.05	97
Table 6-9: Cases with and without the effect of relative velocity	112
Table 7-1: Critical fatigue life for all cases of 8 and 10 wind blocks in USFOS and FRAMEWORK.....	114
Table 7-2: Critical fatigue life for all cases of 12 and 16 wind blocks in FRAMEWORK, WINDPACK and USFOS.....	115
Table 7-3: Critical fatigue life for all comparable cases of 8 wind blocks in FRAMEWORK and WINDPACK	116
Table 7-4: Critical fatigue life for all comparable cases of 10 wind blocks in FRAMEWORK and WINDPACK	117

Table 7-5: Critical fatigue life for all comparable cases of 12 wind blocks in FRAMEWORK and WINDPACK 117

Table 7-6: SCFs for WINDPACK and FRAMEWORK 122

Table 7-7: Critical fatigue life for all comparable cases of 8 wind blocks in FRAMEWORK and USFOS 124

Table 7-8: Critical fatigue life for all comparable cases of 10 wind blocks in FRAMEWORK and USFOS 124

Table 7-9: Critical fatigue life for all comparable cases of 12 wind blocks in FRAMEWORK and USFOS 125

1 Introduction

1.1 Background

Due to the dynamic nature of wind, wind loads are categorized in two categories: mean wind loading coming from mean wind speed (U_{10}), which is used to design for ultimate limit state (ULS), and fatigue loading due to turbulence, which is used to design for fatigue limit state (FLS).

The dynamic loading of the wind causes structural vibrations. Such vibrations produce fluctuating stresses which cause accumulation of fatigue damage and can lead to structural failure. Relying solely on Ultimate Limit State (ULS) in slender structures has proven inadequate as fatigue damage takes place at significantly lower stresses than the material's yield strength. Fatigue Limit State (FLS) is then used to account for high frequency dynamic loads that take place below the yielding resistance of a material.

In slender structures such as flare booms, wind-induced fatigue is usually the governing design basis. This is attributed to the significant effect of fatigue on the life of the subjected elements. Flare booms consist mainly of tubular members which give high stress concentrations at the joints where fatigue cracks usually take place. Complex slender structures such as flare booms may yield inaccurate estimation of fatigue life, with poor FEM modelling.

Fatigue life of a structure is known to be sensitive not only to the stress amplitude but also to the structural modelling and load variation. A reliable calculation method is then required to estimate the fatigue life.

Different types of software have been used in the industry to estimate fatigue life of offshore slender structures using two different approaches, the first of which is time domain nonlinear dynamic analysis and the second is the power spectral density approach.

1.2 Problem Statement

The time domain dynamic analysis relies on stress cycle counting using the rain flow method. Stress histories are generated from the structure's response to simulated wind fields in a nonlinear full dynamic time history analysis. This approach is arguably more accurate in estimating fatigue damage as it takes the nonlinear load effects into account as well as large deformation. However, it is computationally expensive. Power spectral density method is generally simpler, requires less input data, time efficient and depends on frequency domain analysis. However, the fatigue damage estimation in the latter case might be inaccurate as the frequency domain analysis does not consider large deformations caused by nonlinear load effects.

USFOS uses the nonlinear dynamic analysis approach, which gives fatigue stress cycles in time domain. It is then followed by cycle counting using the rain flow method in FATAL to estimate the fatigue life of a flare boom model (Flare 1).

Using the power spectral density approach, DNV SESAM FRAMEWORK and WINDPACK are used to estimate the fatigue life of the same flare boom.

Although the three software has been used to estimate fatigue life of slender structures for many years, a detailed parametric comparison between both software and the estimated fatigue life is yet to be performed.

1.3 Objectives

The main objective of this thesis is to make a comparison between different software results using the same structural model and parameter input. Sensitivity to different parameter changes will also be compared between the different software. Analyses will be performed using the module of an existing flare boom “Flare 1” in DNV SESAM FRAMEWORK and USFOS (with FATAL), and Aker Solution’s in-house program WINDPACK.

The parameters set to be:

- The number of wind blocks used.
- Drag coefficient (Cd).
- Weight factor.
- Relative velocity contribution in USFOS

Time increment in USFOS is also considered as a variable during analysis and is represented as a variable in the comparisons and results to test the effect of a different time increments. However, it is not considered a parameter as it is a case dependent variable.

Stress concentration factors are another factor that might be considered as a parameter. However, in this thesis, stress concentration factors are calculated using Efthymiou theory. The same SCFs are used to run analyses in FRAMEWORK and USFOS, while WINDPACK SCFs differ slightly.

1.4 Limitations

This thesis focuses only on comparing the results between the three software which are based on the two methods. Due to USFOS’ limitations, the effect of vortex-induced vibrations is not included. Such effects should be checked for separately.

The thesis runs only on one flare boom module (Flare 1). 16 wind fields are extracted from Met Ocean report at the location of interest.

FRAMEWORK is limited to read only 12 wind blocks. Therefore, the 16 wind blocks cases are carried out only in USFOS.

1.5 Thesis Outline

1 Chapter 1: Introduction

This chapter provides an overview of the theoretical methods and software used in the thesis. It also presents the main objectives, limitations, and an outline.

2 Chapter 2: Literature Review on Wind-induced Fatigue

This chapter briefly explains the theory behind wind-induced fatigue by reviewing existing literature from different reports on fatigue assessment approaches and the design methods used in the different software.

3 Chapter 3: Model and Methodology of FRAMEWORK, WINDPACK and USFOS

In this chapter, the model used is presented with the required information on the structural properties, geometry, and wind data. Parameters used and a theoretical background on FRAMEWORK, WINDPACK and USFOS are presented as well.

4 Chapter 4: Wind-induced Fatigue Analysis Using FRAMEWORK

This chapter presents results and findings of fatigue life estimation using spectral density approach in FRAMEWORK. It also includes a summary and discussion on the findings.

5 Chapter 5: Wind-induced Fatigue Analysis using WINDPACK

Results and findings of fatigue life calculation using spectral method approach is performed again using WINDPACK. Summary and discussion on the findings are also included.

6 Chapter 6: Wind-induced Fatigue Analysis using USFOS

In this chapter, results and findings of running time domain dynamic nonlinear analysis using USFOS. Summary and discussion on the findings are also included.

7 Chapter 7: Comparisons and Discussions

In this chapter, comparisons are made between the results of the used software. In addition, it discusses the main findings.

8 Chapter 8: Conclusions

This chapter presents the conclusions drawn from the results and findings presented in previous chapters. Furthermore, it provides recommendations for further studies.

2 Literature Review on Wind-induced Fatigue

This chapter briefly explains the theory behind wind-induced fatigue by reviewing existing literature from different reports on fatigue assessment approaches and the design methods used in the different software.

2.1 Wind-induced Fatigue on Slender Structures

Slender structures that are exposed to wind, may also be exposed to wind induced fatigue damage. Based on the structure's dynamic properties, it may vibrate due to wind excited forces. Fluctuating stresses even within the material's yield strength can cause localized micro plastic deformations (such as cracks), and over many cycles of stress may cause a structure to fail. This can happen even if the structure never experiences stresses over the ultimate limit or material's yield strength.

Variations in stress is directly related to the variation of wind speed, which varies with height above sea level and time.

The parameters are defined in (DNV RP-C205, 2019) as follows:

- 1 10-minute mean wind speed (U_{10}) at height 10 m above sea water level is used to express the intensity of the wind, while the standard deviation (σ_U) of the wind speed at the same height is used to express the variation in the wind. Mean wind speed may also be expressed based on an hourly average such as in the Frøya wind profile.
- 2 Turbulence intensity factor to express the turbulence in the wind. It is defined as the ratio σ_U / U_{10}

The short-term wind can be represented by a spectrum. This spectrum is referred to as power spectral density of the wind speed $S_U(f)$. Power spectral density is a function of both mean wind speed U_{10} and the standard deviation σ_U .

Due to the previously mentioned parameters, wind loads are divided into two components. One component expresses the loads coming from mean wind speed. The second component expresses the turbulence in the wind.

(DNV RP-C205, 2019) expresses the fluctuating wind force as follows:

$$F_W = \frac{1}{2} \rho_a C_D S |U_{T,z} + \mathbf{u} - \dot{\mathbf{x}}| (U_{T,z} + \mathbf{u} - \dot{\mathbf{x}}) \quad (2-1)$$

Where:

ρ_a = air density (kg/m^3)

C_D = drag coefficient

$\dot{\mathbf{x}}$ = member velocity

$U_{T,z}$ = mean wind speed at the height z and period T

2.2 Wind Turbulence and Gust

2.2.1 Wind Turbulence

Due to the fluctuating nature of wind, it is common to divide wind characteristics into mean wind and wind turbulence. Wind turbulence represents the fluctuations in the wind. These fluctuations are a result of two main reasons: frictional force and thermal gradients. The former is the product of friction that takes place between the flowing air and the surface of the earth. The latter causes air to move upward and downward rapidly. (Craig MacEachern, 2018)

Statistical approaches are normally used to represent the turbulence in the wind as it is impossible to represent turbulence using deterministic equations.

The 10-minute mean wind speed (U_{10}) is used to measure turbulence and is characterized by the standard deviation (σ_U) as stated in (DNV RP-C205, 2019). Turbulence intensity is a characteristic used to represent turbulence. As stated previously, it is defined as the ratio σ_U / U_{10} . Measurements also show that log normal distribution can be used to represent the relation between the standard deviation (σ_U) and mean wind speed (U_{10}).

Another characteristic that is used to represent turbulence is probability density function. Since the variations in the wind are caused by vortices and eddies within the air flow, these variations are unique and never identical. Using statistical methods, a Gaussian probability density function can then be used to represent the wind velocity components.

The third characteristic that describes wind turbulence is wind gust, which is the main contributor to wind-induced fatigue as explained below.

2.2.2 Wind Gust

As per (DNV RP-C205, 2019), Gust is defined as an abrupt increase in wind speed during a period less than 20 seconds, followed by a decrease in wind speed. Main characteristics of gusts are the rise time, magnitude, and duration.

Gusts occur due to natural fluctuations in wind speed within the 10-minute period of stationary wind conditions without affecting the mean wind speed.

Gusts are essential for fatigue design process as they are accounted for in the dynamic analysis. At any arbitrary point in time resonant response can be triggered by gust excitation close to natural frequency of the structural element.

The gust factor is the ratio of the highest peak wind gust over a certain period to the mean wind speed over the same period. Gust factors are governed by upstream conditions (water surface condition in this case), height above mean water level, and atmospheric stability.

Gust factor can be obtained through the following equation

$$G = \frac{\bar{U} + \sigma_U}{\bar{U}} = 1 + g \cdot I_U \quad (2-2)$$

Where:

\bar{U} is the mean wind speed

σ_U is the standard deviation

I_U is the turbulence intensity factor

Averaging time, τ (s)	Sample time, T (s)	g
3	3600	3.0
3	600	2.5
1	3600	3.4
1	600	2.9
0.2	3600	3.8
0.2	600	3.4

Figure 2-1: Wind loading of structures (Holmes, 2018)

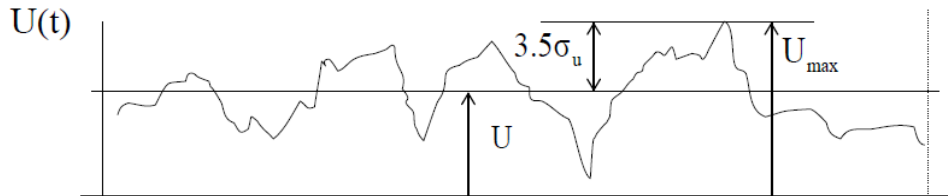


Figure 2-2: Typical wind speed over time (Holmes, 2018)

For maritime conditions and offshore locations, as stated by (DNV RP-C205, 2019) the Frøya wind speed profile is the best documented wind speed profile. This is attributed to the inclusion of the gust factor that helps convert between mean wind speeds at different averaging time periods.

The effect of wind gust is considered in the Frøya wind profile for offshore locations in (DNV RP-C205, 2019) as shown below:

$$U(T, z) = U_0 \cdot \left\{ 1 + C \cdot \ln \frac{z}{H} \right\} \cdot \left\{ 1 - 0.41 \cdot I_U(z) \ln \frac{T}{T_0} \right\} \quad (2-3)$$

Where:

$$H = 10\text{m}$$

$$T_0 = 1 \text{ hr}, T < T_0$$

$$C = 5.73 \cdot 10^{-2} \sqrt{1 + 0.148 U_0}$$

$$I_U = 0.06 \cdot (1 + 0.043 U_0) \cdot \left(\frac{z}{H} \right)^{-0.22}$$

2.3 Fatigue Assessment Methods

Welding is the most common practice of joining steel elements for offshore purposes. Welded joints in fatigue-prone steel structures are considered the most typical locations of crack initiation due to stress concentration, leading to fatigue fracture. This leads to the need for fatigue assessment during phases of design and maintenance. (Dikshant Singh Saini, 2016)

Fatigue assessment methods can be classified based on: Damage variable, damage criterion and stress analysis (S-N curves).

Due to the reasons mentioned above, fatigue assessment based on stress analysis is of more relevance for this thesis.

Fatigue assessment based on stress analysis (S-N curves) can be categorized in the 3 main approaches briefly explained below.

2.3.1 Nominal Stress Approach

This approach uses classical structural mechanics with applying linear elastic theory. It is based on the average global stress in the cross-section, while neglecting the stress concentration that comes from local effects.

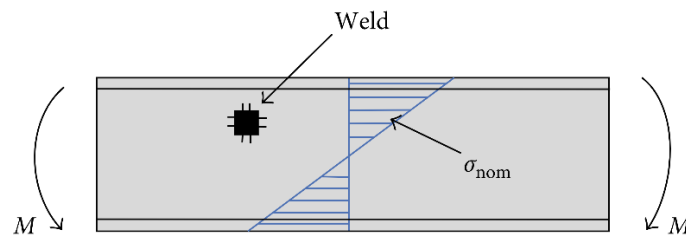


Figure 2-3: Nominal stress concept (Dikshant Singh Saini, 2016)

This method takes into consideration the geometrical changes which impacts stress distribution, however.

Local effects are accounted for in S-N curves through using category of details in standards such as Eurocode or (DNV RP-C203, 2019).

This approach is the most widely used, but it is not suitable for complex geometries where local effects strongly affect stress variation.

2.3.2 Notch Stress Approach

The linear-elastic notch stress approach has gained significant industrial recognition among fatigue design concepts. The primary idea behind this method is to simulate a weld root or toe with a notch of a reference radius, usually $r_{ref} = 0.1\text{mm}$ for thick-walled members ($t > 5\text{mm}$) or $r_{ref} = 0.05\text{mm}$ for thin-walled members ($t < 5\text{mm}$). As stated in (C.M. Sonsino, 2012), assuming linear elastic behavior of the material, the total stress in the weld root is known as effective notch stress.

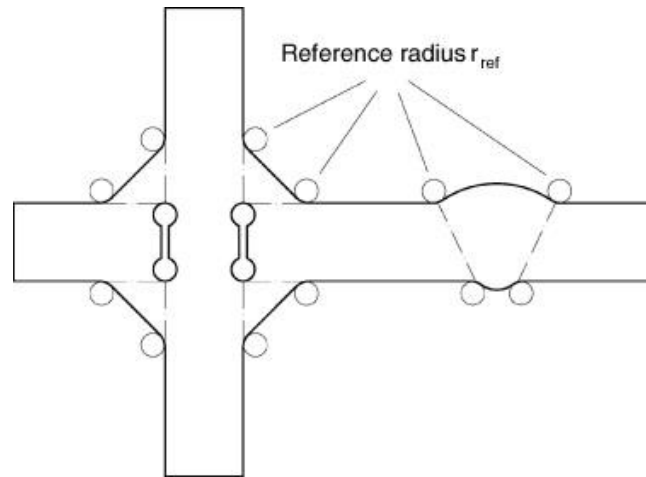


Figure 2-4: Notch stress concept for welded joints (C.M. Sonsino, 2012)

Due to material imperfections and notches in welded connections, local stress concentrations may become significant. Depending on the notch radius or sharpness, the weld stress (toe or root) might be extremely high.

Notch stress fatigue assessment resembles the approach of the nominal stress in theory, with considering local notch stress instead of global stress. Element fatigue resistance can then be represented by S-N curve when local stress is calculated on the crack initiation point. Assessment procedure is used by comparing effective fatigue stress amplitude to the corresponding stress resistance S-N curve.

It should be noted that fatigue strength calculated using this approach is based on perfectly performed samples. Any change in weld shape or material imperfection might affect the resulted fatigue life significantly.

2.3.3 Hot-Spot Stress Approach

Hot spot stress approach considers all the stresses coming to a weld connection except stresses coming from the weld geometry itself. Therefore, local stresses at weld toe or root are excluded from the stress calculations. In this case, the governing parameters in calculation of stress are the global dimensions of the component and the loading case. Hot spot stress approach is used to obtain fatigue crack initiation sites for more complicated geometries where nominal stress is difficult to be obtained. (Hobbacher, 2008)

Hot spot stress approach is suitable for all types of elements. However, in this thesis, hot spot stress on tubular structures is more relevant. It is also worth noting that stress concentration factors and the corresponding S-N curves depend heavily on the geometry and dimensions of different elements.

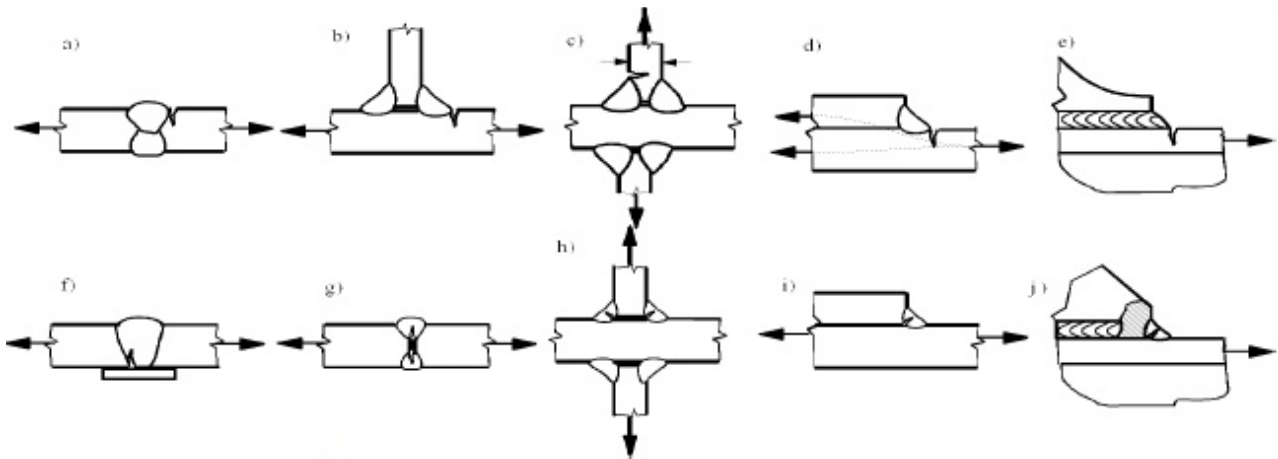


Figure 2-5: Hot-spot stress concept for welded joints (Hobbacher, 2008)

For tubular joints, it is a common practice to use linear extrapolation from simple uniaxial stress calculated at two reference points. Using the stress concentration factor k_{hs} (referred to as SCF), the structural hot spot stress can be correlated to the nominal stress as follows:

$$\sigma_{hs} = k_{hs} \cdot \sigma_{nom} \quad (2-4)$$

Where, σ_{nom} is the nominal axial or bending stress calculated by elementary stress analysis.

Finite element method is used to analytically determine stress concentration factors and hot spot stress, assuming linear elastic material behavior.

It should be noted that the extrapolation method mentioned above gives inconsistent results in some cases. Due to the nonlinearity in the local stresses forming at a notch (weld toe), hot spot stresses depend heavily on the finite element model and the mesh size used.

2.4 Power Spectral Density Method for Fatigue Analysis

In general, power spectral density (PSD) is a method used to measure the content of power in a signal against frequency. It is typically used to represent the distribution of random broadband signals, which are difficult to work with in time domain. PSD represents the proportion contributed of the total power at each frequency.

Due to the stochastic random nature of wind data, it is more convenient to transform the data from time domain to frequency domain using Fast Fourier Transform (FFT). Power Spectral Density (PSD) is then formed. PSD indicates the average power in different frequencies and is usually expressed in radians or hertz.

In case the wind frequency reaches a frequency close to the natural frequency of the component, buffeting will be critical and fatigue stresses are higher. PSD illustrates that by plotting the natural frequency of the indicated element against the wind data.

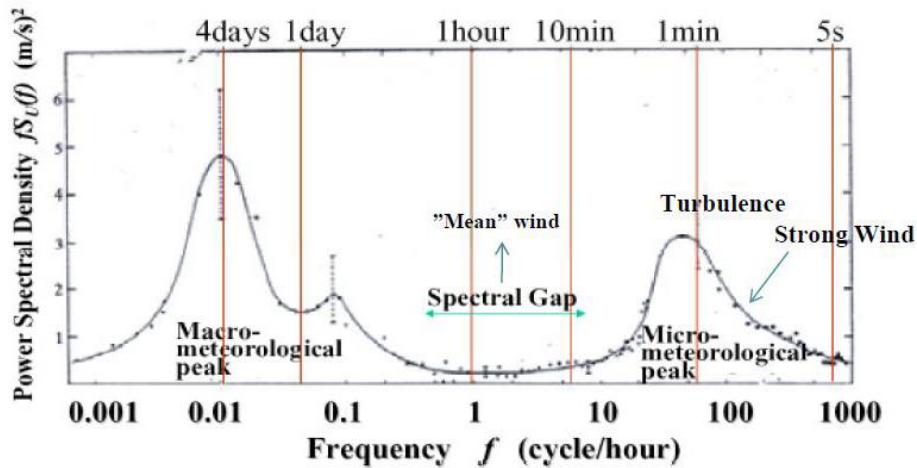


Figure 2-6: Typical spectral density diagram of wind energy (Hoven, 1957)

(DNV RP-C205, 2019) introduces many site-specific wind spectral density formulas such as Davenport, Harris, Frøya, etc. Large differences can be seen in the low frequency range between each spectrum. Among the different spectra introduced, the best suited spectra for offshore structures are the empirical Simiu and Leigh spectrum, Ochi and Shin spectrum, and Frøya model spectral density. The latter is used in DNV SESAM FRAMEWORK as it is the best suited for low-frequency excitation range. Frøya spectrum is also based on neutral conditions over the Norwegian Sea.

Frøya spectral density is represented in (DNV RP-C205, 2019) by the equation:

$$S_U(f) = 320 \cdot \frac{\left(\frac{U_0}{10}\right)^2 \left(\frac{z}{10}\right)^{0.45}}{(1 + \tilde{f}^n)^{5/3n}} \quad (2-5)$$

where:

$$\tilde{f} = 172 \cdot f \cdot \left(\frac{z}{10}\right)^{2/3} \cdot \left(\frac{U_0}{10}\right)^{-0.75} \quad (2-6)$$

$n = 0.468$

U_0 is the hourly mean wind speed at height 10m in m/s

z is the height above sea water level in m.

2.5 Time Domain Fatigue Analysis Method and Rain Flow Counting

It is known that fatigue analysis from spectral method could be very conservative when compared to tested samples. Therefore, more effort has been shifted to time domain method to test for more reliable results.

(A. Naess, 2013) state in their report that time domain fatigue analysis is more accurate than spectral method. However, different standards still rely on spectral method as it is computationally less demanding. On a side note, standards recommend analyzing fatigue using time domain method, when nonlinear analysis is required.

In the time domain method, a structure or structure part is subjected to a stress signal, often done with finite element analysis. A time history graph is then derived of the structure's stress/strain response over a finite amount of time, coming from a dynamic loading which often is irregular in nature. The material loads and unloads repetitively and randomly to form a random stress cycle against time.

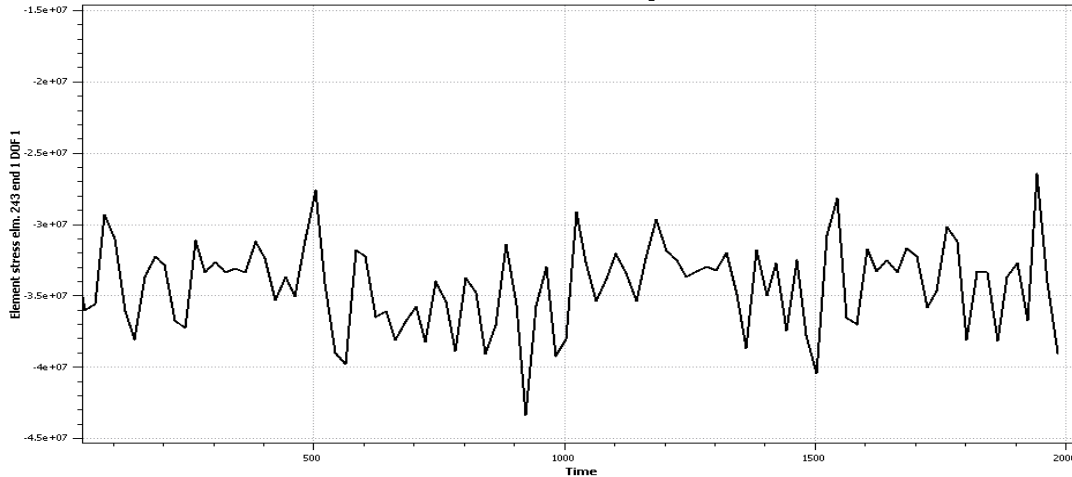


Figure 2-7: Element stress history due to wind loading

2.5.1 Rain Flow Counting Method

Rain flow cycle counting method was initially used to count the cycles stress/strain-time signals. Counting is based on the stress-strain behavior of the material under the elastic behavior range.

Due to the random nature of stress cycles, it is difficult to determine the number of cycles during a certain period. The irregular stress data is translated into several stress ranges with constant amplitude to simplify the data, with the assumption that the impact of each individual stress loop is the same as the impact of a constant amplitude stress loop with equal magnitude. (C.H. McInnes, 2008)



Figure 2-8: Stress history diagram (Yung-Li Lee, 2012)

The signal should first be rotated 90 degrees as shown below. Then a line is drawn from the largest reversal in the same nature as the flow of rain on a rooftop. Further every reversal is included making lines either till “end of flow” or till another line is met. (Yung-Li Lee, 2012)

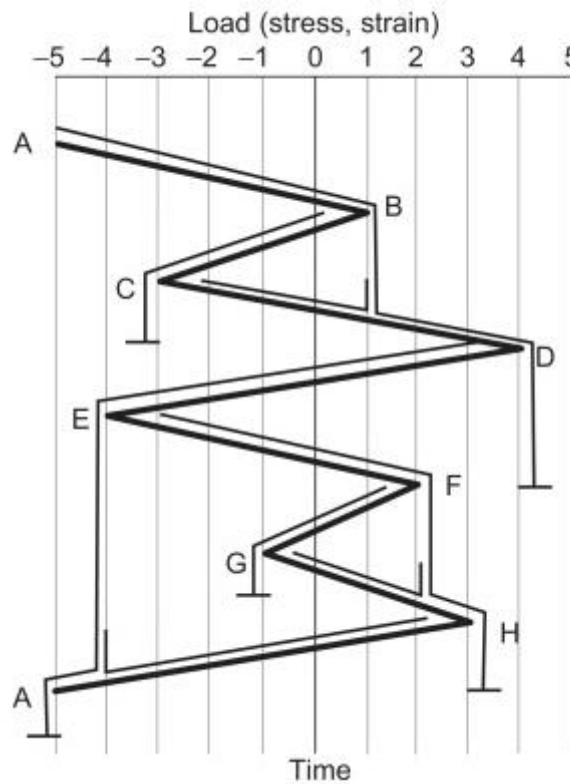


Figure 2-9: Rain flow counting method (Yung-Li Lee, 2012)

Each reversal is then translated into stress ranges (meaning difference from maximum to minimum stress for the current reversal). In the above example point A-D varies from -5 to 4, which then equals a stress range of 9, and that reversal accounts for half a cycle. Reversals with the same range is then added together with number of cycles.

The time history/ rain flow counting method also assumes that the stress signal experienced within a finite period can be scaled to account for the stress signal a structural part experience during its whole lifetime.

2.6 Stress Concentration

In simple structures stresses are determined with the assumption that stress is distributed evenly over the cross section and can be calculated with relatively simple mathematical equations. In a lot of cases, this approach will greatly underestimate the real stress distribution in a member, because uneven shapes or irregularities in design will not distribute stress linearly. The phenomenon is called stress concentration, and may be caused by abrupt changes, contact stresses, discontinuities, initial stresses from fabrication or cracks. (Arthur P. Boresi, 2003)

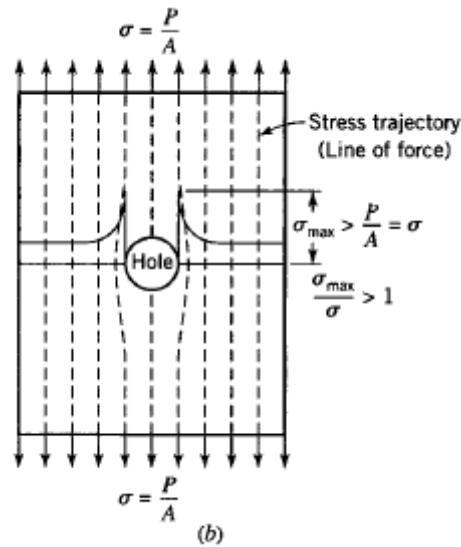


Figure 2-10: Stress concentration around a hole (Arthur P. Boresi, 2003)

As **Figure 2-10** shows, stress distributes evenly, but close to the “crack”, there is significant increase in stress. As mentioned, fatigue is the process of micro plastic deformities propagating with cyclic loading, so stress concentration plays a critical role in this process. The amount a deformity grows from each cycle is directly related to the amount of stress it is subjected to. Stress concentration is expressed in (Arthur P. Boresi, 2003) with the following formula:

$$S_c = \frac{\sigma_{\max}}{\sigma_n} \quad (2-7)$$

Where:

S_c = Stress concentration factor

σ_{\max} = Stress at concentration or critical point to be used in fatigue assessment

σ_n = Nominal stress in member

For fatigue assessment, the effect of stress concentrations must be considered for accurate reliable results. The stress concentration factor is associated to the specific part’s loading and geometry and can be derived either through experimental, analytical, or computational methods.

2.6.1 Hot-spot Stress Method in Welded Pipes

The stress concentration factors (SCFs) are derived based on the joint geometry and the chosen parametric equations. There have been proposed numerous parametric equations over the last 50 years by researchers for determining the right hot spot stresses, with different approaches for determining the stress concentration factors. This thesis uses the equations proposed by Efthymiou in the software analyses.

Stress concentration factors (SCF) in welded pipes are calculated in the joints of chords and braces, with the chord being the pipe with the greater diameter. The hot spot stresses that are used are derived from summation of axial forces, in-plane and out of plane bending multiplied by the respective SCFs

that are presented in the braces. The hot spot stress affects both the brace and the chord and with different concentrations around the cross section of the brace.

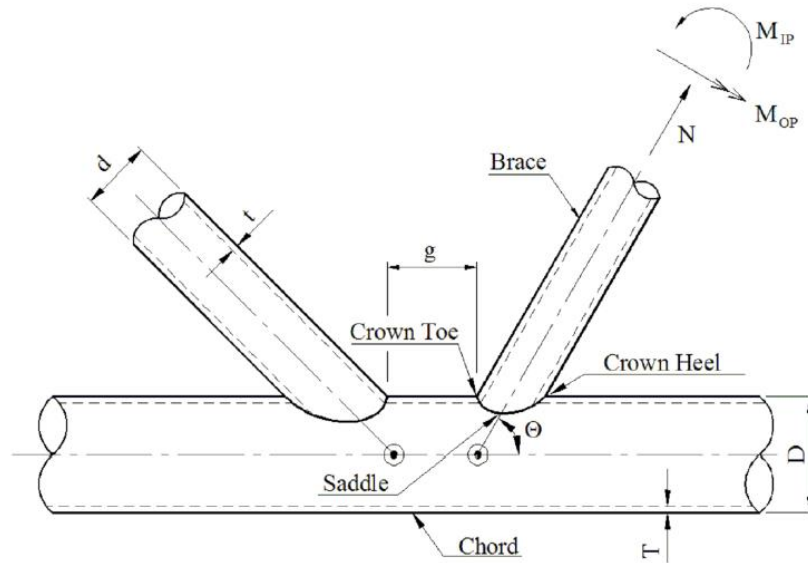


Figure 2-11: Brace and chord configuration (DNV RP-C203, 2019)

The points that generate stress concentrations are in the saddle and the crown in both brace and chord. The intermediate points between saddle and crown may generate higher stresses, so these points are also evaluated. The hot spot stress should therefore be evaluated at 8 points around the cross section of the brace, as shown below.

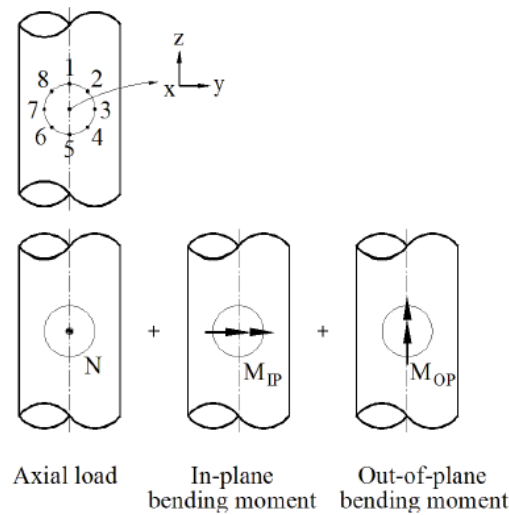


Figure 2-12: Hot-spot locations in pipes (DNV RP-C203, 2019)

Each point then has its own stress equation combining stress concentrations and the type of stress loading that affect the point. The equations are given in (DNV RP-C203, 2019) as follows:

$$\begin{aligned}
\sigma_1 &= SCF_{AC} \sigma_x + SCF_{MIP} \sigma_{my} \\
\sigma_2 &= \frac{1}{2} (SCF_{AC} + SCF_{AS}) \sigma_x + \frac{1}{2} \sqrt{2} SCF_{MIP} \sigma_{my} - \frac{1}{2} \sqrt{2} SCF_{MOP} \sigma_{mz} \\
\sigma_3 &= SCF_{AS} \sigma_x - SCF_{MOP} \sigma_{mz} \\
\sigma_4 &= \frac{1}{2} (SCF_{AC} + SCF_{AS}) \sigma_x - \frac{1}{2} \sqrt{2} SCF_{MIP} \sigma_{my} - \frac{1}{2} \sqrt{2} SCF_{MOP} \sigma_{mz} \\
\sigma_5 &= SCF_{AC} \sigma_x - SCF_{MIP} \sigma_{my} \\
\sigma_6 &= \frac{1}{2} (SCF_{AC} + SCF_{AS}) \sigma_x - \frac{1}{2} \sqrt{2} SCF_{MIP} \sigma_{my} + \frac{1}{2} \sqrt{2} SCF_{MOP} \sigma_{mz} \\
\sigma_7 &= SCF_{AS} \sigma_x + SCF_{MOP} \sigma_{mz} \\
\sigma_8 &= \frac{1}{2} (SCF_{AC} + SCF_{AS}) \sigma_x + \frac{1}{2} \sqrt{2} SCF_{MIP} \sigma_{my} + \frac{1}{2} \sqrt{2} SCF_{MOP} \sigma_{mz}
\end{aligned}$$

(2-8) (DNV RP-C203, 2019)

Where:

$\sigma_{1,2,3\dots}$ = Hot-spot stress at correlating point

σ_x = Nominal stress due to axial stress in brace

$\sigma_{mz/my}$ = Nominal stresses due to in-plane or out-of-plane bending moment.

SCF_{xx} = Stress concentration factor to correlating nominal stress at either crown or saddle (example: AC = means axial at crown).

Hot spots should be investigated in both chord and brace, which makes 16 total points, with stress concentrations for both bending stress and axial stress in both saddle and crown on chord and brace. SCFs for the mirroring point in the cross section (such as 1&5 or 2&6) may be simplified as equal. The intermediate points are estimated using interpolation between the SCFs of both saddle and chord.

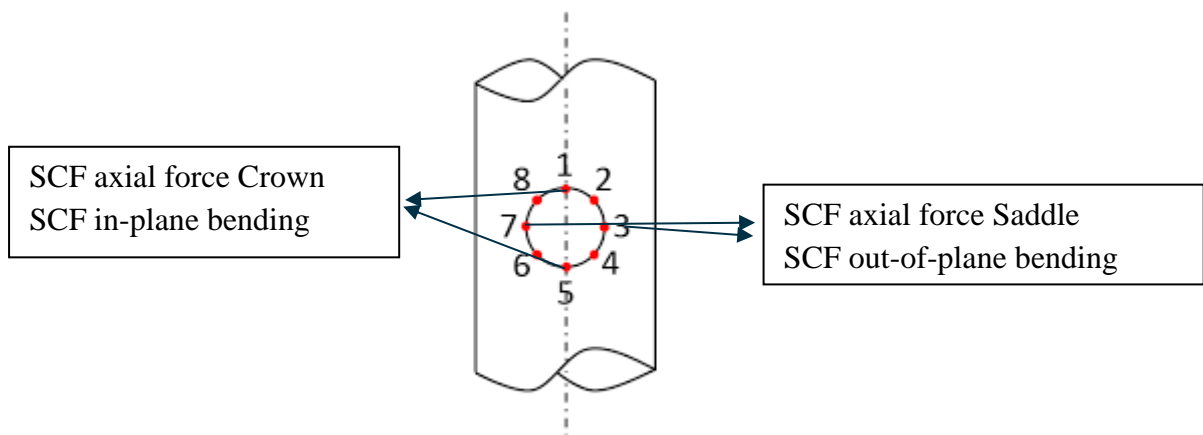


Figure 2-13: SCF naming for tubular joints (Karlsson, 2018)

2.7 Fatigue Analysis Using S-N Curves

Based on experimental testing data, S-N curves are made for different structure materials, environmental conditions, and configurations. Most curves are determined in laboratories by exciting a material with constant stress and counting the number of cycles needed till failure. To derive accurate curves, a lot of specimens are tested with different constant stresses, and the results are plotted on a coordinate grid, with stress-ranges on y-axis and number of cycles on the x-axis, both in logarithmic scale.

The mean of the results is plotted as a graph; however, the mean only ensures 50% probability of survival in real cases. The final S-N curve is then plotted from the mean curve minus two standard deviations to ensure a 97.6% probability of survival. (Yong Bai, 2016)

$$\log \bar{a} = \log a - 2S_{\log N} \quad (2-9)$$

Where:

$\log a$ = Intercept of mean S-N curve

$S_{\log N}$ = Standard deviation of $\log N$

$\log \bar{a}$ = Design S-N strength found in xx (minus 2*standard deviation)

From (DNV RP-C203, 2019)

For every stress range a structure part is subjected to, the S-N curve formulas will provide an estimated number of cycles to failure (N). The formula to estimate N for each stress range is given in (DNV RP-C203, 2019) as follows:

$$\log N = \log \bar{a} - m * \log \left(\Delta\sigma * \left(\frac{t}{t_{ref}} \right)^k \right) \quad (2-10)$$

Where:

N = Predicted number of cycles to failure for a given stress range

$\Delta\sigma$ = Stress range structure is exposed to

m = Negative inverse slope of S-N curve

t_{ref} = Reference thickness

t = Thickness through crack will most likely form

k = Thickness exponent, varies with type weld or bolt connection

2.7.1 S-N Curves for Tubular Joints

The table and graph below show the S-N curve for tubular joints and is the curve used in this thesis' analyses. S-N curves normally consist of two linear slopes with a point of intersection at 10^7 cycles. As for air conditions, the higher stresses are related to a slope that increases the number of cycles with the power 3 as stress changes, and for the lower stress ranges with the power of 5. As mentioned,

the values given in **Table 2-1**, changes with every S-N curve and is based on geometry, material, and structural properties.

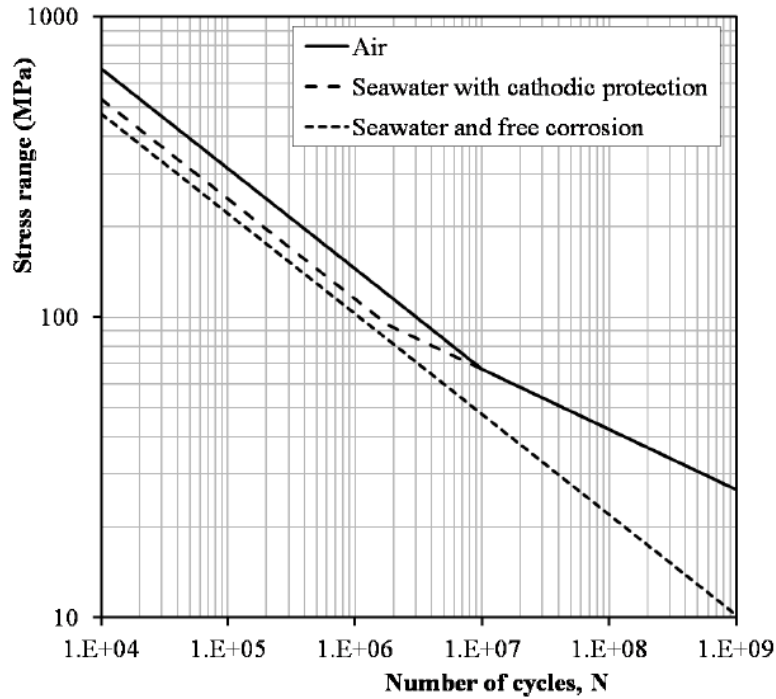


Figure 2-14: S-N curve example (DNV RP-C203, 2019)

<i>Environment</i>	m_1	$\log \bar{a}_1$	m_2	$\log \bar{a}_2$	<i>Fatigue limit at 10^7 cycles [MPa]*</i>	<i>Thickness exponent k</i>
Air	$N \leq 10^7$ cycles		$N > 10^7$ cycles			
	3.0	12.48	5.0	16.13	67.09	0.25
Seawater with cathodic protection	$N \leq 1.8 \cdot 10^6$ cycles		$N > 1.8 \cdot 10^6$ cycles			
	3.0	12.18	5.0	16.13	67.09	0.25
Seawater free corrosion	3.0	12.03	3.0	12.03	0	0.25

Table 2-1: DNV S-N curve for tubular joints (DNV RP-C203, 2019)

2.8 Miner's Rule

If the long-term stress range can be expressed in a stress histogram with a convenient number of stress ranges, the damage accumulated can be calculated with the assumption of linear cumulative damage. The Miner's rule formula is stated in (DNV RP-C203, 2019) as follows:

$$D = \sum_{i=1}^k \frac{n_i}{N_i} = 1, 0 \text{ at failure} \quad (2-11)$$

Where:

D = Accumulated fatigue damage

k = Number of stress ranges

n = Number of cycles at each stress range

N = Predicted number of cycles to failure for a given stress range (as described before)

This relationship assumes that parts of the stress signal can be calculated and accumulated to the total damage separate from the rest of the stress signal. (Sherratt, 1989)

The amount of cycles experienced from each stress range (n) is often and is desirable to express as either daily or yearly exposure, and thus accumulated damage appears as either daily or yearly damage (D_d or D_y). The expected fatigue life (FL), can than be derived by taking the inverse of accumulated damage:

$$FL = \frac{1}{D_y} \text{ or } FL = \frac{1}{D_d * 365 \text{ days}} \quad (2-12)$$

2.9 Research Gap

The frequency domain analysis is a convenient and relatively simple methods, but it has its limitations. Non-linear effects, large deformations and plasticity are some of the factors the method cannot take properly into account. Cross wind induced vibrations, wind directional effects, structural damping and incident turbulence may all effect the bandwidth of the critical stress in the power spectrum, such that the fatigue damage contribution might be underestimated. The spectral methods based on non-Gaussian process are still under development, however. (Junbo Jia, 2010)

Because the time history method cherishes a greater probability for the larger stress values than the Gaussian spectra's, it may cause larger stress ranges that accelerate fatigue contributed damage. Wind sensitive slender structures therefore attract a lot of research effort, especially time domain dynamic analysis. (Junbo Jia, 2010)

Generally, with more accuracy, less over-conservative choices can be made, further optimizing design. This thesis investigates how fatigue life is change with increased accuracy. Multiaxial contribution of wind and correlating probability is an example of how accuracy can decrease the need for conservatism.

Time histories is tedious and require a lot of input data. Large statistical variation and difference is also found within one stress recording to the next one. There is therefore a demand for further research and development in more accurate and simpler assessment methods for time history. More accurate

spectral approach is also desirable because of the simplicity, but it is necessary to confirm numerical models with real behavior through research. (Boris Fuštar, 2018)

3 Model and Methodology of FRAMEWORK, WINDPACK and USFOS

3.1 Flare Boom and Model

The model used in this thesis is of a flare boom on an existing platform in service. Any data that might be revealing is kept for confidentiality.

However, the data necessary for the thesis is stated below and the flare is given the name (Flare 1) for referring purposes.

The model consists of two main parts:

- Flare boom consists of tubular members.
- Supporting structure in shape of box frame consists of box-section and I-section beams. The supporting structure is connected to the topside of the platform by tubular link members.

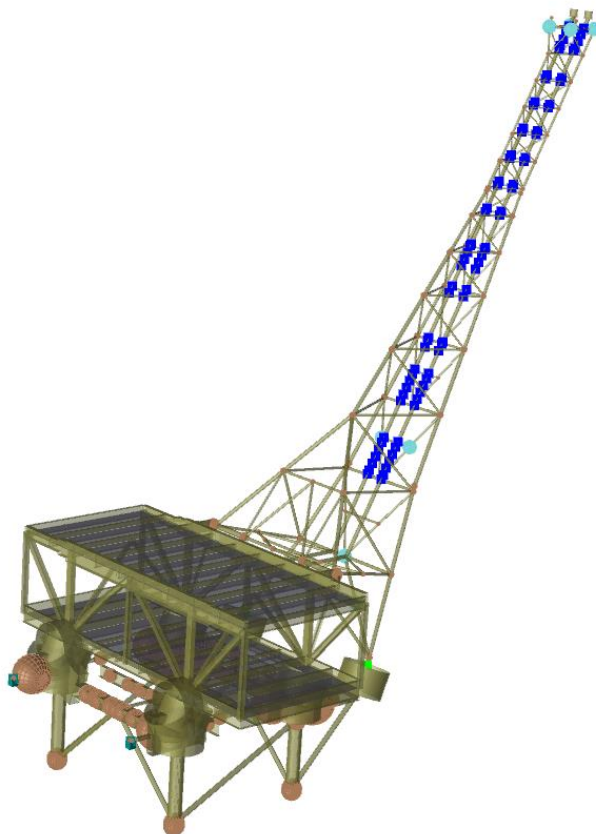


Figure 3-1: Flare boom model in GeniE

The flare boom base point has an elevation of 24.6 m above sea water level at lowest astronomical tide (LAT) and the highest point on the tip of the flare boom has an elevation at 119.8 m above sea water level at lowest astronomical tide (LAT). As shown below in

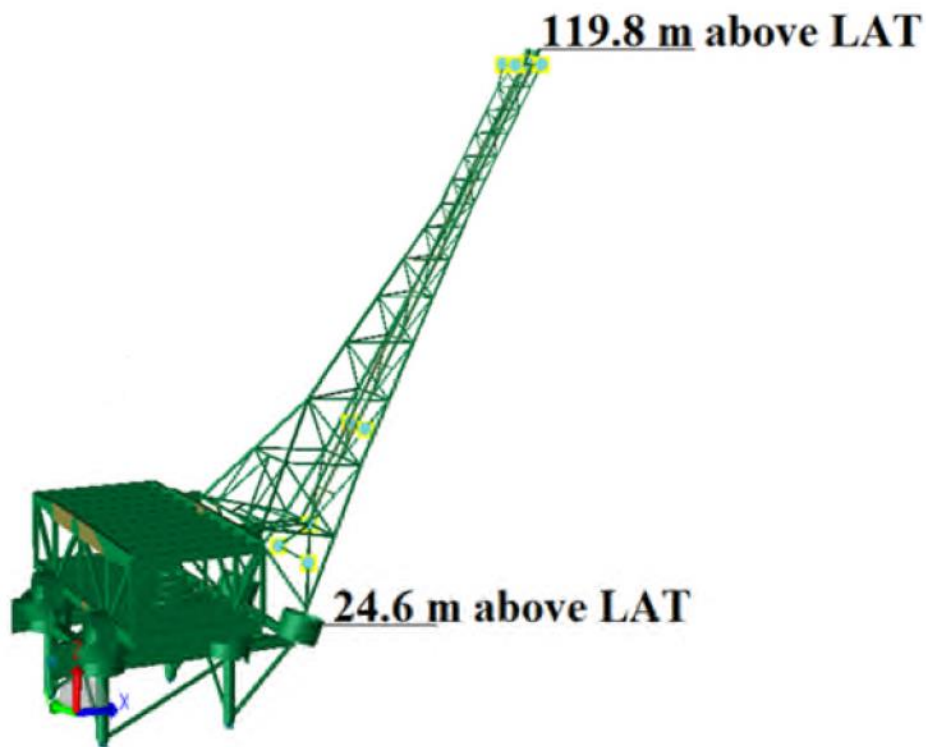


Figure 3-2: Flare boom model showing elevation above LAT (lowest astronomical tide)

The flare boom structure is modeled in DNV GeniE. The model is then used in both DNV SESAM FRAMEWORK and USFOS.

3.1.1 Critical Fatigue Points

To establish a reasonable parametric comparison study between both software used, the fatigue lives of the 5 most critical points are presented.

Figure 3-3, Figure 3-4 and Figure 3-5 show the model with the critical points resulting from analysis in both FRAMEWORK and USFOS.

Joint numbers in FRAMEWORK are different than those in USFOS. Therefore, the correlating name in each software is added to the figures below as the number of 6 digits is the numbering system used in FRAMEWORK, while the number used in USFOS is shown in between parentheses.

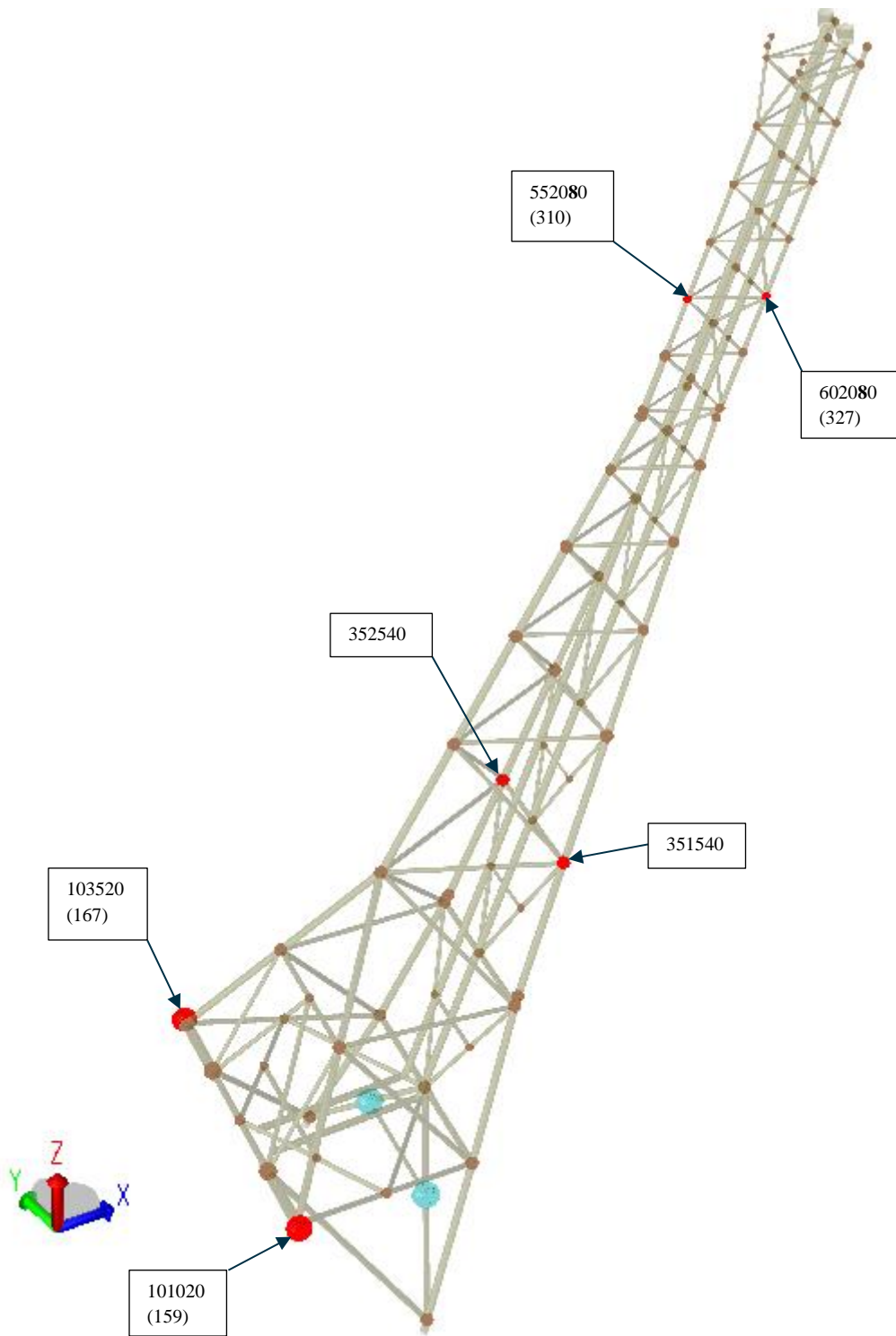


Figure 3-3: Isometric view of the model showing critical points

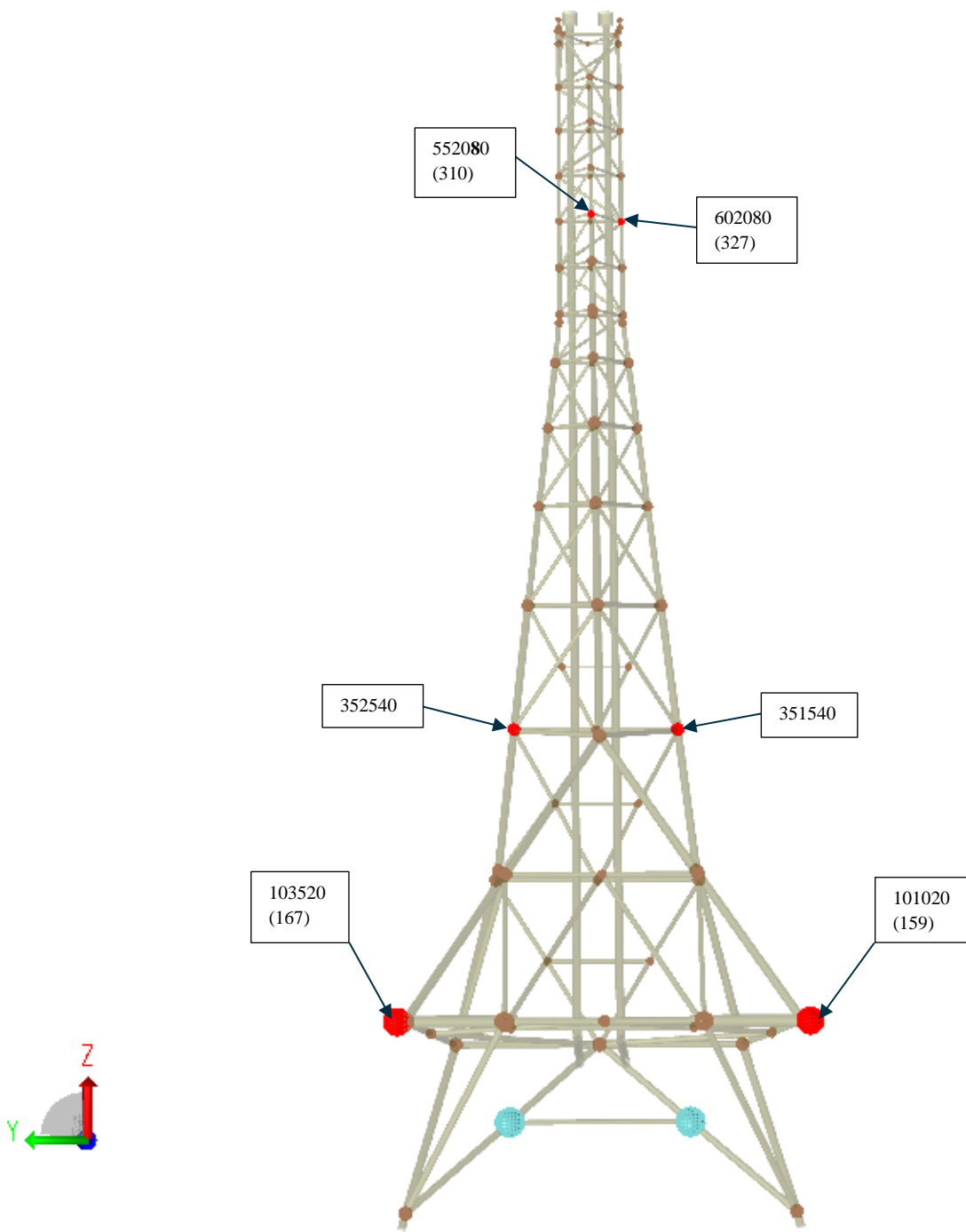


Figure 3-4: Elevation view of the model showing critical points

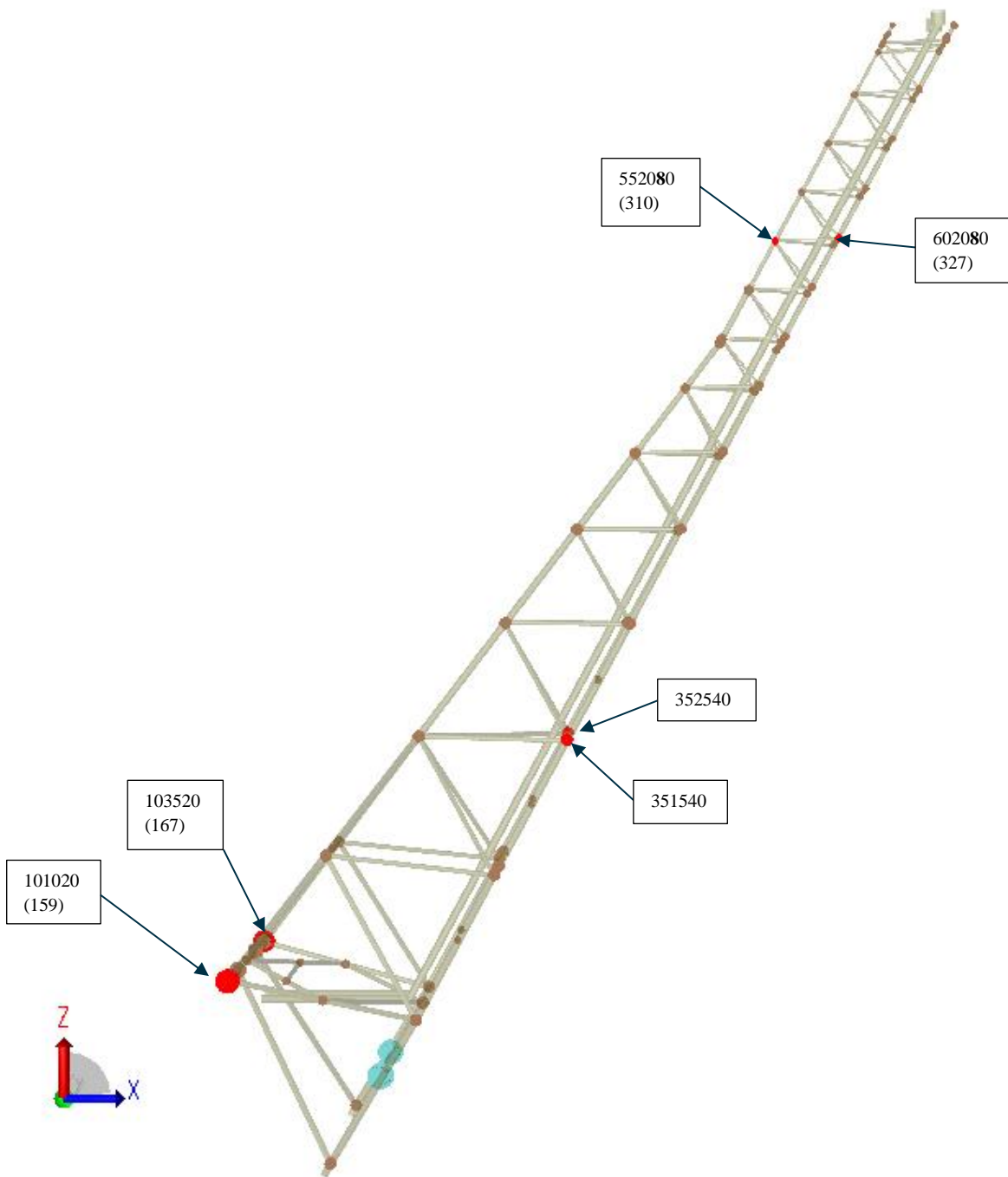


Figure 3-5: Side view of the model showing critical points

3.1.2 Structural Weight

The total weight of the flare boom is 398.15 metric tons. In addition, point masses have been added to approach the target weight and target center of gravity.

There are 9 point added masses, marked in blue and located as shown in **Figure 3-6**, with values of 250-, 500-, and 1000 kg.

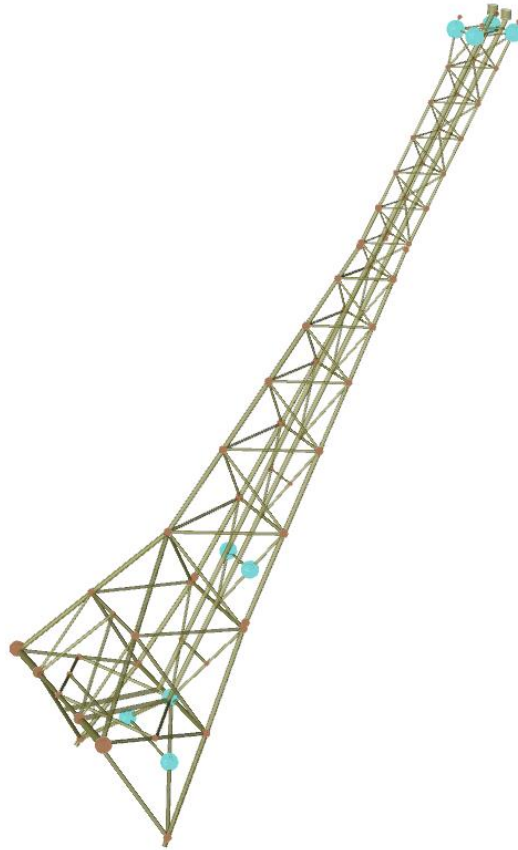


Figure 3-6: Flare boom model showing point added masses

3.1.3 Material Properties

The material used for modelling the flare boom is steel with properties as shown in the table below:

	Value	Members
Yield stress (N/mm ²)	420	Flare boom members
Young's Modulus (N/mm ²)	210000	Flare boom members
Density (kg/m ³)	7850	Flare boom members
Poisson's ratio	0.3	Flare boom members

Table 3-1: Material properties of tubular members

3.1.4 Coordinate System

X-axis: Platform South

Y-axis: Platform East

Z-axis: Up

Platform north is oriented 45° west of geographical north. **Figure 3-7** shows the orientation of the platform with relation to geographical north. X-axis correlates with the flare boom's X-axis.

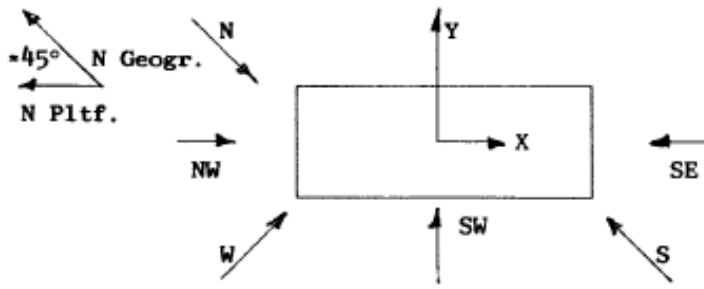


Figure 3-7: Platform orientation relative to global coordinates

3.1.5 Boundary Conditions

The model is supported on the rest of the platform's topside on 6 hinge supports as shown in (Figure 3-8).

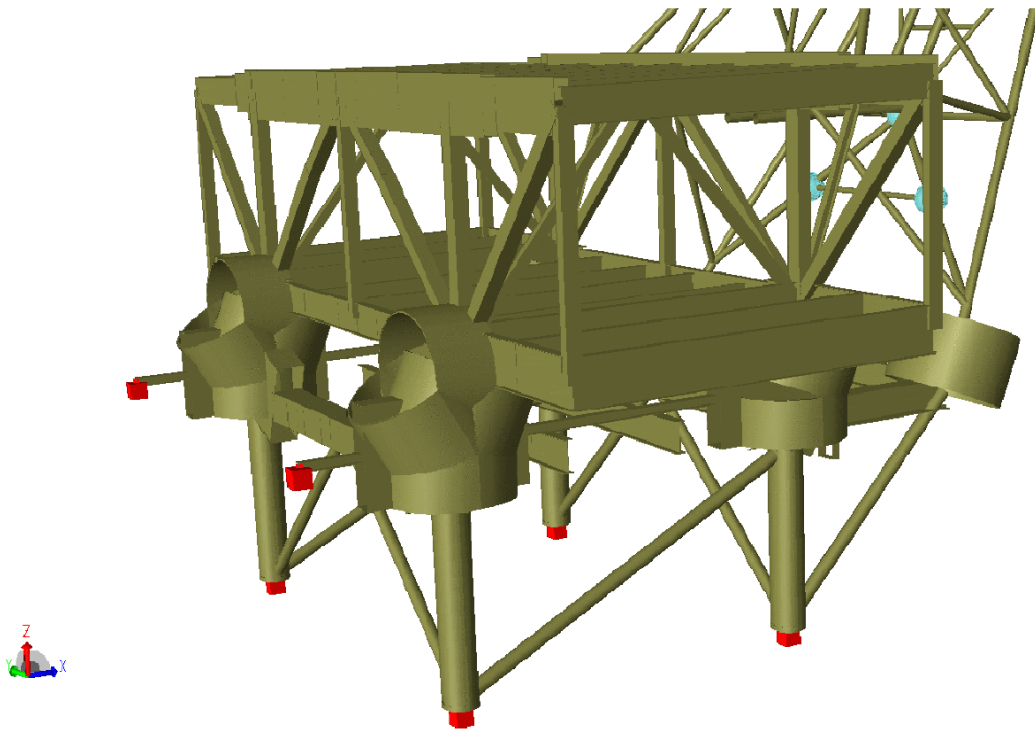


Figure 3-8: Flare boom model showing support points

3.1.6 Wind Data

All wind data used in this thesis is based on data obtained from Metocean Design Basis. This includes the wind profile; all-year wind rose and the scatter diagram.

The specific Metocean field which is used for wind data is preserved for confidentiality purposes. However, the wind rose, wind field, and the scatter diagram are presented in the following figures and equations.

- All-year Wind Rose

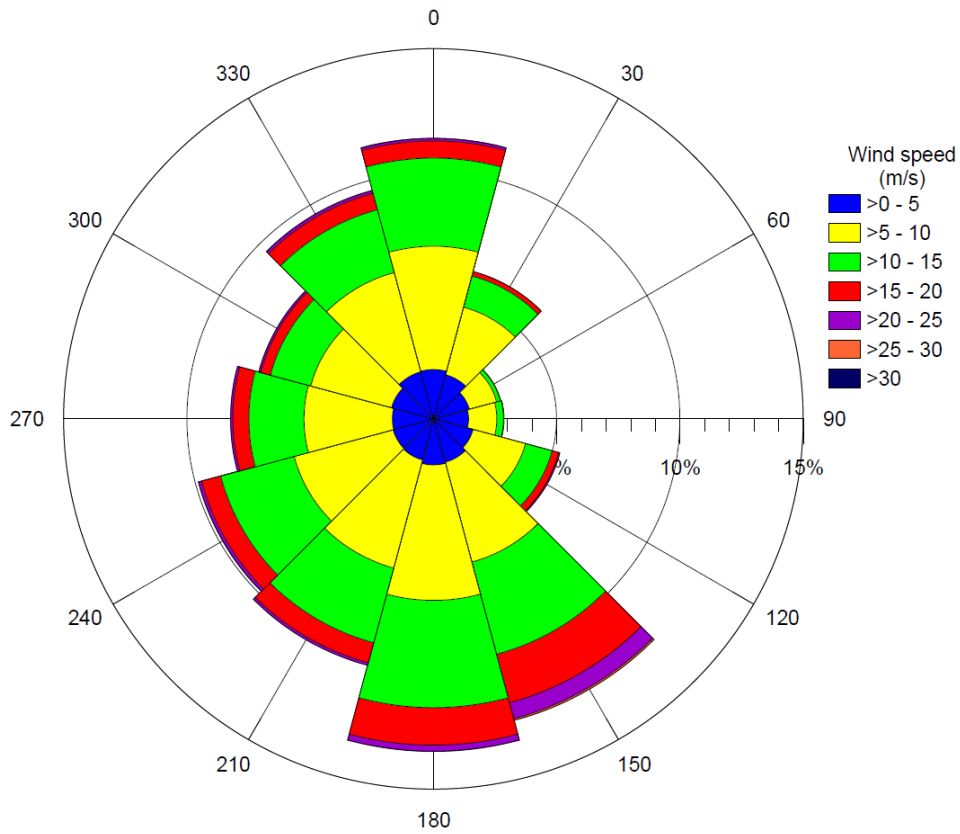


Figure 3-9: All-year wind rose

As the all-year wind rose above shows, the dominant wind directions are South, South-West and North, respectively. While the least-occurring wind comes from the East direction.

- Wind profile and gust

Wind profile and gust are based in this Metocean report on the NORSOK Standard (NORSOK Standard, 2017).

The wind speed $U(z,t)$ at height z (m) above sea level corresponding average period t (s) less than or equal to $t_0 = 3600$ s may be calculated as:

$$u(z, t) = U(z) \cdot \left[1 - 0.41 \cdot I_U(z) \cdot \ln\left(\frac{t}{t_0}\right) \right] \quad (3-1)$$

Where $U(z)$ is the 1-hour mean wind speed and can be represented by:

$$U(z) = U_0 \cdot \left[1 + C \cdot \ln\left(\frac{z}{10}\right) \right] \quad (3-2)$$

and

$$C = 5.73 \cdot 10^{-2} \cdot [1 + 0.15 \cdot U_0]^{1/2} \quad (3-3)$$

Turbulence intensity factor $I_u(z)$ can be represented by the equation:

$$I_u(z) = 0.06 \cdot (1 + 0.043 \cdot U_0) \cdot \left(\frac{z}{10}\right)^{-0.22} \quad (3-4)$$

Where U_0 (m/s) is the 1-hour average wind speed at $z = 10$ m.

Figure 3-10 shows wind profiles for different wind speeds varying with height at the location of interest.

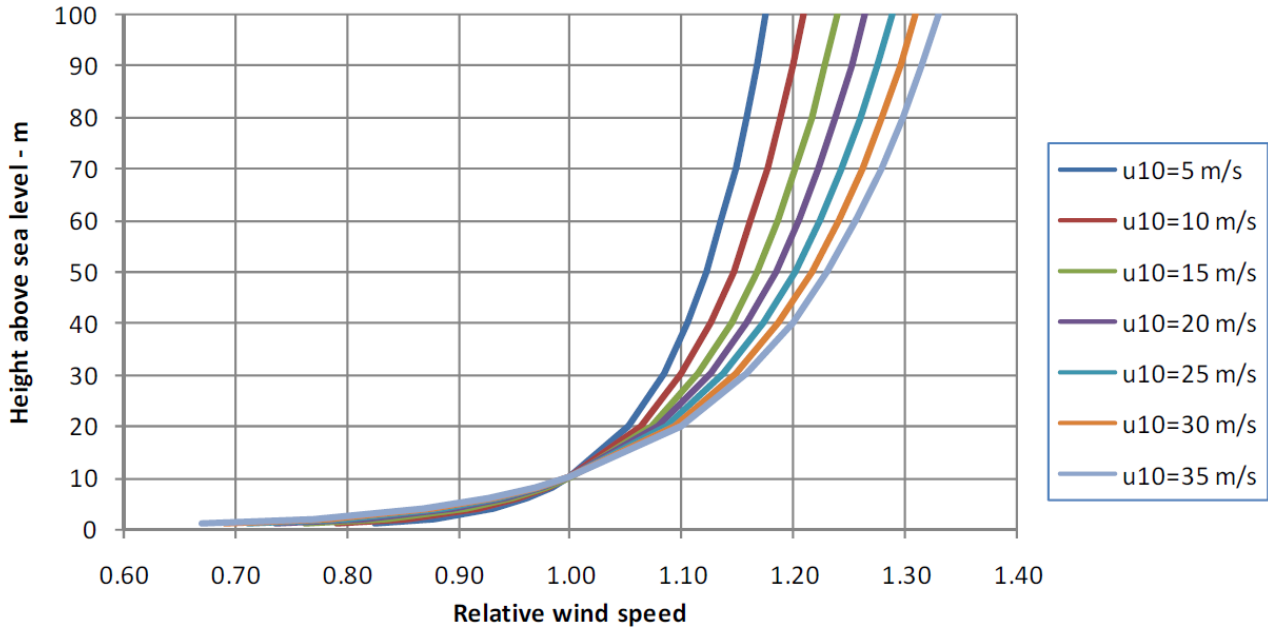


Figure 3-10: Wind profiles at different wind speeds

- Scatter Diagram

The annual direction sample distribution of non-exceedance (%) of 1-hour average wind speed at 10 m above sea level is extracted from the Metocean report as in **Table 3-2**:

Wind (m/s)	0°	30°	60°	90°	120°	150°	180°	210°	240°	270°	300°	330°	Omni
< 2	0.24	0.26	0.27	0.28	0.26	0.25	0.27	0.26	0.27	0.25	0.24	0.29	3.14
< 4	1.17	1.16	0.98	0.96	1.00	1.09	1.07	1.02	1.03	1.02	1.04	1.17	12.70
< 6	2.79	2.49	1.86	1.77	2.09	2.51	2.63	2.44	2.37	2.30	2.40	2.70	28.36
< 8	4.76	3.71	2.42	2.29	3.03	4.12	4.79	4.29	4.04	3.81	3.79	4.45	45.50
< 10	6.90	4.74	2.67	2.55	3.76	5.86	7.22	6.15	5.78	5.22	5.08	6.04	61.97
< 12	8.78	5.49	2.78	2.70	4.29	7.49	9.37	7.76	7.36	6.36	6.02	7.42	75.80
< 14	10.12	5.99	2.83	2.79	4.70	9.02	11.04	8.93	8.49	7.23	6.59	8.34	86.08
< 16	10.83	6.24	2.86	2.83	4.94	10.21	12.18	9.67	9.23	7.77	6.93	8.91	92.60
< 18	11.12	6.34	2.86	2.84	5.04	11.10	12.87	10.05	9.59	8.06	7.12	9.21	96.19
< 20	11.27	6.36	2.86	2.84	5.10	11.72	13.30	10.25	9.76	8.22	7.22	9.39	98.31
< 22	11.34	6.37	2.86	2.84	5.13	12.12	13.48	10.33	9.85	8.27	7.27	9.48	99.34
< 24	11.37	6.37			5.14	12.31	13.54	10.35	9.88	8.31	7.30	9.50	99.76
< 26	11.38				5.15	12.42	13.56	10.36	9.89	8.31	7.30	9.51	99.94
< 28	11.38					12.44	13.57	10.36	9.89	8.31	7.30	9.51	99.99
< 30	11.38					12.45	13.57		9.89		7.30	9.51	100.00
< 32	11.38					12.45			9.89		7.31	9.52	100.00
Total	11.38	6.37	2.86	2.84	5.15	12.45	13.57	10.36	9.89	8.31	7.31	9.52	100.00
Mean	9.0	7.5	5.3	5.6	7.7	10.9	10.0	9.2	9.3	8.9	8.3	8.8	9.0
Maximum	30.5	23.9	20.3	21.0	25.9	30.1	29.0	27.2	30.5	27.5	30.0	30.0	30.5

Table 3-2: Scatter diagram provided by Metocean data

3.1.7 Drag Coefficient

This thesis uses drag factor as a parameter in comparison. Therefore, many drag factors have been picked as explained later in section 3.2. One of the cases is a Reynold's number dependent drag factor. This case is taken from (DNV RP-C205, 2019), with the following limits:

Cd = 0.65 for Reynold's number > 5 * 10⁵

Cd = 1.2 for Reynold's number < 5 * 10⁵

Reynolds number is defined through:

$$Re = \frac{U * D}{\nu} \quad (3-5)$$

Re= Reynold's number

U= Mean wind speed (m/s)

D= Pipe Diameter (m)

ν = Kinematic viscosity (m²/s)

In the case of FRAMEWORK and WINDPACK, drag factor for nontubular members is set to zero (or close to zero; Cd=0.0001) to be excluded from the fatigue analysis.

3.1.8 S-N Curves

S-N curve for tubular members in Air (T-curve) is used for all tubular members and joints according to (DNV RP-C203, 2019).

The S-N curve used is shown in **Figure 3-11** and **Table 3-3**.

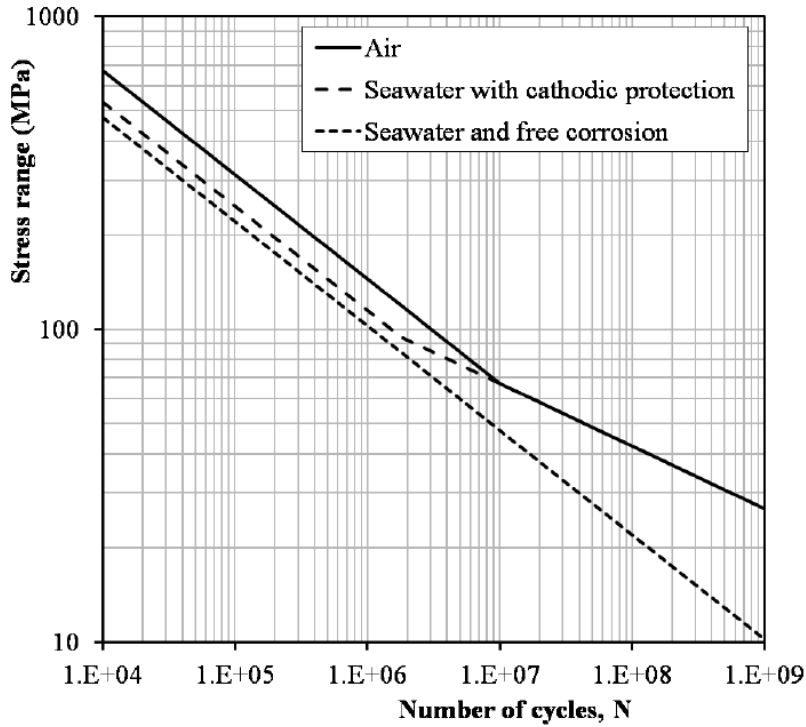


Figure 3-11: S-N curve for tubular joints (DNV RP-C203, 2019)

Environment	m_1	$\log \bar{a}_1$	m_2	$\log \bar{a}_2$	Fatigue limit at 10^7 cycles [MPa]*)	Thickness exponent k
Air	$N \leq 10^7$ cycles		$N > 10^7$ cycles		67.09	0.25
	3.0	12.48	5.0	16.13		
Seawater with cathodic protection	$N \leq 1.8 \cdot 10^6$ cycles		$N > 1.8 \cdot 10^6$ cycles		67.09	0.25
	3.0	12.18	5.0	16.13		
Seawater free corrosion	3.0	12.03	3.0	12.03	0	0.25

Table 3-3: S-N curve for tubular joints (DNV RP-C203, 2019)

3.2 Parametric Study

Fatigue calculation is a complex process with many factors that contribute to the result. Because fatigue is based on repetition and cycles, small changes in the parameters may have large impact on the resulting fatigue life. Several analyses are done to investigate the sensitivity of different parameters.

By varying certain parameters in different cases, the change in fatigue life is observed. In running multiple cases, trends are observed. The following parameters have been investigated along with limitations on the software use.

3.2.1 Software Limitations

1. By running multiple cases of wind block combinations, the ones chosen for further analysis are arguably the most conservative. (See section 3.2.2)
2. FRAMEWORK cannot read more than 12 wind blocks per analysis. Therefore, the case of 16 wind blocks -described below (see section 3.2.2)- is only used in USFOS.
3. FRAMEWORK can analyze up to 7 analysis planes per analysis. Each plane contains all the joints needed for testing at each case. To cover all fatigue-affected joints, multiple analyses must be run with different planes selected. Therefore, the 7 planes, where most critical joints lie, are chosen for analysis.
4. Drag factor on members cannot be set to zero in FRAMEWORK. Therefore, the drag factor for all non-tubular members is set to 0.0001 to avoid computational errors.
5. As USFOS uses time domain nonlinear analysis, sufficient time increment needs to be assigned for each analysis. The decision on time increment is case dependent. As a rule of thumb, time increments are chosen to fall within the range of 10% of the first eigenvalue. Two time-steps are hence chosen for this model: 0.10 seconds and 0.05 seconds (see section 3.2.5).
6. USFOS nonlinear analysis is computationally demanding, therefore the simulation time is shortened from 3600 s (1-hr) to 2000 s. However, FATAL changes back to 1-hr damage before calculating the yearly damage. For sensitivity check, 4 random cases were run using 3600 s and compared to the respective 2000 s cases. The difference is less than 5% in fatigue life.
7. The purpose of this study is to compare the outcome fatigue life of the three software mentioned. Therefore, the comparison is based on the 5 most critical joints in both software.
8. Structural damping is not considered a variable parameter in this thesis, as the same model is used in both software. Structural damping is then assumed to have a set value of 0.05.

3.2.2 Number of Wind Blocks

The less wind blocks used in the analysis; the more conservative choices need to be made. A wind range between two wind speeds is set to the highest wind speed within the range to be more conservative. Choosing fewer blocks gives longer ranges of wind speed. All probabilities related to a given range in the scatter diagram (**Table 3-2**), must therefore correlate to the highest wind speed in

the range. This implies that more wind blocks generally mean less conservative and more accurate fatigue life.

Higher wind speed gives more structural loading and dynamic response, which means more fatigue damage. However, considering the annual probability is generally higher for lower wind speeds, the lower speeds may accumulate more damage. Therefore, it is difficult to decide which wind speed contributes more to fatigue life. To investigate this, four different combinations of wind blocks are used in this analysis.

- **16 wind blocks:**

This scatter diagram is identical to the one provided by the Metocean report, varying wind speed with intervals of 2 m/s. The analysis using these wind blocks is limited to USFOS only, since FRAMEWORK only allows up to 12 wind blocks to be used. This scatter should be the most accurate, also should provide the least fatigue damage.

wind block	m/s	Annual probability / wind direction (%)											Total	
		0°	30°	60°	90°	120°	150°	180°	210°	240°	270°	300°		330°
1	2	0.24	0.26	0.27	0.28	0.26	0.25	0.27	0.26	0.27	0.25	0.24	0.29	3.14
2	4	0.93	0.90	0.70	0.68	0.74	0.84	0.80	0.76	0.76	0.77	0.80	0.88	9.56
3	6	1.62	1.33	0.88	0.81	1.09	1.42	1.56	1.42	1.34	1.28	1.36	1.53	15.64
4	8	1.97	1.22	0.56	0.52	0.94	1.61	2.16	1.85	1.67	1.51	1.39	1.75	17.15
5	10	2.14	1.03	0.25	0.26	0.73	1.74	2.43	1.86	1.74	1.41	1.29	1.59	16.47
6	12	1.88	0.75	0.11	0.15	0.53	1.63	2.15	1.61	1.58	1.14	0.94	1.38	13.85
7	14	1.34	0.50	0.05	0.09	0.41	1.53	1.67	1.17	1.13	0.87	0.57	0.92	10.25
8	16	0.71	0.25	0.03	0.04	0.24	1.19	1.14	0.74	0.74	0.54	0.34	0.57	6.53
9	18	0.29	0.10	0.00	0.01	0.10	0.89	0.69	0.38	0.36	0.29	0.19	0.30	3.6
10	20	0.15	0.02	0.00	0.00	0.06	0.62	0.43	0.20	0.17	0.16	0.10	0.18	2.09
11	22	0.07	0.01	0.00	0.00	0.03	0.40	0.18	0.08	0.09	0.05	0.05	0.09	1.05
12	24	0.03	0.00	0.00	0.00	0.01	0.19	0.06	0.02	0.03	0.04	0.03	0.02	0.43
13	26	0.01	0.00	0.00	0.00	0.01	0.11	0.02	0.01	0.01	0.00	0.00	0.01	0.18
14	28	0.00	0.00	0.00	0.00	0.00	0.02	0.01	0.00	0.00	0.00	0.00	0.00	0.03
15	30	0.00	0.00	0.00	0.00	0.00	0.01	0.00	0.00	0.00	0.00	0.00	0.00	0.01
16	32	0.00	0.00	0.00	0.00	0.00	0.00	0.00	0.00	0.00	0.00	0.01	0.01	0.02
														100

Table 3-4: Scatter diagram of 16 wind blocks

- **8 wind blocks:**

This case is like 16 wind blocks but varying with intervals of 4 m/s. The probability is added for all the wind speeds within the block and the resulting probability is set the highest wind speed.

wind block	m/s	Annual probability / wind direction											Total	
		0°	30°	60°	90°	120°	150°	180°	210°	240°	270°	300°		330°
1	4	1.17	1.16	0.98	0.96	1	1.09	1.07	1.02	1.03	1.02	1.04	1.17	12.71
2	8	3.59	2.55	1.44	1.33	2.03	3.03	3.72	3.27	3.01	2.79	2.75	3.28	32.79
3	12	4.02	1.78	0.36	0.41	1.26	3.37	4.58	3.47	3.32	2.55	2.23	2.97	30.32
4	16	2.05	0.75	0.08	0.13	0.65	2.72	2.81	1.91	1.87	1.41	0.91	1.49	16.78
5	20	0.44	0.12	0	0.01	0.16	1.51	1.12	0.58	0.53	0.45	0.29	0.48	5.69
6	24	0.1	0.01	0	0	0.04	0.59	0.24	0.1	0.12	0.09	0.08	0.11	1.48
7	28	0.01	0	0	0	0.01	0.13	0.03	0.01	0.01	0	0	0.01	0.21
8	32	0	0	0	0	0	0.01	0	0	0	0	0.01	0.01	0.03
														100.0

Table 3-5: Scatter diagram of 8 wind blocks

- **12 wind blocks:**

This case is in intervals of 2 m/s from 2 m/s to 18 m/s cases, and in three ranges: 18-24 m/s, 24-28 m/s and 28-32 m/s. Probabilities are added for all wind speeds in each block, and the resulting probability is set to the highest wind speed. This load case has more wind blocks than the 8 wind blocks case, but larger ranges are made in the upper end of the wind speed spectrum.

wind block	m/s	Annual probability / wind direction (%)											Total	
		0°	30°	60°	90°	120°	150°	180°	210°	240°	270°	300°		330°
1	2	0.24	0.26	0.27	0.28	0.26	0.25	0.27	0.26	0.27	0.25	0.24	0.29	3.14
2	4	0.93	0.90	0.71	0.68	0.74	0.84	0.80	0.76	0.76	0.77	0.80	0.88	9.57
3	6	1.62	1.33	0.88	0.81	1.09	1.42	1.56	1.42	1.34	1.28	1.36	1.53	15.64
4	8	1.97	1.22	0.56	0.52	0.94	1.61	2.16	1.85	1.67	1.51	1.39	1.75	17.15
5	10	2.14	1.03	0.25	0.26	0.73	1.74	2.43	1.86	1.74	1.41	1.29	1.59	16.47
6	12	1.88	0.75	0.11	0.15	0.53	1.63	2.15	1.61	1.58	1.14	0.94	1.38	13.85
7	14	1.34	0.50	0.05	0.09	0.41	1.53	1.67	1.17	1.13	0.87	0.57	0.92	10.25
8	16	0.71	0.25	0.03	0.04	0.24	1.19	1.14	0.74	0.74	0.54	0.34	0.57	6.53
9	18	0.29	0.10	0.00	0.01	0.10	0.89	0.69	0.38	0.36	0.29	0.19	0.30	3.6
10	24	0.25	0.03	0.00	0.00	0.10	1.21	0.67	0.30	0.29	0.25	0.18	0.29	3.57
11	28	0.01	0.00	0.00	0.00	0.01	0.13	0.03	0.01	0.01	0.00	0.00	0.01	0.21
12	32	0.00	0.00	0.00	0.00	0.00	0.01	0.00	0.00	0.00	0.00	0.01	0.01	0.03
													100	

Table 3-6: Scatter diagram of 12 wind blocks

- **10 wind blocks:**

This scatter diagram sets the blocks in intervals of 2 m/s from 4 to 16 m/s like the 16-block, and in three ranges: 16-20 m/s, 20-24 m/s and 24-32 m/s. The 0-2 m/s range is included in the 2-4 m/s range. Probabilities are added for all wind speeds in each block, and the resulting probability is set to the highest wind speed. This load case has more wind blocks than the 8 wind blocks case, but larger ranges are made in the upper end of the wind speed spectrum.

wind block	m/s	Annual probability / wind direction (%)											Total	
		0°	30°	60°	90°	120°	150°	180°	210°	240°	270°	300°		330°
1	4	1.17	1.16	0.98	0.96	1.00	1.09	1.07	1.02	1.03	1.02	1.04	1.17	12.71
2	6	1.62	1.33	0.88	0.81	1.09	1.42	1.56	1.42	1.34	1.28	1.36	1.53	15.64
3	8	1.97	1.22	0.56	0.52	0.94	1.61	2.16	1.85	1.67	1.51	1.39	1.75	17.15
4	10	2.14	1.03	0.25	0.26	0.73	1.74	2.43	1.86	1.74	1.41	1.29	1.59	16.47
5	12	1.88	0.75	0.11	0.15	0.53	1.63	2.15	1.61	1.58	1.14	0.94	1.38	13.85
6	14	1.34	0.50	0.05	0.09	0.41	1.53	1.67	1.17	1.13	0.87	0.57	0.92	10.25
7	16	0.71	0.25	0.03	0.04	0.24	1.19	1.14	0.74	0.74	0.54	0.34	0.57	6.53
8	20	0.44	0.12	0.00	0.01	0.16	1.51	1.12	0.58	0.53	0.45	0.29	0.48	5.69
9	24	0.10	0.01	0.00	0.00	0.04	0.59	0.24	0.10	0.12	0.09	0.08	0.11	1.48
10	32	0.01	0.00	0.00	0.00	0.01	0.14	0.03	0.01	0.01	0.00	0.01	0.02	0.24
													100	

Table 3-7: Scatter diagram of 10 wind blocks

In-depth analysis of the most contributing load cases of wind speed and direction to the damage is possible in USFOS but is comprehensive and not included in this thesis.

3.2.3 Drag Coefficient

Drag coefficient (C_d) is a dimensionless parameter which is used to express the amount of resistance the structure experiences during the dynamic flow of air. It is influenced by shape, surface roughness and size of the structure part. Tubular sections are often chosen for offshore flare booms because of their good drag characteristics (Junbo Jia, 2010).

FRAMEWORK and USFOS has the option to calculate drag factors based on Reynold's number, but there is a chance that the effect of drag is slightly underestimated in that case, because of nonstructural elements, which are not included in the model, but may affect drag on members. Multiple drag factors have therefore been chosen to test the effect between having C_d as a fixed value compared to Reynold's dependent C_d . Varying C_d also gives an indication of the fatigue life's sensitivity to stress since C_d is directly related to the wind force.

Four values of C_d are analyzed.

- **$C_d = 0.65$**
- **$C_d = 1.0$**
- **$C_d = 1.2$**
- **$C_d = \text{Reynold's dependent.}$**

All non-tubular members have been excluded from drag effect by setting C_d to- or close to zero. The supporting structure of the flare boom is not a part of the dynamic analysis for fatigue. However, it is included in the static analysis and determination of the eigenvalues.

3.2.4 Weight and Eigen Frequency

Having the stiffness fixed, the structural weight of the model affects the natural frequency, which further affects the motion and dynamic response. Generally, a heavier structure decreases the natural frequency, which gives a slower motion. Changing the natural frequency of the structure by changing the weight may cause the frequency to approach the wind loading's more present frequencies. This gives a higher chance of resonance which is critical for fatigue damage.

Structural weight is factorized in both software by multiplying material densities and node masses by a **weight factor**. Four different load factor values are used:

- **WF = 0.5**
- **WF = 1.0**
- **WF = 1.1**
- **WF = 1.5**

3.2.5 Time Increment

Time increment governs how often dynamic response is recorded in time. More frequent recording will give a more accurate result; however, it is also more computationally demanding. Time increment is directly related to the number of calculation steps that are done. If the time increment is too large, and response is not recorded frequent enough, critical parts of the response may be missed. In worst

case peaks of stress may be missed several times and the fatigue damage may be severely underestimated.

Optimization of time increment is therefore crucial for accuracy, but also desirable for reducing computational demand. This is done by choosing different time increment values and test its impact on the results. When the difference is of small significance, it can be concluded that the response accurately represents the real motion.

In this thesis, 5 values of time increments were tested on 4 cases. The time increments tested were: 0.02 s, 0.05s, 0.1 s, 0.2 s and 0.5 s. In general, based on software vendors comment, the shorter time increment the more accurate results are expected. Therefore, the case of 0.2 s and 0.5 s gave a very high fatigue life, and therefore excluded. Fatigue life results converge significantly for values less than 0.05 s. The case of 0.02 s gives a difference of 10% in fatigue life compared to the corresponding fatigue life of 0.05 s. However, the case of 0.02 s is very computationally demanding, therefore excluded.

		critical fatigue life					
wind block	Cd	wf	dt = 0.02	dt=0.05	dt=0.1	dt = 0.2	dt = 0.5
8	1	0.5	51.2	71.1	230.9	1103.0	2498.1
		1	24.4	28.1	51.4	317.7	1814.2
		1.1	22.7	25.8	54.3	275.9	1724.1
		1.5	20.5	20.2	32.5	125.7	1395.5

Table 3-8: Critical fatigue life for different time increments for cases with 8 wind-blocks and Cd = 1.0

As a result of the above argument, full analysis is done for all parameters for the cases of 0.10 s and 0.05 s.

The time increment is limited to USFOS, since FRAMEWORK and WINDPACK uses the spectral density approach. Time increment is a case dependent parameter, so the results in this thesis may not be relevant to other cases.

3.2.6 Relative Velocity

For the dynamic analysis of structures under the effect of wind buffeting in time domain, the relative velocity between the structure and the wind might be of interest. As stated in (DNV RP-C205, 2019), for instantaneous wind force, the equation below applies.

$$F_W = \frac{1}{2} \rho_a C_D S |U_{T,z} + u - \dot{x}| (U_{T,z} + u - \dot{x}) \quad (3-6)$$

Where:

ρ_a = air density (kg/m³)

u = gust wind speed (m/s)

C_D = drag coefficient

\dot{x} = member velocity (m/s)

$U_{T,z}$ = mean wind speed at the height z and period T (m/s)

S = projected surface area (m²)

In the equation above the term $(\mathbf{u} - \dot{\mathbf{x}})$ expresses relative velocity between the structure and the wind. For less dynamic structures, structural/member velocity is small related to the wind speed, therefore wind force equation can be linearized to simplify the wind history data computing. Hence, the relative velocity for such structures might not be of interest. However, relative velocity is most impactful in very dynamic structures such as airplanes and wind turbines.

To study the effect of relative velocity on the flare boom model, analysis has been done in the time domain nonlinear analysis using USFOS, with and without including relative velocity. (See section 6.3.2)

3.2.7 Stress Concentration Factors

The Efthymiou equations (see section 2.6.1) are used to calculate SCFs in all three software. In USFOS the SCFs are first calculated in FRAMEWORK and set manually, meaning the values are identical to the ones used in the FRAMEWORK analyses.

Even though WINDPACK also uses the Efthymiou equations, there are slight differences in the values. The SCFs of both software are shown below:

SCFs		Framework	Windpack
Chord	Axial crown	4.436	3.62
	Axial saddle	6.967	6.87
	Out-of-plane (saddle)	5.31	5.31
	In-plane (crown)	2.308	2.31
Brace	Axial crown	3.226	2.89
	Axial saddle	6.04	6.04
	Out-of-plane (saddle)	4.524	4.52
	In-plane (crown)	2.446	2.45

Table 3-9: SCFs for WINDPACK and FRAMEWORK

3.3 DNV SESAM FRAMEWORK Methodology

DNV SESAM FRAMEWORK uses the power spectral density method to analyze fatigue due to buffeting loads coming from wind gusts. As mentioned previously, the effect of vortex shedding is not included in this thesis as FRAMEWORK can include a check for vortex-induced vibration (VIV) separately.

FRAMEWORK requires input information of the eigenmodes, eigen frequencies and structural data along with statistical information about the wind distribution as scatter diagram with drag factors.

FRAMEWORK processes the input data as the annual wind states, then evaluates the response stress power spectra at each local hot spot at every joint.

The hot spot power spectrum response is divided into two parts for buffeting analysis: quasi-static response and dynamic response.

The dynamic response is divided into several excited modal responses at resonance, each of which receives different damage evaluation. This is under the assumption that each of the responses is a narrow-band and independent of other modes.

The quasi-static response deals with the low frequency non-resonant response. The effect from low frequency broad band peak is small to damage and therefore no rigorous evaluation is required to be considered.

Narrow band assumption is used for both dynamic and static responses and it implies a Rayleigh distribution for the hot spot stress range against number of cycles. Fatigue life is then calculated using Miner's Rule with reference to DNV T S-N Curves for Tubular Joints.

Overview of the process done in DNV SESAM FRAMEWORK can be represented in the next flow chart as shown in the user manual (DNV - Framework User Manual, 2020).

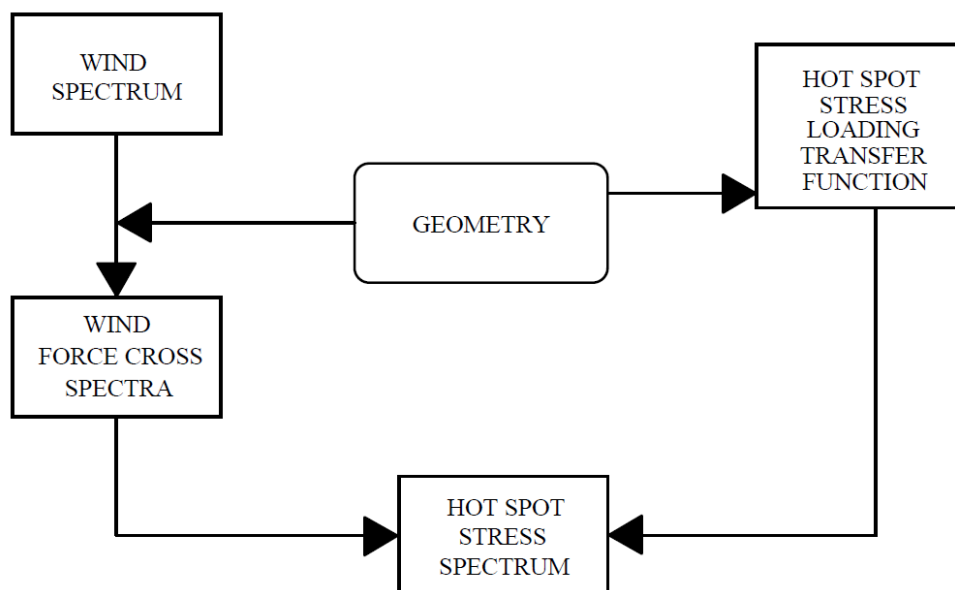


Figure 3-12: Generation of Hot Spot Stress Spectrum (DNV - Framework User Manual, 2020)



Figure 3-13: Typical Hot Spot Stress Spectrum (DNV - Framework User Manual, 2020)

Hot spot stress spectrum is used to predict fatigue life for a given wind state in the following sequence:

- 1 Each peak is treated as narrow-band response with variance equal to the integrand. Close peaks are treated as one peak. Rayleigh distribution is used to represent the stresses with the same variance.
- 2 Stress amplitude distribution is applied to S-N curve at each peak to estimate fatigue damage.
- 3 Damage is accumulated at each peak.

Total damage is then estimated at each wind state by adding the damage at a specified hot spot.

The procedure DNV SESAM FRAMEWORK uses to estimate fatigue life can be described in the following subchapters along with the assumptions used.

3.3.1 Assumptions

1. Low frequency modes at resonance are the main contributors to buffeting damage.
2. Joint stress concentrations are calculated using parametric SCF equations.
3. All structural members need to be tubular members with welded connections.
4. Wind forces are considered linear fluctuating components super-imposed upon mean wind profiles.
5. Wind gust in the mean wind direction, the horizontal crosswind and the vertical crosswind are statistically independent.
6. Fatigue coming from vortex-induced vibration is uncoupled from buffeting-induced vibration and its damage.

3.3.2 Wind Data

Wind data that is required by FRAMEWORK can be categorized into two categories: mean wind data and wind gust data.

Mean wind data required is the mean wind speed, the direction and the probability distribution that describes the percentage ratio of time a specific wind speed is likely to occur. Wind gust data are statistically described in three parameters: power spectrum, cross-correlation function, and probability distribution.

The power spectra represent the energy content of the wind in a frequency domain. The cross-correlation function represents the spatial correlation of the gusts. An example to the spectrum of horizontal wind speed by (Hoven, 1957) is represented previously in section 2.4.

Wind data is used as input wind loads in GeniE model. To account for the flare boom orientation with respect to the geographical north, wind profiles are rotated (-45°).

Mean wind speed and scatter diagram used are extracted from the Metocean data (see 3.1.6).

3.3.3 Wind Spectra

FRAMEWORK requires data for wind speed, height profiles. For each of these, three parameterized gust spectra are calculated, and damage assessment is made. The total damage represents the addition of all damage assessments with accounting for the annual probability.

An example of the probability distribution used is in **Figure 3-14** showing the scatter diagram extracted from the site related Metocean data.

Wind (m/s)	0°	30°	60°	90°	120°	150°	180°	210°	240°	270°	300°	330°	Omni
< 2	0.24	0.26	0.27	0.28	0.26	0.25	0.27	0.26	0.27	0.25	0.24	0.29	3.14
< 4	1.17	1.16	0.98	0.96	1.00	1.09	1.07	1.02	1.03	1.02	1.04	1.17	12.70
< 6	2.79	2.49	1.86	1.77	2.09	2.51	2.63	2.44	2.37	2.30	2.40	2.70	28.36
< 8	4.76	3.71	2.42	2.29	3.03	4.12	4.79	4.29	4.04	3.81	3.79	4.45	45.50
< 10	6.90	4.74	2.67	2.55	3.76	5.86	7.22	6.15	5.78	5.22	5.08	6.04	61.97
< 12	8.78	5.49	2.78	2.70	4.29	7.49	9.37	7.76	7.36	6.36	6.02	7.42	75.80
< 14	10.12	5.99	2.83	2.79	4.70	9.02	11.04	8.93	8.49	7.23	6.59	8.34	86.08
< 16	10.83	6.24	2.86	2.83	4.94	10.21	12.18	9.67	9.23	7.77	6.93	8.91	92.60
< 18	11.12	6.34	2.86	2.84	5.04	11.10	12.87	10.05	9.59	8.06	7.12	9.21	96.19
< 20	11.27	6.36	2.86	2.84	5.10	11.72	13.30	10.25	9.76	8.22	7.22	9.39	98.31
< 22	11.34	6.37	2.86	2.84	5.13	12.12	13.48	10.33	9.85	8.27	7.27	9.48	99.34
< 24	11.37	6.37			5.14	12.31	13.54	10.35	9.88	8.31	7.30	9.50	99.76
< 26	11.38				5.15	12.42	13.56	10.36	9.89	8.31	7.30	9.51	99.94
< 28	11.38					12.44	13.57	10.36	9.89	8.31	7.30	9.51	99.99
< 30	11.38					12.45	13.57		9.89		7.30	9.51	100.00
< 32	11.38					12.45			9.89		7.31	9.52	100.00
Total	11.38	6.37	2.86	2.84	5.15	12.45	13.57	10.36	9.89	8.31	7.31	9.52	100.00
Mean	9.0	7.5	5.3	5.6	7.7	10.9	10.0	9.2	9.3	8.9	8.3	8.8	9.0
Maximum	30.5	23.9	20.3	21.0	25.9	30.1	29.0	27.2	30.5	27.5	30.0	30.0	30.5

Figure 3-14: Scatter Diagram

In FRAMEWORK, for each wind state, wind speed at a height reference of 10 m above sea water level is used to calculate single-sided gust spectrum $S^s_w(f)$, where f is in cycle/s.

FRAMEWORK gives the option of choosing between one of the following spectra for representation of the gust in the same direction as the mean wind:

- HARRIS spectra
- DAVENPORT spectra
- NPD spectra (FRØYA)

While the first and second spectra use data from onshore, hence are more accurate for on shore conditions, NPD spectra use Frøya spectra which are more accurate for offshore representation.

For this reason, this thesis uses NPD spectra in FRAMEWORK analysis.

FRAMEWORK uses PANOFSKY LATERAL spectra and PANOFSKY VERTICAL spectra for the horizontal and vertical crosswind component of the gust, respectively.

3.3.4 Spectral Forcing Function

The spectral density approach to estimate wind fatigue is based on the linear relationship between the forcing spectra and the hot spot stress spectra.

Fluctuating wind components have linear relationship with the fluctuating forcing at a given node. The force on each member is firstly established and then the relationship between member forces and nodal forces is defined.

The total cross power spectral density function is the linear sum of all the three individual spectra: the along mean wind spectra, lateral cross wind spectra, vertical cross wind spectra.

Wind force on a member can be obtained using the drag part of the classic Morison's equation as follows:

$$\mathbf{F} = \frac{1}{2} \rho C_d D L |\mathbf{U}_n| \mathbf{U}_n \quad (3-7)$$

Where:

ρ is the air density

C_d is the drag coefficient

L is member length

D is member diameter

\mathbf{U}_n is the vector normal velocity

This equation can be expanded to include the fluctuating terms as follows: (DNV - Framework User Manual, 2020)

$$\underline{F}(t) = \frac{1}{2} \rho C_d D L a \underline{A} \cdot \begin{pmatrix} \langle U(z,t) \rangle^2 \\ 0 \\ 0 \end{pmatrix} + \frac{1}{2} \rho C_d L a \underline{A} \begin{pmatrix} 2 & b & c \\ 0 & 1 & 0 \\ 0 & 0 & 1 \end{pmatrix} \begin{pmatrix} \langle U(z,t) \rangle \cdot U^1 \\ \langle U(z,t) \rangle \cdot V^1 \\ \langle U(z,t) \rangle \cdot W^1 \end{pmatrix} \quad (3-8)$$

Where:

A is a transformation matrix

a, b, c are constants depending on the mean wind direction and member orientation

$\begin{pmatrix} \langle U(z,t) \rangle \\ 0 \\ 0 \end{pmatrix}$ is the vector representing the mean wind velocity over a period of time t and height z.

$\begin{pmatrix} U^1 \\ V^1 \\ W^1 \end{pmatrix}$ is the vector representing the fluctuation in the wind in along wind, lateral across wind and vertical across wind.

The latter equation represents the force coming on a member due to the fluctuating wind. These member forces can then be distributed on the degree of freedom (dof) at each node.

3.3.5 Spectral Relationships

Using the Fourier transformation, the cross-correlation function yields the cross-power spectral density function. The cross-power spectral density function of the forces between degree of freedoms r and s can therefore be obtained and referred to by $S_{gg}(r,s : \omega)$.

FRAMEWORK accounts for the variation in the mean wind speed with height using the power law as follows:

$$\mathbf{U}(z, t) = \mathbf{U}(10, t) \cdot \left(\frac{z}{10}\right)^\alpha \quad (3-9)$$

Where, α is an exponent depends on the terrain roughness.

FRAMEWORK uses the input dimensions of the points of interest from GeniE, and reads each joint's height above the reference elevation.

The cross-power spectra of the wind $S_{UU}(r,s : \omega)$ can be represented approximately in terms of the power spectral density of the wind $S_{UU}(\omega)$ and a coherence function $coh(r,s : \omega)$ as shown below.

$$\mathbf{S}_{UU}(r, s : \omega) = coh(r, s : \omega) \cdot \mathbf{S}_{UU}(\omega) \quad (3-10)$$

3.3.6 Mode Shape and Eigen Frequency of a Brace

FRAMEWORK uses the following method in estimating vortex induced vibration (VIV). FRAMEWORK treats braces as beam elements with end supports. The ends are treated as pinned,

hence restrained against lateral translation. Rotation is however allowed at the end of the brace and vary between each end unless end support is fully fixed.

(Timoshenko S.P, 1955) shows the classic equation for dynamic bending of a thin beam where shear deformations are neglected can be represented as shown below

$$EI \frac{\partial^4 w}{\partial x^4} = -m \frac{\partial^2 w}{\partial t^2} \quad (3-11)$$

Where:

E: young's modulus

I: the beam's second moment of area

w: transversal deflection

m: mass per unit length

x: co-ordinate along the beam's neutral axis

t: time

The previous fourth-order differential equation yields a general solution which can be shown as:

$$w = (A \cos kx + B \sin kx + C \cosh kx + D \sinh kx) \cos(\omega t + \varphi) \quad (3-12)$$

Where A, B, C and D are constants that can be found using the boundary conditions at beam ends.

ω is the natural frequency in rad/s.

φ is the phase angle.

$$k = \sqrt[4]{\frac{m\omega^2}{EI}}$$

For general support conditions with different rotational spring stiffnesses at the ends, the solution can be

$$K_0\{B + D\} = EIk\{-A + C\}K_L\{-A \sin kL + B \cos kL + C \sinh kL + D \cosh kL\} = EIk\{-A \cos kL - B \sin kL + C \cosh kL + D \sinh kL\} \quad (3-13)$$

K_0 and K_L are the rotational spring stiffnesses at $x = 0$ and $x = L$ respectively.

The solution of the previous equation gives the mode shape and frequency but not the amplitude.

This equation can yield infinite number of choices for kL that satisfies the above equation. However, it is usually the case that the first mode is of most significance.

This step is done using SESTRA to calculate the statical forces and reactions along with the eigen values and the eigen frequencies.

An example for the eigen modes and eigen frequencies is shown below. **Table 3-10** shows the global (flare structure) eigen modes as calculated in GeniE/SESTRA.

NO.	EIGENVALUE UNIT: (SEC) ⁻²	FREQUENCY UNIT: HERTZ	PERIOD UNIT: SEC
1	0.3435015E+02	0.933	1.07205
2	0.4692133E+02	1.090	0.91726
3	0.2714531E+03	2.622	0.38136
4	0.2838375E+03	2.681	0.37295
5	0.3894871E+03	3.141	0.31837
6	0.7010261E+03	4.214	0.23731
7	0.7590830E+03	4.385	0.22805
8	0.9260121E+03	4.843	0.20648
9	0.9357975E+03	4.869	0.20539
10	0.1058297E+04	5.178	0.19314

Table 3-10: Eigen values and eigen frequency with no weight factor

3.3.7 Calculation of Member End Damage

The damage may be higher at the center of the brace or at the end depending on the member end fixity at both ends.

Wind velocities that occur throughout the year are resolved into normal components for each brace member.

The statistical data on wind speeds, directions and probabilities of the year is decomposed into discrete ranges at constant speeds. The total structural damage is then formed by summing up all the damage induced by each wind speed range from each direction.

The damage from two opposing directions is identical. Therefore, the probabilities from opposing directions are added together as shown in the example below.

8 wind block	wind range							
	1	2	3	4	5	6	7	8
Direction	4 m/s	8 m/s	12 m/s	16 m/s	20 m/s	24 m/s	28 m/s	32 m/s
0°+180°	0.0224	0.0731	0.086	0.0486	0.0156	0.0034	0.0004	0
30°+210°	0.0218	0.0582	0.0525	0.0266	0.007	0.0011	0.0001	0
60°+240°	0.02	0.0445	0.0368	0.0195	0.0053	0.0012	0.0001	0
90°+270°	0.0198	0.0412	0.0296	0.0154	0.0046	0.0009	0	0
120°+300°	0.0204	0.0478	0.0349	0.0156	0.0045	0.0012	0.0001	0.0001
150°+330°	0.0226	0.0631	0.0634	0.0421	0.0199	0.007	0.0014	0.0002

Table 3-11: 8 wind blocks scatter diagram

Using the forcing frequency, the total time the wind blows during the year and the probability the total number of vibrations on each brace can be determined. The member stresses at the two nodal ends can be determined using the displacement amplitude and the mode shape.

The stresses mentioned above are the raw stresses. The local hot spot stresses are then found by multiplying the raw stresses by the stress concentration factors (SCF).

3.3.8 Stress Concentration Factors

As previously shown in **section 2.6**, stress concentrations are essential for estimation of fatigue damage in tubular members. The hot spot stresses (HSS) around the welded connection are assumed

to occur at the same place for each mode of response due to buffeting. For flare booms, this assumption is reasonable as the dominating mode of response is normally like that of a cantilever.

At each connection joint, the connecting members are considered as either chords or braces. The chord usually has the greatest diameter and thickness, while all other members are taken as braces. HSSs are then calculated for each connection separately for both chord-side and brace-side of the weld. This can be shown in **Figure 2-11**. This can be controlled by user input in cases where automatic assignment fails.

FRAMEWORK evaluates HSS at each joint by assigning it to one of three schemes: “I”, “E” and “O”.

The “I” and “O” schemes do not recognize an X-joint, while the “E” scheme includes X-joints using Efthymiou equations as explained previously.

In this thesis, “E” scheme has been chosen as it includes all types of connections: X, K, KT and T-joints.

3.3.8.1 Hot Spot Stress Transfer Function from Point Force

Using the model established in GENIE, a finite element model with its mass and stiffness is read by FRAMEWORK. Structural damping is given as a fixed value of 0.005 and it is used by FRAMEWORK to establish the dynamic equation of motion. This damping parameter is assumed to cover both structural and aerodynamic damping. (DNV - Framework User Manual, 2020)

Solving the equation of motion by accounting for the homogeneous part gives the eigenvectors and the eigenvalues. The structural mass and stiffness matrices are then used to establish the equation required to solve for structural displacement vector at each eigenmode at each degree of freedom (dof).

The displacement vector at the master’s degrees of freedom can be translated directly in member stresses. These stresses are then multiplied by stress concentration factors (SCF) to yield the hot spot stresses (HSS) at the joint of application.

3.3.9 Hot Spot Stress Power Spectra

After establishing the stress transfer function between a point load and hot spot stress, hot spot stress power spectrum at a joint can be established.

Hot spot is firstly described in time domain by using Fourier Transformation and convolution theorem. Summing over all the forces at each master’s degree of freedom, the total hot spot spectra at each point can be obtained.

3.3.10 Fatigue Life Calculation

3.3.10.1 Assumptions

- A quasi-static response with numerous separated sharp peaks at structural resonance characterizes the hot spot stress power spectrum.
- The integration of the area under these peaks represents the stress amplitude variation at the corresponding frequency.

- The narrow band stress amplitude within each frequency band follows a Rayleigh Distribution.
- The Palmgren-Miner rule relates fatigue to the number of cycles encountered in each stress range for each frequency band.
- The number of cycles at failure at any stress amplitude is related to DNV T SN curve found in (DNV RP-C203, 2019).

3.3.10.2 Evaluation of Damage

The Palmgren-Miner relationship (see **section 2.8**) is used to estimate the damage sustained due to stress cycles. Using the mentioned SN curve, annual damage for any frequency can be estimated.

As a result, the overall annual damage is the sum of the damages across all wind states and frequency bands.

3.4 WINDPACK Methodology

Like DNV SESAM FRAMEWORK, WINDPACK uses stochastic data to run dynamic analyses of wind buffeting using the power spectral density method.

WINDPACK requires input information of the eigenmodes, eigen frequencies and structural data along with statistical information about the wind distribution as scatter diagram with drag factors.

WINDPACK processes the input data as the annual wind states, then evaluates the response stress power spectra at each local hot spot at every joint.

To run a complete analysis, WINDPACK divides the process into 4 modules. Each module is used to perform different tasks that run in sequence as shown below.

WINDPRE: Generation of input to a stochastic analysis.

WINDSPEC: Calculation of the spectral moments.

WINDFOR: Calculation of dynamic deflection, forces and stresses.

WINDFAT: Calculation of fatigue damage. The SCF-factors are calculated according to Efthymiou. (AS, Aker Jacket Technology, 2022)

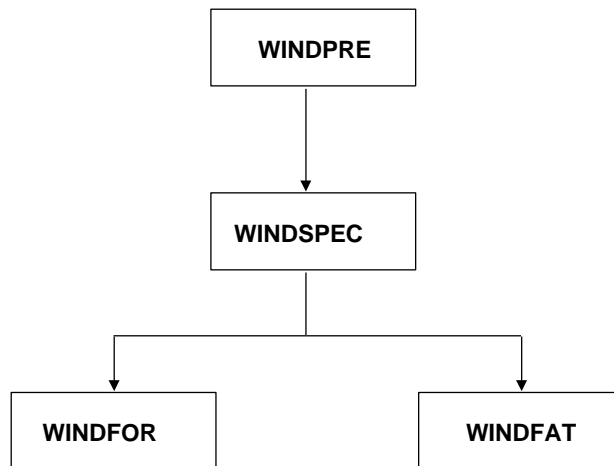


Figure 3-15: Flowchart of WINDPACK modules run sequence

3.4.1 Analysis Procedure

The steps of running WINDPACK can be explained as below:

1. The model for the space frame (Flare 1) is established in GeniE containing the geometry, member properties and material.
2. Sestra is used to run static analysis and generate eigenmodes, eigenvalues and eigen periods.

3. WINDPRE reads the eigenmodes and eigen periods as input along with the joints under investigation. Information about drag coefficients, structural and aerodynamic damping needs to be defined too.
4. Heading angle of the wind is also included as input for WINDPRE with the probability of each direction according to the provided Metocean data. (See **Table 3-2**)
5. WINDPRE gives different output data. Mass for each member is calculated on each of the sticknodes. Coordinated for sticknodes are also given as output along with the eigenvectors of sticknodes. Output data for wind heading angle, probability, drag coefficients used, and unit forces for the members. Sticknodes are defined in the model in GeniE, and they are the nodes in the space frame model which are required for spectral analysis.
6. The probability given for each wind heading direction angle is the summation of percentages for all windspeeds for the same direction angle.
7. WINDSPEC is then run with input about the spectra used. Duration of analysis is set as input along with the main spectra and the cross-correlation spectra.
8. Wind speed and its probability are defined in WINDSPEC. Wind speed given is long term distribution of the mean hourly speed 10 meters above sea level. The probability given for each windspeed is the summation of percentages for all wind direction angles for the same windspeed.
9. WINSPEC gives output data for the response spectra, spectral moments, and deflection levels. Wind loads on each sticknode is also printed.
10. WINDFOR is then used to compute the dynamic node forces and member forces in global coordinates. It also computes dynamic node deflections and von Mises stresses.
11. WINDFAT reads input data from WINDFOR and requires some data about SCFs and S-N curve to be used. The type of each joint under inspection should be defined as (Y, K, KT or X). For each joint, chord and braces should be defined.
12. WINDFAT calculates the stress spectra at each joint then applies SCFs. Palmgren-Miner rule is then used to calculate the total damage in relation to S-N curve.

3.4.2 Units

WINDPACK requires all input data to be in the unit system as shown below.

Length : Meters

Mass : Tonnes

Angles : Radians

Time : Seconds

3.4.3 Wind Speed and Direction Probabilities

WINDPACK separates the probability of wind speed and wind direction coming from scatter diagram and deals with each in separate modules as explained above.

- Wind speed probabilities are summed for each wind direction and then used as input in WINDPRE.
- Wind direction probabilities are summed for each wind speed and then used as input in WINDSPEC.

An example of how the scatter diagram is used in WINDPACK is shown below.

m/s \ deg	0°	30°	60°	90°	120°	150°	180°	210°	240°	270°	300°	330°	Sum	
4		1.17	1.16	0.98	0.96	1.00	1.09	1.07	1.02	1.03	1.02	1.04	1.17	12.71
8		3.59	2.55	1.44	1.33	2.03	3.03	3.72	3.27	3.01	2.79	2.75	3.28	32.79
12		4.02	1.78	0.36	0.41	1.26	3.37	4.58	3.47	3.32	2.55	2.23	2.97	30.32
16		2.05	0.75	0.08	0.13	0.65	2.72	2.81	1.91	1.87	1.41	0.91	1.49	16.78
20		0.44	0.12	0.00	0.01	0.16	1.51	1.12	0.58	0.53	0.45	0.29	0.48	5.69
24		0.10	0.01	0.00	0.00	0.04	0.59	0.24	0.10	0.12	0.09	0.08	0.11	1.48
28		0.01	0.00	0.00	0.00	0.01	0.13	0.03	0.01	0.01	0.00	0.00	0.01	0.21
32		0.00	0.00	0.00	0.00	0.00	0.01	0.00	0.00	0.00	0.00	0.01	0.01	0.03
Sum		11.38	6.37	2.86	2.84	5.15	12.45	13.57	10.36	9.89	8.31	7.31	9.52	

Table 3-12: Scatter diagram of 8 wind blocks showing the input in WINDPACK

Table 3-12 shows the scatter diagram of 8 wind blocks. Each of the rows represents the probability in percentage of wind speed. The sum of all directions for each wind speed is used as input percentage in WINDSPEC.

Each column represents the probability in percentage of wind heading angle. The sum of all wind speeds for each wind heading angle is used as input percentage in WINDPRE.

3.4.4 Wind Turbulence Spectra

Similar to FRAMEWORK, in WINDPACK, for each wind state, wind speed at a height reference of 10 m above sea water level is used to calculate single-sided gust spectrum.

WINDPACK gives the option of choosing between one of the following spectra for representation of the gust in the same direction as the mean wind:

- HARRIS spectra

$$S(\omega) = \frac{V_{10}^2 \cdot 4 \cdot \kappa}{\omega} \cdot \frac{x}{(2 + x^2)^{\frac{5}{6}}}, \quad x = \frac{L \cdot \omega}{V_{10}} \quad (3-14)$$

- DAVENPORT spectra

$$S(\omega) = \frac{V_{10}^2 \cdot 4 \cdot \kappa}{\omega} \cdot \frac{x^2}{(1 + x^2)^{\frac{4}{3}}}, \quad x = \frac{L \cdot \omega}{V_{10}} \quad (3-15)$$

Where,

V_{10} : Windspeed 10 meter above sea level

κ : Ground roughness parameter (for rough open water $\cong 0.003$)

- L : Integral scale length for main wind direction (for rough open water $\cong 1200 \rightarrow 1800$ meter).
- ω : Wind turbulence frequency.

In this thesis, gust spectra are simulated using HARRIS spectra as WINDPACK does not give the option of using Frøya wind spectra from NPD. As stated previously, Frøya wind spectra are best suited for offshore conditions. Therefore, for more reliable results, a comparison between WINDPACK and FRAMEWORK should be held using the same spectra

WINDPACK uses PANOFSKY LATERAL spectra and PANOFSKY VERTICAL spectra for the horizontal and vertical crosswind component of the gust, respectively.

- Wind turbulence spectra in the lateral direction

$$S(\omega) = \frac{V_{10}^2 \cdot 15 \cdot \kappa}{\omega} \cdot \frac{x}{(1 + 9.5x)^{\frac{5}{3}}}, \quad x = \frac{Z \cdot \omega}{V_{10}} \quad (3-16)$$

- Wind turbulence spectra in the vertical direction

$$S(\omega) = \frac{V_{10}^2 \cdot 3.36 \cdot \kappa}{\omega} \cdot \frac{x}{(1 + 10.0x)^{\frac{5}{3}}}, \quad x = \frac{Z \cdot \omega}{V_{10}} \quad (3-17)$$

3.4.5 Stress Concentration Factors (SCFs)

SCFs in WINDPACK are calculated using Efthymiou equations as explained in section 2.7.1.

The terminology for SCFs in WINDPACK is different than that in FRAMEWORK and USFOS. WINDPACK uses the naming system as shown below.

- scs_ax: Axial loading SCF on the chord side at the saddle location.
- scc_ax: Axial loading SCF on the chord side at the crown location.
- sbs_ax: Axial loading SCF on the brace side at the saddle location.
- sbc_ax: Axial loading SCF on the brace side at the crown location.
- sc_ipb: In plane bending SCF on the chord side at the crown location.
- sc_opb: Out of plane bending SCF on the chord side at the saddle location.
- sb_ipb: In plane bending SCF on the brace side at the crown location.
- sb_opb: Out of plane bending SCF on the brace side at the saddle location.

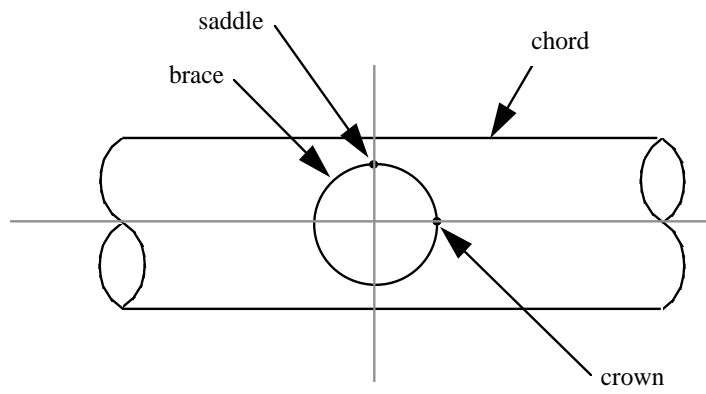


Figure 3-16: Location of saddle and crown as defined in WINDPACK

3.5 USFOS/FATAL Methodology

USFOS is one of DNV SESAM package's software and uses time domain approach to perform a full nonlinear dynamic analysis for the flare boom under the effect of wind buffeting.

To account for mean wind forces from different directions, crosswind interaction and the probability, wind speeds and directions are put in a matrix combining each direction and wind speed with its correlating probability. This correlates to the scatter diagrams shown before in **Table 3-2**. USFOS uses specific input data such as detailed wind fields for the location of interest around the year, the structure model including all the materials and cross-sections and the drag factors. Then a nonlinear dynamic analysis is run to give the resulting stresses of all members and joints.

DNV SESAM FRAMEWORK is only used in evaluation of the stress concentration factors at each of the specified points where fatigue is required to be checked.

FATAL is also included in the SESAM package and uses the time domain rain flow cycle counting method for estimation of fatigue accumulated damage on complex structures. Hotspot stress is calculated at each joint by FATAL using the input SCFs and the output stresses from USFOS. Rain flow cycle counting method (see **section 2.5.1**) is then used by FATAL to derive fatigue induced damage on each joint included in the analysis from input. FATAL then uses DNV T-air S-N curve data (see **section 2.7.1**). The damages calculated on each joint is due to 100% probability from all directions. Therefore, FATAL POST is used to factor down damage from each wind load case by multiplying with the correlating probability.

Figure 3-17 below shows a flowchart of how this methodology works.

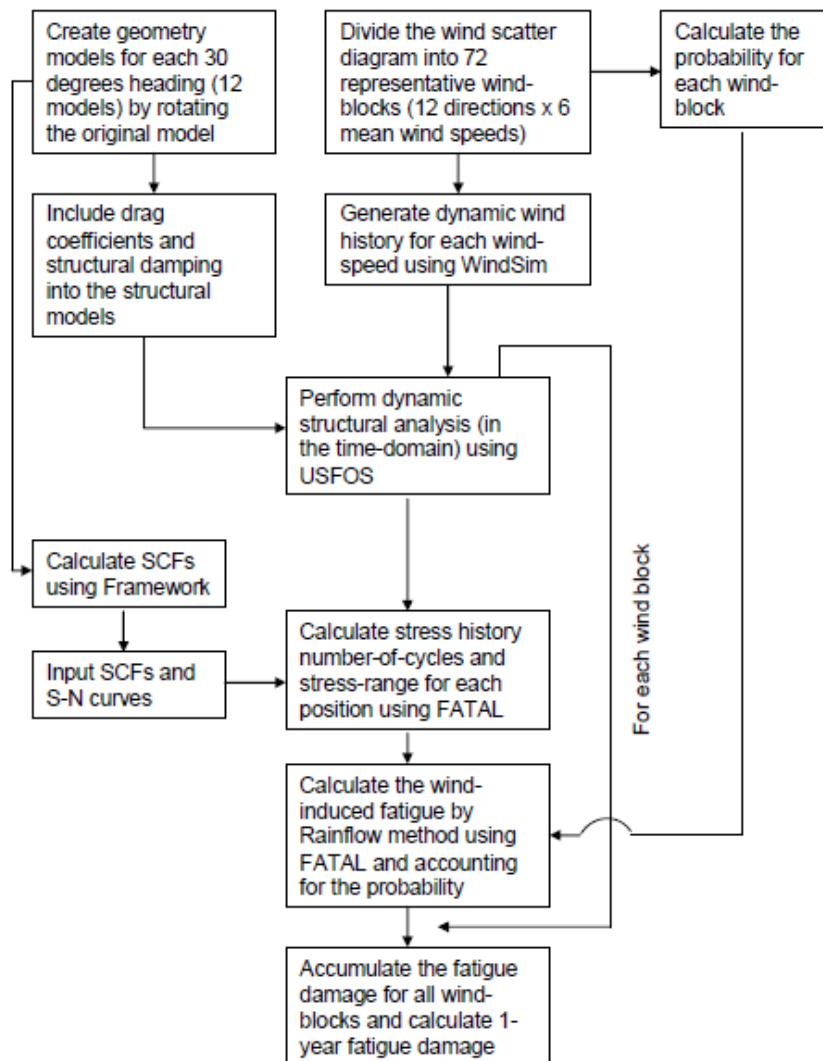


Figure 3-17: USFOS fatigue methodology, flow chart example

3.5.1 Structural Model

As mentioned previously, USFOS performs several dynamic analyses on all selected joints. Changing the wind field direction in USFOS input may result in non-physical cross correlation. Therefore, 12 structural models are used with the same wind fields while rotating the structure 30° degrees counterclockwise to account for the 12 different wind directions in the scatter diagram. (See **Table 3-2**).

The flare boom is modelled using either GeniE or Preframe, which also are parts of SESAM Package. The model must then be converted to USFOS file format in the USFOS utility program StruMan before dynamic analysis can be done in USFOS. For fatigue analysis, StruMan converts dead- and live-loads into point masses. This could also be done directly in USFOS in recent versions.

The structural model gives details for joint coordinates, member cross-sections, material used and the supporting case for each point.

All dimensions are in SI units.

To account for the flare boom orientation with respect to the geographical north, all 12 models used are rotated 45° degrees to the west.



Figure 3-18: USFOS Model showing the rotation of the flare boom

3.5.2 Wind Fields

To subject the structure wind loading on the structure, simulated wind fields are generated by the program WINDSIM. The wind simulations assumes that the wind speed can be split into a mean wind and a fluctuating part (AAS_JAKOBSEN - WindSim User manual, 2020). One wind field should be generated for each wind block in the Metocean data, and the mean wind speed varies with the given wind profile equation, and the fluctuating part is simulated with coherent wind spectra and coherence functions.

The following formulas have been used to simulate wind fields:

For the mean wind speed part:

$$U(z, t) = U(z) * \left[1 - 0.41 * I_u * \ln \frac{t}{t_0} \right] \quad (3-18)$$

$$U(z) = U_0 * \left[1 + C * \ln \frac{z}{10} \right], \text{ where } C = 0.0573 * [1 + 0.15 * U_0]^{0.5} \quad (3-19)$$

$$I_u = 0.06 * [1 + 0.043 * U_0] * \left(\frac{z}{10} \right)^{-0.22} \quad (3-20)$$

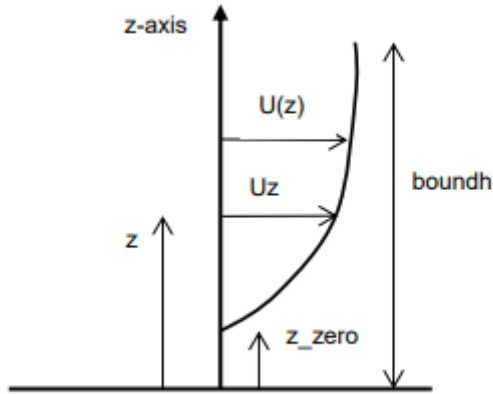


Figure 3-19: Wind profile for simulating wind fields (AAS_JAKOBSEN - WindSim User manual, 2020)

For the fluctuating part:

$$S(f) = \frac{320 * \left(\frac{U_0}{10} \right)^2 * \left(\frac{z}{10} \right)^{0.45}}{(1 + \tilde{f}^n)^{\frac{5}{3n}}} \quad (3-21)$$

$$\tilde{f} = 172 * f * \left(\frac{z}{10} \right)^{\frac{2}{3}} * \left(\frac{U_0}{10} \right)^{-0.75} \quad (3-22)$$

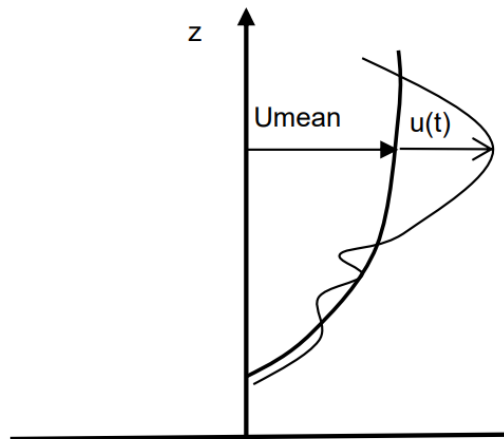


Figure 3-20: Frøya Spectrum for simulating fluctuating wind (AAS_JAKOBSEN - WindSim User manual, 2020)

With a given time increment, simulation length and input the program simulates a varying wind speed in specified grid coordinates over time. The wind grid size specifies the amount of wind speed vector points in the simulation.

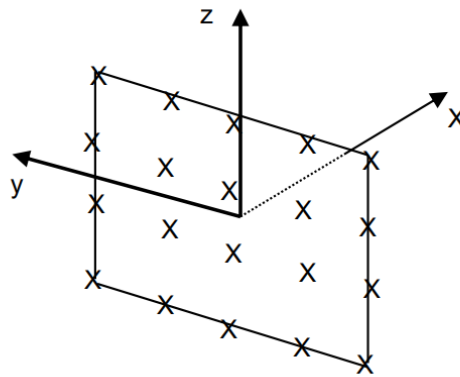


Figure 3-21: Wind grid

In this thesis existing wind fields from previous analysis are used, which were provided to Aker by an external contractor.

Wind fields configurations are parameters which will affect fatigue life. The only parametric study done with wind fields in this thesis is varying which wind fields are included in the analysis, with corresponding probability. (As explained in **3.2.2**)

3.5.3 Dynamic Analysis (USFOS)

USFOS requires a Finite element structural model (FEM file), a command file where specifics for the analysis is set and a simulated wind field file to perform a wind-induced dynamic analysis. One analysis should be done for each wind field in all directions to cover all load combinations coming from all directions and wind speeds.

The key parameters to be specified in the analysis input are:

- All joints or groupings that should be analyzed. Joint 198 is not included in the fatigue analysis. This is attributed to the fact that this joint is difficult to weld on-site and might be a pre-cast connection.
- Simulation length (EndT) is given in seconds. The accumulated fatigue damage is relative to the length of the simulation. To accurately estimate wind gusting turbulence, the length of the simulation should be around 1-hr as recommended by (DNV RP-C203, 2019). However, for making the analysis less computationally demanding, simulation length is set to 2000 s instead of the 3600 s. The difference between both cases is tested on one of the cases and yields a difference within 5% in fatigue life as stated previously. (See **section 3.2.1**)

- Time increment (dT) given in seconds, which specifies how often structural response should be recorded. The smaller this value is, the more accurate the time history graph will represent the full structural response. However, very small is more computationally demanding. A balance is therefore desirable. As a rule of thumb, time increments are chosen to fall within the range of $\pm 10\%$ of the first eigenvalue. Two time-steps are hence chosen for this model: 0.1 sec and 0.05 sec. (See **section 3.2.1**)
- Wind load requires information about drag factor. Drag factor differs according to the wind speed and Reynold's number as stated previously (see **section 3.2.3**). To test the effect of different drag factors, 4 different drag coefficients are chosen: 0.65, 1, 1.2 and Reynold's number dependent. Drag factor is used as a parameter only on tubular members, while set to be zero on all nontubular members in all cases.
- During dynamic analysis, abrupt changes in wind load may be interpreted as a transient short duration impact load giving inaccuracy in results. For the case of Reynold's number dependent Cd, a built-in function (SyrupCd) is used to prevent abrupt changes in Cd, hence abrupt changes in wind load. Abrupt changes in Cd may give inaccurate dynamic response as the structure may then react similarly to that of a dynamic impact load.
- (Rel_Velo) is a function that accounts for the effect of relative wind velocity as in dynamic structures. As stated previously the effect of this phenomenon is tested by setting it on/off. (See **section 3.2.6**)
- Damping ratio, which is given in percentage is not used as a parameter in this thesis and set to a value of 0.005 in all cases.

USFOS then runs analysis where it subjects the structure to the simulated wind field and stores the dynamic structural responses in time history based on specified number of time increments (dT) on every structural member. The member responses of importance in fatigue analysis are the axial, in-plane bending stress and out-of-plane bending stress. These are the stresses required for calculating the 8 hot spot stresses in both brace and chord. (See **section 2.6.1**)

An example on the stress history from USFOS analysis is shown in **Figure 3-22**.

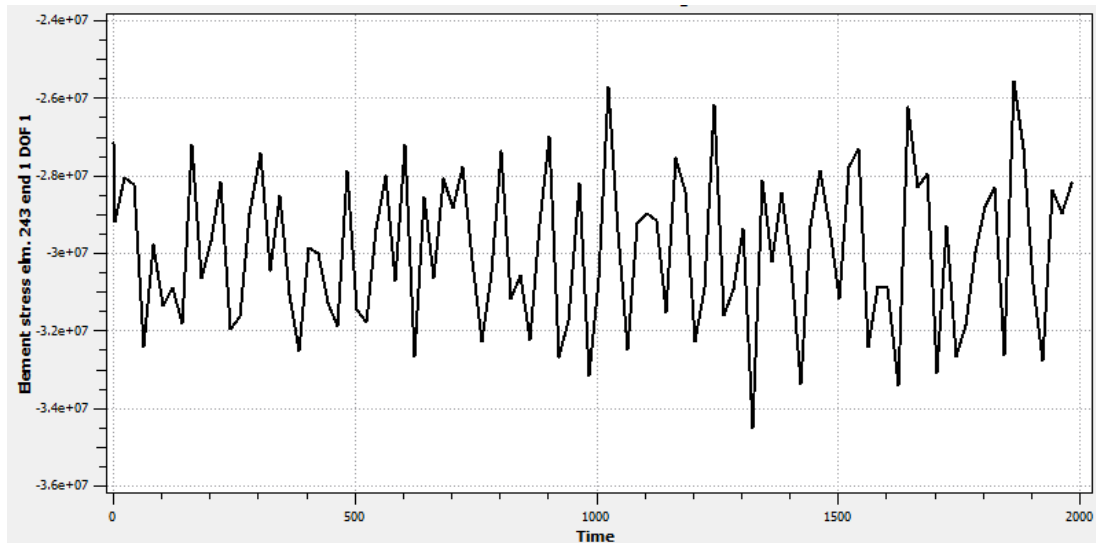


Figure 3-22: Axial stress history of element 243 end 1 example

3.5.4 SCF Calculation

SCF is defined for each point in the analysis using FRAMEWORK. FRAMEWORK uses Efthymiou equations to calculate SCF as shown previously. (See section 2.6.1).

SCFs must be defined for axial and bending stresses in saddles and chords, in both brace- and chord side. For comparing software, the SCFs are derived in FRAMEWORK and equal to those used in the FRAMEWORK analysis.

3.5.5 Cycle Counting (FATAL)

USFOS analysis yields results in output files in “.dyn” extension that can be read by FATAL.

FATAL requires an input file with information about SCFs and S-N curve used.

The S-N curve for tubular joint (DNV T-Air) found in (DNV RP-C203, 2019) is used as a user defined S-N curve in this analysis.

With the use of rain flow cycle counting and the Miner-Palmgren method damage is calculated at 8 stress points around the joint for all load cases. The damage is then scaled to yearly damage according to the simulation length.

The final step goes through FATAL Post, where every load case is factored with its corresponding annual probability. The input needed is therefore the scatter diagram matrix. Finally, the damage from all cases is added.

The joints are then sorted by largest to lowest fatigue damage. Fatigue life can be found by deriving the inverse of yearly damage. The 5 most critical damage points are used in comparison.

4 Wind-induced Fatigue Analysis Using FRAMEWORK

This chapter presents **fatigue life** results for load combinations coming from different parameters, as discussed before, done in FRAMEWORK. A total of **48** analyses have been done categorized into **3** different **wind blocks** cases, **4** different **drag coefficients (Cd)** cases and 4 different **weight factor** cases. (See **section 3.2**)

4.1 Results Tables

The **fatigue life** results from the **5 most critical joints** are presented in the following tables, with the most **critical fatigue life** highlighted in the first cell under the name (**Crt Ftg Life**). The parameters on the left side describe the corresponding load case.

- Joints shown in black in the table correspond to those in black font in the table header.
- Joints shown in yellow correspond to those in yellow in the table header.
- Joints shown in green correspond to joint 602080. (See **Figure 3-3**)
- Joints shown in blue correspond to joint 351540. (See **Figure 3-3**)

8 wind blocks:

Wind Blocks	Cd	wt factor	FRAMEWORK (Fatigue life / years)					
			Crt Ftg Life	jt 101020	jt 103520	jt 552080 / 352540	jt 602080 / 552080	jt 552080 / 351540
8	0.65	0.5	564.1	564	626	45037	101273	104163
		1	331.4	331	343	44801	53107	55356
		1.1	194.7	195	201	23313	27565	28722
		1.5	130.7	131	133	13255	15578	16217
	1	0.5	130.6	131	145	8564	18968	19660
		1	56.9	57	59	5327	6288	6547
		1.1	50.9	51	53	4496	5289	5504
		1.5	35.8	36	37	2638	3076	3197
	1.2	0.5	42.4	42	47	2259	4799	5092
		1	28.5	29	30	2237	2627	2733
		1.1	18.1	18	19	1228	1433	1489
		1.5	13.2	13	14	749	865	899
	Reynold's	0.5	381.5	381	424	26387	63846	56406
		1	230.5	230	239	28991	34330	35747
		1.1	137.3	137	142	15124	17857	18586
		1.5	93.6	94	96	8662	10161	10565

Table 4-1: All results with 8 wind blocks in FRAMEWORK

10 wind blocks:

Wind Blocks	Cd	wt factor	FRAMEWORK (Fatigue life / years)					
			Crt Ftg Life	jt 101020	jt 103520	jt 552080 / 352540	jt 602080 / 552080	jt 552080 / 351540
10	0.65	0.5	221.4	221	239	12908	31102	17434
		1	145.0	145	149	13657	16075	16760
		1.1	92.7	93	95	7139	8386	8740
		1.5	67.8	68	69	4149	4847	5047
	1	0.5	44.8	45	48	2981	3643	4474
		1	31.3	31	32	1673	1948	2027
		1.1	20.5	20	21	937	1080	1122
		1.5	15.3	15	16	603	686	712
	1.2	0.5	23.6	24	25	1355	1505	1795
		1	16.7	17	17	744	856	889
		1.1	11.0	11	11	438	499	517
		1.5	8.3	8	9	295	332	343
	Reynold's	0.5	158.3	158	171	13345	20465	24393
		1	106.3	106	110	8909	10483	10919
		1.1	68.5	69	71	4681	5490	5716
		1.5	50.4	50	51	2759	3211	3339

Table 4-2: All results with 10 wind blocks in FRAMEWORK

12 wind blocks:

Wind Blocks	Cd	wt factor	FRAMEWORK (Fatigue life / years)					
			Crt Ftg Life	jt 101020	jt 103520	jt 552080 / 352540	jt 602080 / 552080	jt 552080 / 351540
12	0.65	0.5	432.5	433	481	13540	77363	80535
		1	245.6	246	254	35652	42246	44059
		1.1	140.7	141	145	18537	21910	22844
		1.5	91.9	92	94	10499	12337	12852
	1	0.5	63.6	64	70	3985	9107	9377
		1	39.6	40	41	4220	4984	5192
		1.1	24.5	25	25	2246	2639	2748
		1.5	17.6	18	18	1317	1534	1596
	1.2	0.5	30.1	30	33	1862	3748	3805
		1	19.8	20	21	1756	2066	2151
		1.1	12.7	13	13	952	1113	1159
		1.5	9.4	9	10	569	660	686
	Reynold's	0.5	292.0	292	325	19806	43020	52157
		1	169.7	170	176	23281	27557	28716
		1.1	98.6	99	102	12129	14317	14914
		1.5	65.7	66	67	6910	8107	8437

Table 4-3: All results with 12 wind blocks in FRAMEWORK

4.2 Result Graphs

This chapter presents **fatigue life for the most critical joint** and how it varies with different parameter changes. One parameter will be fixed and thereby case dependent, while the other parameters are either shown on the x-axis or presented on different graphs.

The shapes of the curves are simplified and should not be interpreted too precise, but rather give an indication of trends. Interpolation between different points shall not be used and will not give accurate representation of reality. More data points would be required to simulate precise reliable curve representation.

All **fatigue life** results correlate with the most critical **fatigue life** in **Table 4-1**, **Table 4-2** and **Table 4-3** and all load cases are presented.

4.2.1 Fatigue life against weight factor for different drag coefficient values

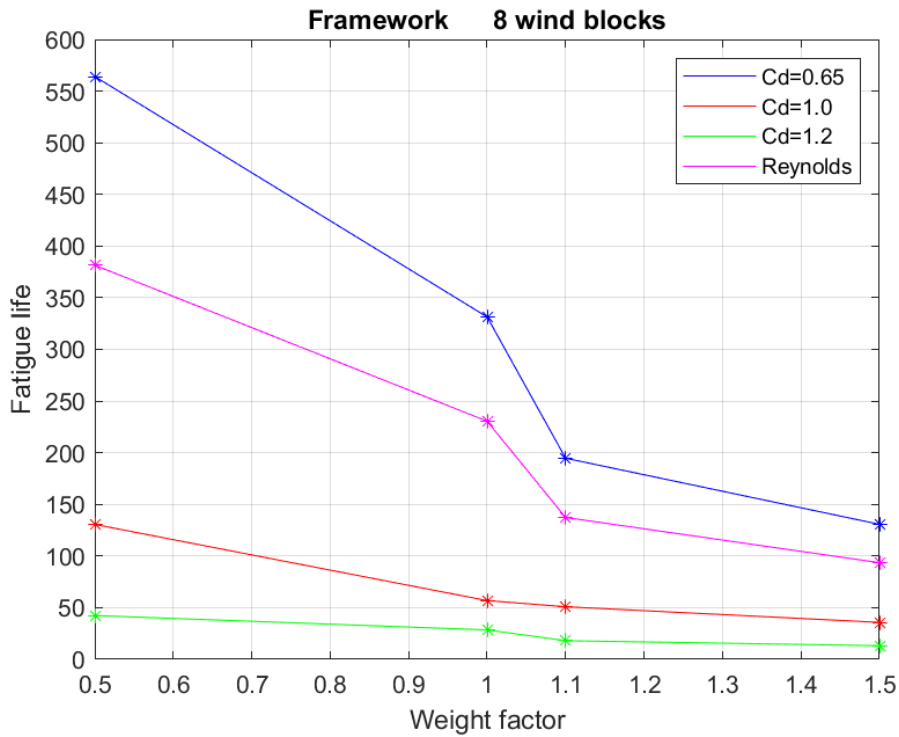


Figure 4-1: Fatigue life against weight factor with 8 wind blocks for different Cd values (FRAMEWORK)

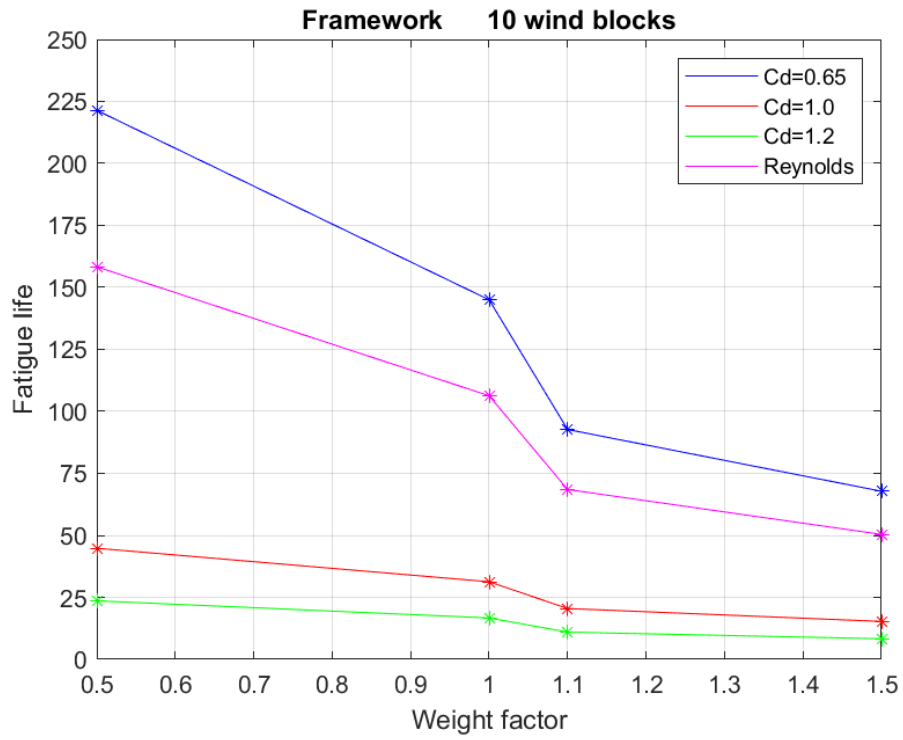


Figure 4-2: Fatigue life against weight factor with 10 wind blocks for different Cd values (FRAMEWORK)

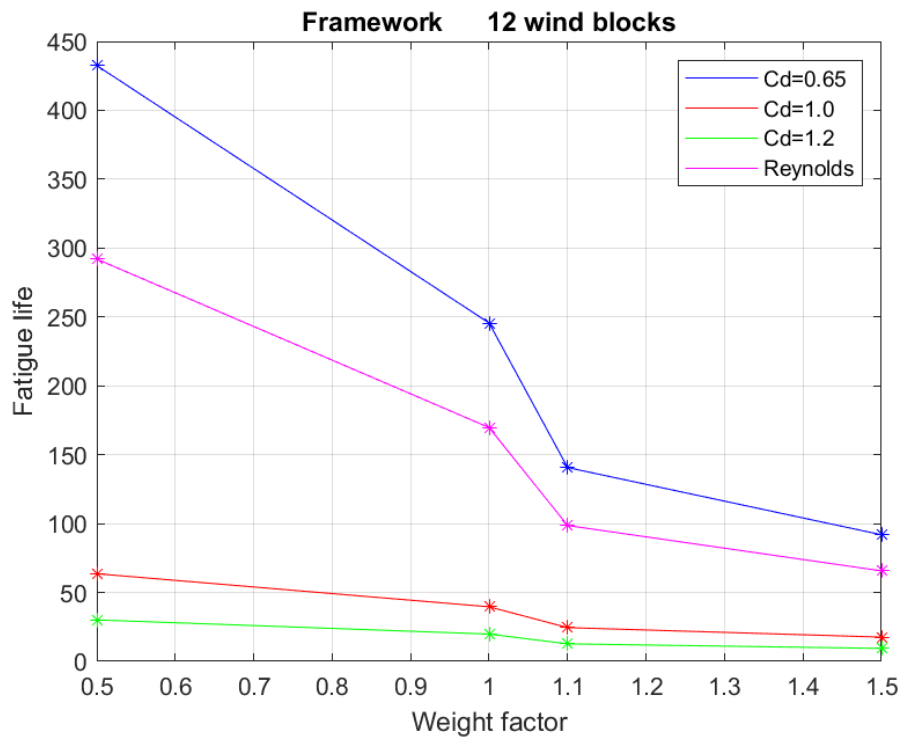


Figure 4-3: Fatigue life against weight factor with 12 wind blocks for different Cd values (FRAMEWORK)

Figure 4-1, Figure 4-2 and Figure 4-3 show variation in **fatigue life** with varying **weight factor** for all variations of **Cd** for the **8, 10 and 12 wind blocks** load cases. The following observations are made:

- **8 wind block** results give longest **fatigue life** overall, and **10 wind block** results give the lowest.
- **Fatigue life** seems to be most sensitive to change in **weight factor** range between **1.0** and **1.1**.
- The lower values of **Cd** seem to be more sensitive to change in **weight factor**. A **30% decrease** in **fatigue life** can be noticed between **weight factor 0.5** and **1.0** in all **wind blocks**.
- The graph for **Cd=0.65** and the **Reynold's** dependent is almost identical in shape.
- The **Reynold's** dependent case gives a higher **fatigue life** than **Cd=1.0** by **60%**, but around **50%** lower than **Cd=0.65** in all **wind blocks**.

4.2.2 Fatigue life against drag coefficient for different weight factor values

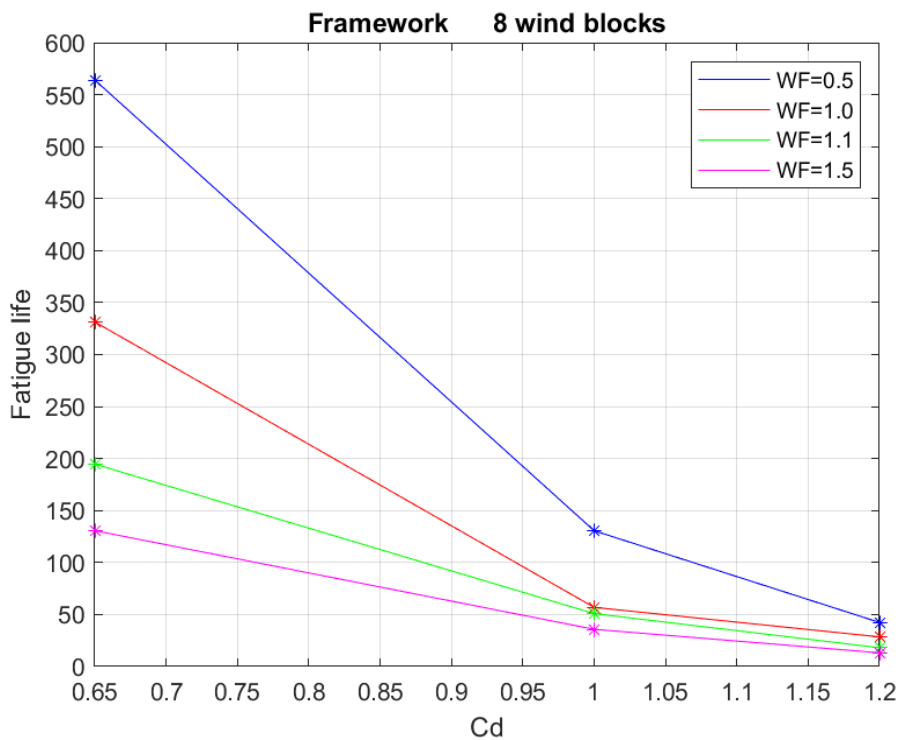


Figure 4-4: Fatigue life against Drag coefficient with 8 wind blocks for different weight factor values (FRAMEWORK)

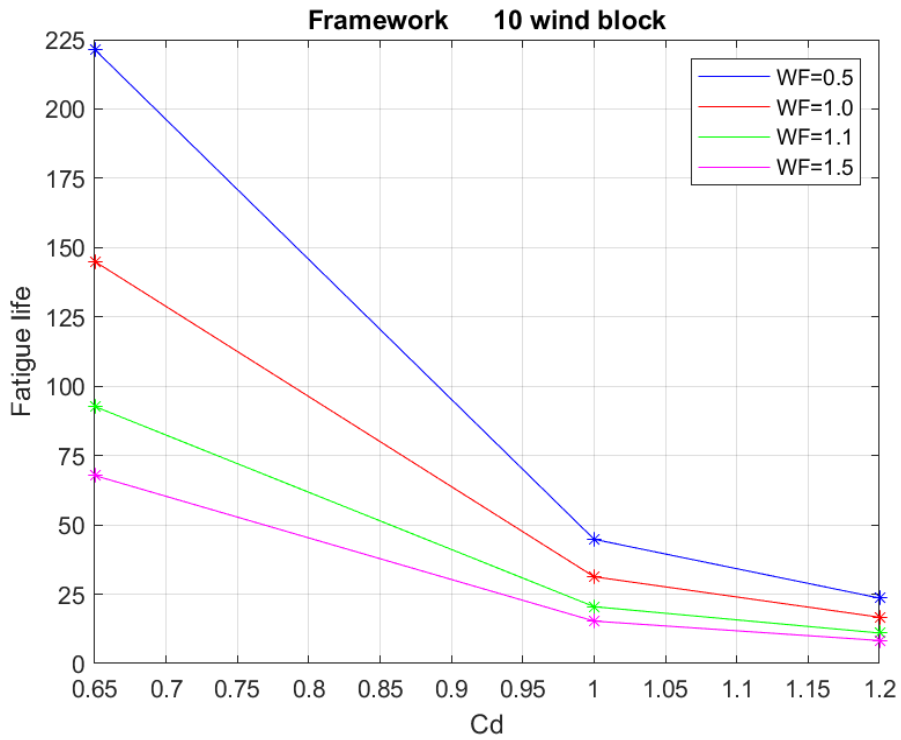


Figure 4-5: Fatigue life against Drag coefficient with 10 wind blocks for different weight factor values (FRAMEWORK)

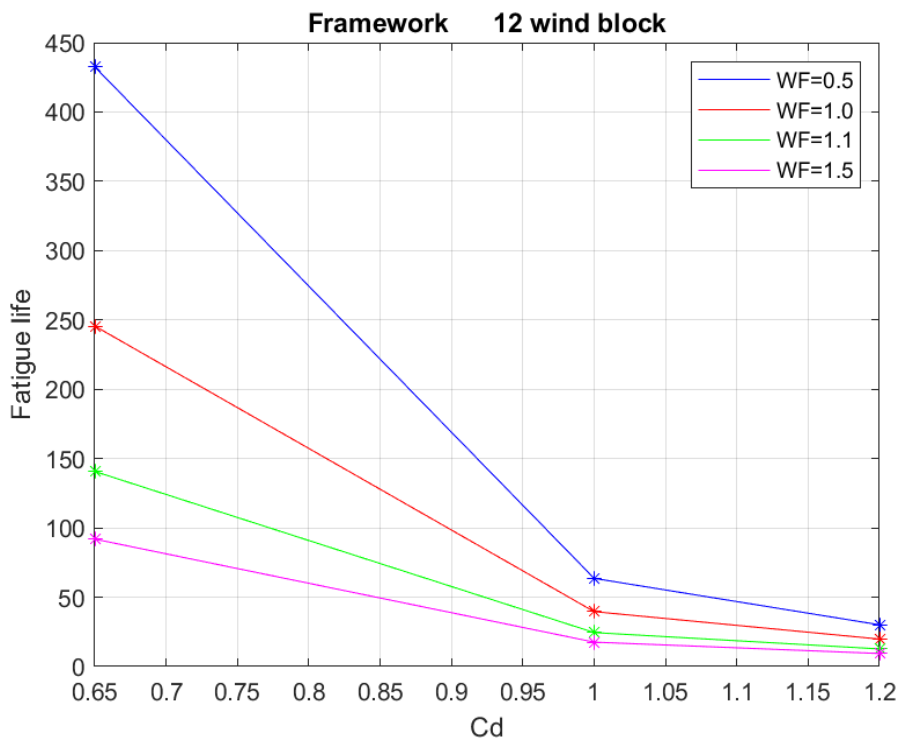


Figure 4-6 Fatigue life against Drag coefficient with 12 wind blocks for different weight factor values (FRAMEWORK)

Figure 4-4, Figure 4-5 and Figure 4-6 show variation in **fatigue life** with variation of **Cd** for all 4 cases of **weight factors** for the **8, 10 and 12 wind block** cases.

Reynold's-dependent drag coefficient is excluded from these graphs as it depends on different values of drag coefficient according to the joint location and the projected wind speed.

The following observations are made:

- **8 wind block** cases give longest **fatigue life** overall, and **10 wind block** cases the lowest overall.
- The trend in all graphs seems to be that **fatigue life** is less sensitive to change in **Cd** after **1**.
- The variation of **Cd** seems to have more impact on **fatigue life** with lower **weight factor**. **Fatigue life** decreases **93%** from **Cd 0.65** to **Cd 1.2** for **weight factor** of **0.5**, while it decreases **82%** from **Cd 0.65** to **Cd 1.2** for **weight factor 1.5**.
- For lower **weight factors**, the drop in **fatigue life** is steeper with increase in **Cd**. **Fatigue life** for **weight factor 0.5** drops from **432.5 years** at **Cd 0.65** to **63.6 years** at **Cd 1.0**, while it drops for **weight factor 1.5** from **91.9 years** to **17.6 years**.

4.2.3 Fatigue life against weight factor for different wind blocks

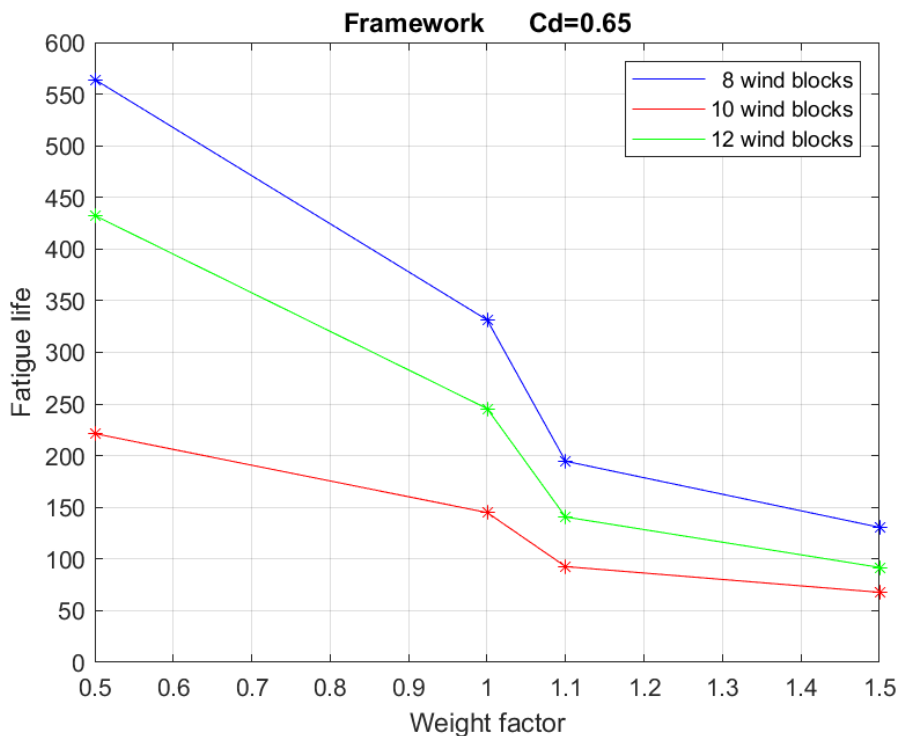


Figure 4-7: Fatigue life against weight factor with Cd=0.65 for different wind block cases (FRAMEWORK)

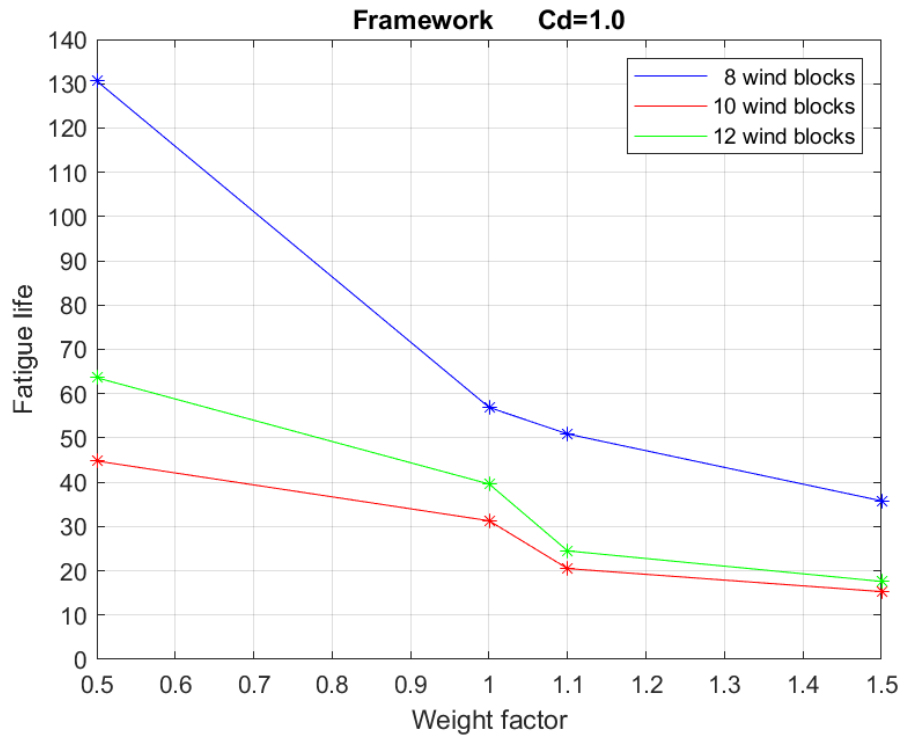


Figure 4-8: Fatigue life against weight factor with Cd=1.0 for different wind block cases (FRAMEWORK)

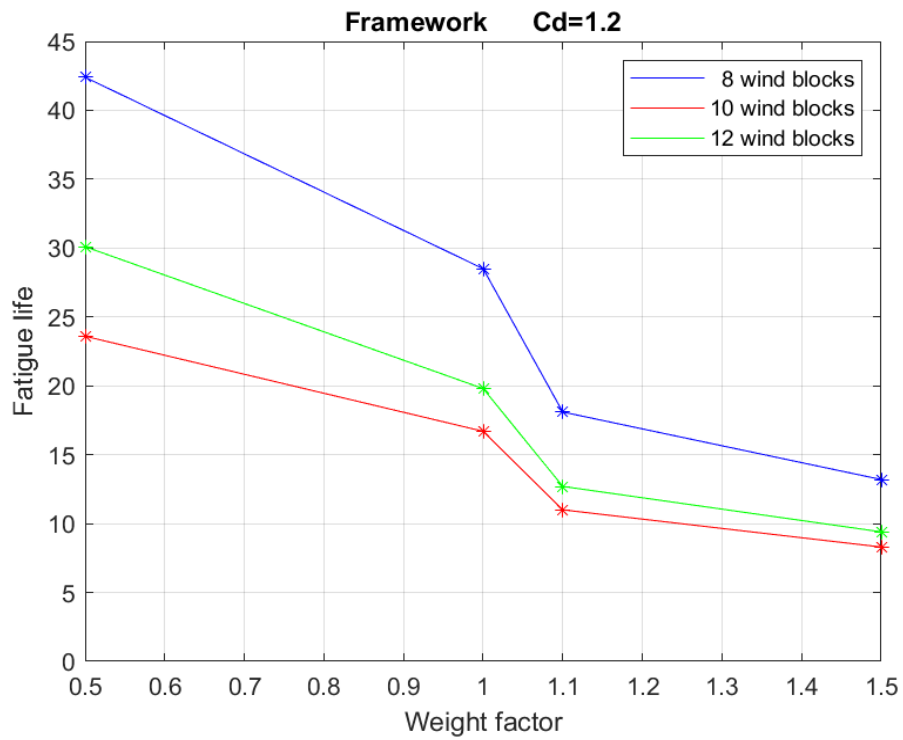


Figure 4-9: Fatigue life against weight factor with Cd=1.2 for different wind block cases (FRAMEWORK)

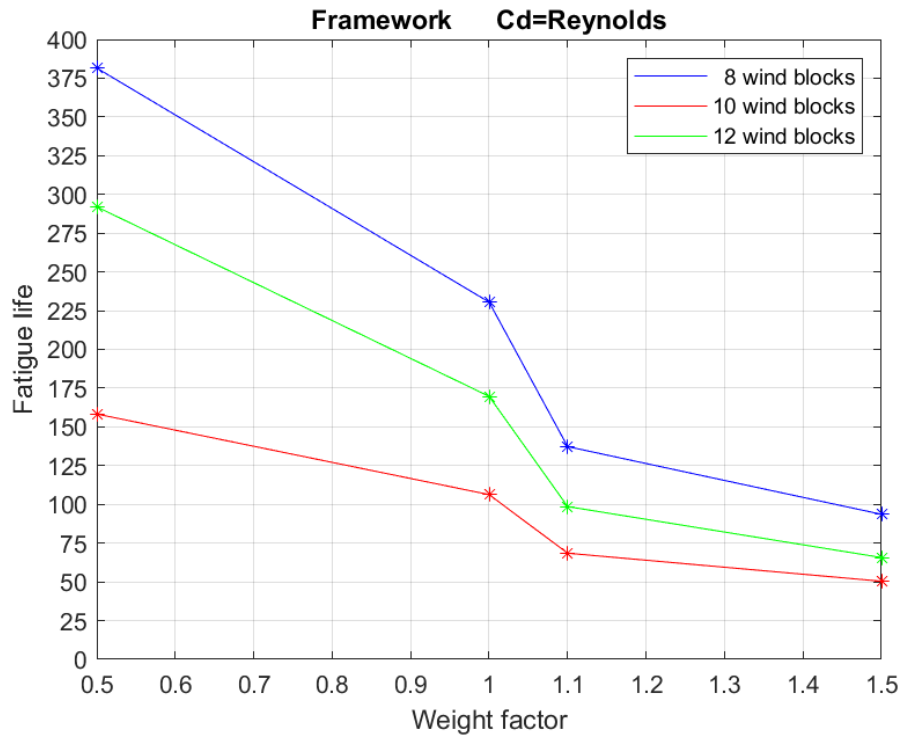


Figure 4-10: Fatigue life against weight factor with Reynold's dependent Cd for different wind block cases (FRAMEWORK)

Figure 4-7, Figure 4-8, Figure 4-9 and Figure 4-10 show variation in **fatigue life** with change in **weight factor** for all **wind block** cases for fixed **Cd** value cases.

The following observations are made:

- **Fatigue life** results seem to be most sensitive to change in **weight factor** from **1** to **1.1** in most cases.
- The **8 wind blocks** case seems to be overall the most sensitive to change in **weight factor**. A drastic **decrease of 80%** shown in case of **8 wind blocks** and **12 wind blocks**, while the case of **10 wind blocks** decreases by **68%**.
- Both the cases of **8 wind blocks** and **12 wind blocks** give similar trends of decrease in **fatigue life** with the increase of **weight factor** from **0.5** to **1.0**.
- The **8 wind blocks** case always give the highest **fatigue life** in all cases, and the **10 wind blocks** case always give the lowest.

4.2.4 Fatigue life against drag factor for different wind blocks

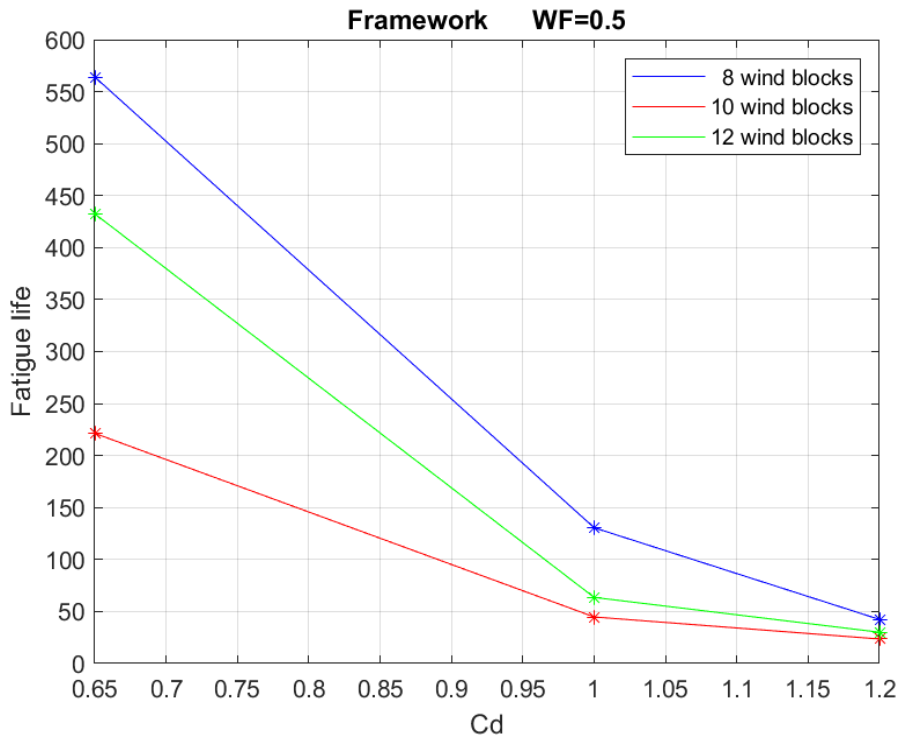


Figure 4-11: Fatigue life against Cd with weight factor 0.5 for different wind block cases (FRAMEWORK)

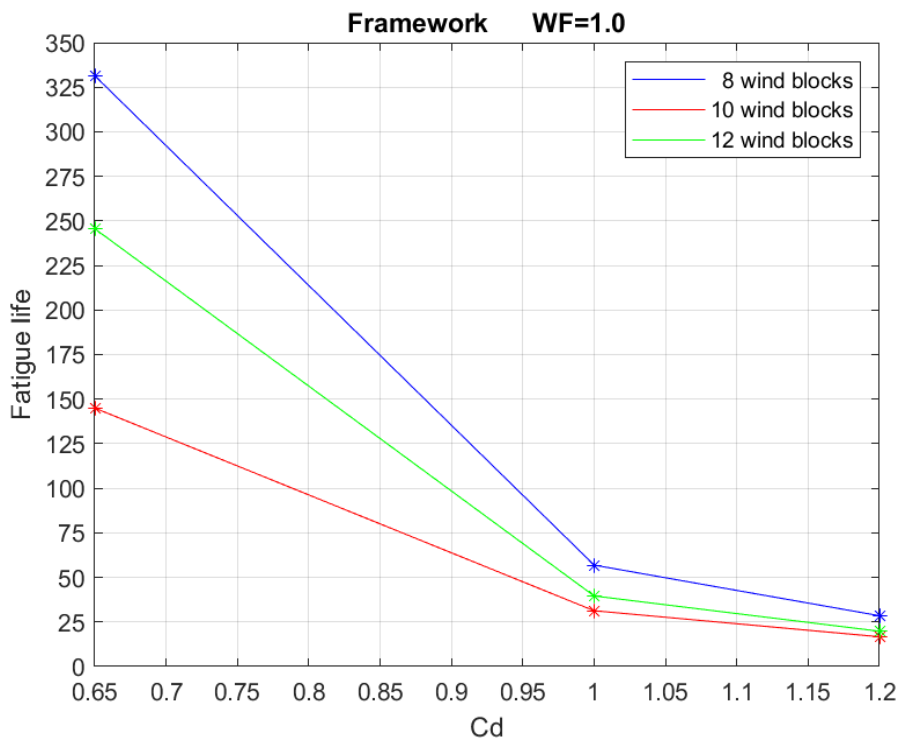


Figure 4-12: Fatigue life against Cd with weight factor 1.0 for different wind block cases (FRAMEWORK)

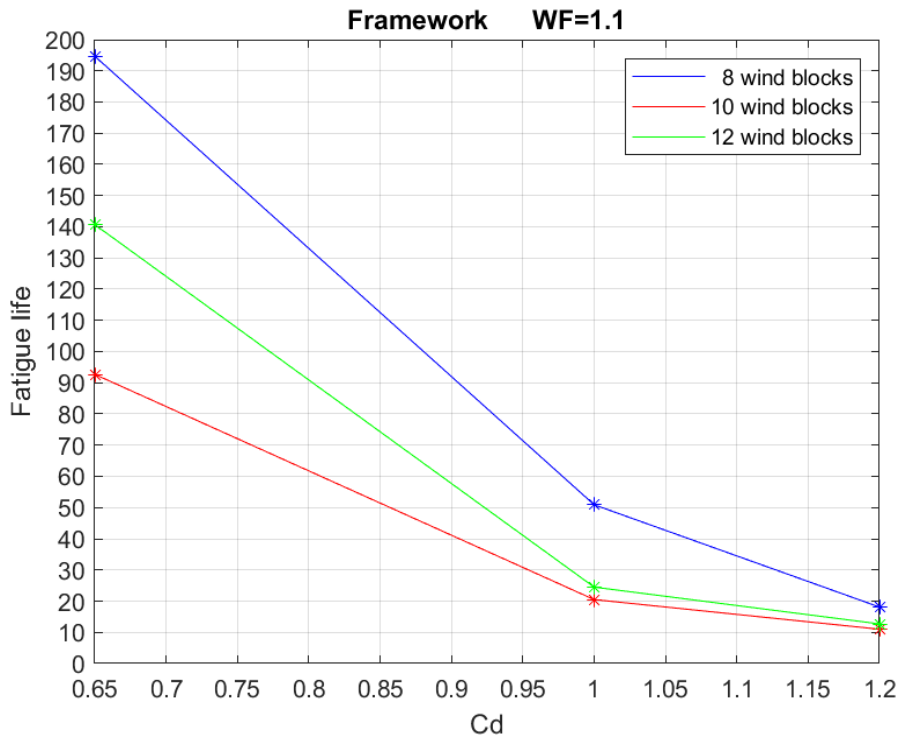


Figure 4-13: Fatigue life against Cd with weight factor 1.1 for different wind block cases (FRAMEWORK)

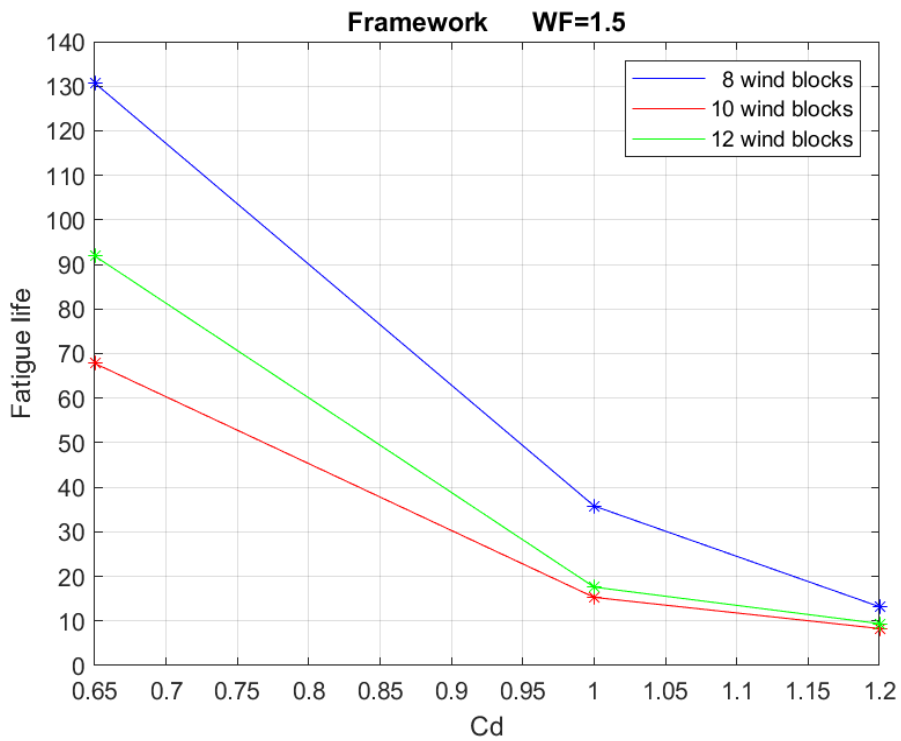


Figure 4-14: Fatigue life against Cd with weight factor 1.5 for different wind block cases (FRAMEWORK)

Figure 4-11, Figure 4-12, Figure 4-13 and Figure 4-14 show change in **fatigue life** with change of **Cd** for all wind block combinations for 4 cases of fixed **weight factor**.

The following observations are made:

- **Fatigue life** is most sensitive to changes of **Cd** under 1.
- The **8 wind blocks** case always gives the highest life and the **10 wind blocks** case always the lowest.
- The **8 wind blocks** case seem to be most sensitive to change in **Cd**. A drastic **88%** drop in **fatigue life** is observed for case of **8 wind blocks**.
- **Fatigue life** drops in close pattern between **Cd = 1** and **1.2** for both **10 wind blocks** and **12 wind blocks** cases. However, for **Cd** less than 1, **12 wind blocks** case drop in **fatigue life** than the corresponding in **10 wind blocks**.

4.3 Summary and Discussion

A general trend can be observed that the **8 wind blocks** case give the highest **fatigue life**, compared to the other **wind block** cases. The **10 wind blocks** case give the lowest **fatigue life** of the three cases under study. **Fatigue life** in the **12 wind blocks** case was on average **68%** lower than the **8 wind blocks** in FRAMEWORK. On a similar trend, **fatigue life** in the **10 wind blocks** case was on average **49%** lower than the **8 wind blocks** in FRAMEWORK. Although the **10- and 12 wind blocks** case includes more **wind blocks**, the bigger blocks of the top wind speeds make a larger impact on the resulting **fatigue life**. This can be attributed to a larger effect of the top wind speeds than the lower, even though the probability of occurrence is lower. As the high wind speed blocks are governing, it might be suggested that the lower wind speed blocks are combined instead of the high wind speed blocks for a more accurate -less conservative- result.

It can be observed from all graphs that **fatigue life** is more sensitive to change of **Cd** under 1 than above 1. One of the main reasons why could be the logarithmic scale of the S-N curves. Since **Cd** directly affects the wind force, **Cd** is linearly related to stress. Lower **Cd** gives less stress ranges, which in turn give less fatigue damage and higher **fatigue life** according to the S-N curve.

In most of the graphs, there is a drop of **34-42%** in **fatigue life** when **weight factor** increases from **1.0** to **1.1**. In comparison, the **fatigue life** drops with about **28%** between **weight factor 1.1** and **1.5**. This may be explained by the relation between structure's mass and its natural frequency. The spectral method uses frequencies to represent wind loading to simulate turbulence (see section 2.4). When weight is changed in the range of **1.0** to **1.1**, the natural frequency of the structure may come closer to one of the wind spectra's main frequencies, causing more resonant motions, hence higher fatigue stresses.

5 Wind-induced Fatigue Analysis Using WINDPACK

This chapter presents **fatigue life** results for load combinations coming from different parameters, as discussed before, done in WINDPACK. A total of **36** analyses have been done categorized into **3** different **wind block cases**, **3** different **drag coefficients (Cd)** and **4** different **weight factors**. (See section 3.2)

5.1 Results Tables

The **fatigue life** results from the **5 most critical joints** are presented in the following tables, with the most **critical fatigue life** highlighted in the first cell under the name (**Crt Ftg Life**). The parameters on the left side describe the corresponding load case.

8 wind blocks:

Wind Blocks	Cd	wt factor	Windpack (Fatigue life / years)					
			Crt Ftg Life	jt 209590	jt 200590	jt 103520	jt 103520	jt 101020
8	0.65	0.5	1259.7	1260	1289	5813	5813	5813
		1	787.1	787	802	3025	3025	3028
		1.1	720.9	721	734	2752	2752	2752
		1.5	546.5	547	555	2171	2171	2193
	1	0.5	151.0	151	154	523	523	523
		1	109.4	109	111	333	333	334
		1.1	102.5	103	104	311	311	313
		1.5	84.8	85	85	260	260	262
	1.2	0.5	69.3	69	71	218	218	219
		1	52.2	52	53	148	148	148
		1.1	49.2	49	50	139	139	139
		1.5	42.0	42	43	119	119	120

Table 5-1: All results with 8 wind blocks in WINDPACK

10 wind blocks:

Wind Blocks	Cd	wt factor	Windpack (Fatigue life / years)					
			Crt Ftg Life	jt 209590	jt 200590	jt 103520	jt 103520	jt 101020
10	0.65	0.5	583.1	583	593	1860	1860	1864
		1	386.8	387	392	1092	1092	1093
		1.1	359.5	360	364	1041	1041	1078
		1.5	284.0	284	287	941	941	944
	1	0.5	99.0	99	101	277	277	278
		1	71.8	72	73	186	186	186
		1.1	67.5	68	68	179	179	184
		1.5	56.0	56	57	164	164	164
	1.2	0.5	49.2	49	50	133	133	133
		1	36.8	37	37	92	92	92
		1.1	34.7	35	35	89	89	91
		1.5	29.4	29	30	82	82	82

Table 5-2: All results with 10 wind blocks in WINDPACK

12 wind blocks:

Wind Blocks	Cd	wt factor	Windpack (Fatigue life / years)					
			Crt Ftg Life	jt 209590	jt 200590	jt 103520	jt 103520	jt 101020
12	0.65	0.5	871.8	872	893	4662	4662	4678
		1	532.6	533	543	2282	2282	2286
		1.1	487.0	487	496	2053	2053	2071
		1.5	361.1	361	367	1511	1511	1522
	1	0.5	101.8	102	104	350	350	350
		1	76.7	77	78	222	222	222
		1.1	72.3	72	73	207	207	208
		1.5	58.7	59	59	168	168	168
	1.2	0.5	48.8	49	50	146	146	146
		1	38.8	39	39	101	101	101
		1.1	36.8	37	37	95	95	95
		1.5	30.5	31	31	79	79	79

Table 5-3: All results with 12 wind blocks in WINDPACK

5.2 Result Graphs

This chapter presents graphs showing for **the most critical joint in fatigue life** and how it varies with different parameter changes. One parameter will be fixed and thereby case dependent, while the other parameters are either shown on the x-axis or presented in different graphs. All reasonable representations are shown.

The shapes of the curves are simplified and should not be interpreted too precisely, but they rather give an indication of trends. Interpolation between different points shall not be used and will not give an accurate representation of reality. More data points would be required to simulate precise reliable curve representation.

All **fatigue life** results correlate with the most **critical fatigue life** in **Table 5-1, Table 5-2 and Table 5-3**. All load cases are presented.

5.2.1 Fatigue life against weight factor for different drag coefficient values:

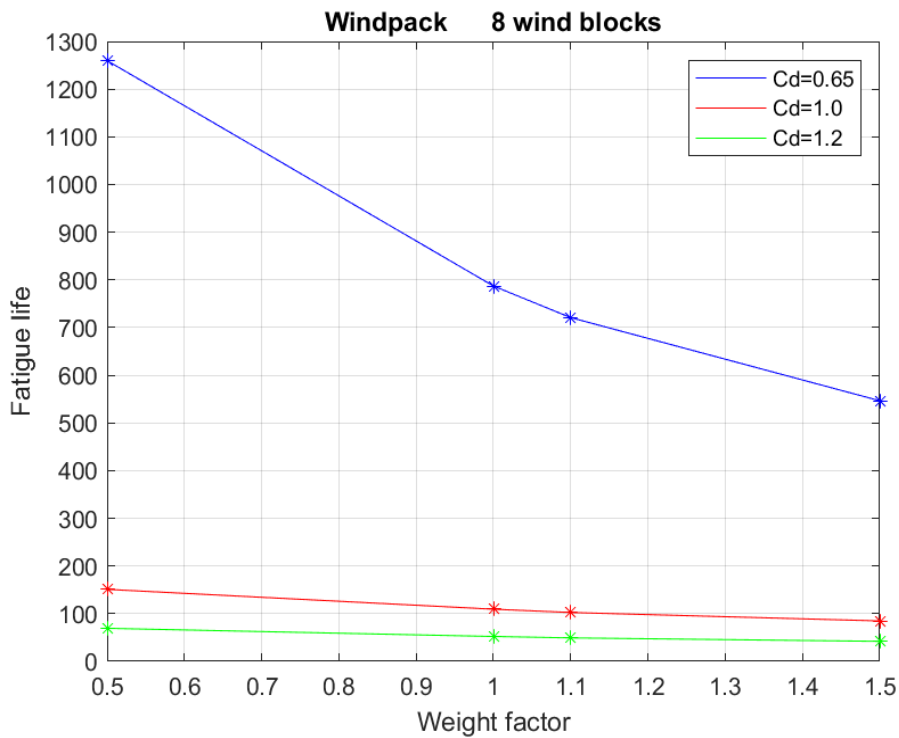


Figure 5-1: Fatigue life against weight factor with 8 wind blocks for different Cd values (WINDPACK)

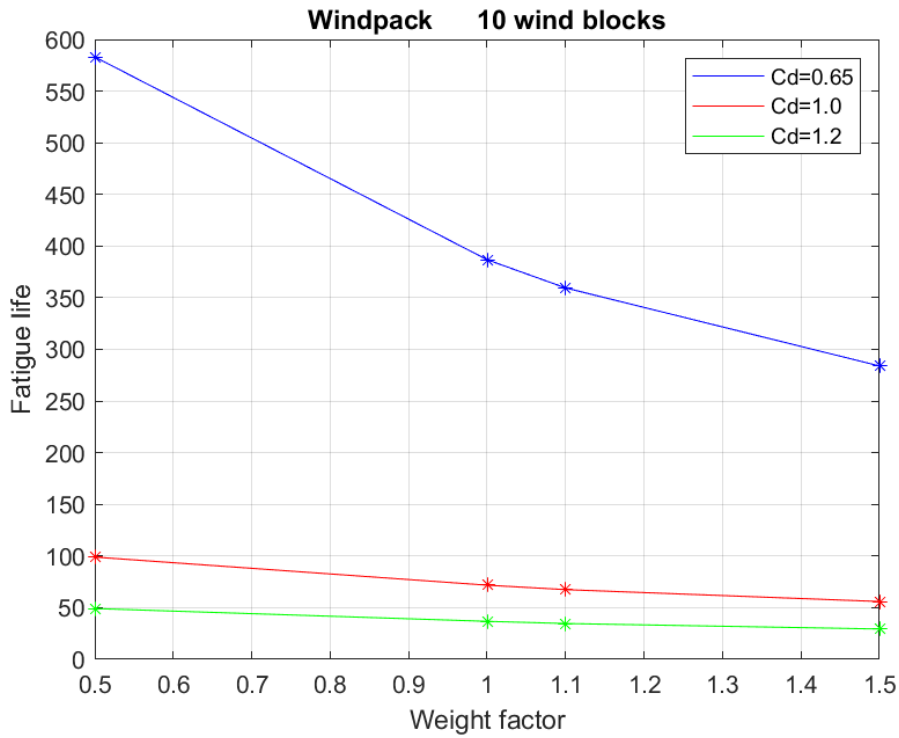


Figure 5-2: Fatigue life against weight factor with 10 wind blocks for different Cd values (WINDPACK)

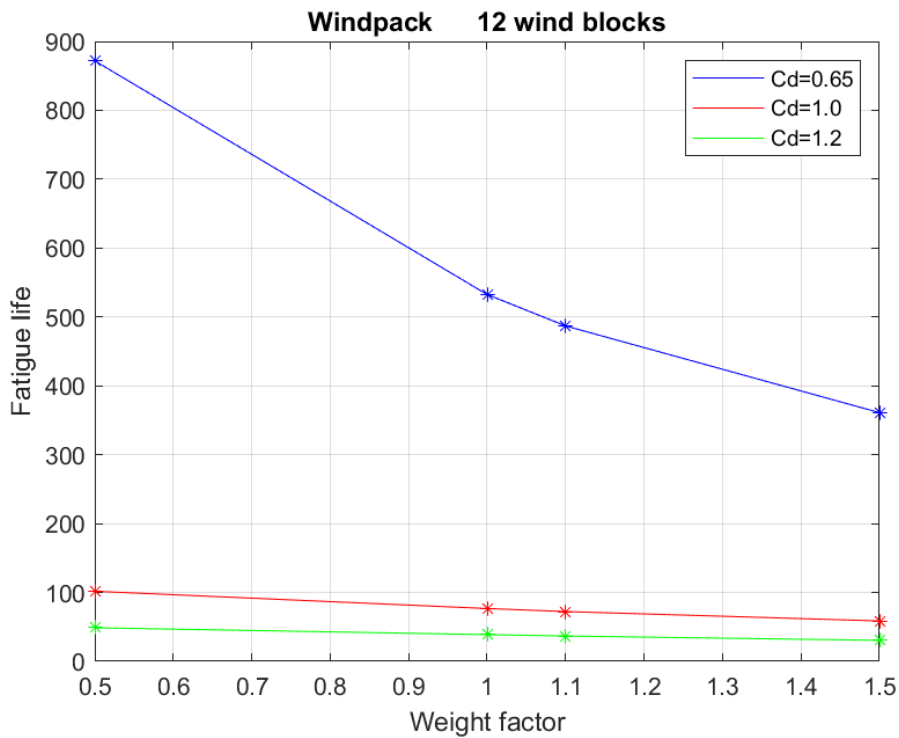


Figure 5-3: Fatigue life against weight factor with 12 wind blocks for different Cd values (WINDPACK)

Figure 5-1, Figure 5-2 and Figure 5-3 show variation in fatigue life with varying weight factor, for all Cd, for the 8, 10 and 12 wind blocks load cases. The following observations are made:

- **8 wind block** results give highest **fatigue life** overall, and **10 wind block** results give the lowest.
- **Fatigue life** is much higher in the case of **Cd = 0.65** when compared with **1.0** and **1.2** for all **wind block** cases. **Fatigue life** for **weight factor** of **0.5** and **Cd = 0.65** is between **6** and **8** times more than the corresponding in **Cd = 1.0**.
- The case of **Cd = 0.65** seems to be more sensitive to change in **weight factor**. An average drop of **55%** in **fatigue life** is observed between all **wind blocks** between **weight factor** of **0.5** and **1.5**.
- **Fatigue life** drop shows milder slope for the case of **Cd = 1.0** and **1.2**. Both trends are very close to be parallel. The average drops between all **wind block** cases are **43%** and **38%** for **Cd = 1.0** and **1.2**, respectively.

5.2.2 Fatigue life against drag coefficient for different weight factor values:

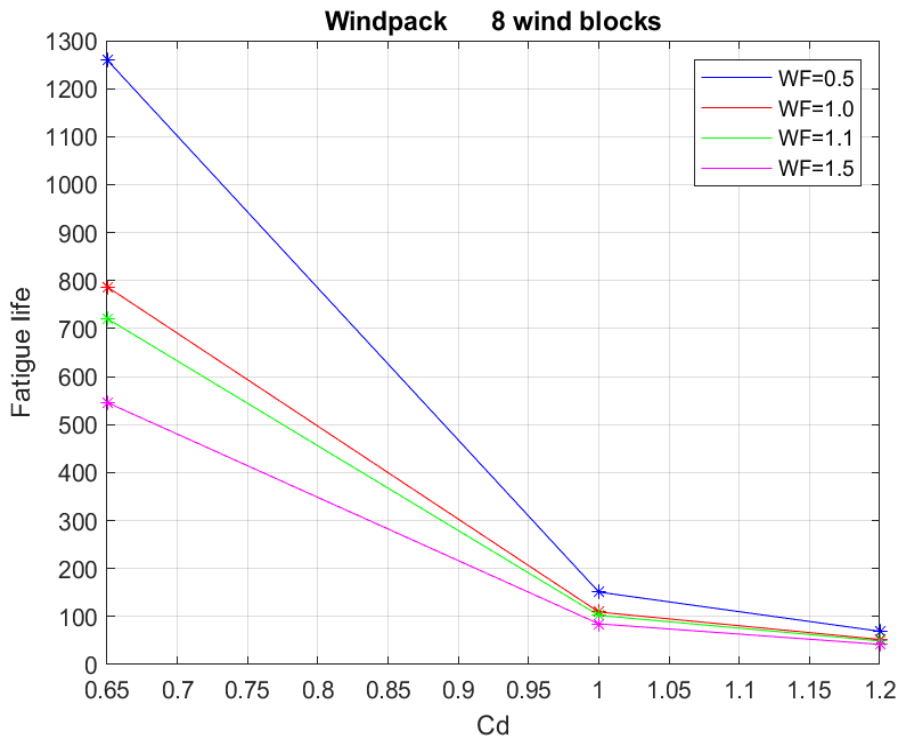


Figure 5-4: Fatigue life against Drag coefficient with 8 wind blocks for different weight factor values (WINDPACK)

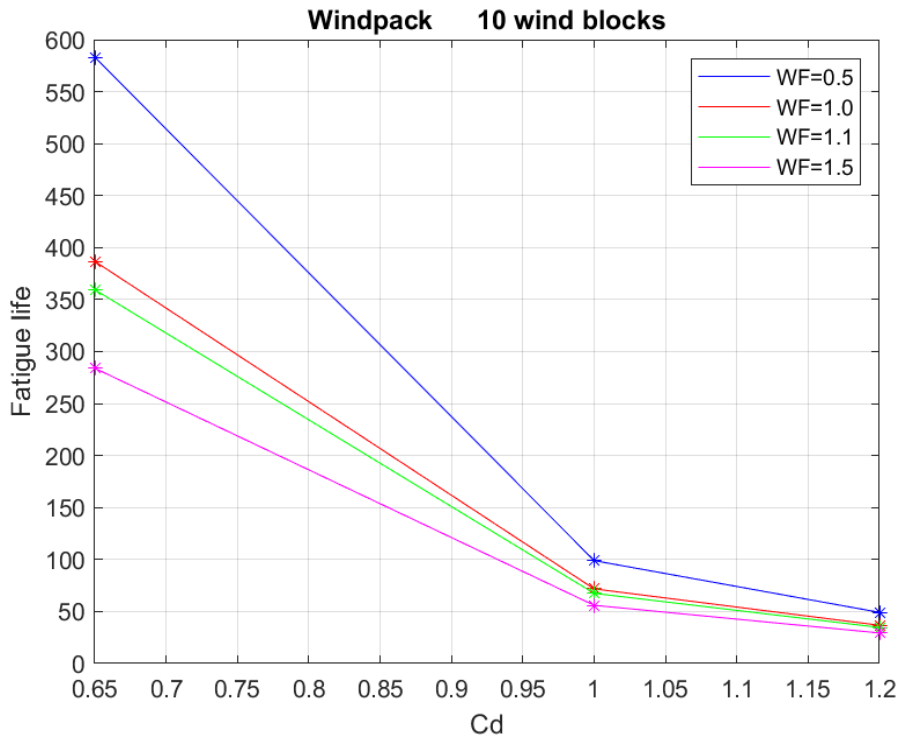


Figure 5-5: Fatigue life against Drag coefficient with 10 wind blocks for different weight factor values (WINDPACK)

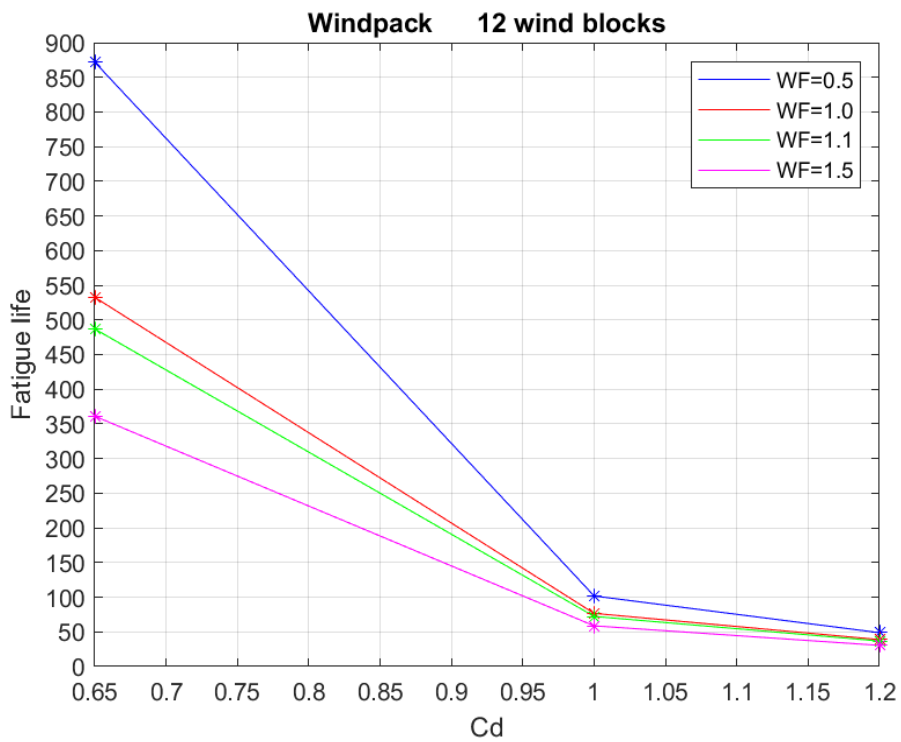


Figure 5-6: Fatigue life against Drag coefficient with 12 wind blocks for different weight factor values (WINDPACK)

Figure 5-4, Figure 5-5 and Figure 5-6 show variation in **fatigue life** with variation of **Cd**, for all 4 cases of **weight factors**, for the **8, 10 and 12 wind block** cases.

The following observations are made:

- **8 wind block** cases give highest **fatigue life** overall, and **10 wind block** cases the lowest overall.
- The trend in all graphs seems to be that **fatigue life** is less sensitive to change in **Cd** after 1.
- The variation of **Cd** seems to have more impact on **fatigue life** with lower **weight factor**. **Fatigue life** decreases **94%** from **Cd 0.65** to **Cd 1.2** for **weight factor** of **0.5**, while it decreases **91%** from **Cd 0.65** to **Cd 1.2** for **weight factor 1.5**.
- For lower **weight factors**, the drop in **fatigue life** is steeper with increase in **Cd**. **Fatigue life** for **8 wind blocks** and for **weight factor 0.5** drops from **1259.7 years** at **Cd 0.65** to **151 years** at **Cd 1.0**, while it drops from **546.5 years** to **42 years** for **weight factor 1.5**.

5.2.3 Fatigue life against weight factor for different wind block cases:

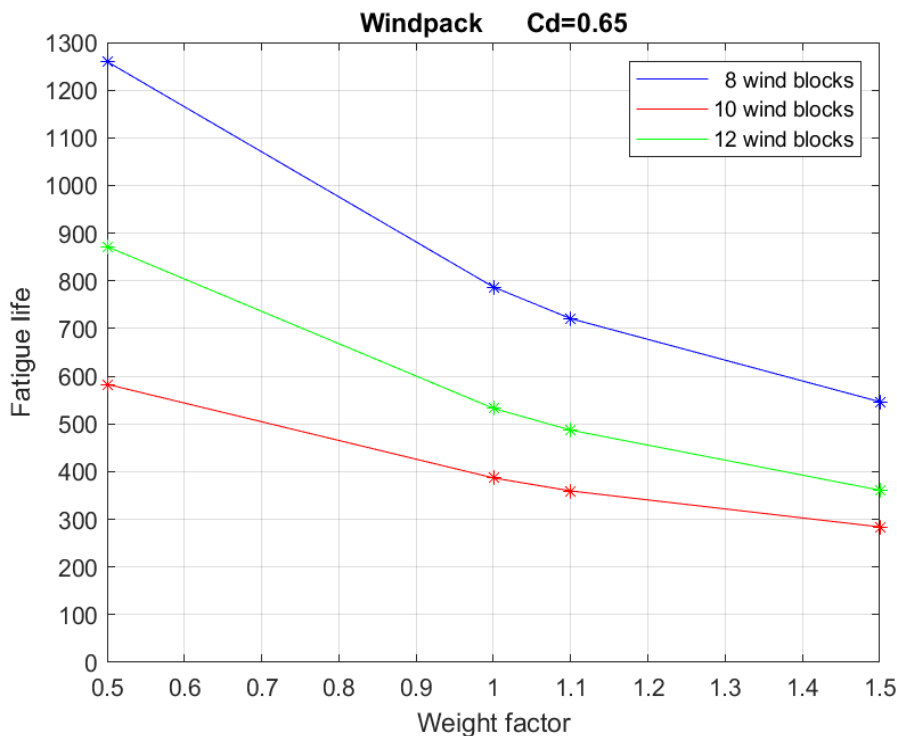


Figure 5-7: Fatigue life against weight factor with Cd=0.65 for different wind block cases (WINDPACK)

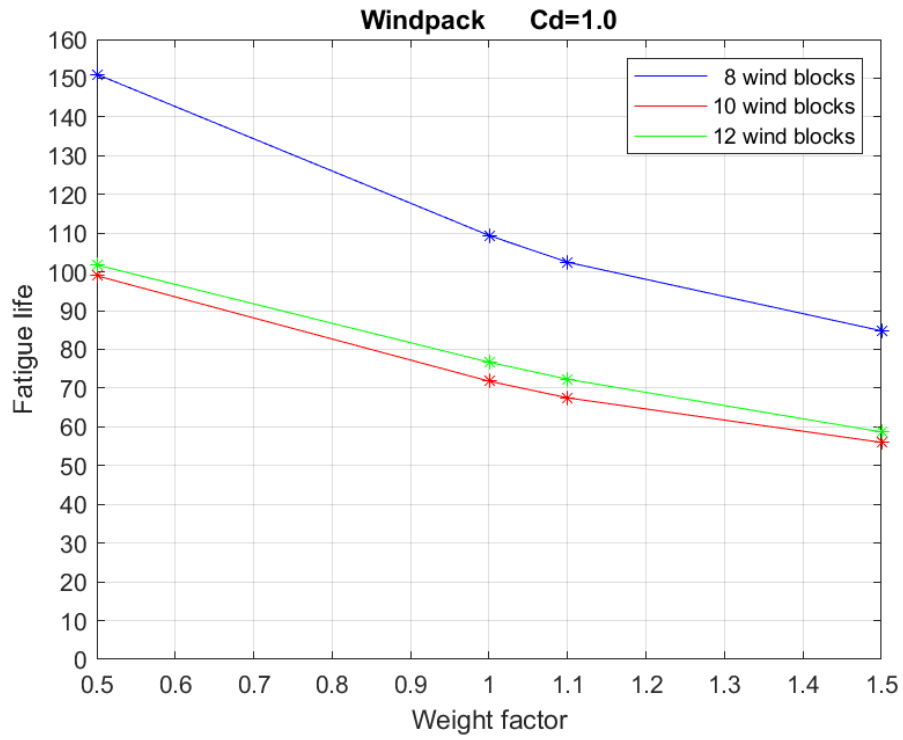


Figure 5-8: Fatigue life against weight factor with Cd=1.0 for different wind block cases (WINDPACK)

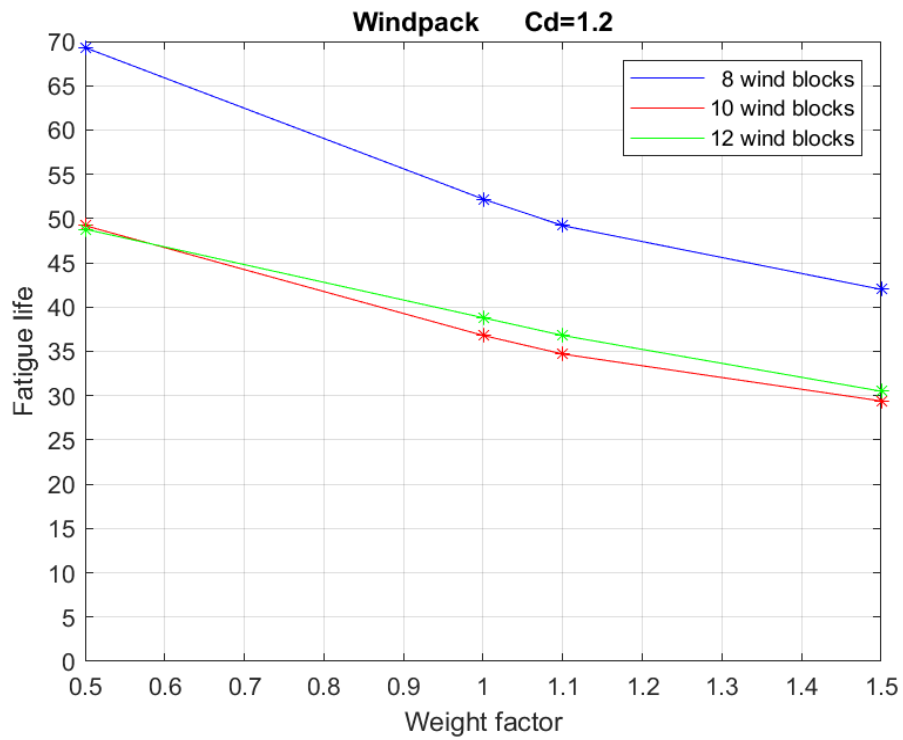


Figure 5-9: Fatigue life against weight factor with Cd=1.2 for different wind block cases (WINDPACK)

Figure 5-7, Figure 5-8 and Figure 5-9 show variation in **fatigue life** with change in **weight factor** for all **wind blocks**, for fixed **Cd** value cases.

The following observations are made:

- **Fatigue life** results from **8 wind blocks** are generally the highest followed by those from **12 wind blocks** and **10 wind blocks**, respectively.
- For **Cd = 1 and 1.2**, **fatigue life** from the **10 wind blocks** case and **12 wind blocks** case are close and follow almost the same pattern.
- The **8 wind blocks** case seems to be overall the most sensitive to change in **weight factor**, however the trend is milder than that in FRAMEWORK.
- Both the cases of **8 wind blocks** and **12 wind blocks** give similar trends of decrease in **fatigue life** with the increase of **weight factor** from **0.5 to 1.0**.
- The **8 wind blocks** case always give the highest **fatigue life** in all cases, and the **10 wind blocks** case

5.2.4 Fatigue life against drag coefficient for different wind blocks:

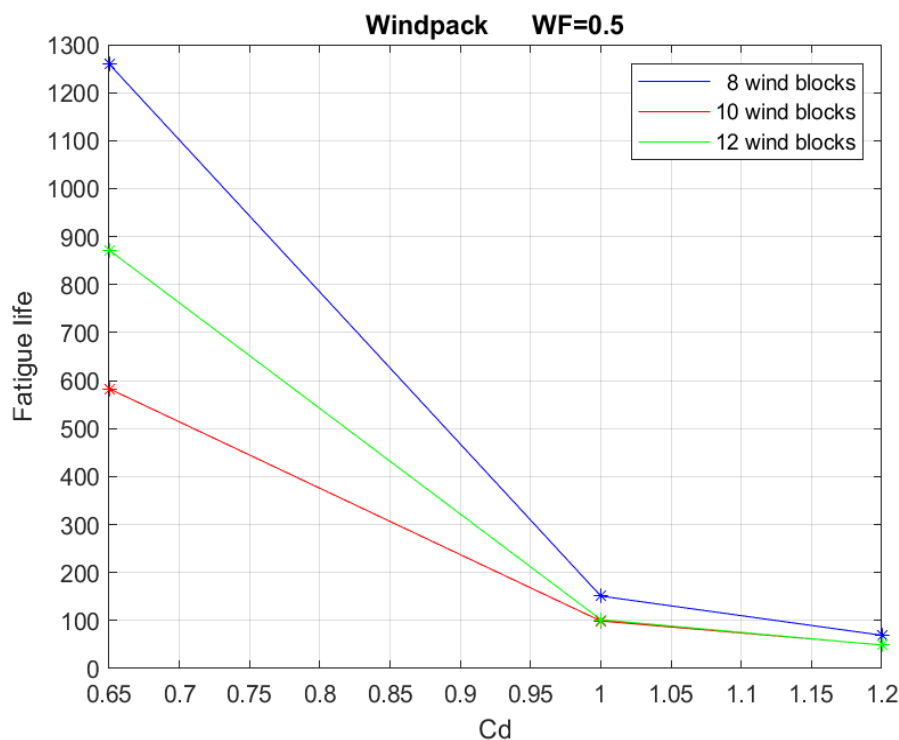


Figure 5-10: Fatigue life against Cd with weight factor 0.5 for different wind block cases (WINDPACK)

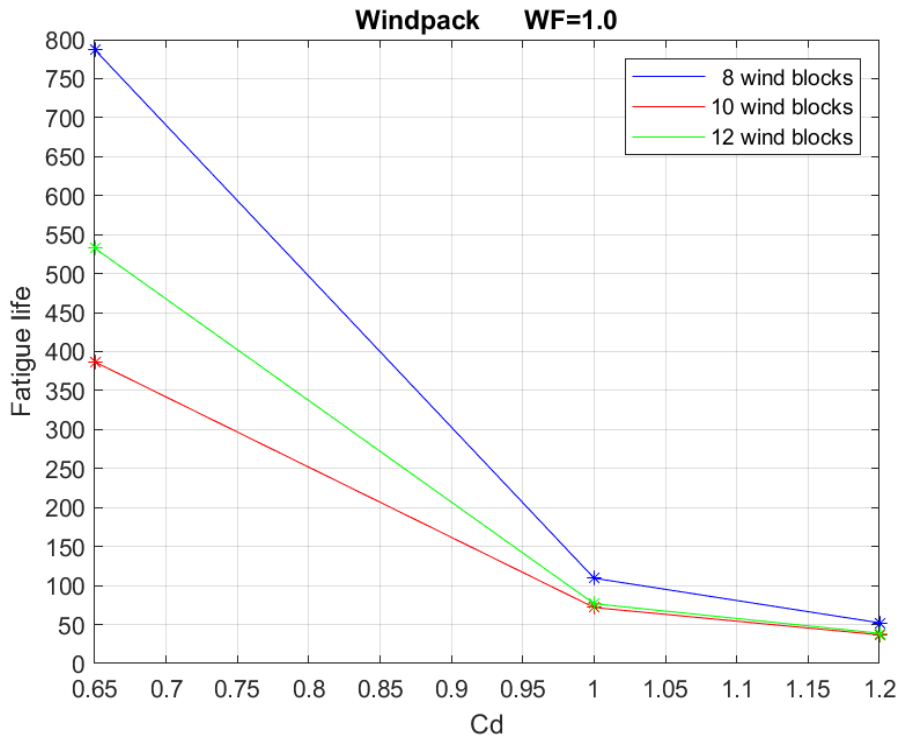


Figure 5-11: Fatigue life against Cd with weight factor 1.0 for different wind block cases (WINDPACK)

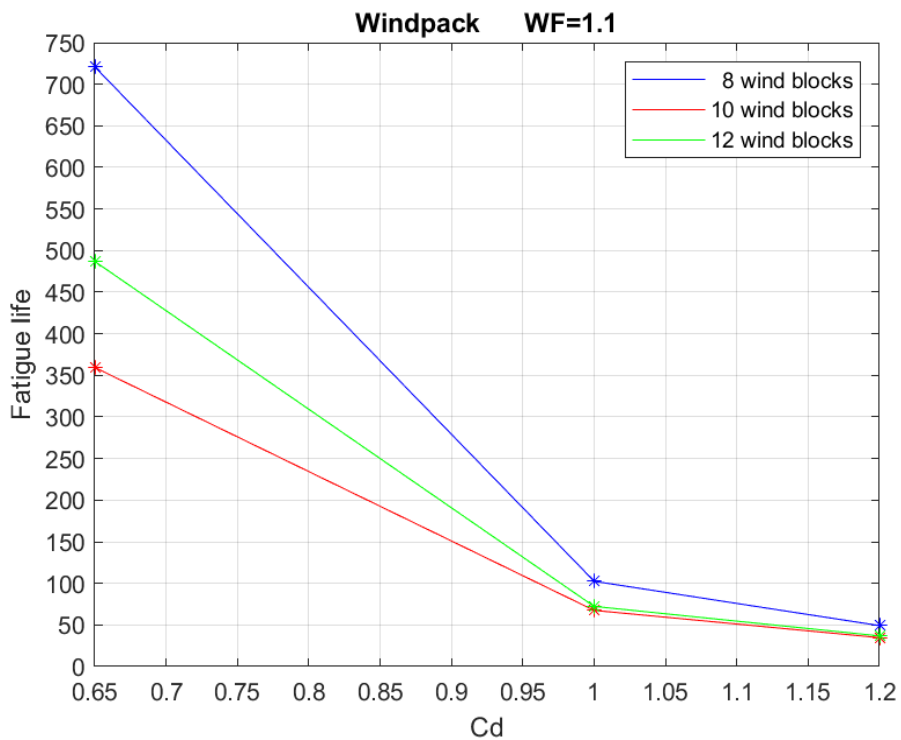


Figure 5-12: Fatigue life against Cd with weight factor 1.1 for different wind block cases (WINDPACK)

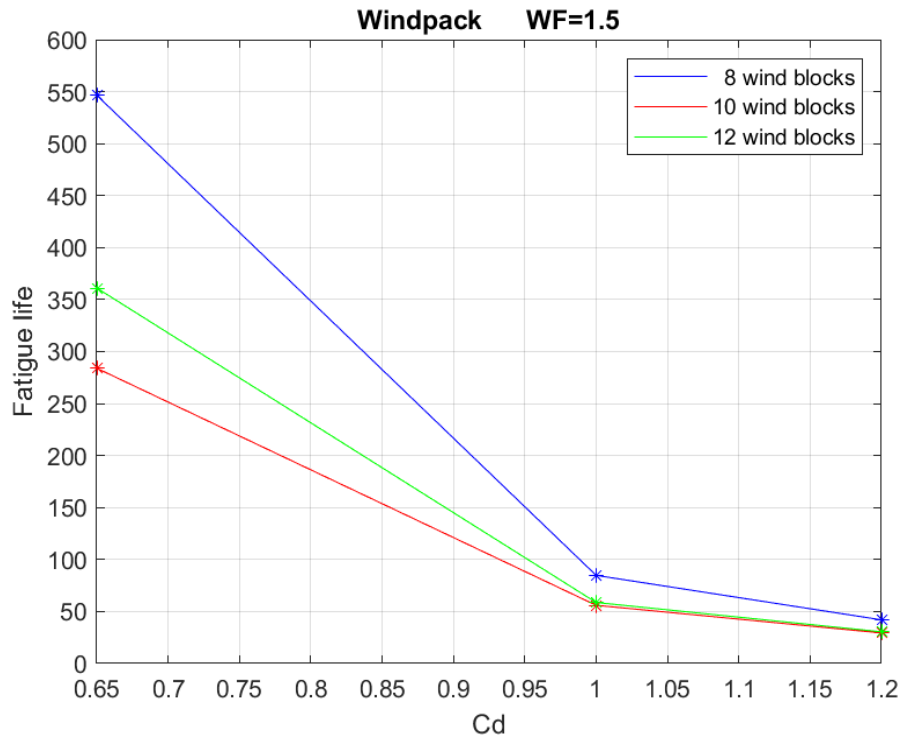


Figure 5-13: Fatigue life against Cd with weight factor 1.5 for different wind block cases (WINDPACK)

Figure 5-10, Figure 5-11, Figure 5-12 and Figure 5-13 show change in **fatigue life** with change of **Cd**, for all **wind block** combinations, for 4 cases of fixed **weight factor**.

The following observations are made:

- **Fatigue life** is most sensitive to changes of **Cd** under 1.
- The **8 wind blocks** case always gives the highest **fatigue life** and the **10 wind blocks** case always the lowest.
- **Fatigue life** results and their trend from **Cd = 1.0** to **1.2** is almost identical for both cases of **10 wind blocks** and **12 wind blocks** for all **weight factors**.
- The **8 wind blocks** case seem to be most sensitive to change in **Cd**. A drastic **92%** drop in **fatigue life** is observed for case of **8 wind blocks** between **weight factor** of **0.5** and **1.5**. While the drop was **89%** and **91%** in cases of **10 wind blocks** and **12 wind blocks**, respectively.

5.3 Summary and Discussion

A general trend can be observed that the **8 wind blocks** case give the highest **fatigue life**, compared to the other **wind block** cases. The **10 wind blocks** case give the lowest **fatigue life** of the three cases under study. However, the difference between **10 wind blocks** and **12 wind blocks** using WINDPACK is not as evident as in FRAMEWORK. **Fatigue life** in the **12 wind blocks** case was on average **70%** lower than the **8 wind blocks** in FRAMEWORK. On a similar trend, **fatigue life** in the **10 wind blocks** case was on average **61%** lower than the **8 wind blocks** in WINDPACK. Although the **10- and 12 wind blocks** case includes more **wind blocks**, the bigger blocks of the top wind speeds

make a larger impact on the resulting **fatigue life**. This can be attributed to a larger effect of the top wind speeds than the lower, even though the probability of occurrence is lower.

It can be observed from all graphs that **fatigue life** is more sensitive to change of **Cd** under **1** than above **1**. One of the main reasons why could be the logarithmic scale of the S-N curves along with the variation of slope between 3 and 5 ($m = 3$ and 5). Since **Cd** directly affects the wind force, **Cd** is linearly related to stress. Lower **Cd** values give less stress ranges, which in turn give less fatigue damage and higher **fatigue life** according to the S-N curve.

For **Cd=1.0** and **1.2** the **10-** and **12 wind blocks** cases almost overlapped.

In most of the graphs, there is a drop of **5%-10%** in **fatigue life** when **weight factor** increases from **1.0** to **1.1**. In comparison, the **fatigue life** drops with about **20%-30%** between **weight factor 1.1** and **1.5**. **Fatigue life** changed almost linearly with changing **weight factor** in WINDPACK.

6 Wind-induced Fatigue Analysis Using USFOS

This chapter presents the results gathered from numerous analyses done in USFOS. **124** cases have been analyzed categorized in: **4** different **wind block combinations**, **4** values for **Cd**, **4** different **weight factors** and with **time increment (dt)** of **0.05 seconds** and **0.1 seconds**, for all cases. Besides the main analysis, some cases have also been run with and without the **relative velocity** formula.

6.1 USFOS Analysis with Time Increment (dt) of 0.10 seconds

USFOS is used to analyze fatigue using two **time increments** as stated previously. (See section 3.2.5) In this section, all **fatigue life** results from the analysis with **time increment 0.1 seconds** are presented.

6.1.1 Results Tables

The **fatigue life** results from the **5 most affected joints** are presented in the following tables, with the most critical **fatigue life** highlighted with darker color under the header (**Crt Ftg Life**). The parameters on the left side describe the corresponding load case.

All cases for 8 wind blocks:

Wind Blocks	Cd	wt factor	Usfos dt=0.10 (Fatigue life / years)					
			Crt Ftg Life	jt 167	jt 159	jt 310	jt 327	jt 310/327
8	0.65	0.5	1416	1416	1683	44033	61767	96246
		1	264	264	280	4822	6784	10322
		1.1	299	299	318	6180	8045	11935
		1.5	167	167	176	3271	4181	6165
	1	0.5	231	231	265	5330	7407	11912
		1	51	51	54	723	958	1398
		1.1	54	54	57	858	1086	1458
		1.5	33	33	34	466	580	777
	1.2	0.5	113	113	128	2266	3116	4926
		1	27	27	28	344	448	645
		1.1	28	28	29	391	490	629
		1.5	17	17	18	215	264	341
	Reynold's	0.5	853	853	985	24361	34235	49529
		1	170	170	179	2623	3698	5444
		1.1	200	200	211	3587	4690	7215
		1.5	116	116	121	1965	2531	3824

Table 6-1: All results with 8 wind blocks in USFOS with dt=0.10

All cases for 10 wind blocks:

Wind Blocks	Cd	wt factor	Usfos dt=0.10 (Fatigue life / years)					
			Crt Ftg Life	jt 167	jt 159	jt 310	jt 327	jt 310/327
10	0.65	0.5	576	576	662	14239	20178	32541
		1	116	116	122	1543	2152	3174
		1.1	149	149	157	2327	3042	4005
		1.5	87	87	91	1094	1371	2013
	1	0.5	114	114	128	1853	2593	3994
		1	27	27	28	278	365	503
		1.1	33	33	34	370	463	620
		1.5	20	20	21	207	252	351
	1.2	0.5	60	60	67	833	1150	1726
		1	15	15	16	145	188	254
		1.1	18	18	18	185	229	299
		1.5	11	11	11	107	129	174
	Reynold's	0.5	313	313	353	6601	9363	14830
		1	69	69	72	767	1055	1494
		1.1	91	91	96	1170	1511	2045
		1.5	55	55	57	592	740	1048

Table 6-2: All results with 10 wind blocks in USFOS with dt=0.10

All cases for 12 wind blocks:

Wind Blocks	Cd	wt factor	Usfos dt=0.10 (Fatigue life / years)					
			Crt Ftg Life	jt 167	jt 159	jt 310	jt 327	jt 310/327
12	0.65	0.5	1140	1140	1321	36443	50150	77882
		1	215	215	225	4270	5851	9025
		1.1	248	248	260	5342	6793	6944
		1.5	121	121	126	2602	3262	3279
	1	0.5	180	180	201	4398	6010	9814
		1	40	40	41	611	794	1076
		1.1	44	44	45	729	830	906
		1.5	23	23	24	350	414	431
	1.2	0.5	87	87	96	1852	2512	4050
		1	21	21	21	282	360	451
		1.1	23	23	23	326	353	400
		1.5	13	13	13	156	184	190
	Reynold's	0.5	688	688	785	20730	28450	41118
		1	140	140	146	2399	3309	4963
		1.1	162	162	170	3136	4019	4543
		1.5	83	83	86	1597	2027	2256

Table 6-3 All results with 12 wind blocks in USFOS with dt=0.10

All cases for 16 wind blocks:

Wind Blocks	Cd	wt factor	Usfos dt=0.10 (Fatigue life / years)					
			Crt Ftg Life	jt 167	jt 159	jt 310	jt 327	jt 310/327
16	0.65	0.5	2324	2324	2680	71994	103488	163988
		1	437	437	461	8361	11752	17921
		1.1	478	478	506	9542	12588	19566
		1.5	272	272	283	5348	7027	10832
	1	0.5	372	372	420	8711	12382	19646
		1	84	84	88	1220	1637	2393
		1.1	86	86	90	1367	1753	2627
		1.5	52	52	54	767	978	1452
	1.2	0.5	180	180	202	3694	5189	8123
		1	43	43	45	575	759	1092
		1.1	44	44	45	628	800	1184
		1.5	27	27	28	356	447	655
	Reynold's	0.5	1402	1402	1571	39510	56980	83963
		1	286	286	299	4619	6502	9588
		1.1	321	321	336	5485	7257	10952
		1.5	190	190	197	3201	4228	6301

Table 6-4: All results with 16 wind blocks in USFOS with dt=0.10

6.1.2 Results Graphs

This chapter presents **fatigue life** for **the most critical joint** only and how it varies with different parameter changes for USFOS **dt=0.10** seconds cases. One parameter will be fixed and thereby case dependent, while the other parameters are either shown on the x-axis or presented in different graphs. All reasonable representations are shown.

The shapes of the curves are simplified and should not be interpreted too precisely, but rather give an indication of trends. Interpolation between different points shall not be used and will not give an accurate representation of reality. More data points would be required to simulate precise reliable curve representation.

All **fatigue life** results correlate with the most **critical fatigue life** in **Table 6-1, Table 6-2, Table 6-3** and **Table 6-4**.

6.1.2.1 Fatigue life against weight factor for different drag coefficient values

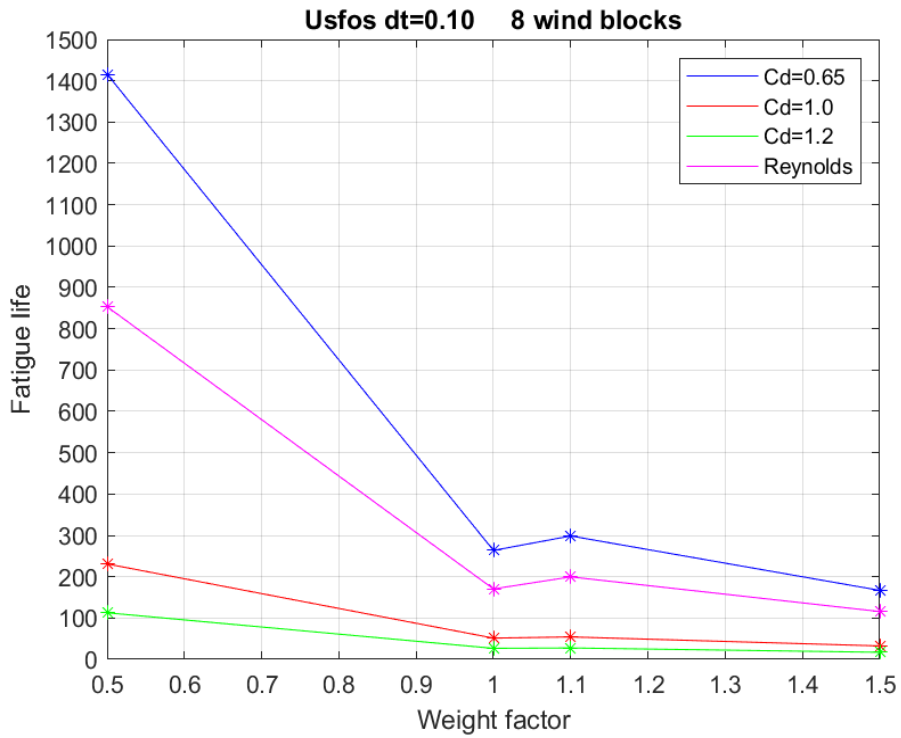


Figure 6-1: Fatigue life against weight factor with dt=0.10 and 8 wind blocks for different Cd values

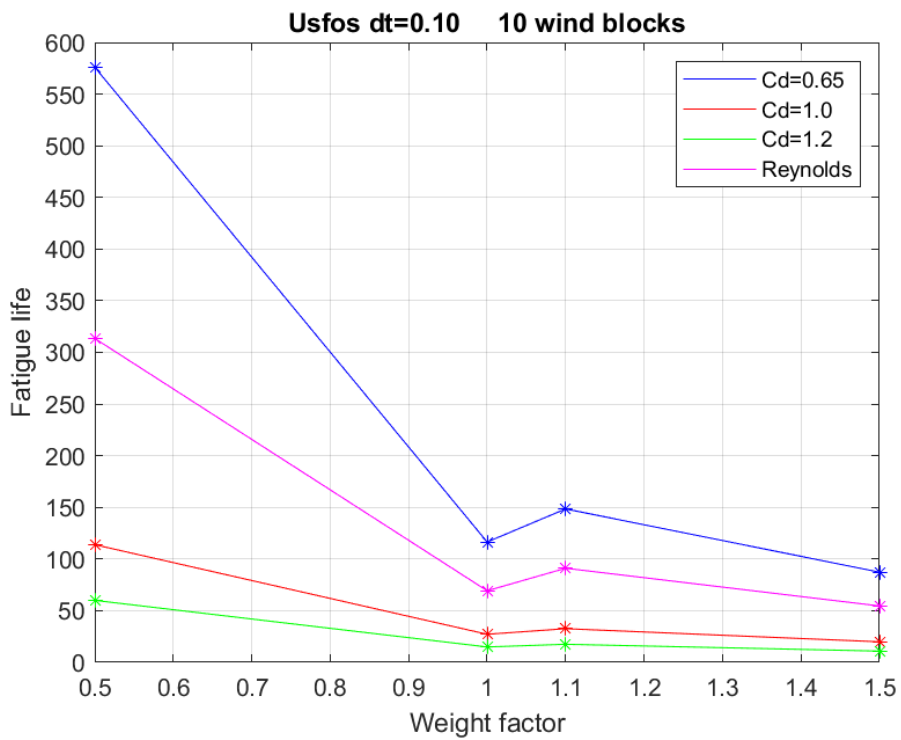


Figure 6-2: Fatigue life against weight factor with dt=0.10 and 10 wind blocks for different Cd values

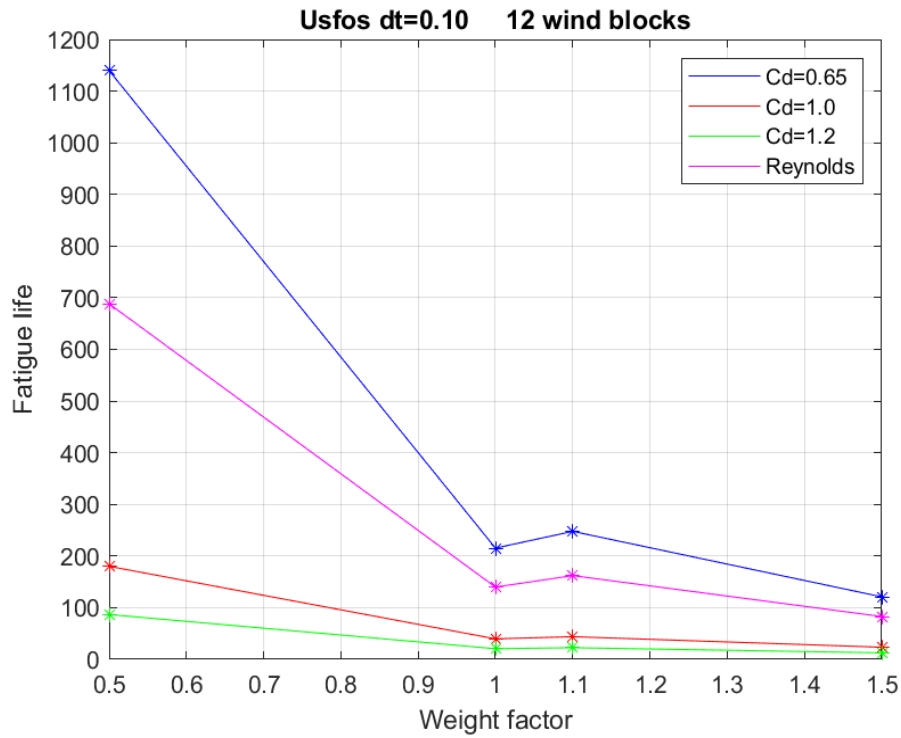


Figure 6-3: Fatigue life against weight factor with $dt=0.10$ and 12 wind blocks for different Cd values

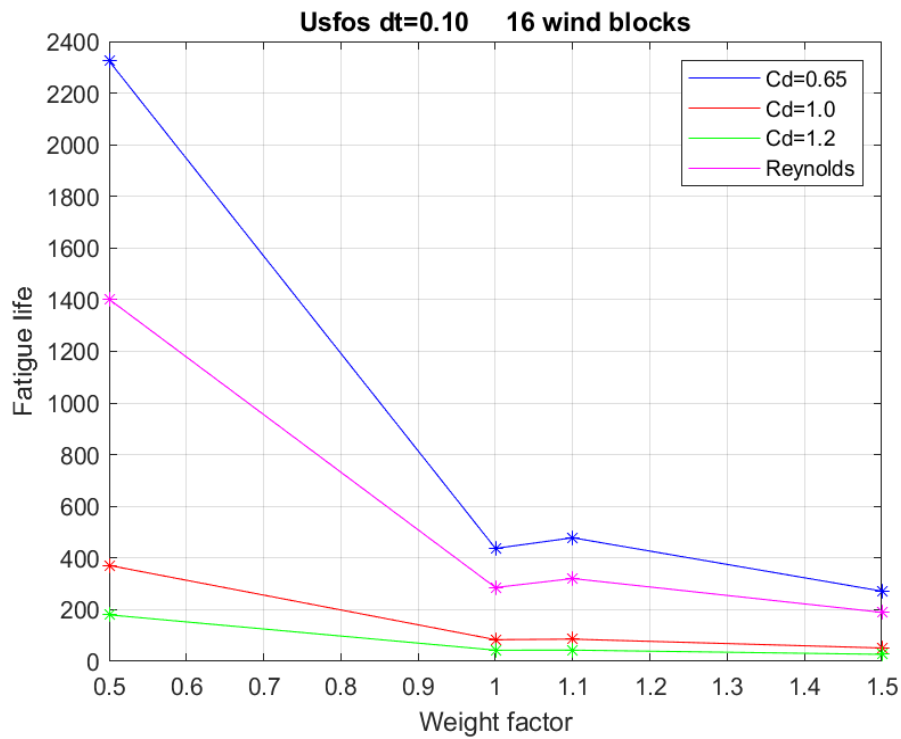


Figure 6-4: Fatigue life against weight factor with $dt=0.10$ and 16 wind blocks for different Cd values

Figure 6-1, Figure 6-2, Figure 6-3 and Figure 6-4 show variation in **fatigue life** with varying **weight factor**, for all variations of **Cd** for, the **8, 10, 12 and 16 wind blocks**.

The following observations were made:

- The trends of **fatigue life** are very similar to the trends observed in FRAMEWORK and in the USFOS analysis with **dt = 0.05 seconds**.
- For all cases run with **0.10 seconds time increment**, **fatigue life** increases when **weight factor** changed from **1 to 1.1**. This is unique for cases with **0.10 seconds time increment** only, and the slope of this increase appears to be more for lower values of **Cd**.
- The slope of this increase flattens out for cases of **16 wind blocks** and **8 wind blocks**.

6.1.2.2 Fatigue life against drag coefficient for different weight factor values

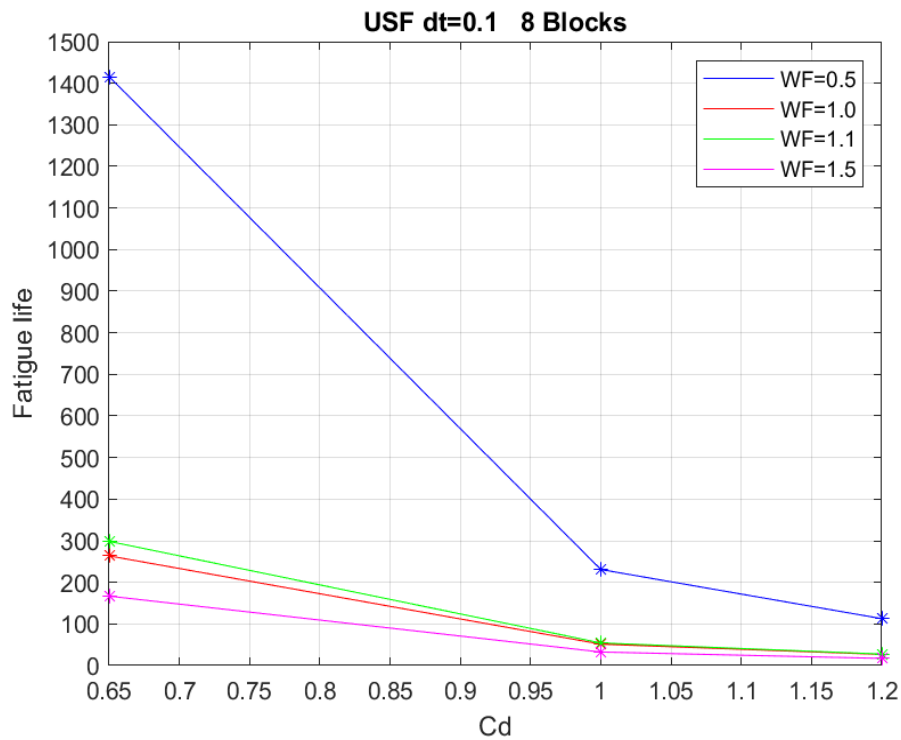


Figure 6-5: Fatigue life against Cd with dt=0.10 and 8 wind blocks for different weight factors

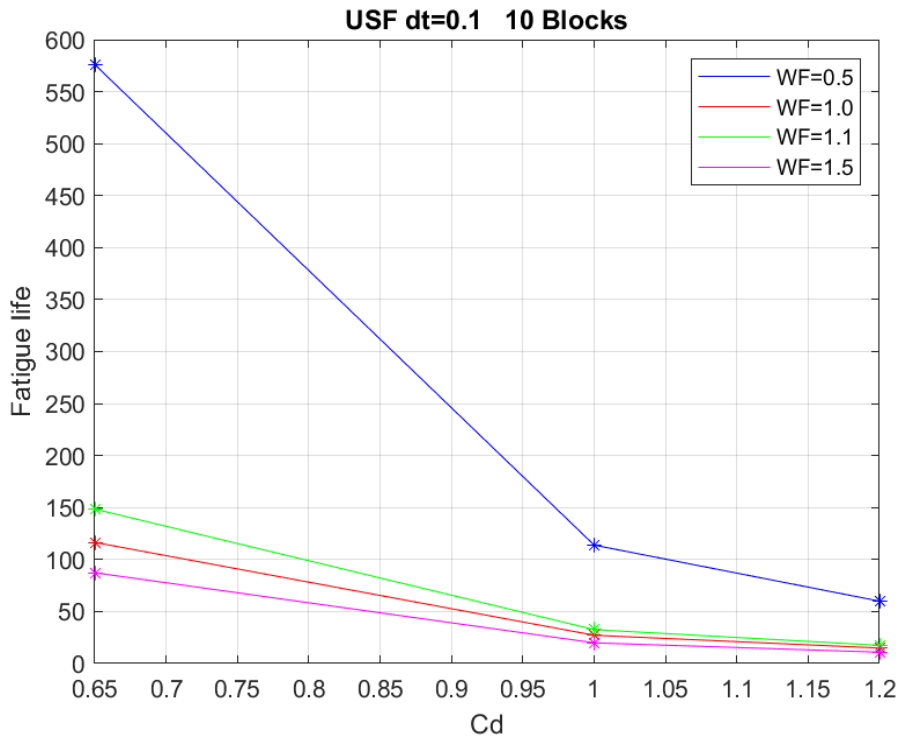


Figure 6-6: Fatigue life against Cd with dt=0.10 and 10 wind blocks for different weight factors

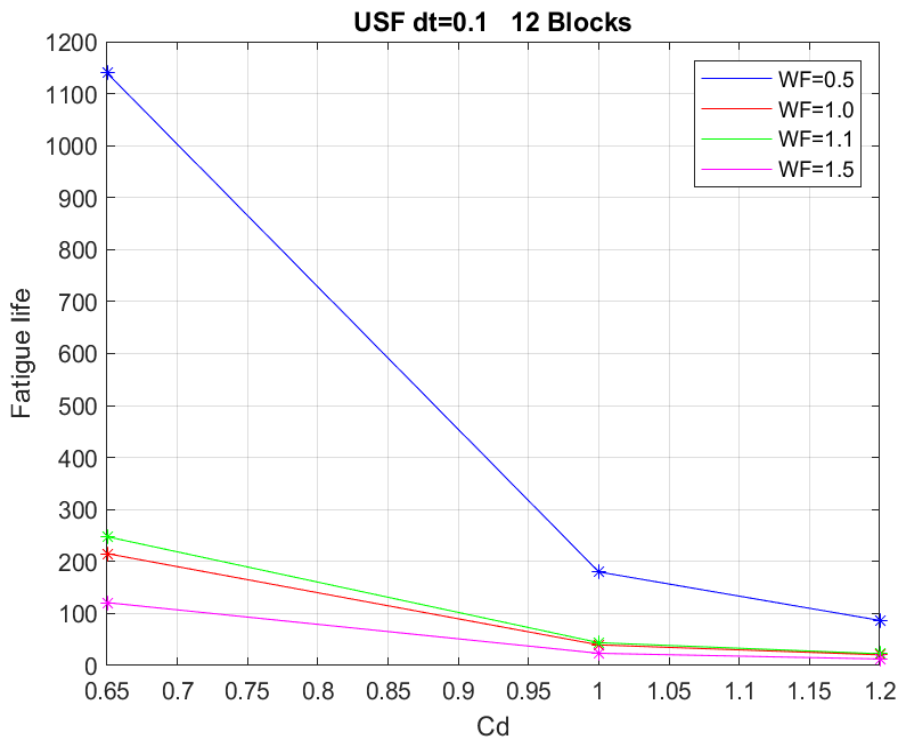


Figure 6-7: Fatigue life against Cd with dt=0.10 and 12 wind blocks for different weight factors

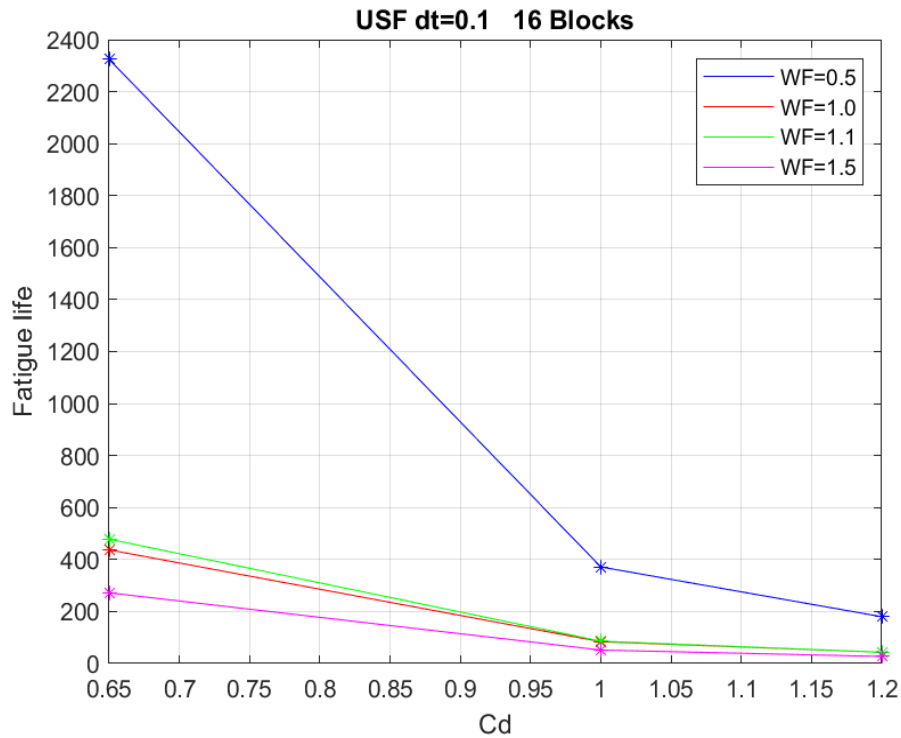


Figure 6-8: Fatigue life against Cd with dt=0.10 and 16 wind blocks for different weight factors

Figure 6-5, Figure 6-6, Figure 6-7 and Figure 6-8 show variation in **fatigue life** with variation of **Cd**, for all 4 cases of **weight factors**, for the 8, 10, 12 and 16 wind block cases.

The following observations are made:

- The trend in all graphs seems to be that **fatigue life** is less sensitive to change in **Cd** after 1.
- For **Cd = 0.65**, **fatigue life** for **weight factor** of 0.5 is on average 4 times higher than **fatigue life** of **weight factor** of 1.0.
- Lower **weight factor** values are more sensitive to the increase of **Cd**. The case of **weight factor 0.5** shows the highest decrease in **fatigue life** with the increase of **Cd** from 0.65 to 1.0. A decrease of 80% is average among all **wind blocks** for **weight factor** of 0.5. An average decrease of 77% is observed for **weight factor** of 1.0.

6.1.2.3 Fatigue life against weight factor for different wind blocks

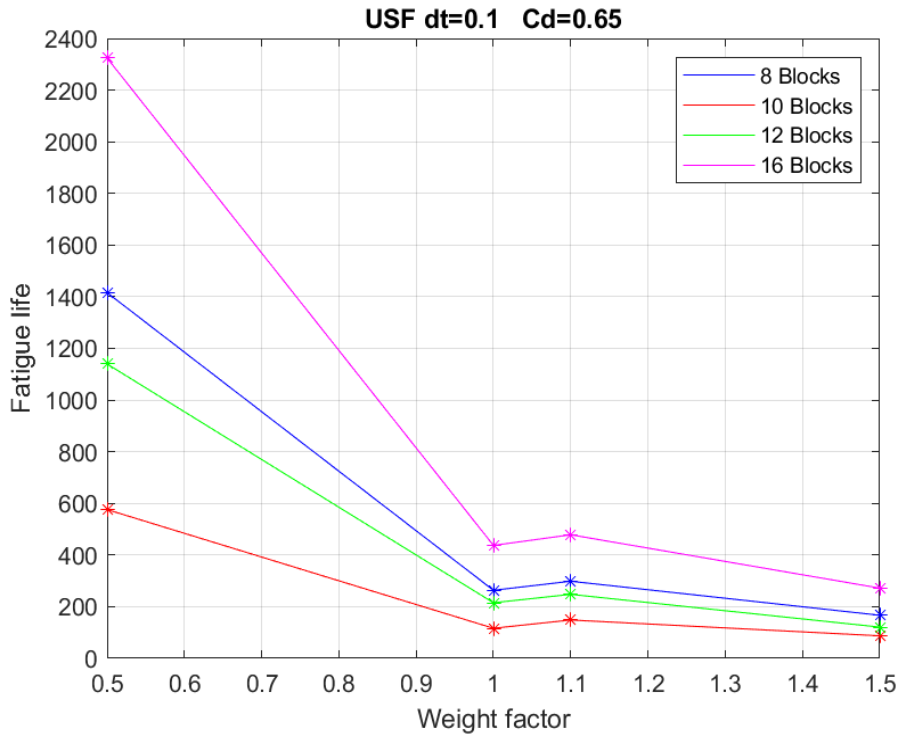


Figure 6-9: Fatigue life against weight factor with dt=0.10 and Cd=0.65 for different wind block cases

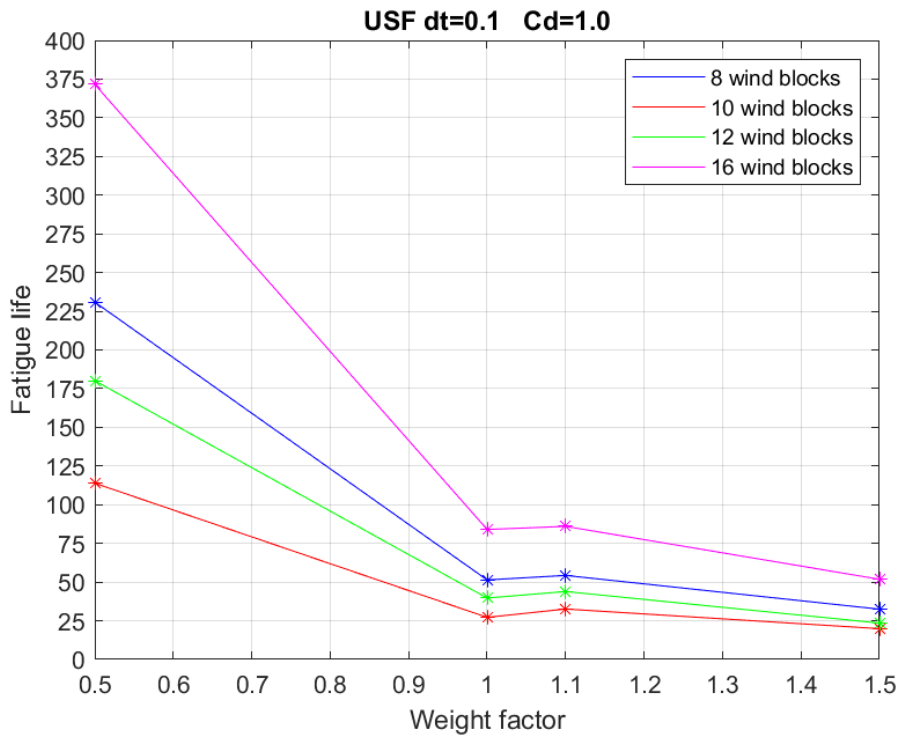


Figure 6-10: Fatigue life against weight factor with dt=0.10 and Cd=0.10 for different wind block cases

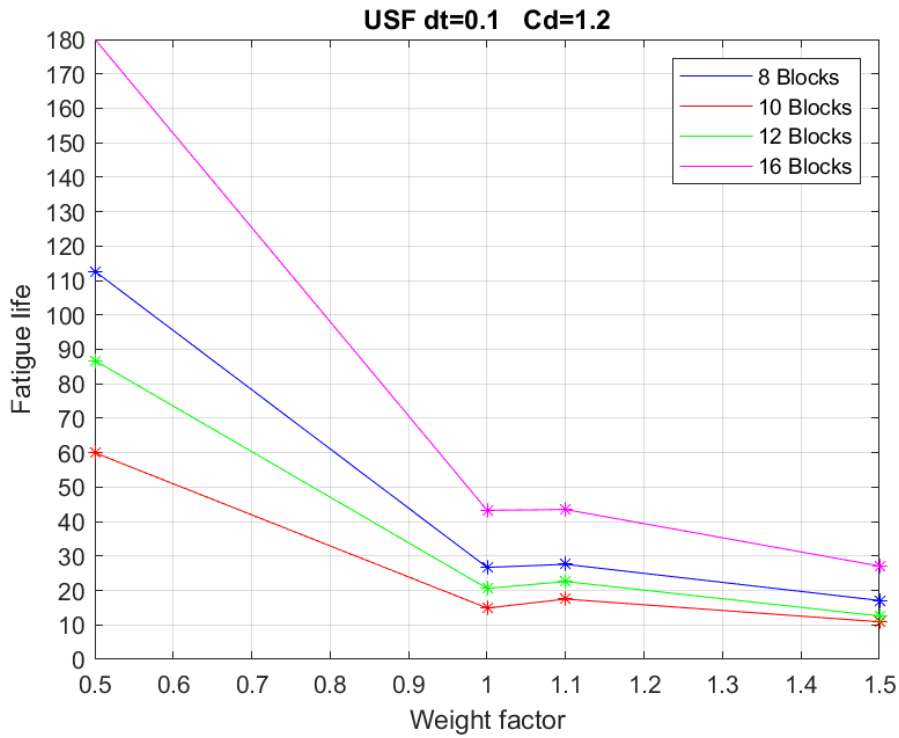


Figure 6-11: Fatigue life against weight factor with dt=0.10 and Cd=1.2 for different wind block cases

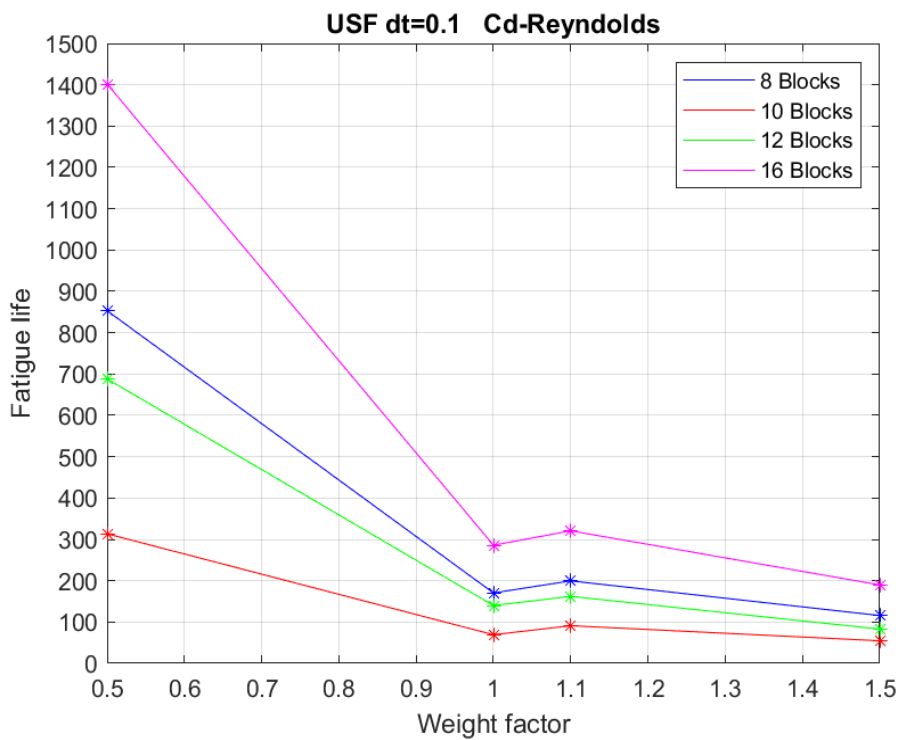


Figure 6-12: Fatigue life against weight factor with dt=0.10 and Reynold's dependent Cd for different wind block cases

Figure 6-9, Figure 6-10, Figure 6-11 and Figure 6-12 show variation in **fatigue life** with change in **weight factor**, for all **wind block** cases, for fixed **Cd** value cases.

The following observations are made:

- **Fatigue life** results seem to be most sensitive to change in **weight factor** that is **below 1**.
- Parameter sensitivity seem to decrease with decreasing **fatigue life**.
- The **16 wind blocks** case give the highest **fatigue life**, followed by the **8 wind blocks** case, then the **12 wind blocks** case in all cases. The **10 wind blocks** case give the lowest in all cases. Same trend is evident in all cases of **Cd**.
- For all cases run with **0.10 seconds time increment**, **fatigue life** increases when **weight factor** increased from **1 to 1.1**. This is unique for cases with **0.10 second time increment** only, and the slope of this increase appears to be more sensitive to lower values of **Cd**.

6.1.2.4 Fatigue life against drag factor for different wind blocks

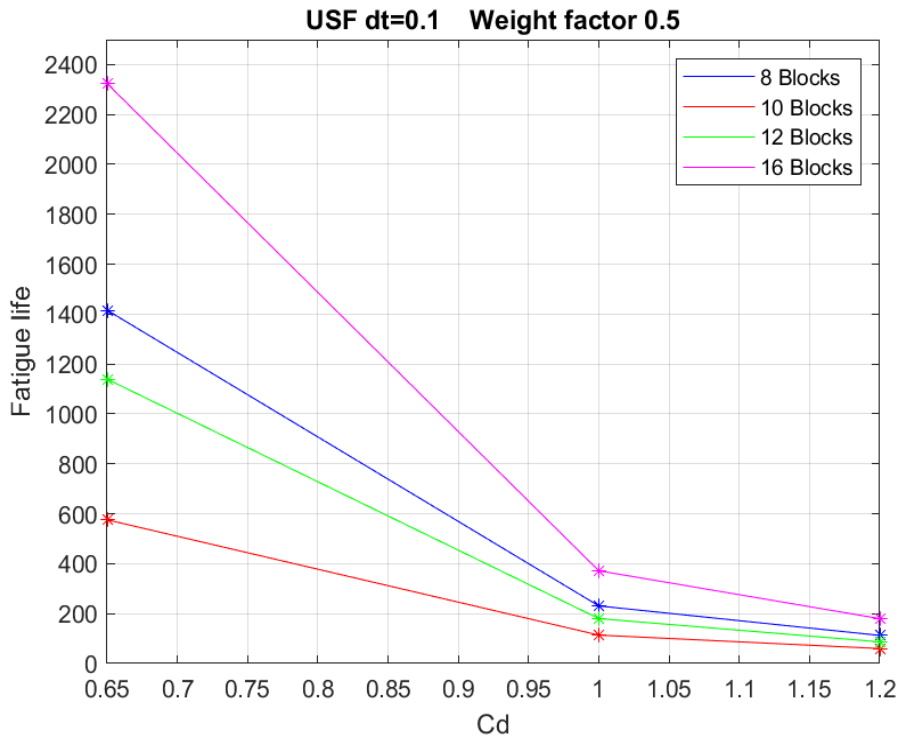


Figure 6-13: Fatigue life against Cd with dt=0.10 and weight factor 0.5 for different wind block cases

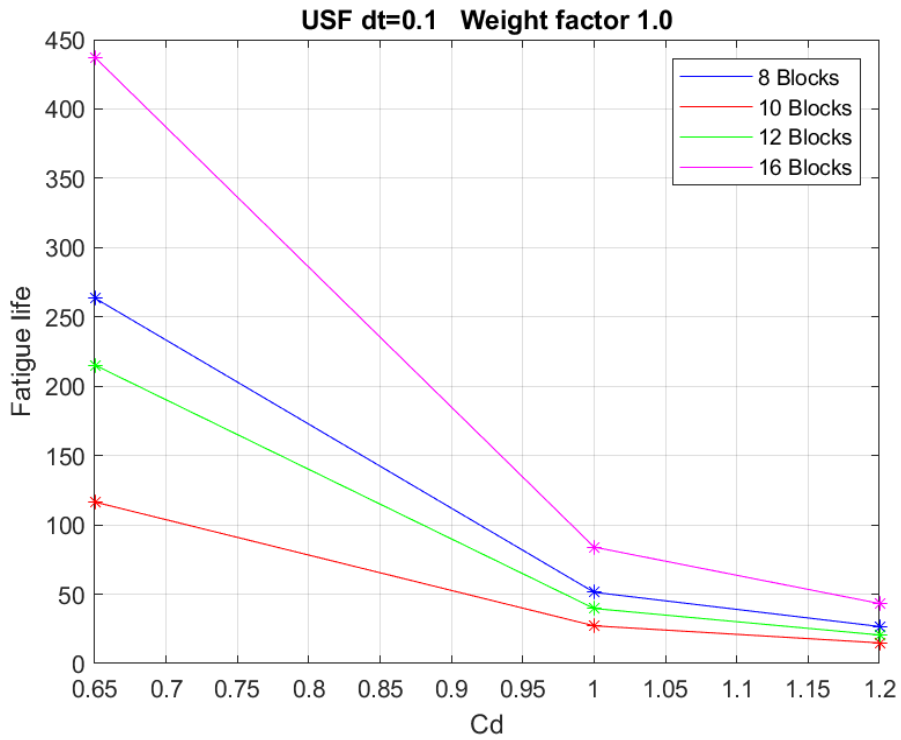


Figure 6-14: Fatigue life against Cd with dt=0.10 and weight factor 1.0 for different wind block cases

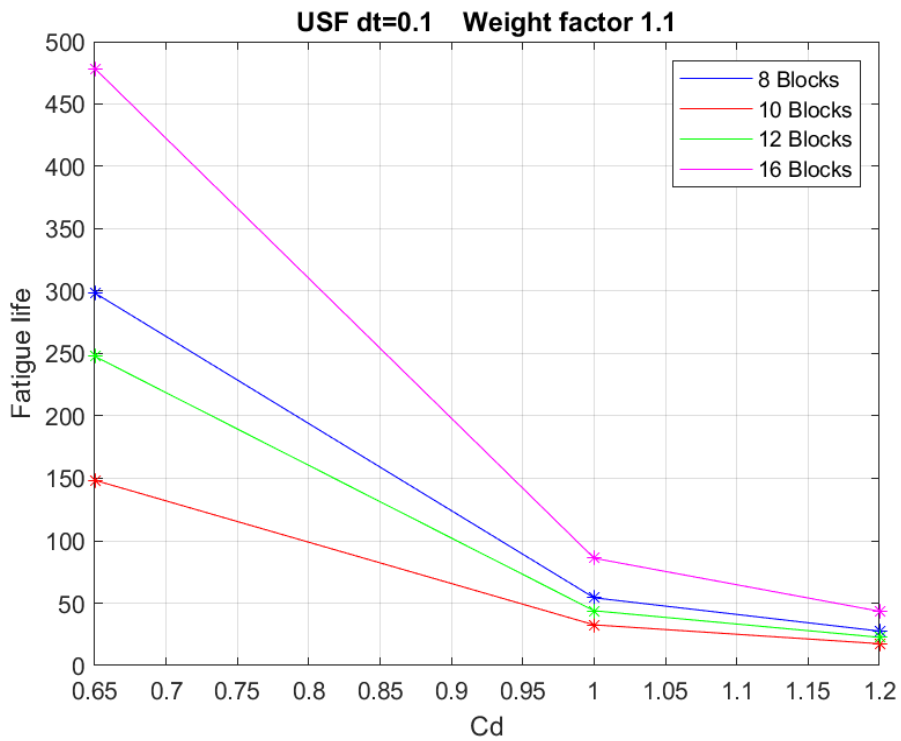


Figure 6-15: Fatigue life against Cd with dt=0.10 and weight factor 1.1 for different wind block cases

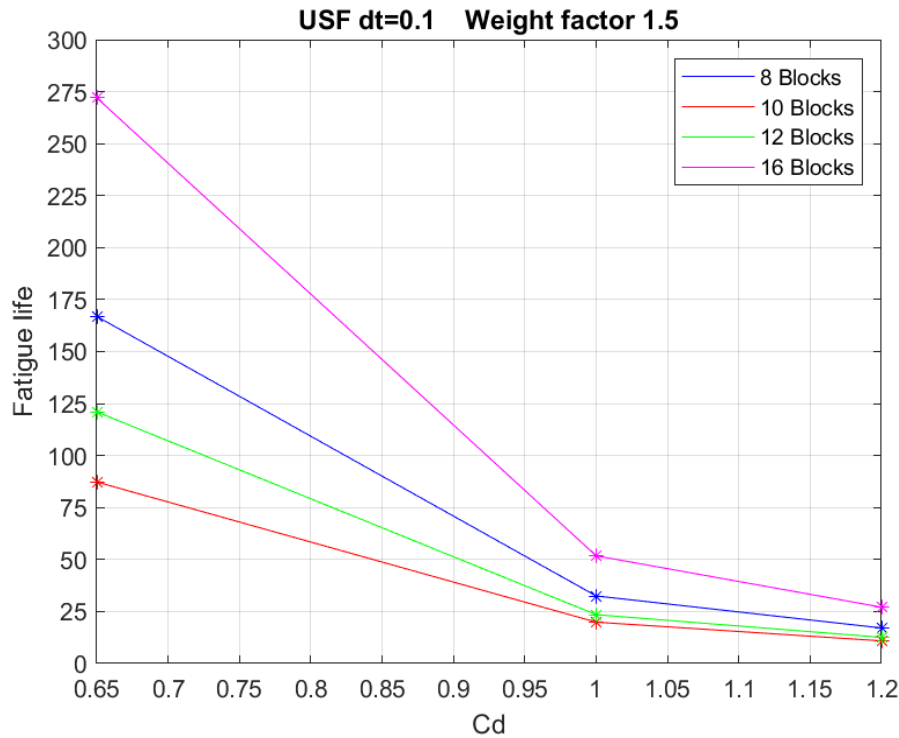


Figure 6-16: Fatigue life against Cd with dt=0.10 and weight factor 1.5 for different wind block cases

Figure 6-13, Figure 6-14, Figure 6-15 and Figure 6-16 show change in **fatigue life** with change of **Cd**, for all **wind block** combinations, for 4 cases of **weight factor**.

The following observations are made:

- **Fatigue life** is most sensitive to changes when **Cd** is lower than **1.0**.
- The **16 wind blocks** case give the highest **fatigue life**, followed by the **8 wind blocks** case, then the **12 wind blocks** case in all cases. The **10 wind blocks** case give the lowest in all cases of different **weigh factors**.
- The **16 wind blocks** case seem to be overall the most sensitive to change in **Cd**. Sensitivity to change seems to decrease with lower **fatigue life**.

6.1.3 Summary and Discussion

For time history fatigue analysis method, increasing weight makes the structure more dynamically sensitive and thereby more prone to fatigue damage. This increase of **fatigue life** with increasing **weight factor** from **1.0** to **1.1** seems contradicting. Considering that the analysis with different **time increments** shows the opposite, it can be concluded that the mentioned increase may not be due to any physical phenomenon, but rather a numerical inaccuracy in the analysis.

Changing mass of the structure through multiplication by a **weight factor** also changes the **natural frequency** of the structure, as mass is inversely related to **natural frequency**. As **time increment** is set as certain value for each analysis, the frequency of computing the loads and stresses changes

according to the **time increment**. Due to the two previous facts, changing **weight factor** could lead to inaccurate representation of the stress history, as the peaks in stress history might not be captured by the **time increment**. This inaccuracy might result in overestimated **fatigue life**. This could explain why **fatigue life** increases between **weight factor 1.0** and **1.1**.

The conclusion is that using a **time increment** of **0.10** seconds for the flare tower under study (Flare boom 1) is inaccurate and should be avoided.

6.2 USFOS Analysis with Time Increment (dt) of 0.05 seconds

6.2.1 Results Tables

The **fatigue life** results from the **5 most affected joints** are presented in the following tables, with the most **critical fatigue life** highlighted with darker color under the header (**Crt Ftg Life**). The parameters on the left side describe the corresponding load case.

- Joints shown in black in the table correspond to those in black font in the table header.
- Joints shown in red in the table correspond to those in red font in the table header.

All cases for 8 wind blocks:

Wind Blocks	Cd	wt factor	Usfos dt=0.05 (Fatigue life / years)					
			Crt Ftg Life	jt 167	jt 159	jt 310	jt 327	jt 310/327
8	0.65	0.5	418	418	453	10271	14605	22857
		1	138	138	144	2261	3024	4550
		1.1	125	125	130	1934	2581	3808
		1.5	95	95	97	1518	1916	2358
	1	0.5	71	71	76	1287	1798	2746
		1	28	28	29	353	453	659
		1.1	26	26	27	314	402	538
		1.5	20	20	21	233	284	321
	1.2	0.5	36	36	38	560	775	1165
		1	15	15	15	169	214	293
		1.1	14	14	14	152	191	238
		1.5	11	11	11	112	135	149
	Reynold's	0.5	267	267	285	5848	8354	12930
		1	92	92	95	1309	1757	2556
		1.1	85	85	88	1160	1549	2214
		1.5	67	67	68	920	1171	1594

Table 6-5: All results with 8 wind blocks in USFOS with dt=0.05

All cases for 10 wind blocks:

Wind Blocks	Cd	wt factor	Usfos dt=0.05 (Fatigue life / years)					
			Crt Ftg Life	jt 167	jt 159	jt 310	jt 327	jt 310/327
10	0.65	0.5	204	204	215	3890	5461	8503
		1	79	79	82	922	1192	1755
		1.1	56	56	58	610	822	1156
		1.5	49	49	50	536	678	958
	1	0.5	43	43	45	539	734	1085
		1	18	18	19	176	216	288
		1.1	14	14	14	125	161	216
		1.5	12	12	12	109	134	178
	1.2	0.5	23	23	24	256	342	490
		1	10	10	10	92	112	141
		1.1	8	8	8	67	85	113
		1.5	7	7	7	58	70	90
	Reynold's	0.5	120	120	126	1893	2651	4054
		1	49	49	51	497	632	898
		1.1	36	36	36	343	454	618
		1.5	31	31	31	294	371	506

Table 6-6: All results with 10 wind blocks in USFOS with dt=0.05

All cases for 12 wind blocks:

Wind Blocks	Cd	wt factor	Usfos dt=0.05 (Fatigue life / years)					
			Crt Ftg Life	jt 167	jt 159	jt 310	jt 327	jt 310/327
12	0.65	0.5	302	302	324	7710	10893	17129
		1	103	103	106	1816	2400	3117
		1.1	96	96	99	1578	2075	2266
		1.5	64	64	65	1165	1432	1473
	1	0.5	49	49	51	951	1328	2048
		1	20	20	21	269	343	384
		1.1	20	20	20	243	284	307
		1.5	14	14	14	165	194	204
	1.2	0.5	25	25	26	407	563	853
		1	11	11	11	125	157	165
		1.1	11	11	11	116	127	143
		1.5	8	8	8	78	90	94
	Reynold's	0.5	195	195	207	4566	6468	10043
		1	69	69	71	1083	1441	2085
		1.1	65	65	67	955	1260	1511
		1.5	46	46	46	727	928	945

Table 6-7: All results with 12 wind blocks in USFOS with dt=0.05

All cases for 16 wind blocks:

Wind Blocks	Cd	wt factor	Usfos dt=0.05 (Fatigue life / years)					
			Crt Ftg Life	jt 167	jt 159	jt 310	jt 327	jt 310/327
16	0.65	0.5	727	727	779	17464	25323	39216
		1	219	219	227	3309	4480	6623
		1.1	201	201	208	3111	4186	6161
		1.5	170	170	170	2855	3610	5534
	1	0.5	124	124	132	2222	3143	4739
		1	44	44	45	551	714	1015
		1.1	41	41	42	508	657	942
		1.5	35	35	35	429	525	773
	1.2	0.5	63	63	66	979	1369	2029
		1	23	23	24	269	344	486
		1.1	22	22	22	247	313	444
		1.5	18	18	19	204	247	281
	Reynold's	0.5	457	457	483	9524	13881	21186
		1	147	147	151	1912	2587	3682
		1.1	138	138	142	1870	2516	3577
		1.5	121	121	123	1741	2225	3292

Table 6-8: All results with 16 wind blocks in USFOS with dt=0.05

6.2.2 Results Graphs

This chapter presents **fatigue life** for **the most critical joint** only and how it varies with different parameter changes for USFOS **dt=0.05** seconds cases. One parameter will be fixed and thereby case dependent, while the other parameters are either shown on the x-axis or presented in different graphs. All reasonable representations are shown.

The shapes of the curves are simplified and should not be interpreted too precisely, but they rather give an indication of trends. Interpolation between different points shall not be used and will not give an accurate representation of reality. More data points would be required to simulate precise reliable curve representation.

All **fatigue life** results correlate with the most **critical fatigue life** in **Table 6-5, Table 6-6, Table 6-7** and **Table 6-8**.

6.2.2.1 Fatigue life against weight factor for different Drag coefficient values

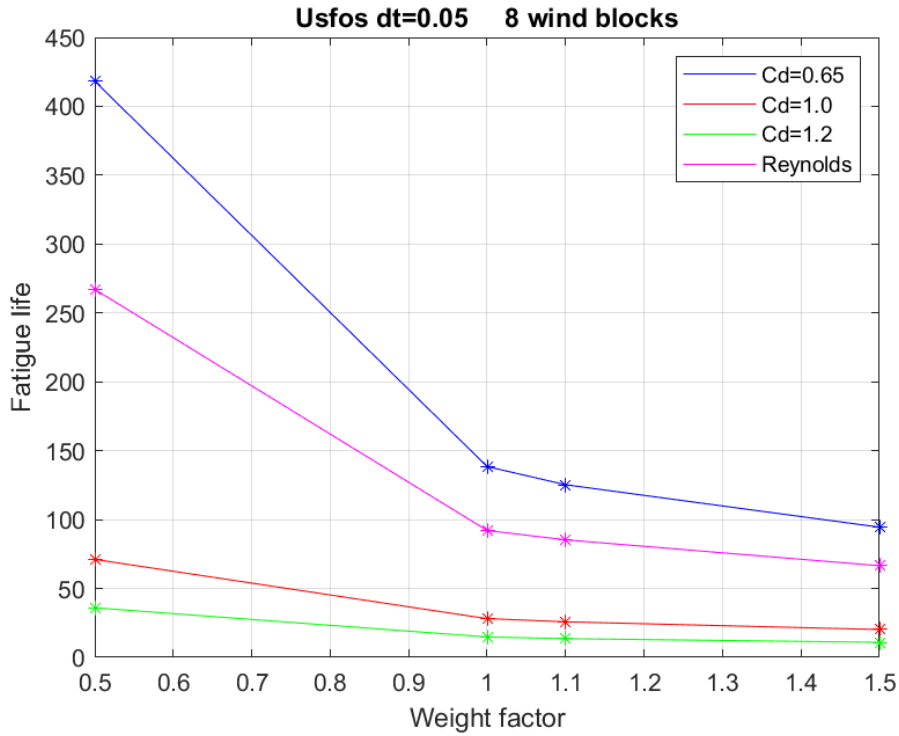


Figure 6-17: Fatigue life against weight factor with dt=0.05 and 8 wind blocks for different Cd values

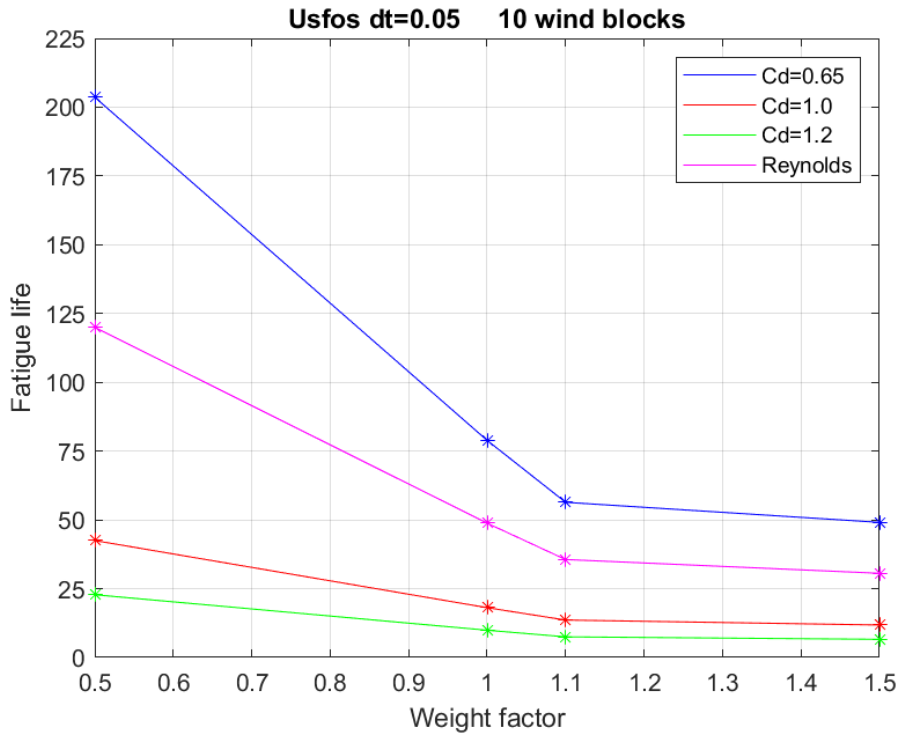


Figure 6-18: Fatigue life against weight factor with dt=0.05 and 10 wind blocks for different Cd values

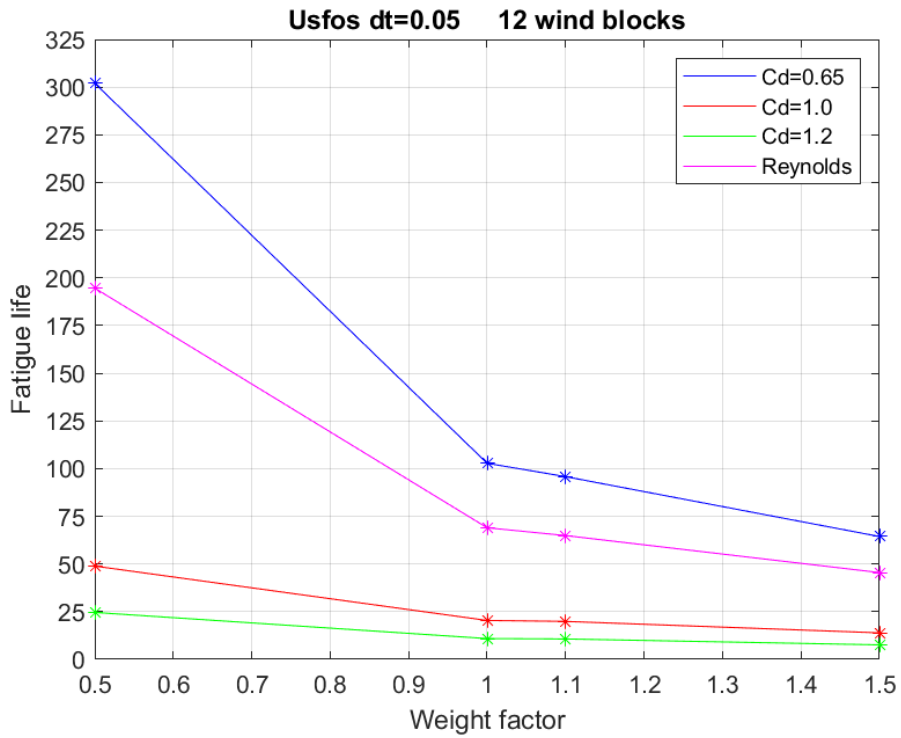


Figure 6-19: Fatigue life against weight factor with dt=0.05 and 12 wind blocks for different Cd values

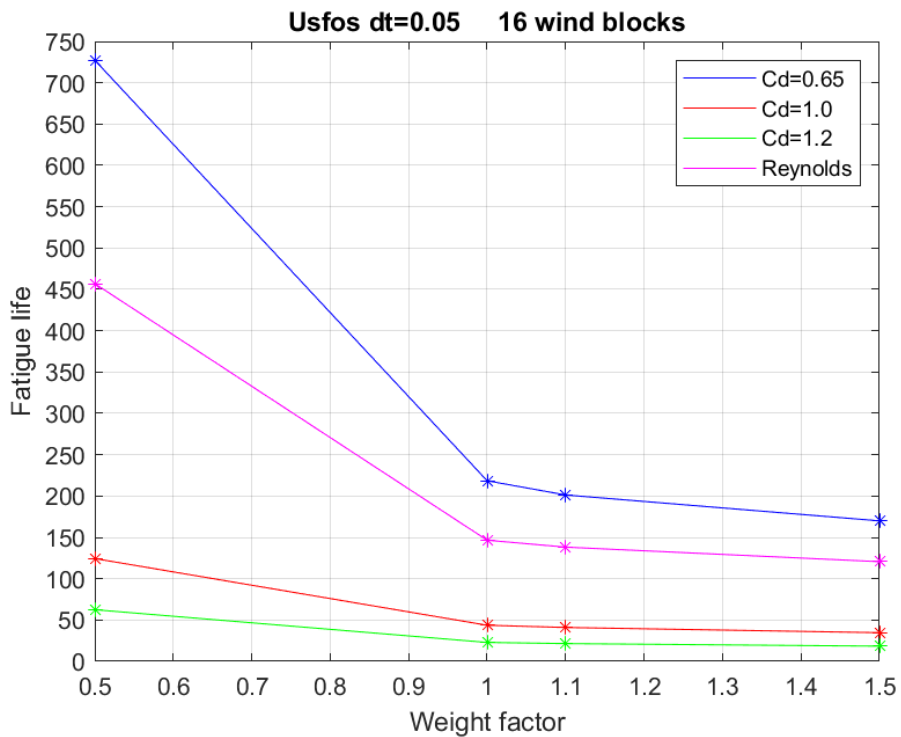


Figure 6-20: Fatigue life against weight factor with dt=0.05 and 16 wind blocks for different Cd values

Figure 6-17, Figure 6-18, Figure 6-19 and Figure 6-20 show variation in **fatigue life** with varying **weight factor**, for all variations of **Cd**, for the **8, 10, 12 and 16 wind blocks**.

The following observations are made:

- **Fatigue life** seem to be more sensitive to change of **weight factor** under **1** for most cases
- In **Figure 6-18** for **10 wind blocks** case, for all **Cd** values, the slope of the curve remains almost constant until **weight factor of 1.1**. However, this trend changes for other **wind blocks**, as the slope remain almost constant after **weight factor of 1.0**.
- **Fatigue life** for the lower values of **Cd** seem to be more sensitive to change in **weight factor**. An average decrease of **77%** in **fatigue life** is observed between **weight factor of 0.5 and 1.5** for **Cd = 0.65**. However, the decrease in case of **Cd = 1.0** is on average **71%** for all **wind blocks**
- **Reynold's dependent Cd** case seems to give longer life than **Cd = 1.0**.

6.2.2.2 Fatigue life against Drag coefficient for different weight factor values

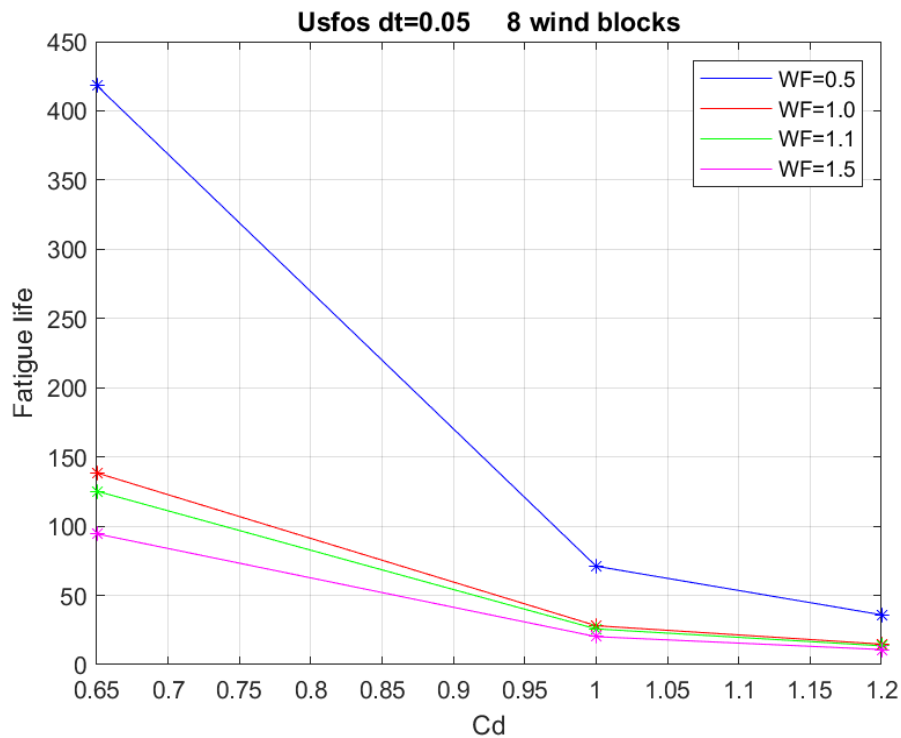


Figure 6-21: Fatigue life against Cd with dt=0.05 and 8 wind blocks for different weight factors

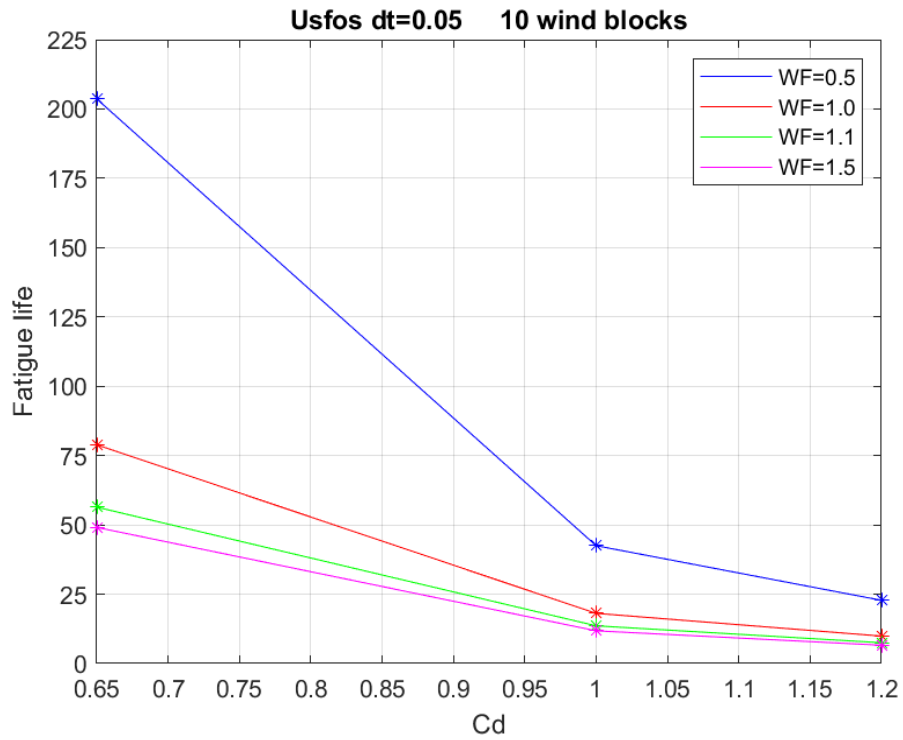


Figure 6-22: Fatigue life against Cd with dt=0.05 and 10 wind blocks for different weight factors

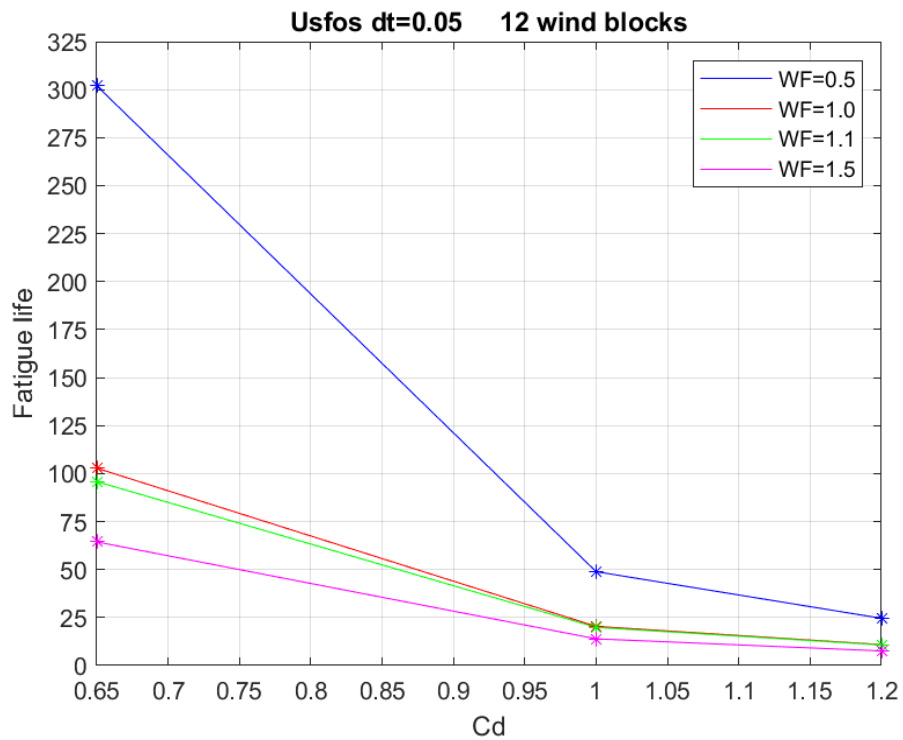


Figure 6-23: Fatigue life against Cd with dt=0.05 and 12 wind blocks for different weight factors

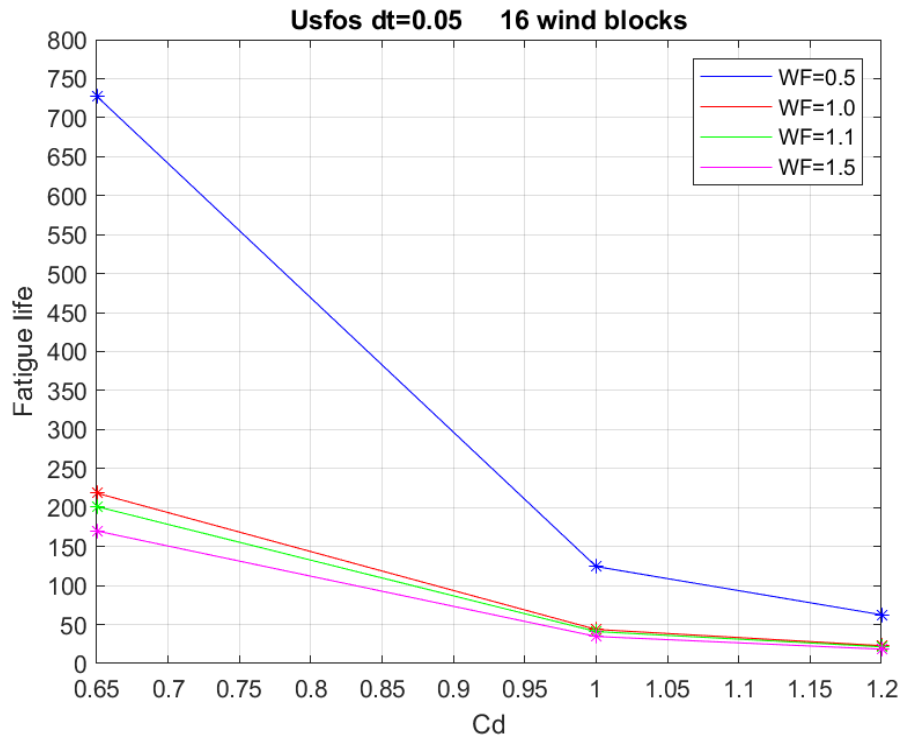


Figure 6-24: Fatigue life against Cd with dt=0.05 and 16 wind blocks for different weight factors

Figure 6-21, Figure 6-22, Figure 6-23 and Figure 6-24 show variation in **fatigue life** with variation of **Cd**, for all 4 cases of **weight factors**, for the **8, 10, 12 and 16 wind block**.

The following observations are made:

- The trend in all graphs seems to be that **fatigue life** is less sensitive to change in **Cd** after **1**.
- For **Cd = 0.65**, **fatigue life** for **weight factor** of **0.5** is on average **3 times** higher than **fatigue life** of **weight factor** of **1.0**.
- Lower **weight factor** values are more sensitive to the increase of **Cd**. The case of **weight factor 0.5** shows the highest decrease in **fatigue life** with the increase of **Cd** from **0.65** to **1.0**. A decrease of **82%** is average among all **wind blocks** for **weight factor** of **0.5**. An average decrease of **80%** is observed for **weight factor** of **1.0**.
- In cases of **8 wind blocks** and **16 wind blocks**, the trends of decrease in **fatigue life** for **weight factors 1.0, 1.1 and 1.5** are similar and close to identical.

6.2.2.3 Fatigue life against weight factor for different wind blocks

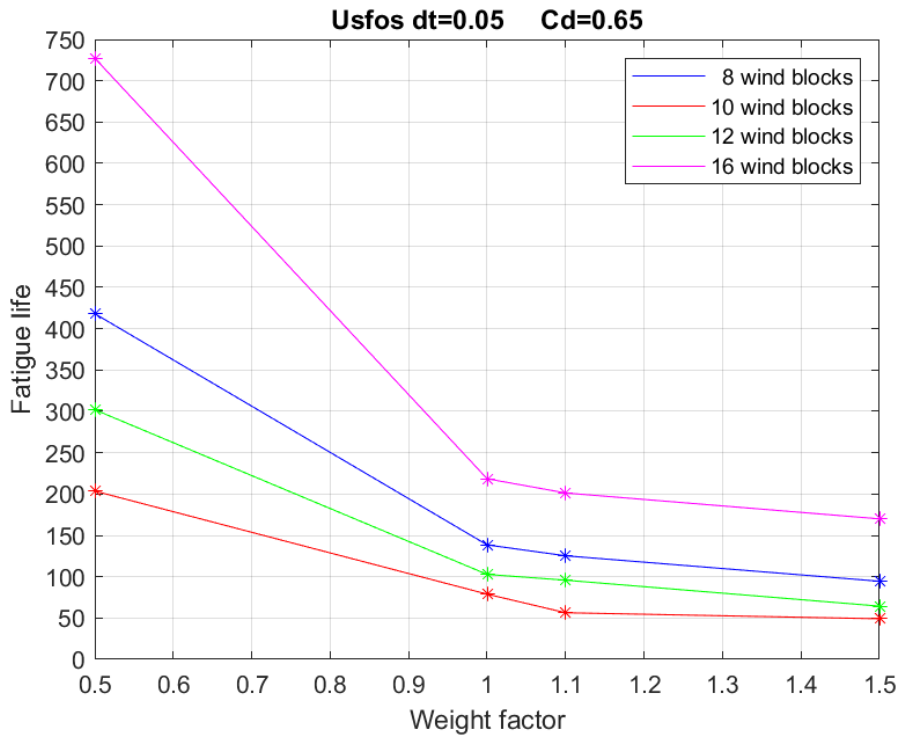


Figure 6-25: Fatigue life against weight factor with dt=0.05 and Cd=0.65 for different wind block cases

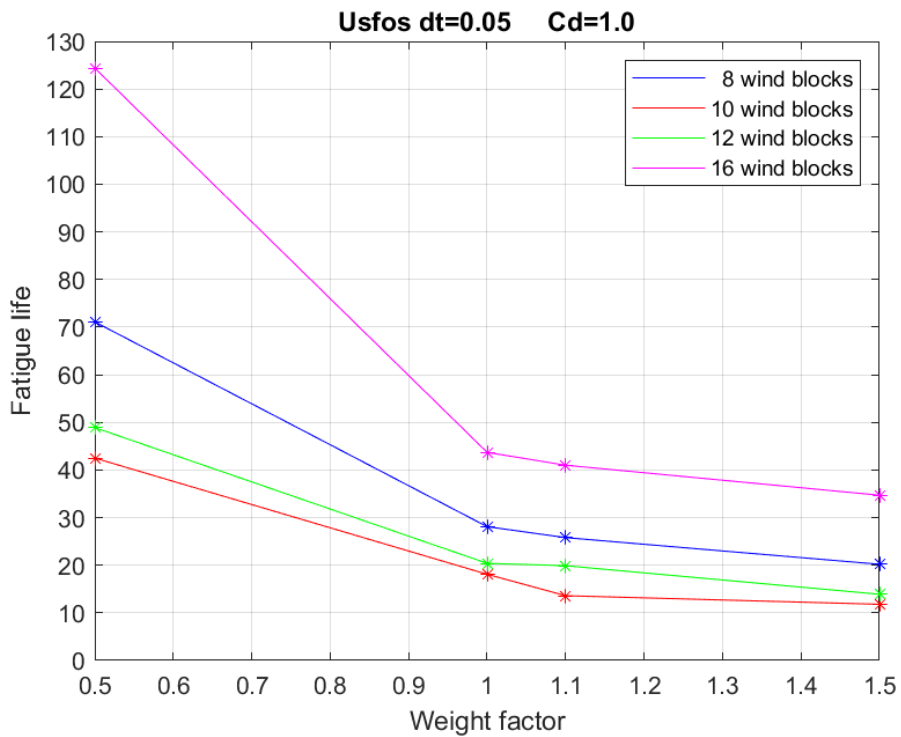


Figure 6-26: Fatigue life against weight factor with dt=0.05 and Cd=1.0 for different wind block cases

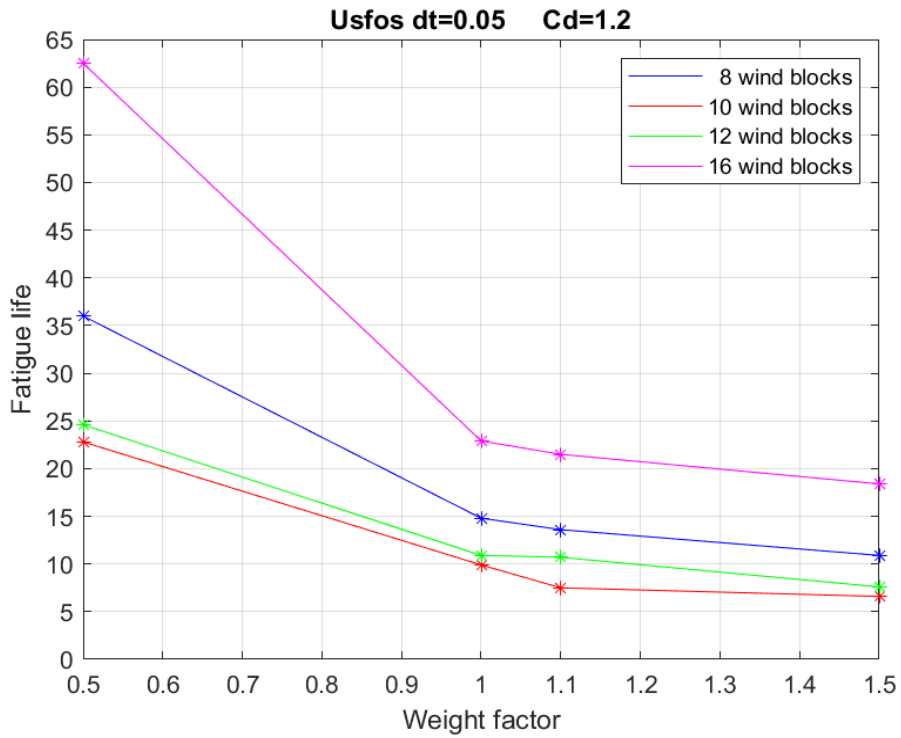


Figure 6-27: Fatigue life against weight factor with dt=0.05 and Cd=1.2 for different wind block cases

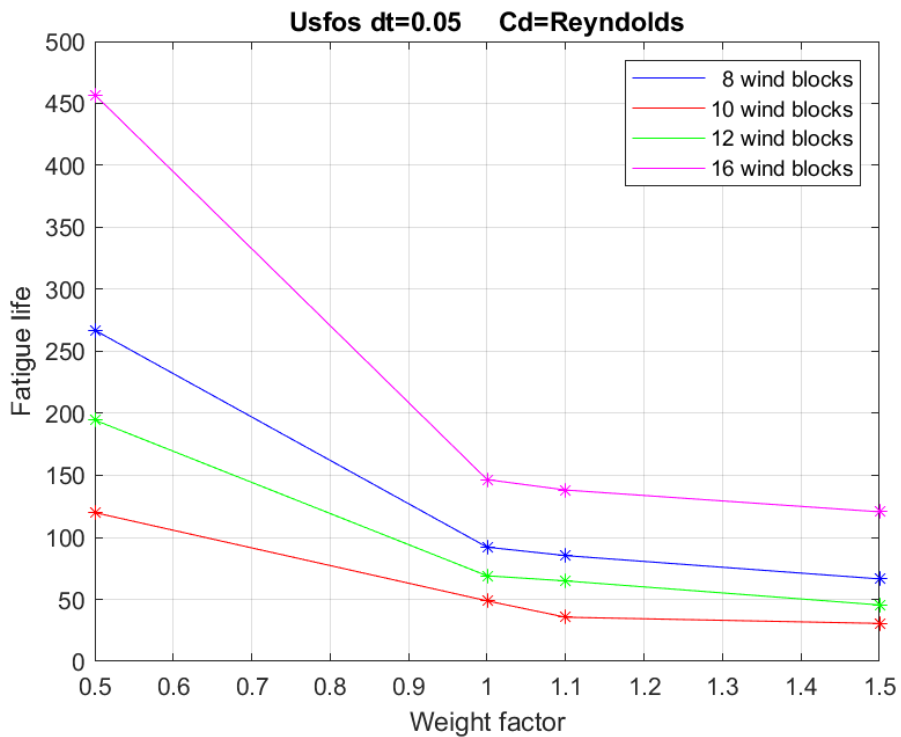


Figure 6-28: Fatigue life against weight factor with dt=0.05 and Reynold's dependent Cd for different wind block cases

Figure 6-25, Figure 6-26, Figure 6-27 and Figure 6-28 show variation in **fatigue life** with change in **weight factor**, for all **wind block** cases, for fixed **Cd** value cases.

The following observations are made:

- **Fatigue life** results seem to be most sensitive to change in **weight factor** that is **below 1**.
- The **16 wind blocks** case seem to be overall the most sensitive to change in **weight factor**. Sensitivity then seems to decrease with decreasing **fatigue life**. **16 wind blocks** case gives an average decrease of **73%** between **weight factor** of **0.5** and **1.5**.
- The **16 wind blocks** case gives the highest **fatigue life** readings, followed by the **8 wind blocks** case, then the **12 wind blocks** case in all cases. The **10 wind blocks** case give the lowest in all cases.
- The trend of decrease in **fatigue life** in case of **10 wind blocks** seems to be linear between **weight factor** of **0.5** and **1.1** for all **wind blocks**.

6.2.2.4 Fatigue life against Drag factor for different wind blocks

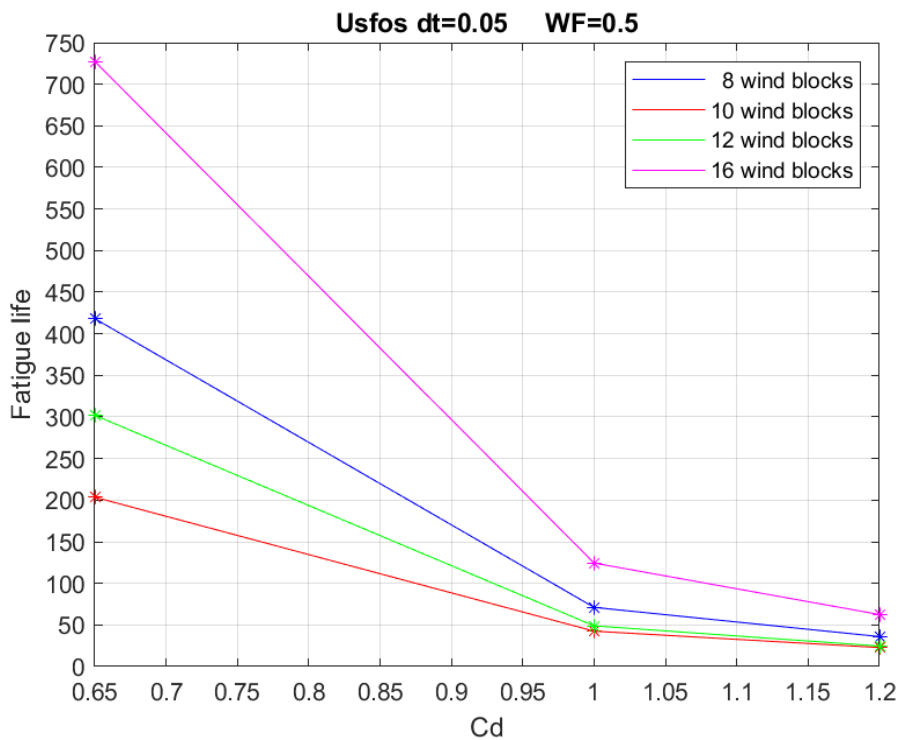


Figure 6-29: Fatigue life against Cd with dt=0.05 and weight factor 0.5 for different wind block cases

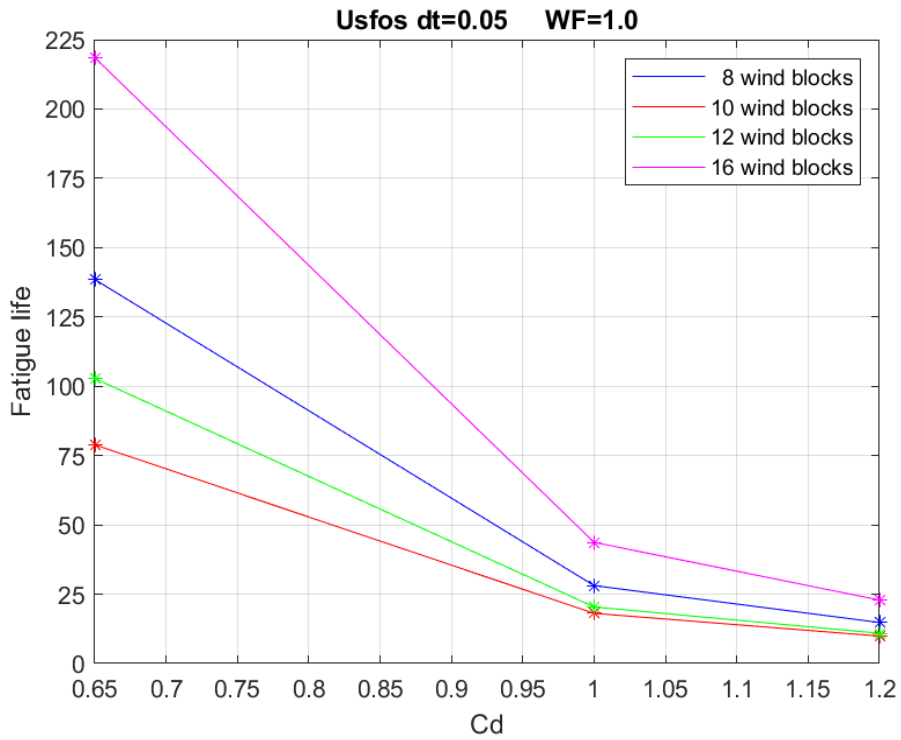


Figure 6-30: Fatigue life against Cd with dt=0.05 and weight factor 1.0 for different wind block cases

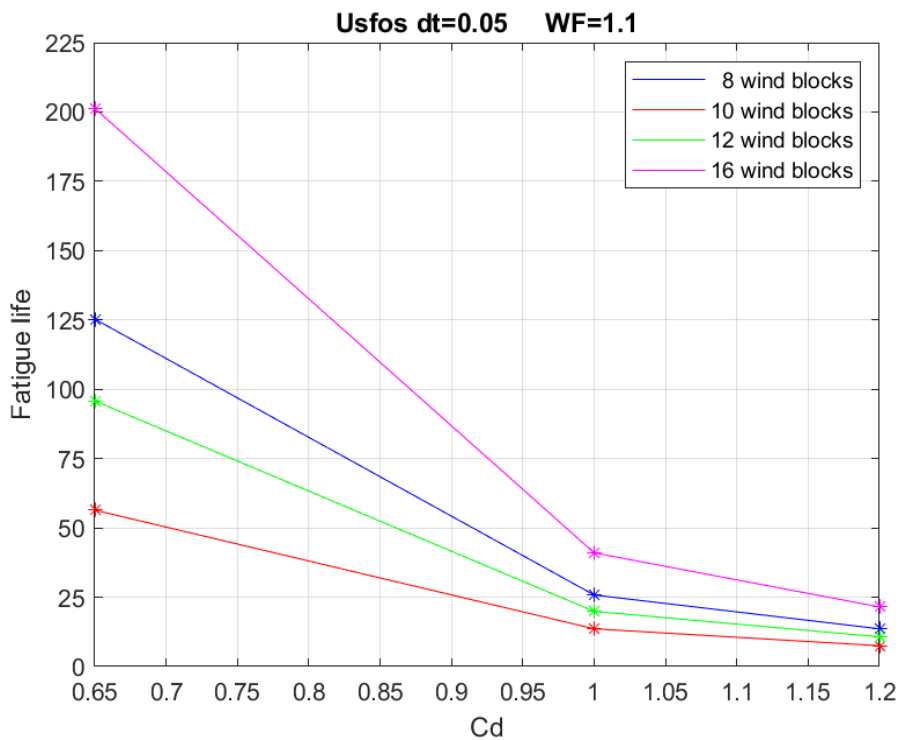


Figure 6-31: Fatigue life against Cd with dt=0.05 and weight factor 1.1 for different wind block cases

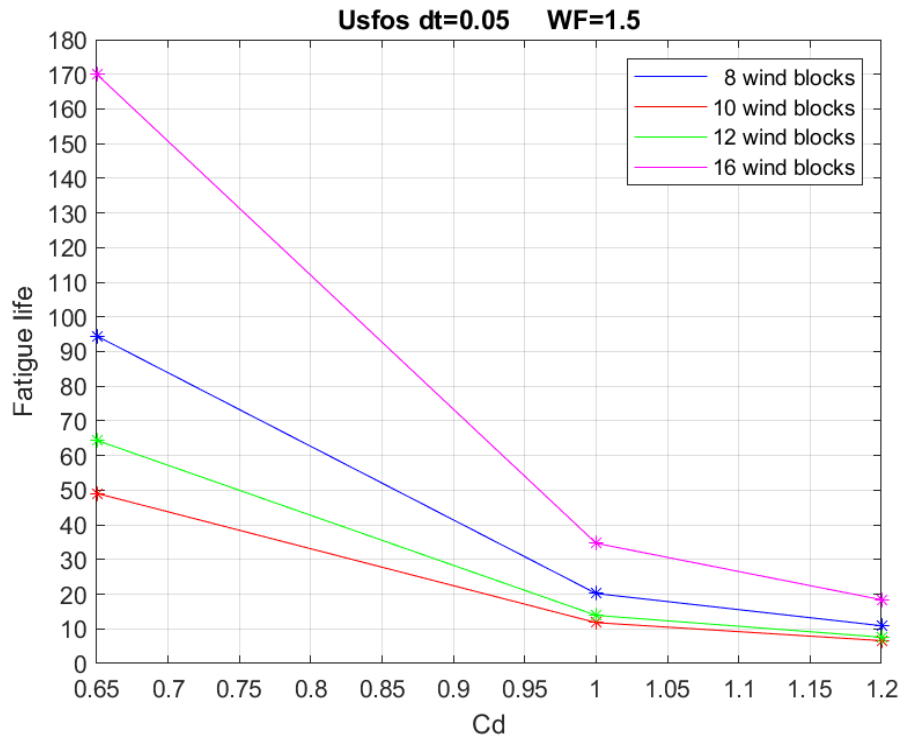


Figure 6-32: Fatigue life against Cd with dt=0.05 and weight factor 1.5 for different wind block cases

Figure 6-29, Figure 6-30, Figure 6-31 and Figure 6-32 show change in **fatigue life** with change of **Cd** for all **wind block** combinations for 4 cases of **weight factor**. The following observations are made:

- **Fatigue life** is most sensitive to changes of **Cd** under 1.
- The **16 wind blocks** case give the highest **fatigue life**, followed by the **8 wind blocks** case, then the **12 wind blocks** case in all cases. The **10 wind blocks** case give the lowest in all cases.
- The **16 wind blocks** case seem to be overall the most sensitive to change in **Cd**. Sensitivity then seems to decrease with decreasing **fatigue life**.

6.2.3 Summary and Discussion

All the graphs in the figures show that the **16 wind blocks** cases give the highest **fatigue life**, **34%** higher on average than the **8 wind block** cases. The **10 wind blocks** case give the lowest **fatigue life** of the three, and **27%** lower than **8 wind blocks**. The **12 wind blocks** cases give slightly higher **fatigue life** than **10 wind blocks** but remains **46%** lower than **8 wind blocks**. This is true for all cases, but the percentages may vary. Even though the **10-** and **12 wind blocks** cases include more **wind blocks** than the **8 wind blocks**, the longer ranges of the top wind speeds make a larger difference than having more **wind blocks**. This gives the impression that the top wind speeds have a larger effect than the lower, even though the probability of occurrence is lower.

Fatigue life is most sensitive to change of **Cd** in the range between **0.65** and **1.0**, and less so in the range of **1.0** to **1.2** in all cases. Generally, the trend for both **Cd** and **weight factor** seem to be that

the higher the values become, the smaller the **fatigue life** sensitivity seem to get. In the case of **10 wind blocks** and **Cd = 1.2**, **fatigue life** only changes from **8** to **7** years by increasing **weight factor** from **1.1** to **1.5**. This decrease is relatively large percentage wise, but small compared to the general scale of **fatigue life** in all cases. Cases with lower parameter values like **8 wind blocks** and **Cd = 0.65**, **fatigue life** decreases from **418** to **138** when increasing **weight factor** from **0.5** to **1.0**, and that seem to be the trend in all cases. The trend is clear that with increasing parameter values or fatigue damage, the damage seems to converge.

In all wind block cases, there seem to be a drastic increase in **fatigue life** for cases with **weight factor** of **0.5** compared to all the other **weight factor** cases. When looking time histories for the critical joint for the cases: **16 wind blocks** and **Cd = 1.0** for **weight factor** of **0.5** and **1.0** there is clear difference in the dynamic response of the structure.

Case of **32 m/s**, wind coming from **330 degrees**. With **weight factor 0.5**:

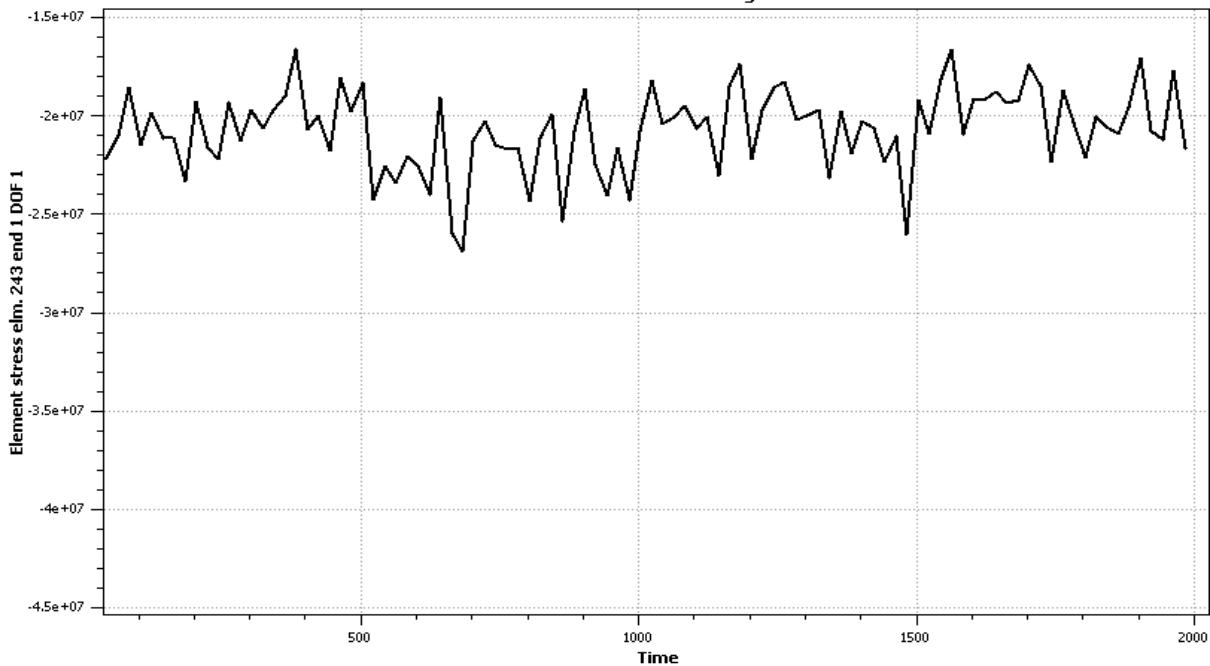


Figure 6-33: Axial stress time history in element 243 from load case 192, with weight factor 0.5

Case of **32 m/s**, wind coming from **330 degrees**. With **weight factor 1.0**:

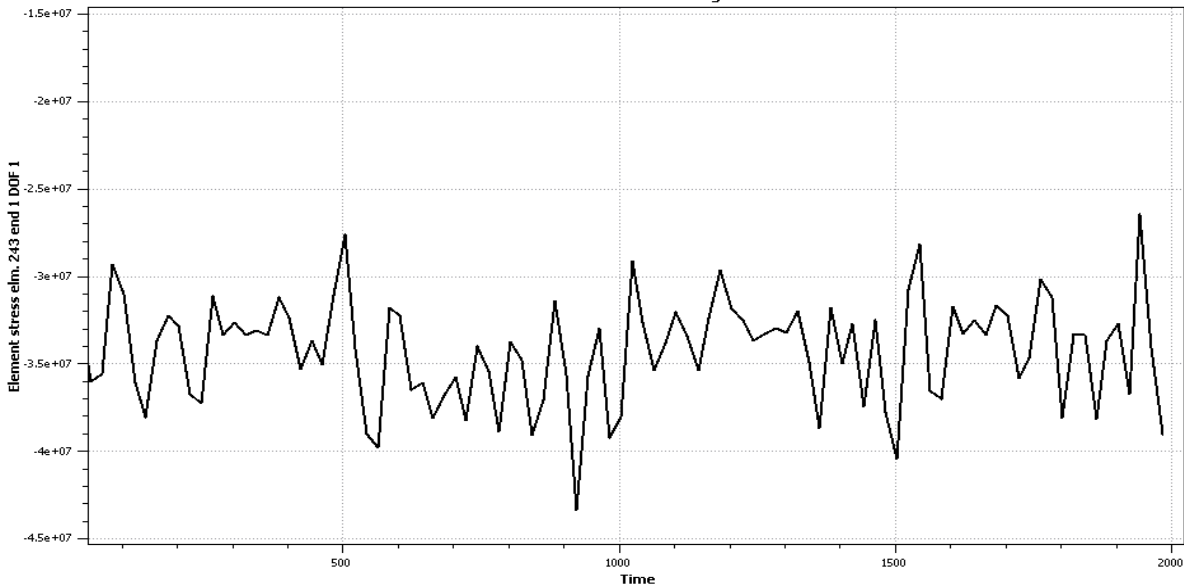


Figure 6-34: Axial stress time history in element 243 from load case 192, with no weight factor

The difference in overall stress is visually different in the two cases; while the stress varies mostly in the range between **16 to 27 MPa** for the **0.5 weight factor** case, it varies mostly in the range of **26 to 43 MPa** for the other case. Changing the weight clearly affects the structures dynamic behavior and could be the main reason for the drastic change in **fatigue life** between **weight factor 0.5** and **1.0**. The values used for estimating and comparing against the S-N, are however determined by the stress ranges ($\Delta\sigma$). The figures illustrate clearly that the latter case (**weight factor = 1.0**), has the longest ranges of about **14 MPa** compared to **8 MPa** in the former (**weight factor = 0.5**).

Large difference in **fatigue life** is observed when **Cd** changes from **0.65** to **1.0** in all cases. Two load cases with equal input except **Cd** show the following stress time history:

Case 1 - 16 wind blocks, no weight factor and $C_d=0.65$:

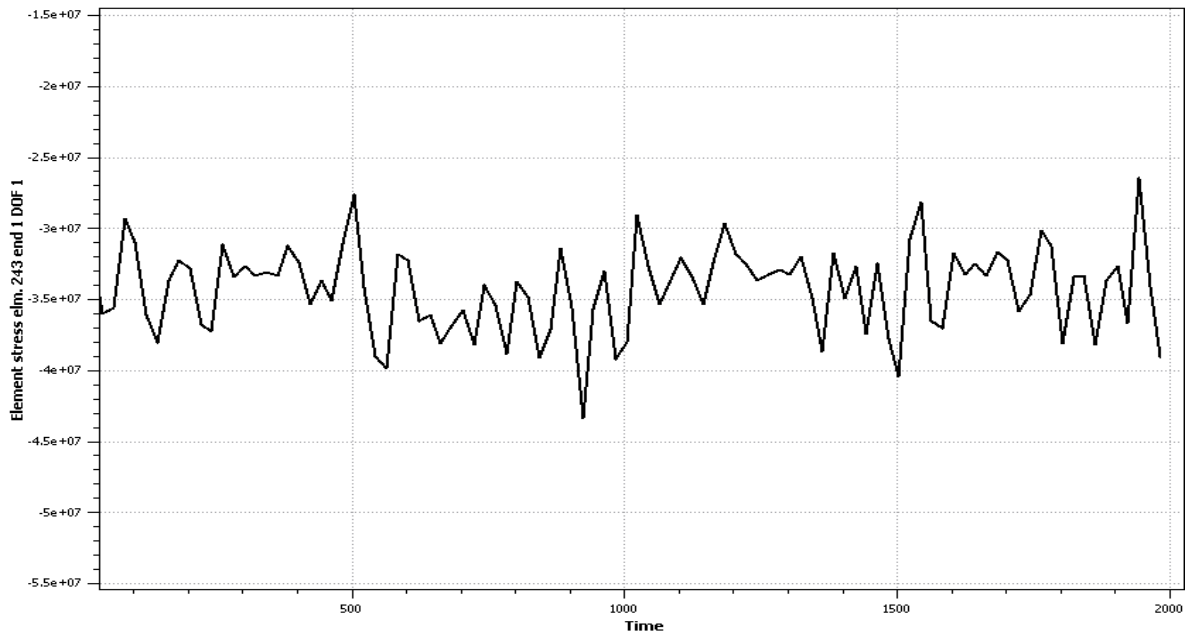


Figure 6-35: Axial stress time history in element 243 from 16 wind blocks' load case 192, with $C_d=0.65$

Case 2 - 16 wind blocks, no weight factor and $C_d=1.0$:

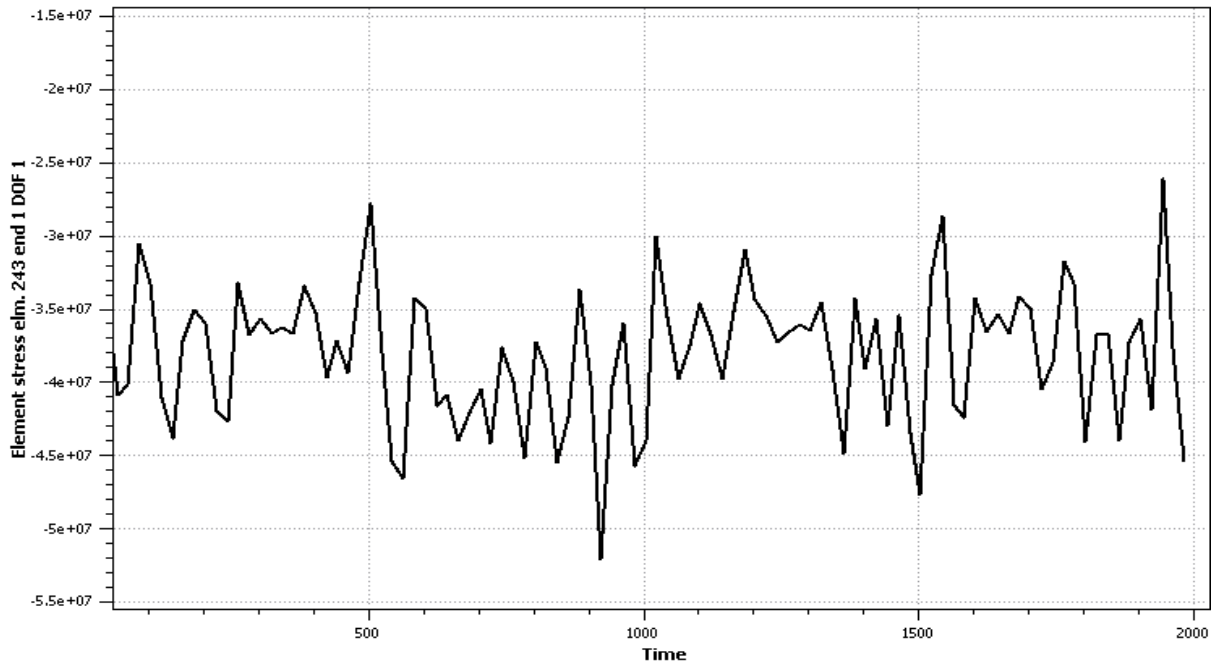


Figure 6-36: Axial stress time history in element 243 from 16 wind blocks' load case 192, with $C_d=1.0$

As **Figure 6-35** and **Figure 6-36** show the same stress pattern, with only magnitude in difference. This proves that **Cd** only works as an amplification factor but does not change the overall stress behavior. This shows that the dynamic behavior not changing, i.e., the vibration frequency seems close to identical. While case 1 shows a stress range of about **12 MPa**, case 2 shows the same stress range with a value of about **19 MPa**, which differs with a factor close to **0.65**. So, while the stress ranges vary linearly with the value for **Cd**, the logarithmic scaling of the S-N curve causes lower change in **fatigue life** as **Cd** increases.

6.3 Parameters

Before comparing USFOS to other software, values of certain parameters which are limited to USFOS must be set. That includes the formula for **relative velocity** and decision on **time increment**. This chapter investigate the effect both the mentioned parameters have on **fatigue life**.

6.3.1 Decision on Time Increment

The lower the **time increment** value is, the more accurate the results will be. However, denser analysis requires more time and storage capacity. Therefore, analysis with different **time increment** to compare time and storage use with accuracy have been done.

Multiple **time increments** have been adopted: **dt=0.02, 0.05, 0.10, 0.20** and **0.50 seconds**. **Fatigue life** converged significantly with decreasing **time increment**, especially for the biggest **time increments**. **Fatigue life** difference from **0.05** and **0.02** was small enough to be neglected, and the analysis spent twice the amount of time to run with **0.02 seconds** (see section **Error! Reference source not found.**).

Cases with **0.05 seconds** compared to **0.10 seconds**, on average gave about half the **fatigue life**, so the most reasonable **time increment** to use in the final analysis was **0.05 seconds**. This value provides sufficient accuracy and is also practical as it is less computationally expensive.

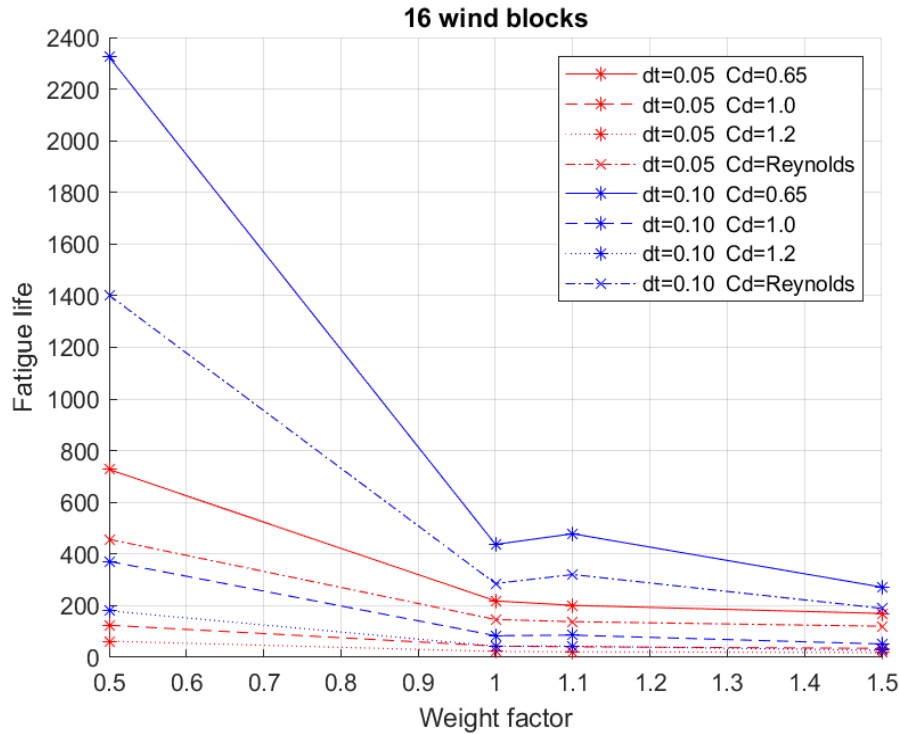


Figure 6-37: Fatigue life against weight factor for all cases of Cd of both dt=0.05 and dt=0.10

As Figure 6-37 shows, there is a significant difference in **fatigue life** of coherent cases with **time increments** of **0.10 seconds** compared to **0.05 seconds**, especially with lower **weight factors**.

6.3.2 Relative Velocity

Relative velocity is a phenomenon which mainly affect large motion structures such as wind turbines (see section 3.2.6). USFOS has a built-in function that accounts for this phenomenon. To analyze the effect of this function, comparison cases have been done with and without this function active for **16 wind blocks** with **Reynold's number dependent Cd** and **Cd=1.0** for all cases of **weight factor**. The results are presented in **Table 6-9** below:

Wind Blocks	Cd	wt factor	Rel vel on	Rel vel off
16	1	0.5	471.9	124.4
		1	140.2	43.7
		1.1	127.9	41.0
		1.5	89.4	34.7
	Reynold's	0.5	1507.8	457.0
		1	402.7	146.6
		1.1	370.8	138.2
		1.5	273.0	120.6

Table 6-9: Cases with and without the effect of relative velocity

On average the use of this formula gives an **196%** increase (i.e., approximately 3 times) in **fatigue life** compared to the cases excluding it. The effect of **relative velocity** most likely does not have such significant impact at relatively small displacements on slender structure such as this flare in real life. For further analyses, this formula is therefore turned off.

7 Comparisons and Discussions

The main objective of this thesis is to compare **fatigue life** results and parameter sensitivity from different software approaches. Since FRAMEWORK and WINDPACK both use the spectral density method, comparisons of the two are presented first. FRAMEWORK is then compared to USFOS, as FRAMEWORK input spectra and fatigue life results correlate to those from USFOS.

7.1 Comparison Table

Results from the different software with parameters are presented in the tables below:

Wind Blocks	Cd	wt factor	Critical fatigue life			
			Framework	Windpack	Usfos dt=0.05	Usfos dt=0.10
8	0.65	0.5	564	1260	418	1416
		1	331	787	138	264
		1.1	195	721	125	299
		1.5	131	547	95	167
	1	0.5	131	151	71	231
		1	57	109	28	51
		1.1	51	103	26	54
		1.5	36	85	20	33
	1.2	0.5	42	69	36	113
		1	29	52	15	27
		1.1	18	49	14	28
		1.5	13	42	11	17
	Reynold's	0.5	381		267	853
		1	230		92	170
		1.1	137		85	200
		1.5	94		67	116
10	0.65	0.5	221	583	204	576
		1	145	387	79	116
		1.1	93	360	56	149
		1.5	68	284	49	87
	1	0.5	45	99	43	114
		1	31	72	18	27
		1.1	20	68	14	33
		1.5	15	56	12	20
	1.2	0.5	24	49	23	60
		1	17	37	10	15
		1.1	11	35	8	18
		1.5	8	29	7	11
	Reynold's	0.5	158		120	313
		1	106		49	69
		1.1	69		36	91
		1.5	50		31	55

Table 7-1: Critical fatigue life for all cases of 8 and 10 wind blocks in USFOS and FRAMEWORK

Wind Blocks	Cd	wt factor	Critical fatigue life			
			Framework	Windpack	Usfos dt=0.05	Usfos dt=0.10
12	0.65	0.5	433	872	302	1140
		1	246	533	103	215
		1.1	141	487	96	248
		1.5	92	361	64	121
	1	0.5	64	102	49	180
		1	40	77	20	40
		1.1	25	72	20	44
		1.5	18	59	14	23
	1.2	0.5	30	49	25	87
		1	20	39	11	21
		1.1	13	37	11	23
		1.5	9	31	8	13
	Reynold's	0.5	292		195	688
		1	170		69	140
		1.1	99		65	162
		1.5	66		46	83
16	0.65	0.5	Not possible		727	2324
		1			219	437
		1.1			201	478
		1.5			170	272
	1	0.5			124	372
		1			44	84
		1.1			41	86
		1.5			35	52
	1.2	0.5			63	180
		1			23	43
		1.1			22	44
		1.5			18	27
	Reynold's	0.5			457	1402
		1			147	286
		1.1			138	321
		1.5			121	190

Table 7-2: Critical fatigue life for all cases of 12 and 16 wind blocks in FRAMEWORK, WINDPACK and USFOS

7.2 FRAMEWORK and WINDPACK

The two software have very similar methods of estimating **fatigue life**, as they both use spectral density method in estimating fatigue damage. However, the main difference between the two are how the scatter diagram is treated. While FRAMEWORK combine the directional probabilities opposing each other (such as 0° and 180°), WINDPACK adds all the probabilities of each wind direction in different wind speeds together and all probabilities of each wind speed in different directions together. Meaning all wind speed probabilities coming from one direction are added as the overall probability from that direction. The same is done for wind speeds.

The analyses done for the flare model also differ in which spectral density function used in the two software. While FRAMEWORK uses the **NPD (Frøya)** spectral equation, WINDPACK does not have that option available and uses **HARRIS** spectra.

It is worth noting that WINDPACK can run 16 wind blocks; however, this case is excluded as FRAMEWORK is incapable of running more than 12 wind blocks.

7.2.1 Results Tables

Results from the different software with parameters are presented in the tables below:

Wind Blocks	Cd	wt factor	Critical fatigue life	
			Framework	Windpack
8	0.65	0.5	564	1260
		1	331	787
		1.1	195	721
		1.5	131	547
	1	0.5	131	151
		1	57	109
		1.1	51	103
		1.5	36	85
	1.2	0.5	42	69
		1	29	52
		1.1	18	49
		1.5	13	42

Table 7-3: Critical fatigue life for all comparable cases of 8 wind blocks in FRAMEWORK and WINDPACK

Wind Blocks	Cd	wt factor	Critical fatigue life	
			Framework	Windpack
10	0.65	0.5	221	583
		1	145	387
		1.1	93	360
		1.5	68	284
	1	0.5	45	99
		1	31	72
		1.1	20	68
		1.5	15	56
	1.2	0.5	24	49
		1	17	37
		1.1	11	35
		1.5	8	29

Table 7-4: Critical fatigue life for all comparable cases of 10 wind blocks in FRAMEWORK and WINDPACK

Wind Blocks	Cd	wt factor	Critical fatigue life	
			Framework	Windpack
12	0.65	0.5	433	872
		1	246	533
		1.1	141	487
		1.5	92	361
	1	0.5	64	102
		1	40	77
		1.1	25	72
		1.5	18	59
	1.2	0.5	30	49
		1	20	39
		1.1	13	37
		1.5	9	31

Table 7-5: Critical fatigue life for all comparable cases of 12 wind blocks in FRAMEWORK and WINDPACK

7.2.2 Results Graphs

This chapter presents **fatigue life** for **the most critical joint** and how it varies with different parameter changes. One parameter will be fixed and thereby case dependent, while the other parameters are either shown on the x-axis or presented on different graphs.

The shapes of the curves are simplified and should not be interpreted too precise, but rather give an indication of trends. Interpolation between different points shall not be used and will not give accurate representation of reality. More data points would be required to simulate precise reliable curve representation.

All **fatigue life** results correlate with the most critical **fatigue life** in Table 7-3, Table 7-4 and Table 7-5 and all reasonable load cases are presented.

7.2.2.1 Fatigue life against weight factor for different wind blocks

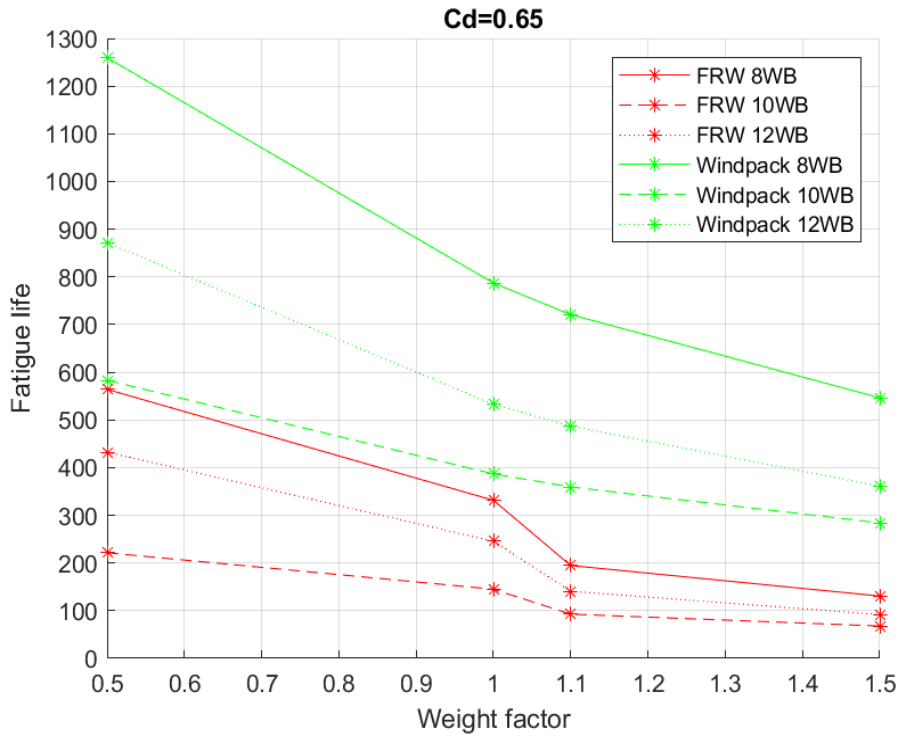


Figure 7-1: Fatigue life against weight factor with Cd=0.65 for different wind block cases in FRAMEWORK and WINDPACK

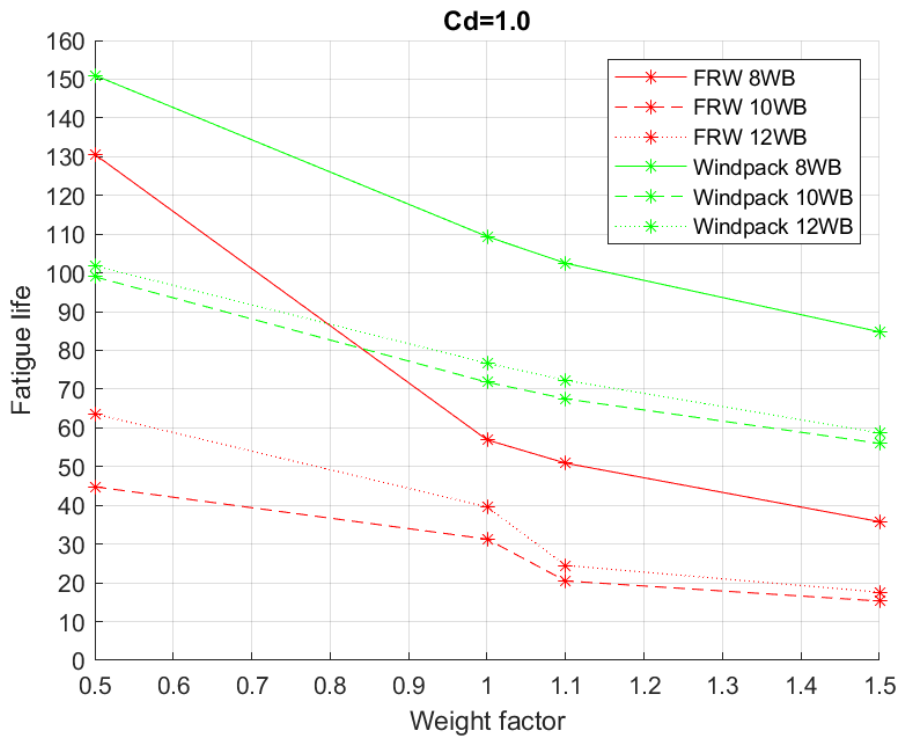


Figure 7-2: Fatigue life against weight factor with Cd=1.0 for different wind block cases in FRAMEWORK and WINDPACK

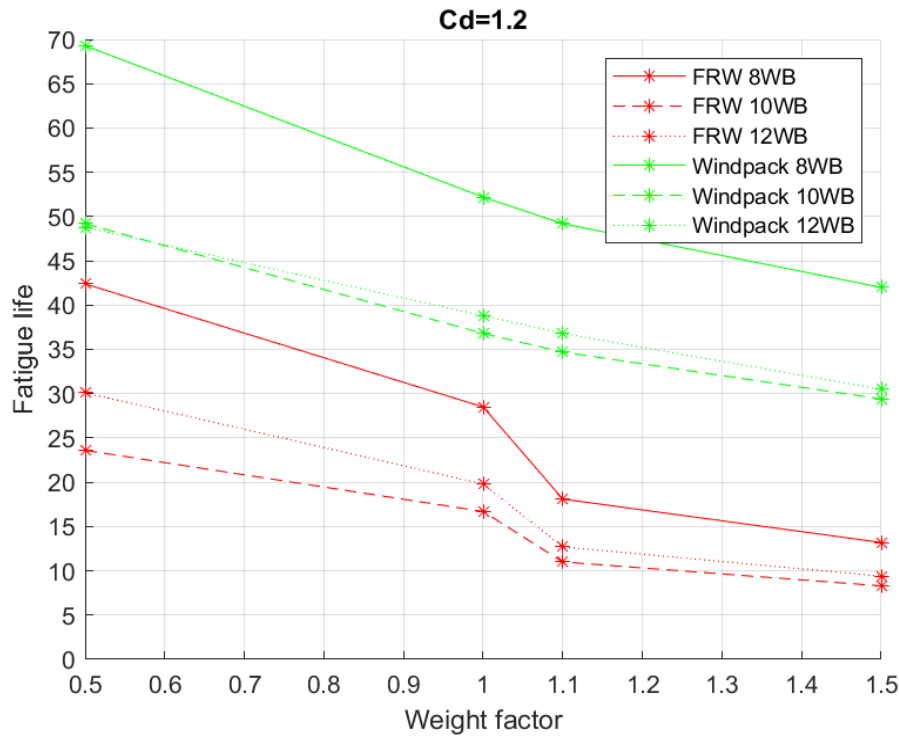


Figure 7-3: Fatigue life against weight factor with Cd=1.2 for different wind block cases in FRAMEWORK and WINDPACK

Figure 7-1, Figure 7-2 and Figure 7-3 show variation in **fatigue life** with varying **weight factor** for FRAMEWORK and WINDPACK, for all **wind block** combinations, for different **Cd** cases.

The following observations are made:

- WINDPACK predicts longer **fatigue life** than FRAMEWORK in each corresponding **wind block** case.
- For the same **Cd** and **weight factor**, all **wind block** cases in WINDPACK predict longer fatigue than all wind block cases in FRAMEWORK, except FRAMEWORK's **8 wind blocks**, **WF=0.5** and **Cd=1.0**.
- **Fatigue life** in WINDPACK decreases almost linearly with **weight factor** while **fatigue life** in FRAMEWORK is very sensitive around **weight factor 1.0** to **1.1**. A significant drop between weight factor 1.0 and 1.1 can be observed as a trend in all FRAMEWORK cases, while this trend is not observed in WINDPACK.

7.2.2.2 Fatigue life against drag coefficient for different wind blocks

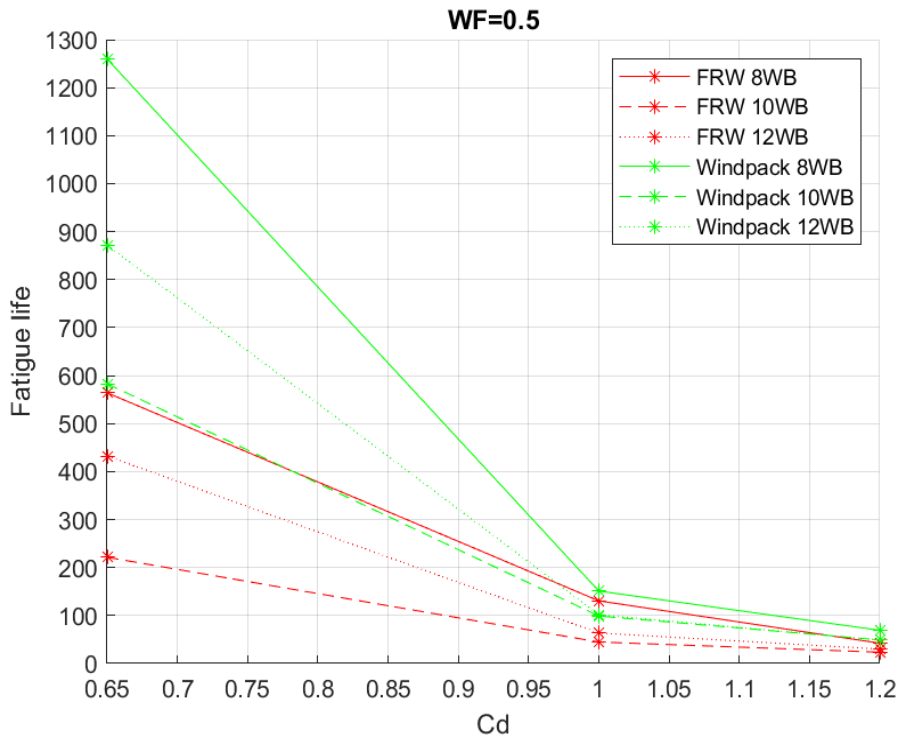


Figure 7-4: Fatigue life against Cd with weight factor 0.5 for all wind block cases in FRAMEWORK and WINDPACK

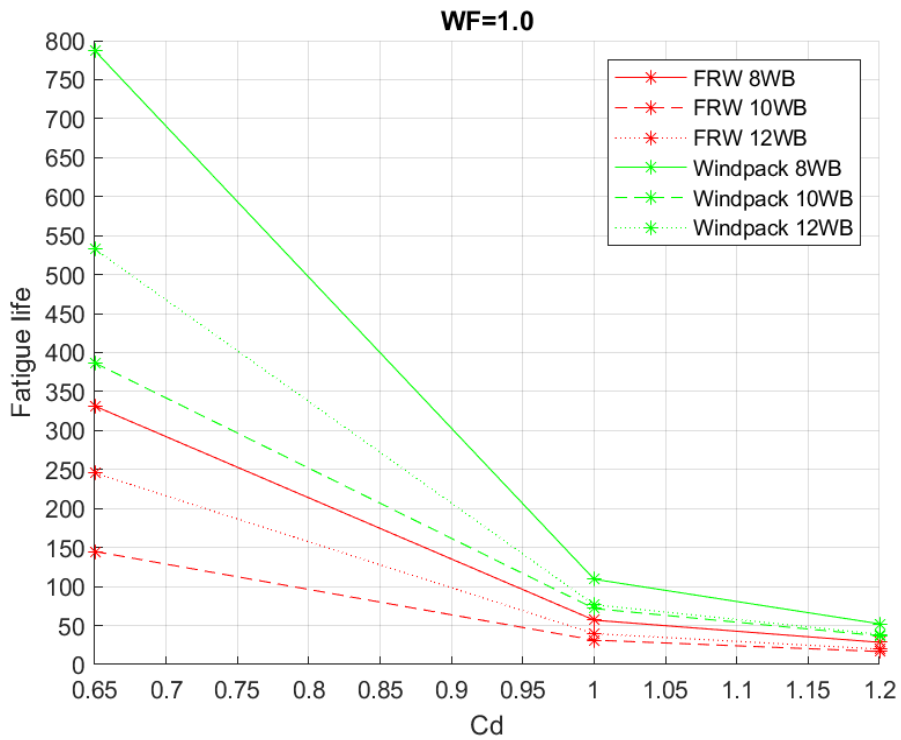


Figure 7-5: Fatigue life against Cd with weight factor 1.0 for all wind block cases in FRAMEWORK and WINDPACK

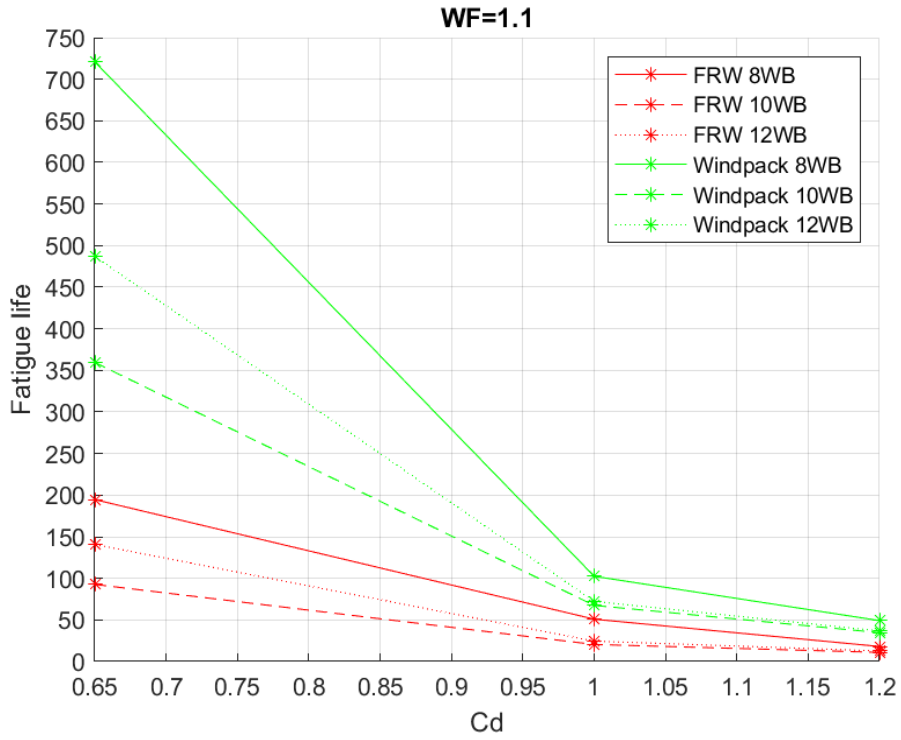


Figure 7-6: Fatigue life against Cd with weight factor 1.1 for all wind block cases in FRAMEWORK and WINDPACK

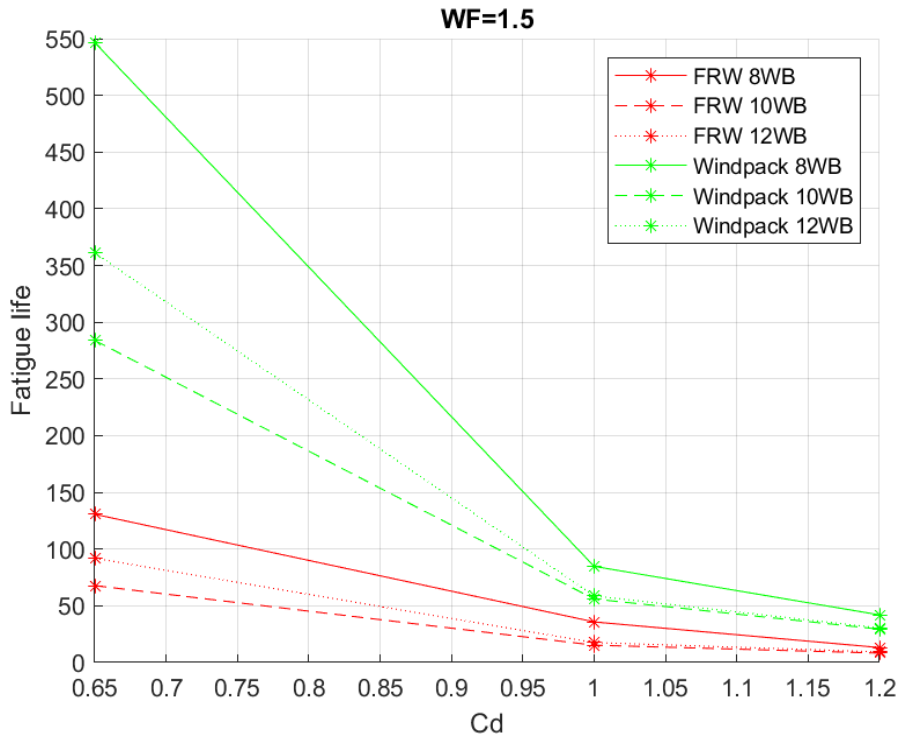


Figure 7-7: Fatigue life against Cd with weight factor 1.5 for all wind block cases in FRAMEWORK and WINDPACK

Figure 7-4, Figure 7-5, Figure 7-6 and Figure 7-7 show variation in **fatigue life** with varying **Cd** for FRAMEWORK and WINDPACK, for all **wind block** combinations, for different **weight factor** cases.

The following observations are made:

- WINDPACK predicts longer **fatigue life** than FRAMEWORK in each corresponding **wind block** case.
- With the same **Cd** and **weight factor**, almost all wind block cases in WINDPACK predict longer fatigue than almost all wind block cases in FRAMEWORK.
- **Fatigue life** is most sensitive for **Cd** values between **0.65** and **1.0** for both software. This sensitivity seems milder in FRAMEWORK than that in WINDPACK. For the case of **weight factor** of **1.0** and **8 wind blocks**, **fatigue life** drops **91%** and **93%** between **Cd** of **0.65** and **1.2** for FRAMEWORK and WINDPACK, respectively.
- **Fatigue life** of the two software converge with increasing **Cd**.

7.2.3 Summary and Discussion

In all cases with correlating input, WINDPACK predicts a longer **fatigue life** than FRAMEWORK. On average FRAMEWORK predicts **41%** the **fatigue life** that WINDPACK predicts, if **weight factor** cases are excluded the same difference is **47%**. On the basis that WINDPACK uses the HARRIS spectra, which is originally developed for wind over land (DNV RP-C205, 2019), and FRAMEWORK uses the NPD spectrum, which is developed for offshore wind, FRAMEWORK may be more accurate for analysis of this type of offshore structure. FRAMEWORK gives more conservative **fatigue life** for (Flare boom 1).

As the table below show, the **SCFs** used in the two software are almost identical, except for the **SCFs** for axial force in crown. Higher **SCFs** mean lower **fatigue life**, so one of the reasons why FRAMEWORK predicts shorter **fatigue life** than WINDPACK is the difference in **SCF**.

SCFs		Framework	Windpack
Chord	Axial crown	4.436	3.62
	Axial saddle	6.967	6.87
	Out-of-plane (saddle)	5.31	5.31
	In-plane (crown)	2.308	2.31
Brace	Axial crown	3.226	2.89
	Axial saddle	6.04	6.04
	Out-of-plane (saddle)	4.524	4.52
	In-plane (crown)	2.446	2.45

Table 7-6: SCFs for WINDPACK and FRAMEWORK

Fatigue life in each software seems to react almost equally to change of **weight factor** except in the range of **weight factor** of **1.0** to **1.1**. As mentioned, there seems to be a specific sensitivity in

FRAMEWORK around this range. This might be attributed to the structure's natural frequency shifting closer to a spectral peak frequency when **weight factor** increases from **1.0** to **1.1**. Considering that the two software do not use the same spectra models, therefore may not contain energy peaks around the same frequencies, the previous conclusion is further substantiated.

In both software the **fatigue life** sensitivity to parameter change seem to converge in most cases when **fatigue life** becomes lower. That is the overall trend; however, deviation from this norm is observed. As explained, with FRAMEWORK being sensitive to change in the **weight factor** range of **1.0** to **1.1**. The overall trend is either way obvious and represent the same mechanism as the actual nature of fatigue. This is not a proof of one software's preference over the other; however, since this may be explained by the fact that the **S-N curve** has a logarithmic scaling, meaning that small changes in stress ranges makes larger difference in **fatigue life** in the lower stress range.

Looking at wind block combinations the two software are not very comparable since the probabilities are treated differently along with the different spectra. It should be noted that further comparison between FRAMEWORK and WINDPACK using the same spectra (HARRIS) is strongly recommended.

7.3 FRAMEWORK and USFOS

Compared with WINDPACK, FRAMEWORK seem to be more conservative, more relevant for offshore structures and have results closer to that of USFOS. USFOS analysis of **time increment 0.05 seconds** is also more accurate and gives more conservative results than the analysis with **time increment of 0.1 seconds**.

Based on these conclusions, this chapter will focus on comparing FRAMEWORK to USFOS (dt = 0.05).

The main difference of FRAMEWORK and USFOS is the design methods of calculating fatigue as the former uses spectral density method while the latter uses time history nonlinear dynamic analysis. FRAMEWORK also treats probabilities differently as it combines the directional probabilities of opposing directions, while USFOS treats probabilities of each direction separately.

7.3.1 Results Tables

Results from the different software with parameters are presented in the tables below:

Wind Blocks	Cd	wt factor	Critical fatigue life	
			Framework	Usfos dt=0.05
8	0.65	0.5	564	418
		1	331	138
		1.1	195	125
		1.5	131	95
	1	0.5	131	71
		1	57	28
		1.1	51	26
		1.5	36	20
	1.2	0.5	42	36
		1	29	15
		1.1	18	14
		1.5	13	11
	Reynold's	0.5	381	267
		1	230	92
		1.1	137	85
		1.5	94	67

Table 7-7: Critical fatigue life for all comparable cases of 8 wind blocks in FRAMEWORK and USFOS

Wind Blocks	Cd	wt factor	Critical fatigue life	
			Framework	Usfos dt=0.05
10	0.65	0.5	221	204
		1	145	79
		1.1	93	56
		1.5	68	49
	1	0.5	45	43
		1	31	18
		1.1	20	14
		1.5	15	12
	1.2	0.5	24	23
		1	17	10
		1.1	11	8
		1.5	8	7
	Reynold's	0.5	158	120
		1	106	49
		1.1	69	36
		1.5	50	31

Table 7-8: Critical fatigue life for all comparable cases of 10 wind blocks in FRAMEWORK and USFOS

Wind Blocks	Cd	wt factor	Critical fatigue life	
			Framework	Usfos dt=0.05
12	0.65	0.5	433	302
		1	246	103
		1.1	141	96
		1.5	92	64
	1	0.5	64	49
		1	40	20
		1.1	25	20
		1.5	18	14
	1.2	0.5	30	25
		1	20	11
		1.1	13	11
		1.5	9	8
	Reynold's	0.5	292	195
		1	170	69
		1.1	99	65
		1.5	66	46

Table 7-9: Critical fatigue life for all comparable cases of 12 wind blocks in FRAMEWORK and USFOS

7.3.2 Results Graphs

This chapter presents **fatigue life** for **the most critical joint** and how it varies with different parameter changes. One parameter will be fixed and thereby case dependent, while the other parameters are either shown on the x-axis or presented on different graphs.

The shapes of the curves are simplified and should not be interpreted too precise, but rather give an indication of trends. Interpolation between different points shall not be used and will not give accurate representation of reality. More data points would be required to simulate precise reliable curve representation.

All **fatigue life** results correlate with the most critical **fatigue life** in **Table 7-7**, **Table 7-8** and **Table 7-9** and all reasonable load cases are presented.

7.3.2.1 Fatigue life against weight factor for different wind blocks and Cd values

7.3.2.1.1 Cd = 0.65

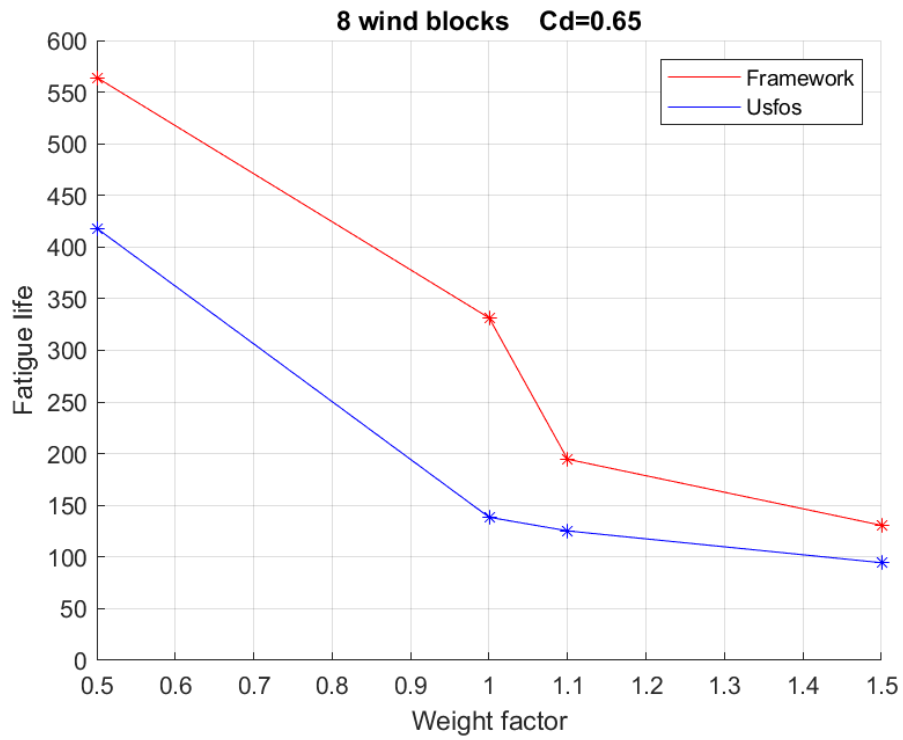


Figure 7-8: Fatigue life against weight factor with Cd=0.65 and 8 wind blocks for USFOS and FRAMEWORK

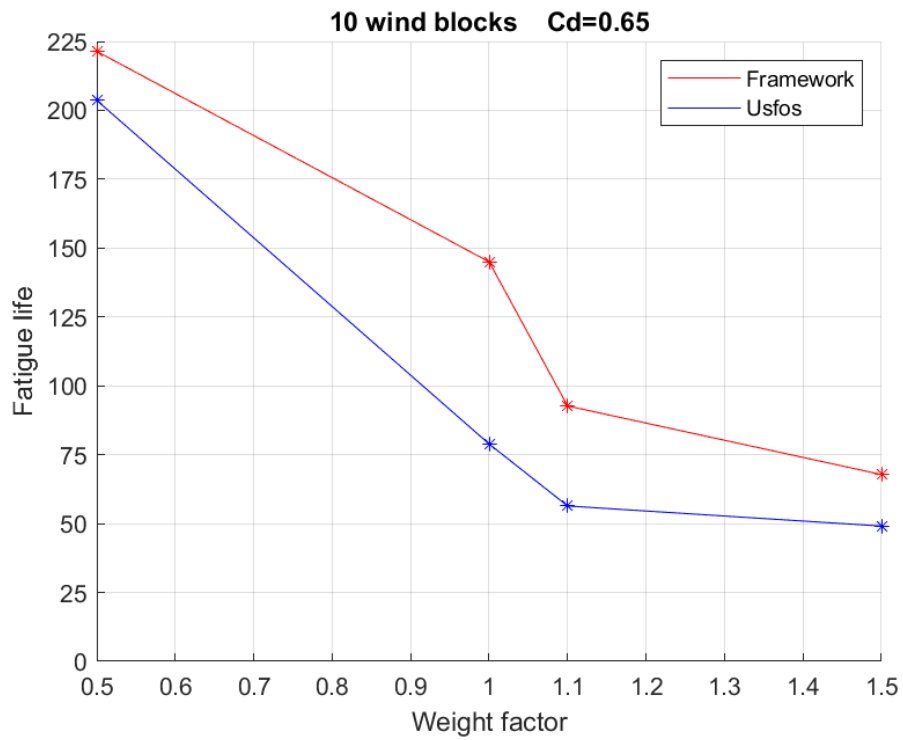


Figure 7-9: Fatigue life against weight factor with Cd=0.65 and 10 wind blocks for USFOS and FRAMEWORK

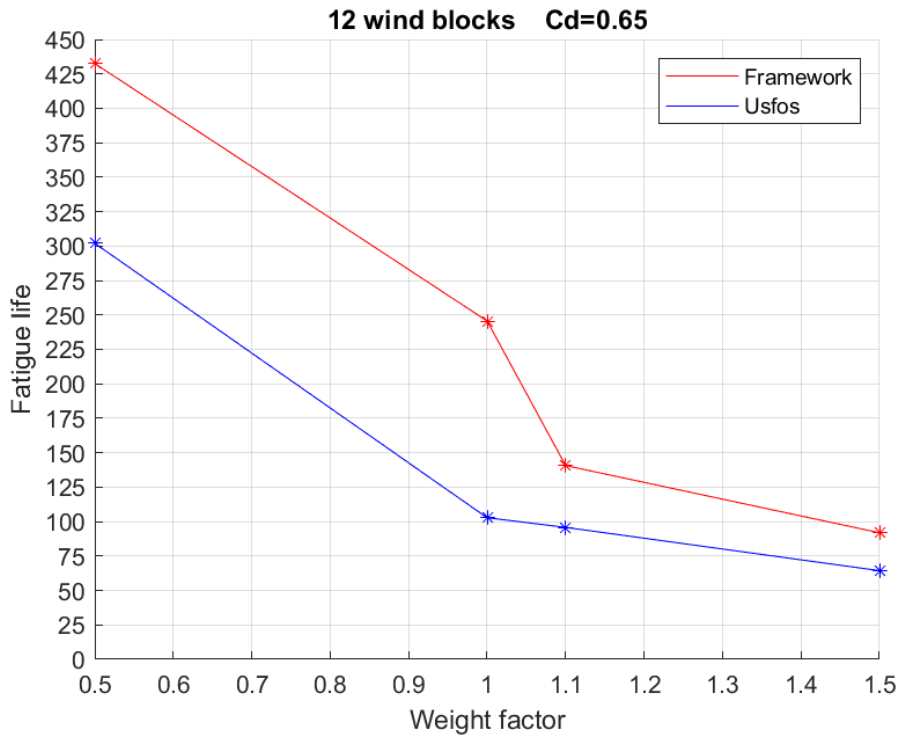


Figure 7-10: Fatigue life against weight factor with Cd=0.65 and 12 wind blocks for USFOS and FRAMEWORK

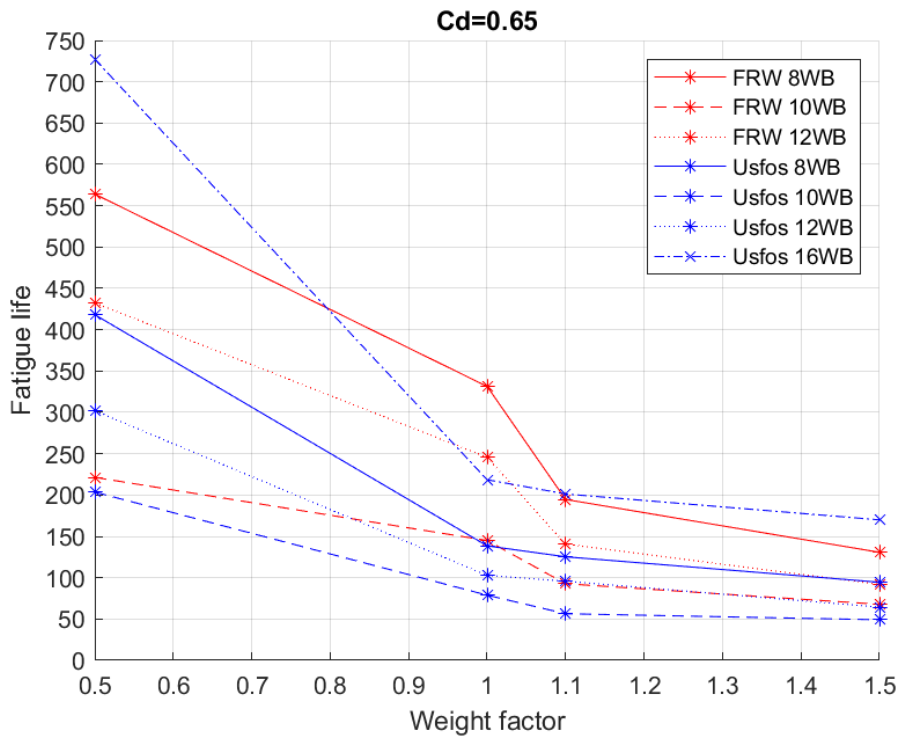


Figure 7-11: Fatigue life against weight factor with Cd=0.65 for all wind block cases in USFOS and FRAMEWORK

Figure 7-8, Figure 7-9 and Figure 7-10 show variation in fatigue life with varying weight factor, for FRAMEWORK and USFOS, for all wind block cases with Cd=0.65. Figure 7-11 show all wind block cases of both software.

The following observations are made:

- FRAMEWORK predicts longer **fatigue life** in each corresponding **wind block** case.
- The largest difference is observed in the **weight factor** range from **0.5** to **1.0**.
- There is a significant drop in **fatigue life** between **weight factor 1.0** and **1.1** in FRAMEWORK. However, this trend is not similar in the corresponding USFOS results as **fatigue life** drop seems linear between **weight factor 1.0** and **1.5**.
- **Fatigue life** results in USFOS **16 wind blocks** case is close to FRAMEWORK **12 wind block** case at **weight factor 1.0**.

7.3.2.1.2 Cd = 1.0

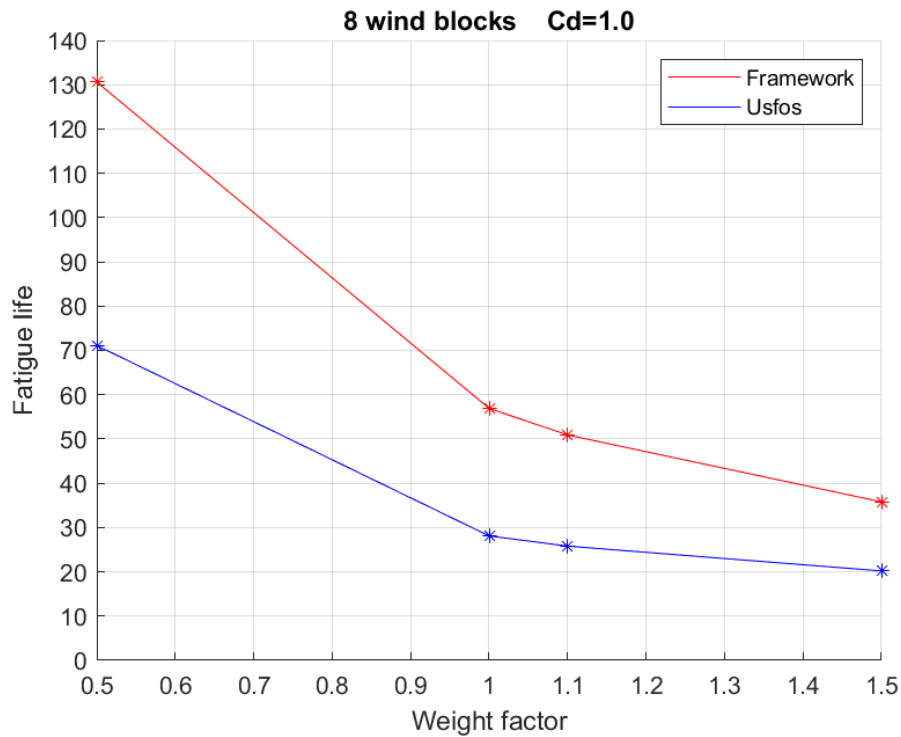


Figure 7-12: Fatigue life against weight factor with Cd=1.0 and 8 wind blocks for USFOS and FRAMEWORK

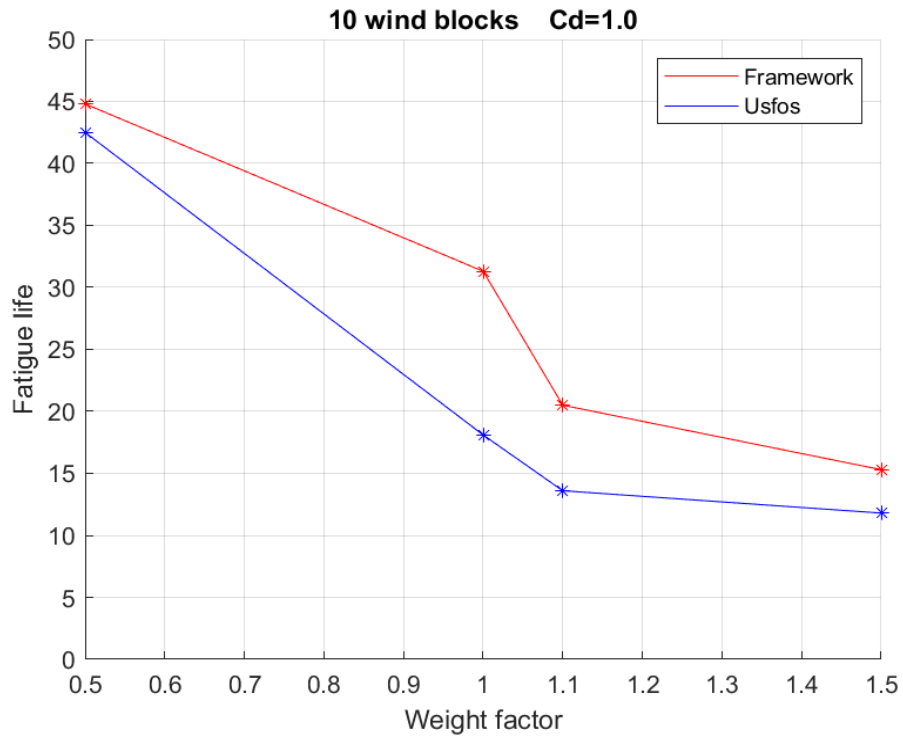


Figure 7-13: Fatigue life against weight factor with Cd=1.0 and 10 wind blocks for USFOS and FRAMEWORK

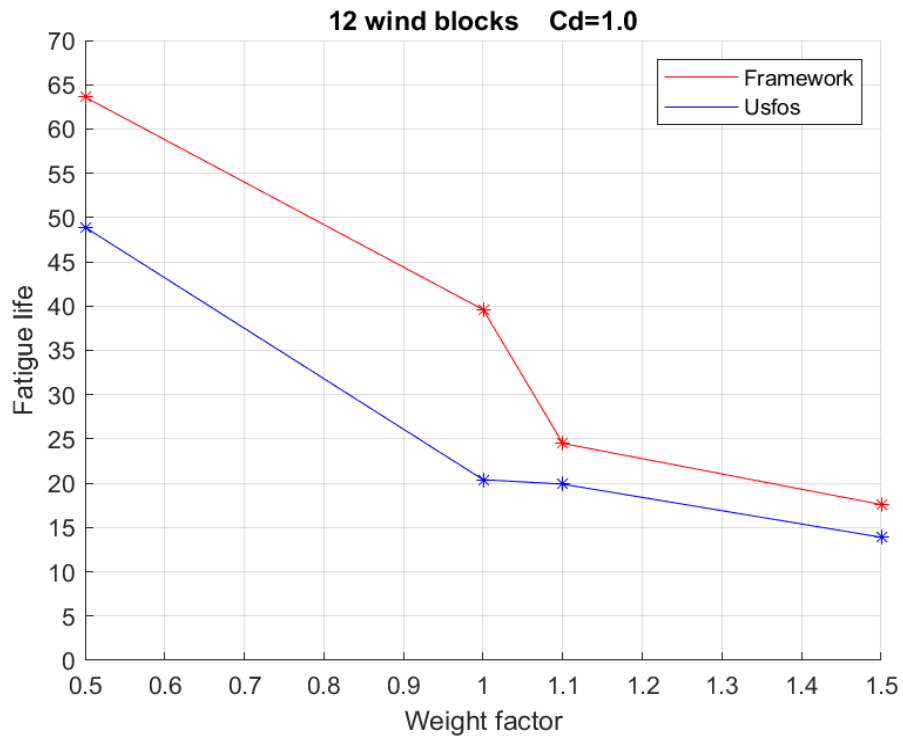


Figure 7-14: Fatigue life against weight factor with Cd=1.0 and 12 wind blocks for USFOS and FRAMEWORK

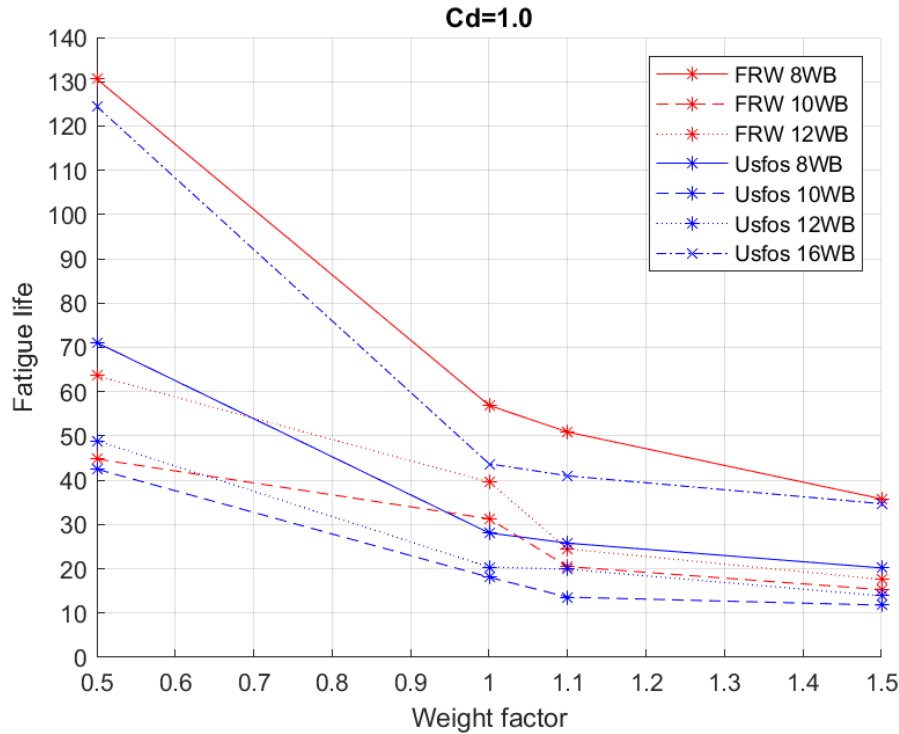


Figure 7-15: Fatigue life against weight factor with Cd=1.0 for all wind block cases in USFOS and FRAMEWORK

Figure 7-12, Figure 7-13 and Figure 7-14 show variation in **fatigue life** with varying **weight factor** for FRAMEWORK and USFOS for each **wind block** case with **Cd=1.0**. **Figure 7-15** show all **wind block** cases of both software.

The following observations are made:

- FRAMEWORK predicts longer **fatigue life** in each corresponding **wind block** case.
- The largest difference is observed in the **weight factor** range from **0.5** to **1.0**.
- There is a significant drop in **fatigue life** between **weight factor 1.0** and **1.1** in FRAMEWORK. However, this trend is not similar in the corresponding USFOS results as **fatigue life** drop seems linear between **weight factor 1.0** and **1.5**.
- **Fatigue life** results in USFOS **16 wind blocks** case is close to FRAMEWORK **12 wind block** case at **weight factor 1.0**.
- **Fatigue life** decrease trend in FRAMEWORK **8 wind blocks** case and USFOS **16 wind blocks** case are similar and close in results. For the mentioned cases, FRAMEWORK predicts a **fatigue life** of **130.6 years** for **weight factor** of **0.5**, while USFOS predicts **124.4 years** for the same **weight factor**. While for the same mentioned cases, FRAMEWORK predicts a **fatigue life** of **35.8** for **weight factor** of **1.5**, while USFOS predicts **34.7 years** for the same **weight factor**.

7.3.2.1.3 Cd = 1.2

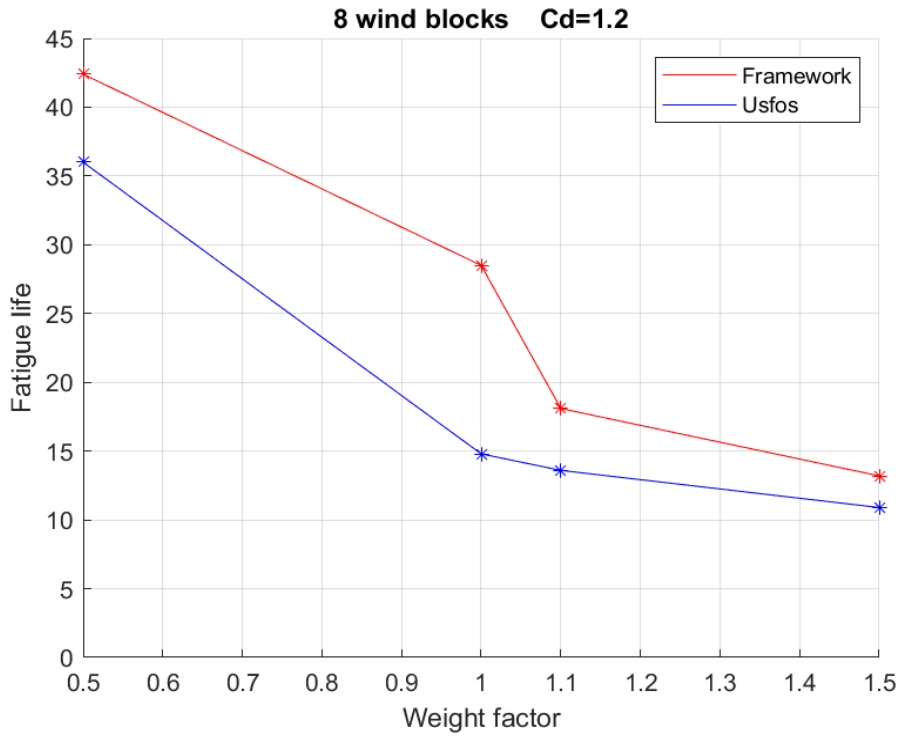


Figure 7-16: Fatigue life against weight factor with Cd=1.2 and 8 wind blocks for USFOS and FRAMEWORK

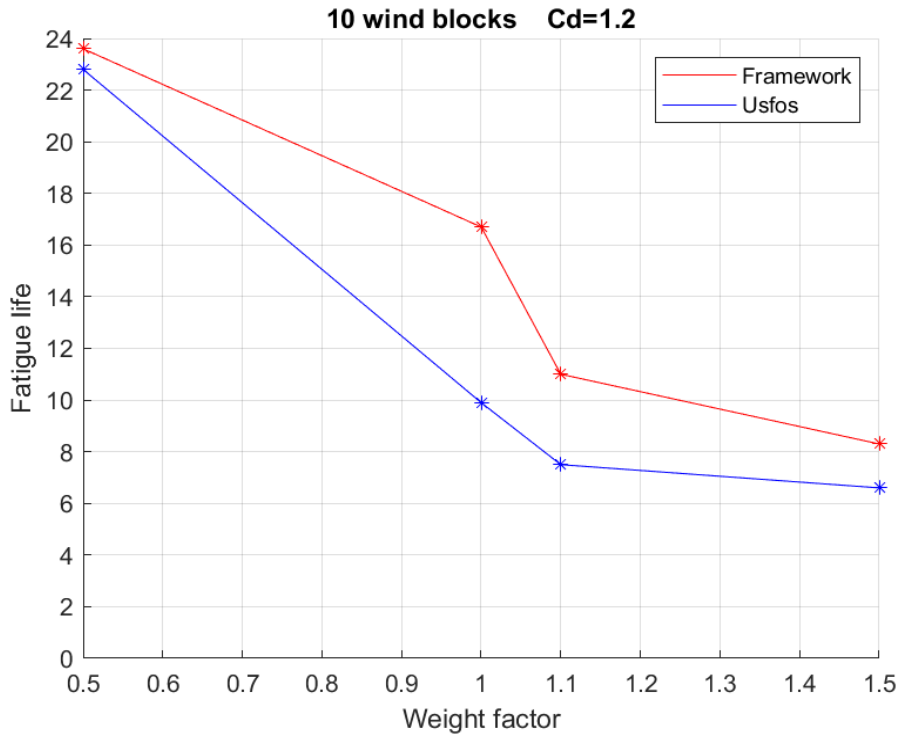


Figure 7-17: Fatigue life against weight factor with Cd=1.2 and 10 wind blocks for USFOS and FRAMEWORK

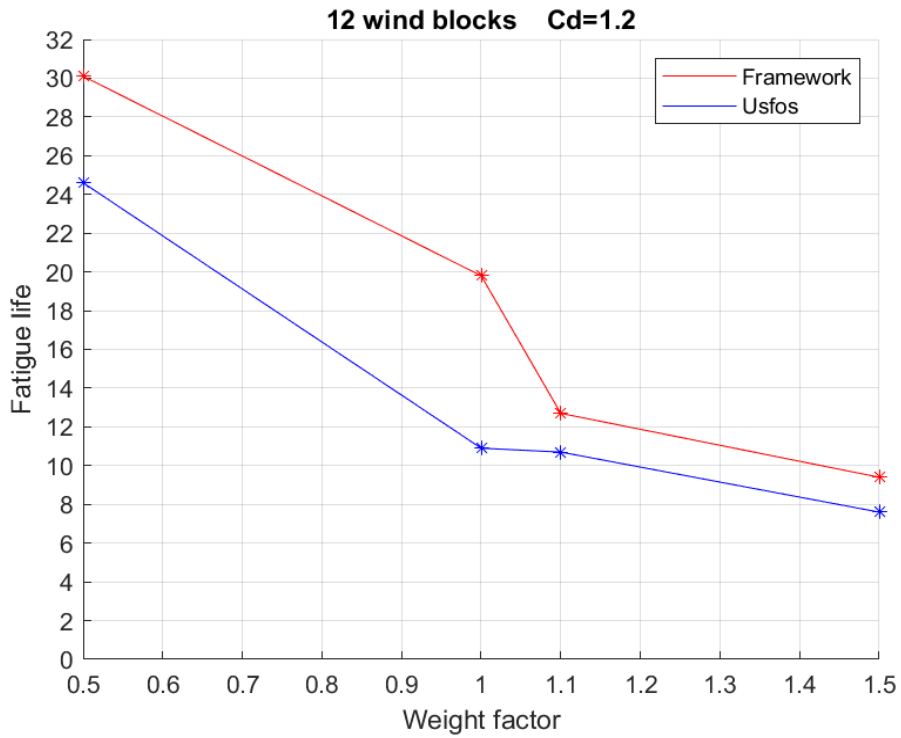


Figure 7-18: Fatigue life against weight factor with Cd=1.2 and 12 wind blocks for USFOS and FRAMEWORK

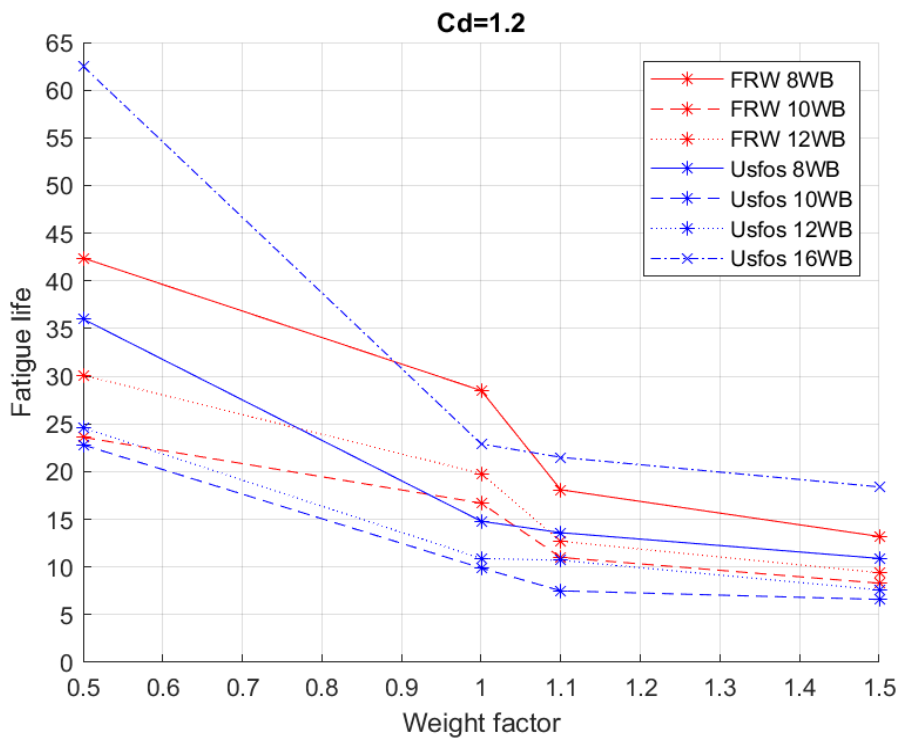


Figure 7-19: Fatigue life against weight factor with Cd=1.2 for all wind block cases in USFOS and FRAMEWORK

Figure 7-16, Figure 7-17 and Figure 7-18 show variation in **fatigue life** with varying **weight factor** for FRAMEWORK and USFOS for each **wind block** case with **Cd=1.2**. Figure 7-19 show all **wind block** cases of both software.

The following observations are made:

- FRAMEWORK predicts longer **fatigue life** in each corresponding **wind block** case.
- The largest difference is observed in the **weight factor** range from **0.5** to **1.0**.
- **Fatigue life USFOS 16 wind blocks case** is close to FRAMEWORK **12 wind block case** with **weight factor 1.0**.
- There is a significant drop in **fatigue life** between **weight factor 1.0** and **1.1** in FRAMEWORK. However, this trend is not similar in the corresponding USFOS results as **fatigue life** drop seems linear between **weight factor 1.0** and **1.5**.
- Both software results seem to show the same trend of decrease in **fatigue life** between **weight factor** of **1.1** and **1.5** especially in the case of **12 wind blocks**.

7.3.2.1.4 Cd = Reynold's dependent

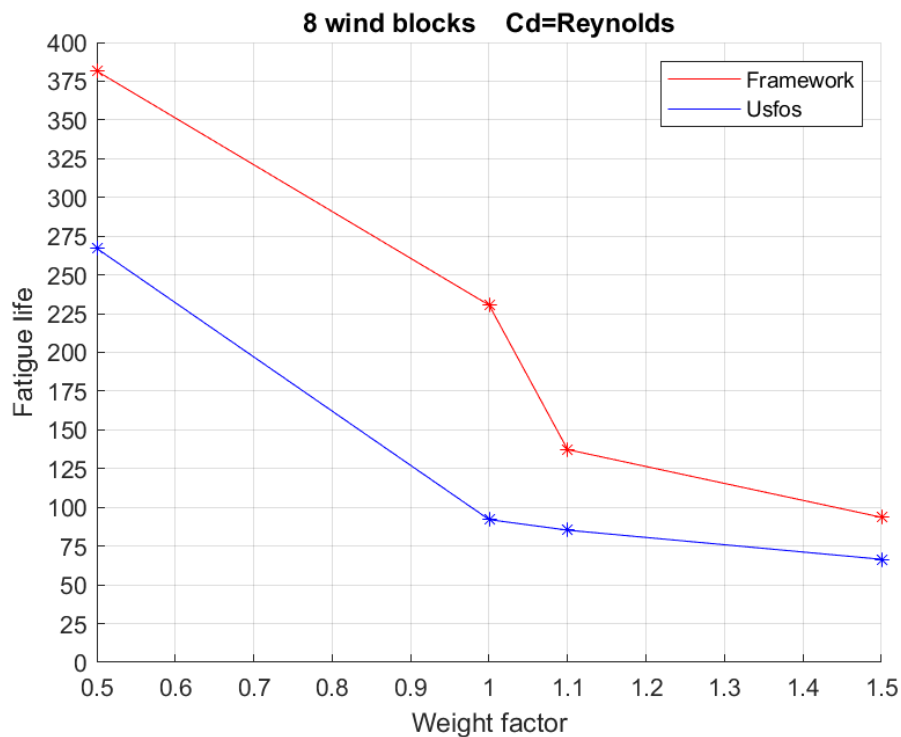


Figure 7-20: Fatigue life against weight factor with Reynold's number dependent Cd and 8 wind blocks for USFOS and FRAMEWORK

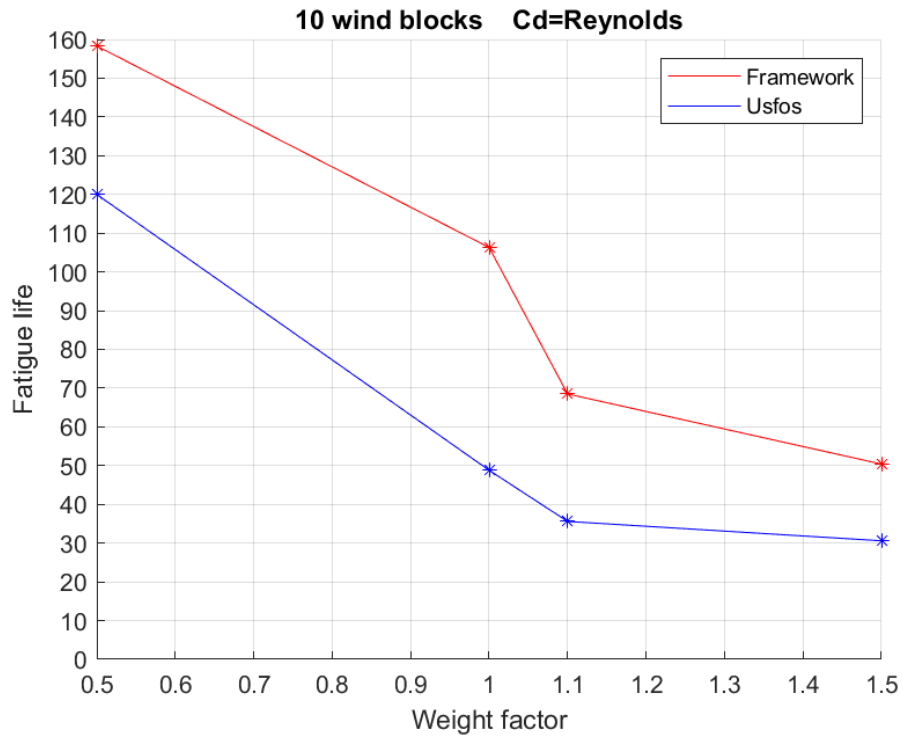


Figure 7-21: Fatigue life against weight factor with Reynold’s number dependent Cd and 10 wind blocks for USFOS and FRAMEWORK

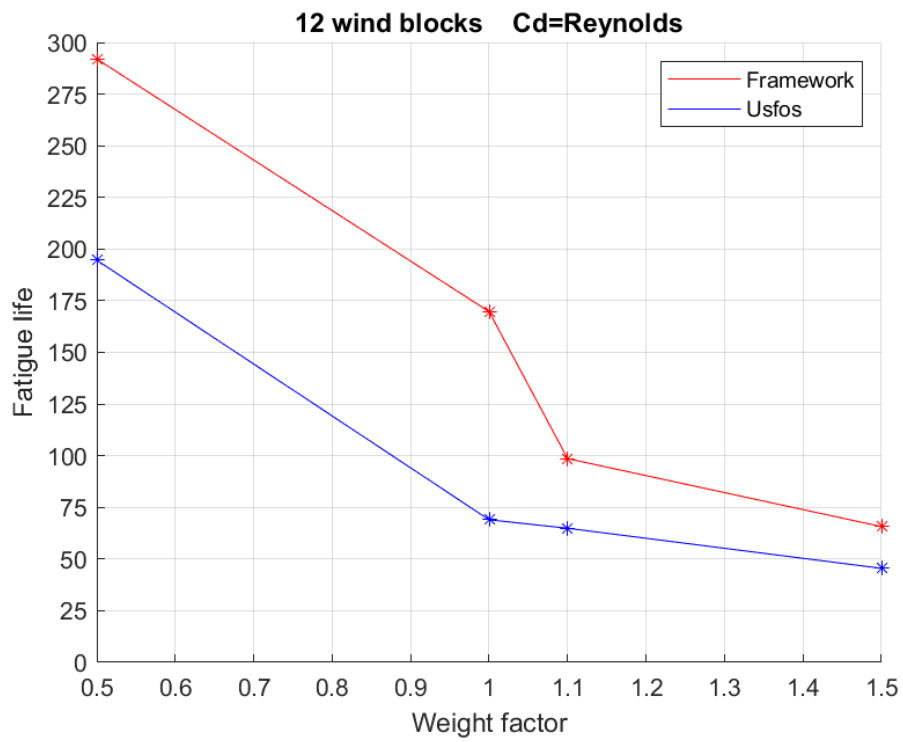


Figure 7-22: Fatigue life against weight factor with Reynold’s number dependent Cd and 12 wind blocks for USFOS and FRAMEWORK

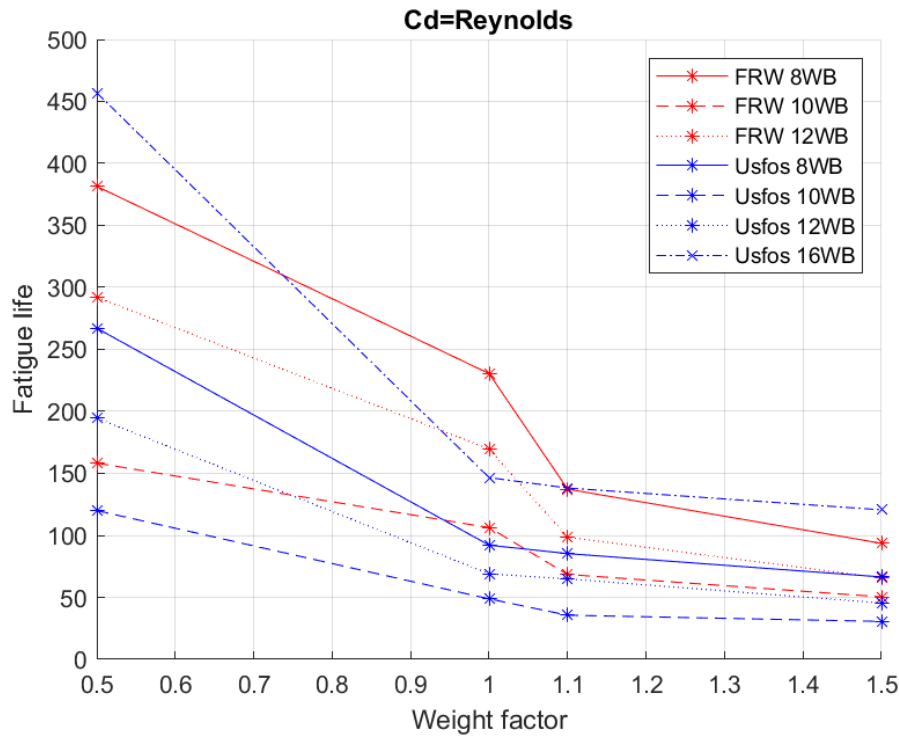


Figure 7-23: Fatigue life against weight factor with Reynold's number dependent Cd for all wind block cases in USFOS and FRAMEWORK

Figure 7-20, Figure 7-21 and Figure 7-22 show variation in **fatigue life** with varying **weight factor** for FRAMEWORK and USFOS for each **wind block** case with **Reynold's number dependent Cd**. Figure 7-23 show all **wind block** cases of both software.

The following observations are made:

- FRAMEWORK predicts longer **fatigue life** in each corresponding **wind block** case.
- The largest difference is observed in the **weight factor** range from **0.5** to **1.0**.
- **Fatigue life** USFOS **16 wind blocks** case is close to FRAMEWORK **12 wind block** case with **weight factor 1.0**.
- There is a significant drop in **fatigue life** between **weight factor 1.0** and **1.1** in FRAMEWORK. However, this trend is not similar in the corresponding USFOS results as **fatigue life** drop seems linear between **weight factor 1.0** and **1.5**.
- Both software results seem to show the same trend of decrease in **fatigue life** between **weight factor** of **1.1** and **1.5** especially in the case of **12 wind blocks**.

7.3.2.2 Fatigue life against Cd for different wind blocks and weight factors

7.3.2.2.1 Weight factor of 0.5

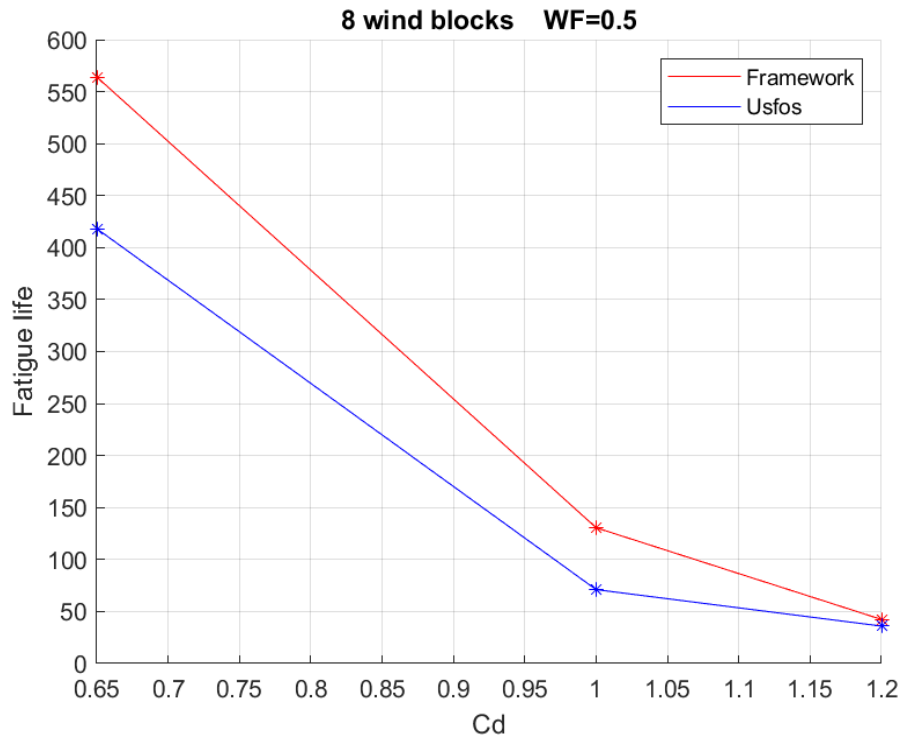


Figure 7-24: Fatigue life against Cd with weight factor 0.5 and 8 wind blocks for USFOS and FRAMEWORK

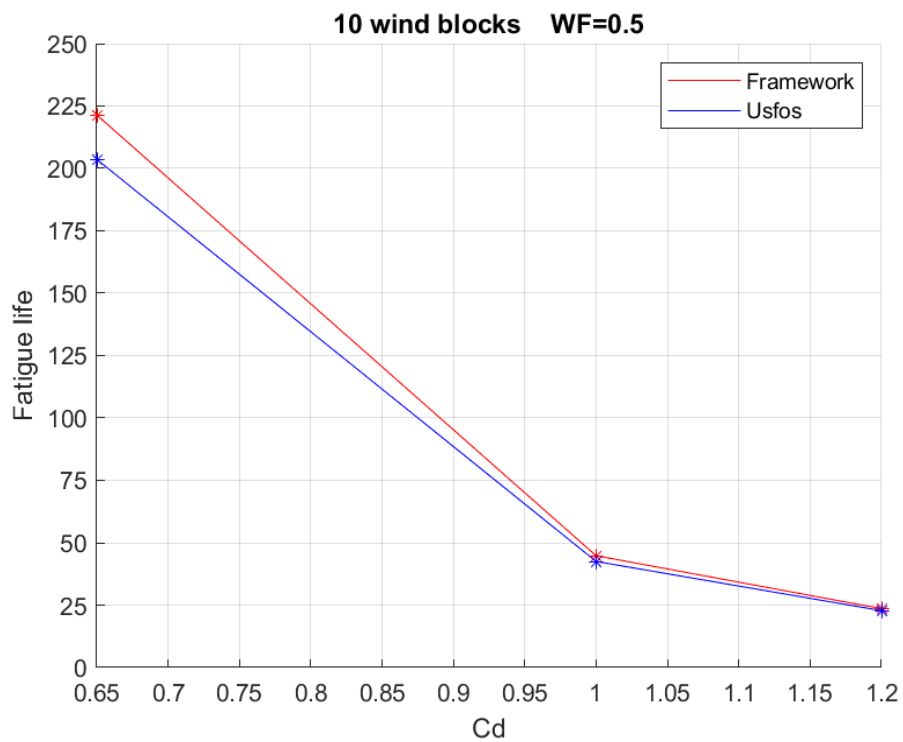


Figure 7-25: Fatigue life against Cd with weight factor 0.5 and 10 wind blocks for USFOS and FRAMEWORK

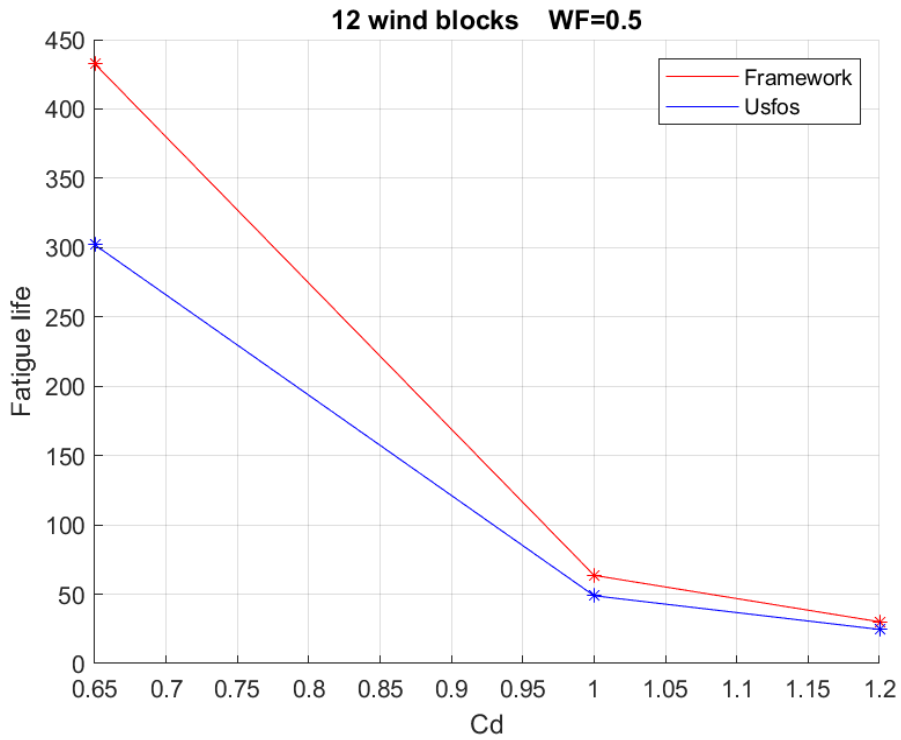


Figure 7-26: Fatigue life against Cd with weight factor 0.5 and 12 wind blocks for USFOS and FRAMEWORK

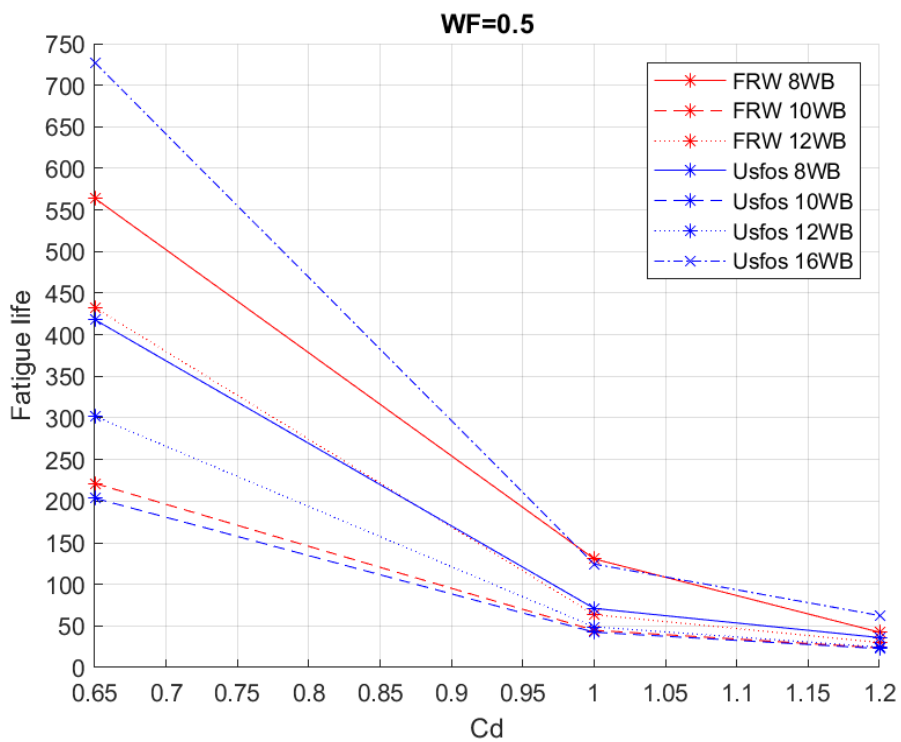


Figure 7-27: Fatigue life against Cd with weight factor 0.5 for all wind block cases in USFOS and FRAMEWORK

Figure 7-24, Figure 7-25 and Figure 7-26 show variation in **fatigue life** with varying **Cd** for FRAMEWORK and USFOS for each **wind block** case with **weight factor** of **0.5**. Figure 7-27 show all **wind block** cases of both software.

The following observations are made:

- FRAMEWORK predicts longer **fatigue life** in each corresponding **wind block** case.
- **Fatigue life** is closer in value for all cases when **Cd=1.2**, relative to other values of **Cd**.
- **Fatigue life** is most sensitive for **Cd** values between **0.65** to **1.0** for both software.
- **Fatigue life** of the two software come closer with increasing **Cd**. For the case of **Cd = 1.2**, **fatigue life** in both software is close to equal in all different **weight factor** cases.
- **Fatigue life** in the **10 wind blocks** case shows the same trend and is close to equal in both software.
- **Fatigue life** drop trends in case of USFOS **8 wind blocks** and FRAMEWORK **12 wind blocks** are almost identical.
- USFOS case of **16 wind blocks** show higher drop in fatigue life between **Cd = 0.65** and **1.0** than the corresponding in FRAMEWORK case of **8 wind blocks**.
- USFOS case of **16 wind blocks** predicts the highest **fatigue life** among all cases presented, with an increase of **29%** at **Cd = 0.65** than the corresponding in FRAMEWORK case of **8 wind blocks** and **47%** at **Cd = 1.2** for the same cases. The average increase in **fatigue life** between USFOS and FRAMEWORK is **35%** for the mentioned cases.

7.3.2.2.2 Weight factor of 1.0

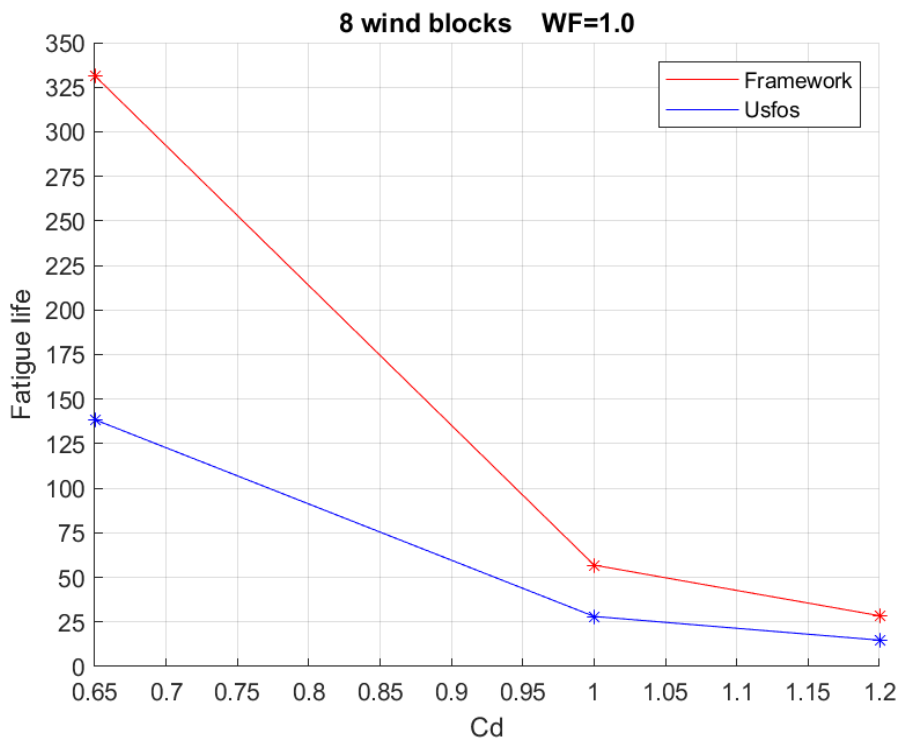


Figure 7-28: Fatigue life against Cd with weight factor 1.0 and 8 wind blocks for USFOS and FRAMEWORK

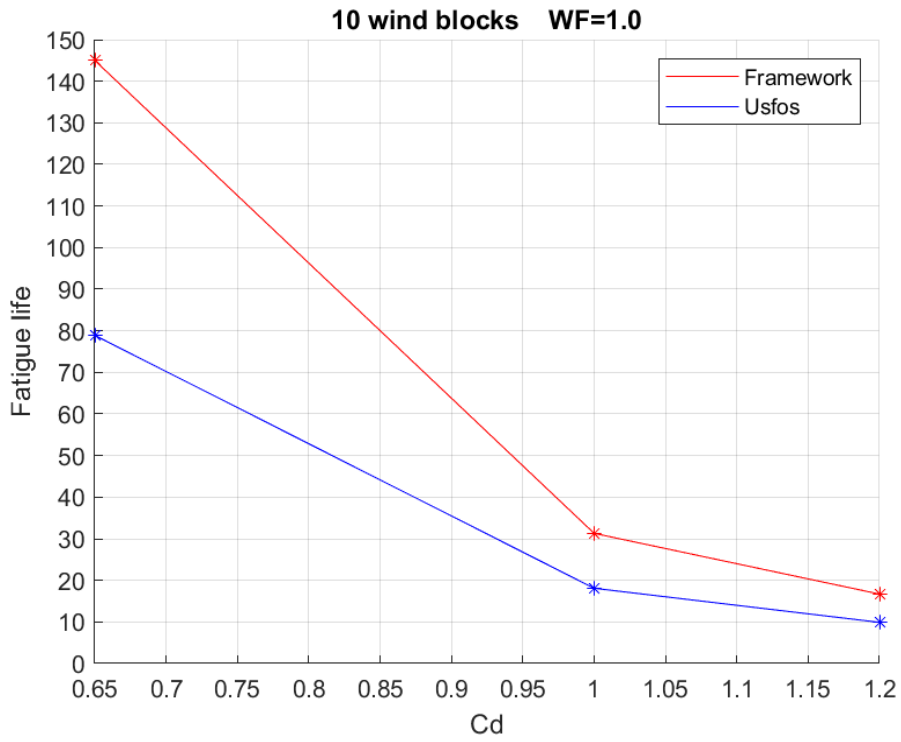


Figure 7-29: Fatigue life against Cd with weight factor 1.0 and 10 wind blocks for USFOS and FRAMEWORK

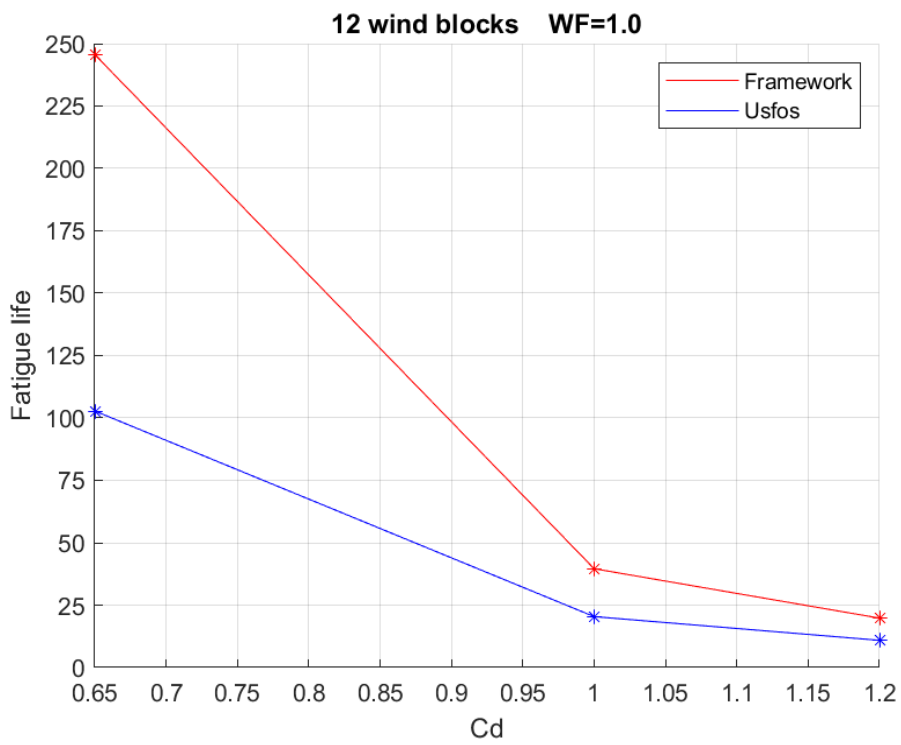


Figure 7-30: Fatigue life against Cd with weight factor 1.0 and 12 wind blocks for USFOS and FRAMEWORK

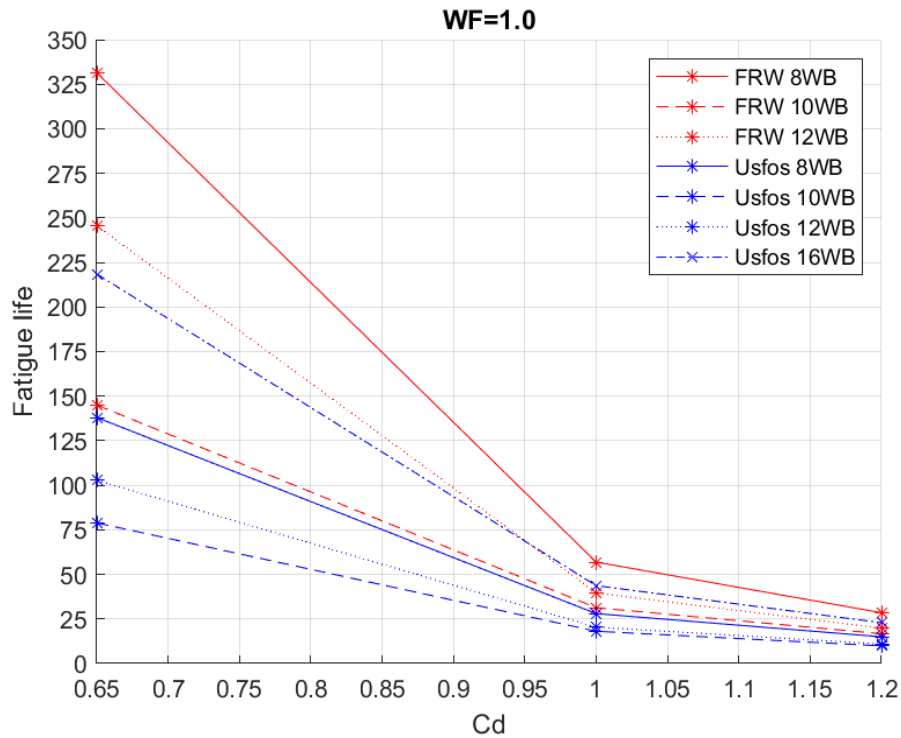


Figure 7-31: Fatigue life against Cd with weight factor 1.0 for all wind block cases in USFOS and FRAMEWORK

Figure 7-28, Figure 7-29 and Figure 7-30 show variation in **fatigue life** with varying **Cd**, for FRAMEWORK and USFOS, for each **wind block** case with **weight factor** of **0.5**. Figure 7-31 shows all **wind block** cases of both software.

The following observations are made:

- FRAMEWORK predicts longer **fatigue life** in each corresponding **wind block** case.
- **Fatigue life** is closer in value for all cases when **Cd=1.2**, relative to other values of **Cd**.
- **Fatigue life** is most sensitive for **Cd** values between **0.65** to **1.0** for both software.
- **Fatigue life** of the two software come closer with increasing **Cd**. For the case of **Cd = 1.2**, **fatigue life** in both software is close to equal in all different **weight factor** cases.
- The case of USFOS **10 wind blocks** predicts the lowest **fatigue life** among all cases.
- **Fatigue life** drop trend in USFOS is milder in slope than the corresponding in FRAMEWORK in all cases.
- **Fatigue life** drop trends in case of USFOS **16 wind blocks** and FRAMEWORK **12 wind blocks** are close for **Cd = 1.0** and **1.2**.
- **Fatigue life** drop trends in case of USFOS **8 wind blocks** and FRAMEWORK **10 wind blocks** are almost identical. FRAMEWORK case gives higher **fatigue life** than the corresponding in USFOS with an average increase of **8%**.

- USFOS case of **16 wind blocks** predicts the highest **fatigue life** among all USFOS cases, while FRAMEWORK case of **8 wind blocks** predicts the highest **fatigue life** among all cases **presented**. For the mentioned cases, FRAMEWORK **fatigue life** results are on average **35%** higher than USFOS results.

7.3.2.2.3 Weight factor of 1.1

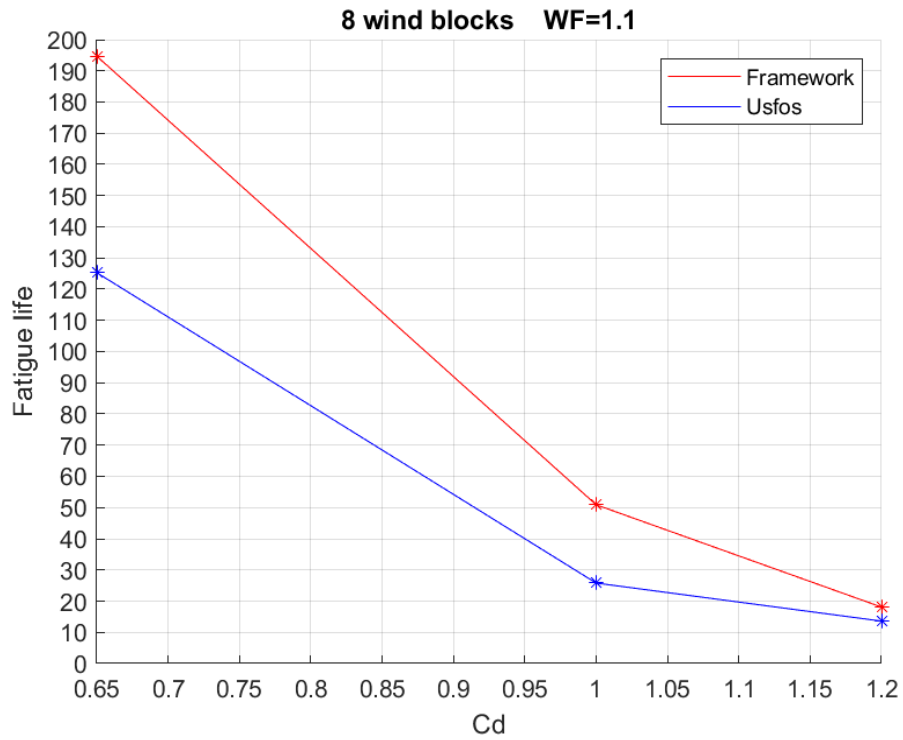


Figure 7-32: Fatigue life against Cd with weight factor 1.1 and 8 wind blocks for USFOS and FRAMEWORK

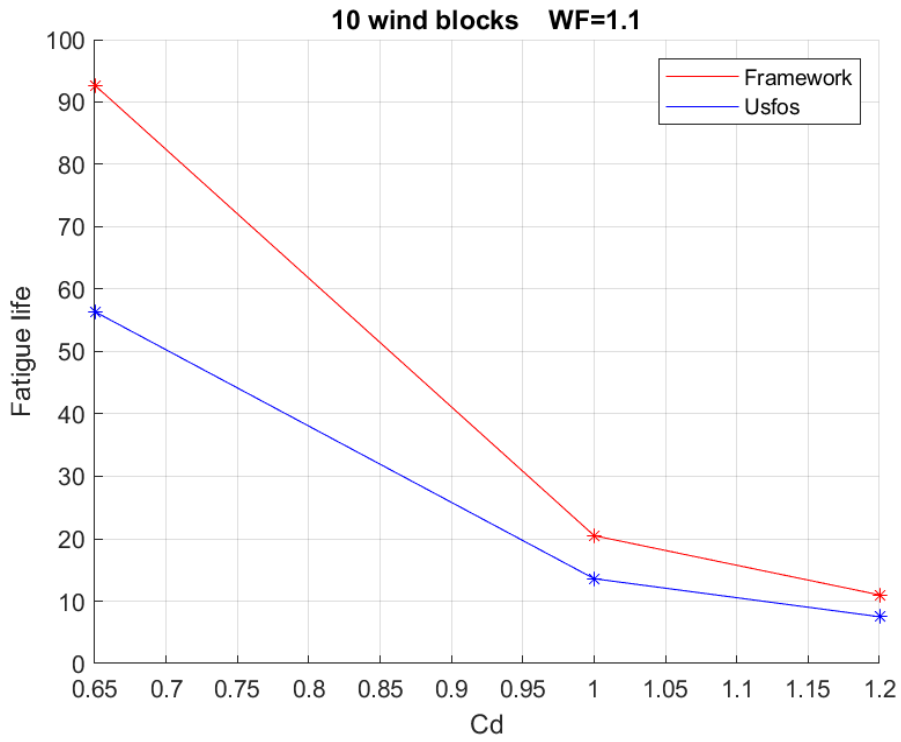


Figure 7-33: Fatigue life against Cd with weight factor 1.1 and 10 wind blocks for USFOS and FRAMEWORK

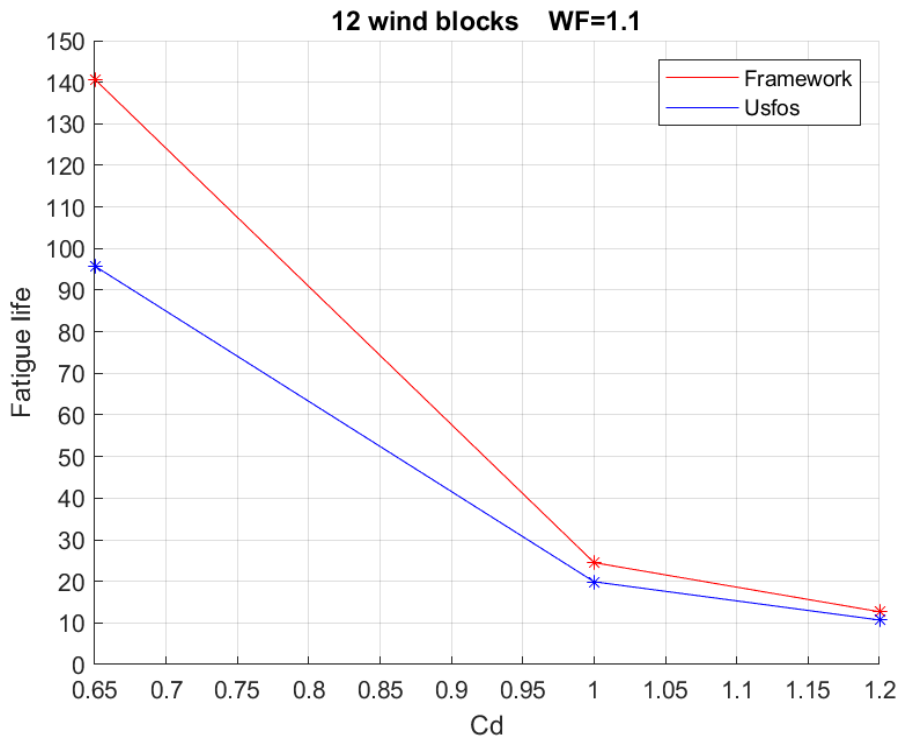


Figure 7-34: Fatigue life against Cd with weight factor 1.1 and 12 wind blocks for USFOS and FRAMEWORK

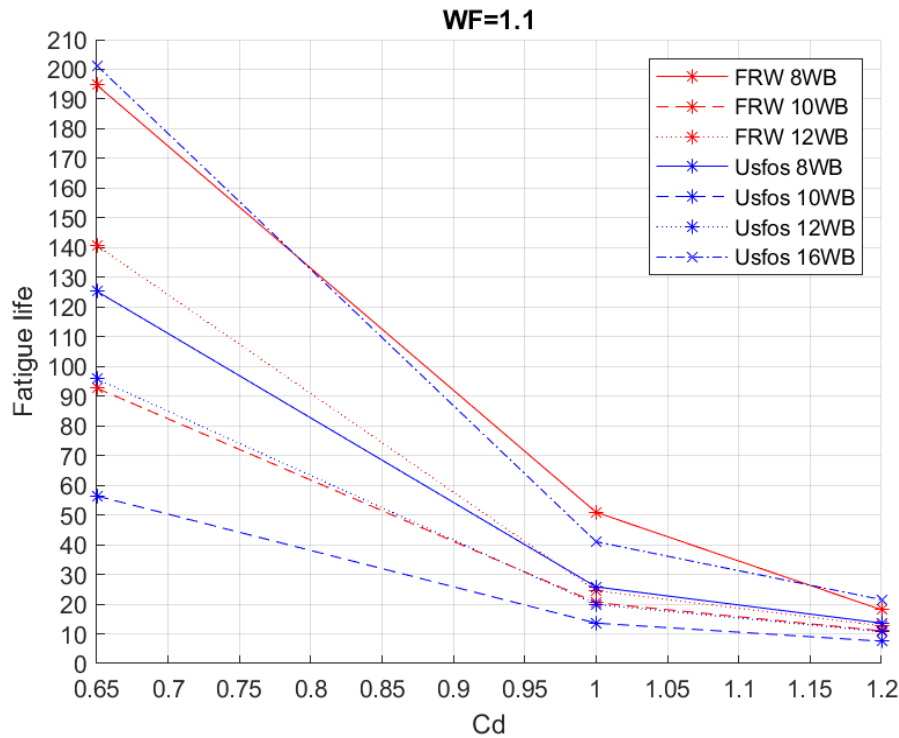


Figure 7-35: Fatigue life against Cd with weight factor 1.1 for all wind block cases in USFOS and FRAMEWORK

Figure 7-32, Figure 7-33 and Figure 7-34 show variation in fatigue life with varying Cd for FRAMEWORK and USFOS for each wind block case with weight factor of 1.5. Figure 7-35 and Figure 7-27 show all wind block cases of both software.

The following observations are made:

- FRAMEWORK predicts longer **fatigue life** in each corresponding **wind block** case.
- **Fatigue life** is closer in value for all cases when **Cd=1.2**, relative to other values of **Cd**.
- **Fatigue life** is most sensitive for **Cd** values between **0.65** to **1.0** for both software.
- **Fatigue life** of the two software come closer with increasing **Cd**. For the case of **Cd = 1.2**, **fatigue life** in both software is close to equal in all different **weight factor** cases.
- The case of **USFOS 10 wind blocks** predicts the lowest **fatigue life** among all cases.
- **Fatigue life** drop trend in **USFOS** is milder in slope than the corresponding in **FRAMEWORK** in all cases.
- **Fatigue life** drop trends in case of **USFOS 16 wind blocks** and **FRAMEWORK 8 wind blocks** are close.
- **Fatigue life** drop trends in case of **USFOS 8 wind blocks** and **FRAMEWORK 12 wind blocks** are close to identical for **Cd = 1.0** and **1.2**.

- **Fatigue life** drop trends in case of USFOS **12 wind blocks** and FRAMEWORK **10 wind blocks** are almost identical. The percentage increase/decrease between both cases is $\pm 3\%$.
- USFOS case of **16 wind blocks** predicts the highest **fatigue life** for **Cd = 0.65** and **1.2**, while FRAMEWORK case of **8 wind blocks** predicts the highest **fatigue life** for **Cd = 1.0**. For the mentioned cases, FRAMEWORK **fatigue life** results for **Cd = 1.0** is **24%** higher in FRAMEWORK, while higher in USFOS for **Cd = 0.65** and **1.2** by **3%** and **18%** respectively.

7.3.2.2.4 Weight factor of 1.5

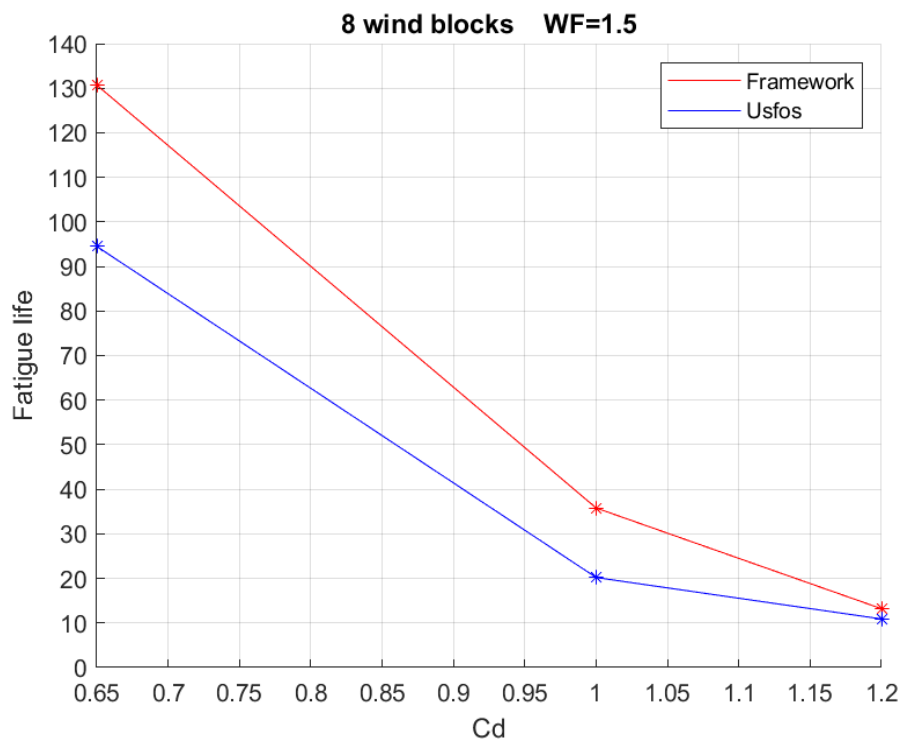


Figure 7-36: Fatigue life against Cd with weight factor 1.5 and 8 wind blocks for USFOS and FRAMEWORK

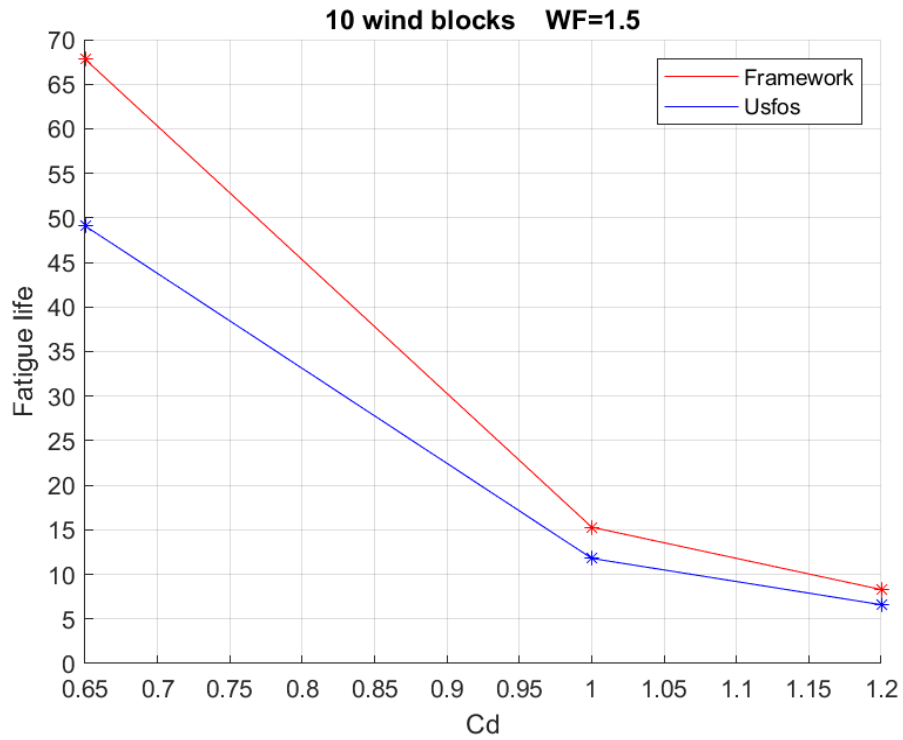


Figure 7-37: Fatigue life against Cd with weight factor 1.5 and 10 wind blocks for USFOS and FRAMEWORK

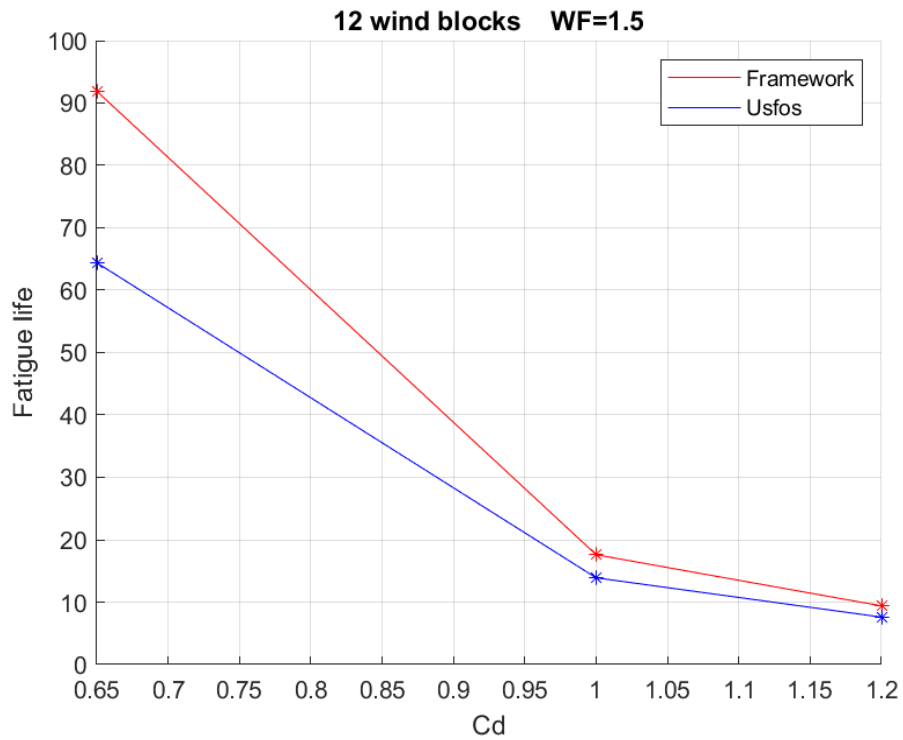


Figure 7-38: Fatigue life against Cd with weight factor 1.5 and 12 wind blocks for USFOS and FRAMEWORK

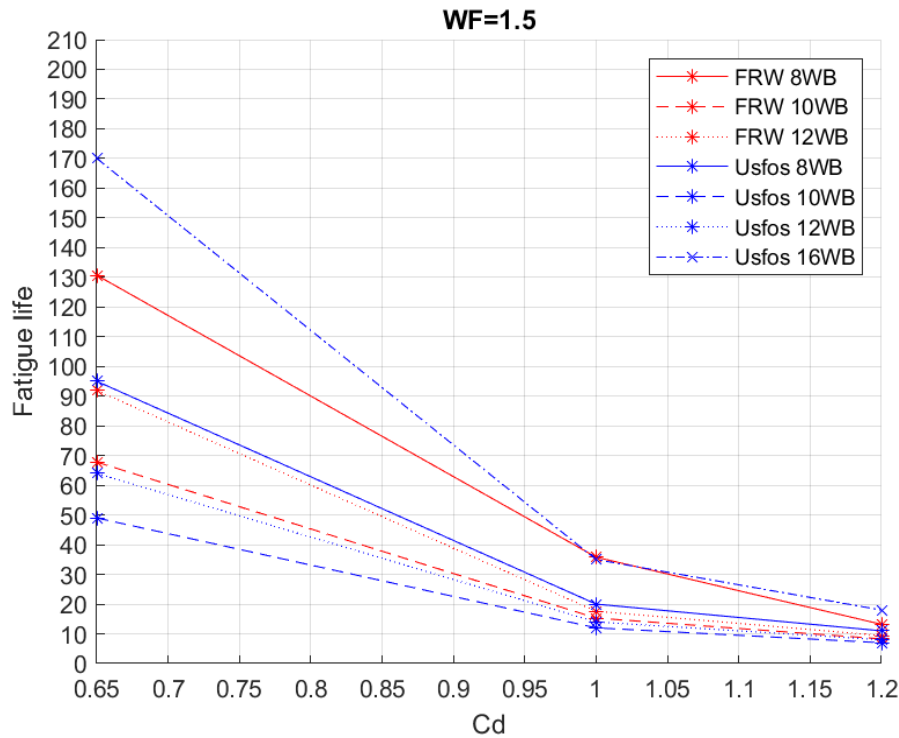


Figure 7-39: Fatigue life against Cd with weight factor 1.5 for all wind block cases in USFOS and FRAMEWORK

Figure 7-36, Figure 7-37 and Figure 7-38 show variation in **fatigue life** with varying Cd, for FRAMEWORK and USFOS, for each **wind block** case with **weight factor** of 1.5. Figure 7-39 shows all **wind block** cases of both software.

The following observations are made

- FRAMEWORK predicts longer **fatigue life** in each corresponding **wind block** case.
- **Fatigue life** is closer in value for all cases when **Cd=1.2**, relative to other values of **Cd**.
- **Fatigue life** is most sensitive for **Cd** values between **0.65** to **1.0** for both software.
- **Fatigue life** of the two software come closer with increasing **Cd**. For the case of **Cd = 1.2**, **fatigue life** in both software is close to equal in all different **weight factor** cases.
- The case of **USFOS 10 wind blocks** predicts the lowest **fatigue life** among all cases.
- **Fatigue life** drop trend in **USFOS** is milder in slope than the corresponding in **FRAMEWORK** in all cases.
- **Fatigue life** result in case of **USFOS 16 wind blocks** and **FRAMEWORK 8 wind blocks** converges to become almost identical while it diverges in case of **Cd = 0.65** and **1.2**. For the mentioned cases, **fatigue life** is predicted to be higher in **USFOS** than that in **FRAMEWORK** by **30%** and **40%** respectively.

- **Fatigue life** drop trends in case of USFOS **8 wind blocks** and FRAMEWORK **12 wind blocks** are close to identical with USFOS predicting higher **fatigue life** with an average **11%** among all the cases.
- **Fatigue life** drop trends in case of USFOS **12 wind blocks** and FRAMEWORK **10 wind blocks** are close to identical. **Fatigue life** in this case is predicted to be higher in FRAMEWORK by **8%**.
- USFOS case of **16 wind blocks** predicts the highest **fatigue life** for **Cd = 0.65** and **1.2**, while FRAMEWORK case of **8 wind blocks** predicts the highest **fatigue life** for **Cd = 1.0**. For the mentioned cases, FRAMEWORK **fatigue life** results for **Cd = 1.0** is **3%** higher in FRAMEWORK, while higher in USFOS for **Cd = 0.65** and **1.2** by **30%** and **39%** respectively.

7.3.3 Summary and Discussion

In all cases with correlating input data, FRAMEWORK predicts a longer **fatigue life** than USFOS for the corresponding cases.

On average, USFOS predicts **66%** of the **fatigue life** that FRAMEWORK predicts. For **weight factor** of **1.0** cases, USFOS predicts **49%** of the fatigue life that FRAMEWORK predicts. Concluding which software is more reasonable to use for such structure is difficult as there are many assumptions made and there is limited data available on real **fatigue life** of similar structures.

The most critical joint in FRAMEWORK (**jt 101020**) is the mirror of the most critical joint in USFOS (**jt 167**) (see **Figure 3-3**), while the opposite is the case for the second most critical joint. Both joints are in the connection between the flare tower and the support structure. This may be explained by the difference the scatter diagrams are treated in USFOS and FRAMEWORK, where the latter simplifies the analysis by adding all opposing direction's probabilities and calculate fatigue damage from 6 directions instead of 12. This simplification distributes the wind loading differently throughout the structure than USFOS. Wind from two opposing directions, may affect two opposing joints in the same scale if the structure is somewhat symmetrical.

USFOS **16 wind blocks** case could have the most accurate representation of reality out of the USFOS analyses, as it includes more data on the probabilities by having more wind blocks. For that reason, a close representation by FRAMEWORK is sought after. By studying the comparisons given in this chapter, it could be argued that FRAMEWORK case of **8 wind blocks** correlates closest to the **16 wind blocks** case in USFOS. However, the **8 wind blocks** case in FRAMEWORK predicts slightly higher **fatigue life** on average.

Fatigue life predicted by USFOS **16 wind blocks** and FRAMEWORK **8 wind blocks** are close in results in cases of **weight factor** of **0.5** and **1.1**.

Fatigue life decrease trends in case of USFOS **12 wind blocks** and FRAMEWORK **10 wind blocks** are close to identical in cases of **weight factor** of **1.1** and **1.5**, with variance of around $\pm 8\%$. This could be attributed to the change in eigen frequencies with the increase in mass.

The **12 wind blocks** case in FRAMEWORK come close to the **16 wind blocks** case in USFOS in case of **weight factor 1.0** and for the most part predicts slightly shorter life than USFOS. It is arguable which of these analyses is more accurate; however, the **12 wind block** cases seem to be the more conservative. This could be attributed to the bigger wind blocks at higher wind speeds used in case of **12 wind blocks**.

There seem to be a large difference in **fatigue life** sensitivity of the two software around **weight factor** range of **1.0** and **1.1**. As mentioned previously, there is a relatively large difference in **fatigue life** due to a relatively small difference in weight compared to the other weight factors in FRAMEWORK, whereas the USFOS analysis generally does not have a significant sensitivity to **fatigue life** in the same range. This further indicate that this specific increase in FRAMEWORK may be due to the shift in **natural frequency** of the structure as time history analysis is not as sensitive to natural frequency.

In both software the **fatigue life** sensitivity to parameter change seem to converge in most cases when **fatigue life** decreases. However, deviation from this norm is observed, as explained with FRAMEWORK's extra sensitivity in **weight factor 1.0** to **1.1**. This could be explained by the fact that the **S-N curve** has a bi-linear scaling, hence small changes in stress ranges make larger difference in **fatigue life** in the lower stress range realm.

8 Conclusions

Two methods of estimating fatigue life have been studied, with significant difference in results. The two methods are the spectral density approach which is used in FRAMEWORK and WINDPACK and the time domain non-linear dynamic approach which is used in USFOS. The same structural model has been used and only the most critical joint in the analysis has been compared in studies. Sensitivity to parameter changes (i.e., parametric study) have been studied and compared between the different software approaches. Structural weight factor, drag factor, wind block combination and relative velocity are the main parameters that have been investigated. The effect of changing time increment has also been investigated in USFOS; however, it is not considered as a parameter since sufficient time increment must always be used and is case dependent. Furthermore, interesting behavior was observed with time increment $dt = 0.10$ seconds.

8.1 Concluding Remarks

- FRAMEWORK estimates a shorter **fatigue life** than WINDPACK in all cases with corresponding input. On average FRAMEWORK predicts **41%** of the **fatigue life** that WINDPACK predicts in all cases. For **weight factor 1.0** cases, the difference becomes **47%**. One reason for this difference due to slightly higher SCF values in FRAMEWORK. Considering that WINDPACK is using the HARRIS spectra, which is meant for onshore wind, and FRAMEWORK using the Frøya spectra, which is better suited for offshore wind, the latter software may be the more accurate of the two.
- The time history method in USFOS predicts a shorter **fatigue life** than the spectral density method in FRAMEWORK using corresponding input. On average USFOS predicts **66%** the **fatigue life** that FRAMEWORK predicts. For **weight factor 1.0** cases, the difference becomes **49%**.
- USFOS most critical joint (jt 167 / 103520) (see **Figure 3-3**) is located at the base connection between flare tower and the supporting structure, which seems reasonable since the flare boom mostly acts as a cantilever and therefore has the max global bending moments at this point. WINDPACK's most critical joint is the same as in USFOS; however, in FRAMEWORK the most critical joint (jt 159 / 101020) (see **Figure 3-3**) is the mirror of that in USFOS, located on the opposite connection between flare boom and support structure. This may be explained by the difference in which the scatter diagrams are treated in USFOS, WINDPACK and FRAMEWORK. The latter simplifies the analysis by adding all opposing direction's probabilities and calculate fatigue damage from 6 directions instead of 12; however, this simplification is not used in USFOS and WINDPACK. This simplification distributes the wind loading differently throughout the structure. Wind from two opposing directions, may affect two opposing joints in the same scale if the structure is relatively symmetrical, as symmetry in geometry and material properties causes structure to respond equally but in opposing directions to loads of same magnitude with opposing directions.

- Use of more **wind blocks** generally means less predicted fatigue damage. This is due to less conservative roundups. This is proven with USFOS **16 wind blocks** cases having an average **66%** higher **fatigue life** than the **8 wind blocks** cases. In the cases of **10-** and **12 wind blocks**, the top wind speeds are added with corresponding probabilities in longer ranges, yielding shorter **fatigue life** than the **8 wind blocks** cases, in which all wind speeds are distributed evenly. **Fatigue life** in the **12 wind blocks** cases is on average **73%** and **68%** of that in the **8 wind blocks** cases in USFOS and FRAMEWORK, respectively. **Fatigue life** in the **10 wind blocks** cases is on average **54%** and **49%** of that in the **8 wind blocks** cases in USFOS and FRAMEWORK, respectively. Even though the probability of occurrence for the top wind speeds are low, they make a significant impact on **fatigue life**.
- The trend in all software seems that parameters sensitivity decreases with lower **fatigue life**. This may be explained by the logarithmic scale of the S-N curves. Changes in stress in the lower stress region means more significant changes in the cycles a material can endure, compared to these in the higher stress region.
- The largest change in **fatigue life** due to **weight factor** is in the range of **weight factor 0.5 to 1.0** in USFOS, decreasing with **62%** on average. **Fatigue life** decreased almost linearly with increasing **weight factor** in WINDPACK with **29%** on average in the range of **weight factor 0.5 to 1.0**. **Fatigue life** in FRAMEWORK has a similar decrease trend with **weight factor** as that in USFOS, where the graphs of the two are almost parallel, except in the range of **weight factor 1.0 to 1.1**.
- On average **fatigue life** decreases with **36%** in the **weight factor** range of **1.0 to 1.1** in FRAMEWORK, which is relatively large compared to the small increase in weight. FRAMEWORK shows an increase in sensitivity in this range in all cases, while this trend does not appear in the other two software. This could be attributed to the wind spectra generated by FRAMEWORK, which might have an energy peak frequency close to the natural frequency the structure has with **weight factor 1.1**, causing resonant reactions. WINDPACK uses a different spectrum (HARRIS), and therefore may not have the same energy peak frequencies, while USFOS uses time history and therefore is not as frequency sensitive. This could be the reason why this **weight factor** range is not as critical in USFOS and WINDPACK.
- USFOS and FRAMEWORK show similar behavior in **fatigue life** by change of **Cd**, FRAMEWORK is slightly more sensitive on average. Cases with the use of **Reynold's dependent Cd** give higher **fatigue life** than cases with **Cd = 1.0**, but lower than cases with **Cd = 0.65**.
- **Fatigue life** predicted by USFOS **16 wind blocks** and FRAMEWORK **8 wind blocks** are close in results in different cases of **weight factors** and more comparable than the cases of USFOS **8 wind blocks** and FRAMEWORK **8 wind blocks**. This is clearly seen in case of **weight factor 0.5** and **1.1**.

- **Fatigue life** in WINDPACK is sensitive to change in **Cd** in the range between **0.65** to **1.0**, decreasing with **84%**. Great caution should be practiced when deciding on **Cd** in WINDPACK.
- While investigating time histories from different values of **Cd** in USFOS the same stress pattern is observed, only with varying magnitude. The difference in stress at the same stress range from two cases of different **Cd** are almost equal to the factored difference of **Cd**. This concludes that **Cd** directly affects the structure's stress in USFOS.
- **Relative velocity** is a built-in function in USFOS, and **8** analyses have been done with and without this formula active. On average the use of this formula gives an increase of **196%** in **fatigue life**. This formula should be used with great caution when analyzing wind induced fatigue.
- While changing the **time increment**, there is negligible change in **fatigue life** when going lower than **dt = 0.05 seconds**, while it generally doubles when changing from **dt = 0.10 seconds** to **dt = 0.05 seconds**. The denser **time increment** significantly increases the run time for the analysis (double the time for **dt = 0.05** than **dt = 0.10** seconds). The most reasonable **time increment** for this structure (Flare boom 1) is therefore concluded to be **0.05 seconds**, based on need for accuracy and analysis time.
- While investigating how **weight factor** changes **fatigue life** in USFOS **dt=0.10 seconds** analyses, **fatigue life** increases in every case between **weight factor 1.0** to **1.1**. However, a heavier structure generally increases the natural period and generates more stress response, especially when considering the slender nature of the structure. The reason could be linked to numerical issues in calculations. All other analyses that are done show the opposite behavior i.e., decrease in **fatigue life** with increase in weight. **Time increment** of **0.10** seconds should be avoided for this specific case.
- The practical differences of the three software may be concluded as follows. FRAMEWORK is slightly easier to setup and requires less input data. USFOS needs simulated wind field. Errors are easily detected in USFOS, while FRAMEWORK does not provide the same overview. It is possible to view all stress histories for all cases in USFOS, which means more control and confirmation opportunities, while with FRAMEWORK the spectra approaches provide less control due to load cases being translated into frequency-domain spectral stresses.
- A general conclusion can be drawn from all graphs that for cases with higher **fatigue life**, most of the damage may fall in the slope region of 5 ($m = 5$) on the SN-curve, while cases with lower **fatigue life**, the slope 3 ($m = 3$) dominates. Hence, an increase in load (by e.g., **Cd**) the high **fatigue life** cases will drop more rapidly than the lower **fatigue life** cases.

8.2 Further Work

This thesis has investigated the differences in 3 different software based on a comparative study. However, further comparisons are recommended. Running analysis with FRAMEWORK and WINDPACK with the same wind spectrum and equal SCFs is recommended for further insight.

FRAMEWORK shows significant sensitivity to change of weight factor in this structural model (Flare 1). Weight is inversely related to natural frequency as explained, and further investigation of the correlation of a structure's natural frequency and the peak frequencies present in different wind spectra are encouraged. This might provide insight to the limitations or drawbacks to avoid when using the spectral density approach.

FRAMEWORK yields the most critical point in fatigue analysis for (Flare 1) as the mirror of the most critical point resulting from USFOS analysis. Further investigation of this result could be done by putting wind directions opposite to the ones used in this thesis (for example $180^\circ - 330^\circ$).

This thesis is based on wind blocks with highest wind speed in each block to give the most conservative results. Different cases of wind block arrangement are therefore encouraged to be studied further for better understanding of the effect in change in wind blocks. As the high wind speed blocks are governing, it might be suggested that the lower wind speed blocks are combined instead of the high wind speed blocks for a more accurate -less conservative- result.

Further studies on the difference between time history and spectral density methods should also be investigated to provide insight for the limitations and inaccuracies of both. Accuracy of both can only be confirmed through experimental testing, which can confirm integrity of both methods for the industry.

Further studies on the effect of relative velocity on slender structures with relatively small displacements are recommended.

Other comparative studies of flare towers or similar slender structures can further confirm large differences in the different methods used.

9 References

1. A. Naess, T. M. (2013). *Stochastic dynamics of marine structures*. New York: Cambridge University Press.
2. Arthur P. Boresi, R. J. (2003). *Advanced Mechanics of Materials*. John Wiley & Sons Inc.
3. AS, Aker Jacket Technology. (2022). Windpack User Manual. AS, *Aker Jacket Technology*.
4. Boris Fuštar, I. L. (2018). *Review of Fatigue Assessment Methods for Welded Steel Structures*. Advances in Civil Engineering.
5. C.H. McInnes, P. M. (2008). *Equivalence of four-point and three-point rainflow cycle counting algorithms*. International Journal of Fatigue.
6. C.M. Sonsino, W. F. (2012). *Notch stress concepts for the fatigue assessment of welded joints*. International Journal of Fatigue.
7. Craig MacEachern, Í. Y. (2018). *Comprehensive Energy Systems*.
8. Dikshant Singh Saini, D. K.-C. (2016). *A review of stress concentration factors in tubular and non-tubular joints for design of offshore installations*. Kanpur: Journal of Ocean Engineering and Science.
9. DNV - Framework User Manual. (2020). *Framework User Manual*. DNV AS.
10. DNV RP-C203. (2019). *Fatigue design of offshore steel structures (RP-C203)*.
11. DNV RP-C205. (2019, September). *Environmental conditions and environmental loads (RP-C205)*. DNV AS.
12. Hobbacher, A. I. (2008). *Recommendations for Fatigue Design of Welded Joints and Components*. IIW.
13. Holmes, J. D. (2018). *Wind loading of structures*. CRC Press.
14. Hoven, I. v. (1957). *Power spectrum of horizontal wind speed in the frequency range of 0.0007 to 900 cycles per hour*. Journal of Meteorology.
15. Junbo Jia, R. E.-J. (2010). *The Effects of Wind Modeling Considerations and Wind Direction on an Accurate Fatigue Life Assessment*. The International Society of Offshore and Polar Engineers.
16. Karlsson, H. (2018). *Static and Fatigue Analyses of Welded*. Karlskrona: Faculty of Mechanical Engineering, Blekinge Institute of Technology.
17. NORSOK Standard. (2017). *Actions and action effects (N-003)*.
18. Sherratt, D. N. (1989, January). Fatigue life prediction from power spectral density data. *Environmental Engineering*, s. 12.
19. Timoshenko S.P, .. a. (1955). *Vibration Problems in Engineering*.

20. Yong Bai, W.-L. J. (2016). *Marine Structural Design (Second Edition), Chapter 25 - Fatigue Capacity*. Butterworth-Heinemann.
21. Yung-Li Lee, T. T. (2012). *Rainflow Cycle Counting Techniques, Metal Fatigue Analysis Handbook*. Butterworth-Heinemann.
22. AAS_JAKOBSEN - WindSim User manual. (2020, 01 31). *User manual WindSim*. Hentet fra http://www.aas-jakobsen.net/download/windsim/User%20manual%20Windsim_v47.pdf